**Universidade de Brasília – UnB**
**Instituto de Ciências Biológicas – IB**
**Programa de Pós-graduação em Zoologia - PPGZoo**

**TESE DE DOUTORAMENTO**

# OSTEOLOGIA E ANÁLISE MORFOMÉTRICA DE ESPÉCIMES ADULTOS E JUVENIS DE BAURUSUCHIDAE (NOTOSUCHIA, MESOEUCROCODYLIA) DA FORMAÇÃO ADAMANTINA, GRUPO BAURU, CRETÁCEO SUPERIOR.

**MSc. Daniel Martins dos Santos**

19/0005823

Orientador: Prof. Dr. Rodrigo Miloni Santucci

Brasília, outubro de 2023

**Universidade de Brasília – UnB**
**Instituto de Ciências Biológicas – IB**
**Programa de Pós-graduação em Zoologia - PPGZoo**

**TESE DE DOUTORAMENTO**

# OSTEOLOGIA E ANÁLISE MORFOMÉTRICA DE ESPÉCIMES ADULTOS E JUVENIS DE BAURUSUCHIDAE (NOTOSUCHIA, MESOEUCROCODYLIA) DA FORMAÇÃO ADAMANTINA, GRUPO BAURU, CRETÁCEO SUPERIOR.

**Aluno:** MSc. Daniel Martins dos Santos 19/0005823

**Orientador:** Prof. Dr. Rodrigo Miloni Santucci

Tese de doutorado apresentada ao Instituto de Ciências Biológicas da Universidade de Brasília (IB-UnB), Programa de Pós-graduação em Zoologia, como requisito para obtenção do título de Doutor em Zoologia, na área de concentração em Sistemática e Biogeografia.

Brasília, outubro de 2023

**Tese apresentada na forma de três artigos científicos conforme permitido pela resolução 03/2021 do Colegiado do Programa de Pós-graduação em Zoologia, Instituto de Ciências Biológicas, Universidade de Brasília.**

MSc. Daniel Martins dos Santos

19/0005823

Brasília, outubro de 2023

## BANCA EXAMINADORA

**Presidente**

**Prof. Dr. Rodrigo Miloni Santucci (UnB)**

Paleontólogo especializado em saurópodos titanossauros e análise cladística. Conduz pesquisas nas Bacia Bauru e Sanfranciscana.

**Membro interno**

**Prof. Dra. Angele Martins dos Reis (UnB)**

Herpetóloga atuando principalmente nos seguintes temas: anatomia descritiva, anatomia comparada, morfologia e aplicação de dados morfológicos para sistemática de serpentes.

**Membros externos**

**Prof. Dr. André Piacentini Pinheiro (UERJ)**

Paleontólogo atuando na área da biologia, geologia sedimentar e paleontologia de vertebrados, com especialidade em Crocodylomorpha (Archosauria).

**Prof. Dr. Felipe Chinaglia Montefeltro (Unesp)**

Paleontólogo atuante nos temas de sistemática filogenética de Rhynchosauria, Crocodyliformes, e na evolução da região ótica de Crocodyliformes.

**Suplentes**

**Prof. Dra. Julia Klaczko (UnB)**

Desenvolve projetos nas áreas de Zoologia nos seguintes temas: macroevolução de répteis, evolução da genitália de Squamata e evolução da forma do crânio em vertebrados.

**Prof. Dr. Pedro Lorena Godoy (USP)**

Paleontólogo atuante na taxonomia e sistemática de Crocodylomorpha e outros répteis extintos. Busca documentar padrões macroevolutivos no registro fóssil.

## Página de Aprovação

Osteologia e Análise Morfométrica de Espécimes Adultos e Juvenis de Baurusuchidae (Notosuchia, Mesoeucrocodylia) da Formação Adamantina, Grupo Bauru, Cretáceo Superior

MSc. Daniel Martins dos Santos

Orientador: Prof. Dr. Rodrigo Miloni Santucci

Tese de Doutorado apresentada ao Programa de Pós-graduação em Zoologia, Instituto de Ciências Biológicas, da Universidade de Brasília, como parte dos requisitos necessários à obtenção do título de Mestre/Doutor(a) em Zoologia.

Aprovada por

(Prof. Dr. Rodrigo Miloni Santucci) Presidente – UnB

(Prof. Dra. Angele Martins dos Reis) – UnB
(Prof. Dr. André Piacentini Pinheiro) – UERJ
(Prof. Dr. Felipe Chinaglia Montefeltro) – Unesp

(Prof. Dra. Julia Klaczko) – UnB
(Prof. Dr. Pedro Lorena Godoy) - USP

Brasília

Outubro de 2023

**Ficha catalográfica elaborada automaticamente,com os dados fornecidos pelo(a) autor(a)**

MS237 Martins dos Santos, Daniel

Osteologia e Análise Morfométrica de Espécimes Adultos e Juvenis de Baurusuchidae (Notosuchia, Mesoeucrocodylia) da Formação Adamantina, Grupo Bauru, Cretáceo Superior / Daniel Martins dos Santos; Orientador, Rodrigo Miloni Santucci.

-- Brasília, 2023.225 p.

Tese (Doutorado em Zoologia) -- Universidade de Brasília,2023.

1. Crocodylomorpha. 2. Bacia Bauru. 3. Baurusuchidae. 4.Osteologia. 5. ontogenia. I. Miloni Santucci, Rodrigo , orient. II. Título.

## AGRADECIMENTOS

Como animais sociais que somos, esta tese jamais poderia ter sido concluída sem as interações, ensinamentos, apoio e acolhimento de um grupo considerável de pessoas. Grande demais para citar nominalmente. Contudo, agradeço especialmente aos meus pais e minha irmã, Edgar, Eloisa e Bruna, que me cercaram de amor e me incentivaram ao longo de toda a minha vida.

À minha esposa Raiane, com quem navego as águas da vida adulta. Obrigado por aturar meus monólogos sobre a biologia de répteis extintos e outros assuntos.

Ao meu orientador, Prof. Dr. Rodrigo Miloni Santucci. Não somente um grande paleontólogo, Rodrigo também é um incrível ser humano que me orientou com paciência e dedicação.

Aos meus colegas de pós-graduação, por todos esses anos de gostosas risadas que compartilhamos nas saídas de campo e no laboratório. Só nós sabemos como foi difícil seguir nossos sonhos em um contexto de turbulência política e pandemia.

Agradeço também aos meus amigos e amigas de infância, da geologia e do intercâmbio, que coloriram a minha vida com momentos marcantes e diferentes perspectivas. Tenho certeza de que sou uma pessoa melhor graças a essas interações.

Por fim, agradeço profundamente o apoio financeiro recebido. O presente trabalho foi realizado com apoio da Coordenação de Aperfeiçoamento de Pessoal de Nível Superior – Brasil (CAPES) – Código de Financiamento 001.

Daniel Martins dos Santos

“Organisms are not billiard balls, propelled by simple and measurable external forces to predictable new positions on life’s pool table. Sufficiently complex systems have greater richness. Organisms have a history that constrains their future in myriad, subtle ways.”

**— Stephen Jay Gould**

“Here we are, the most clever species ever to have lived. So how is it we can destroy the only planet we have?”

**— Jane Goodall**

## Título

**OSTEOLOGIA E ANÁLISE MORFOMÉTRICA DE ESPÉCIMES ADULTOS E JUVENIS DE BAURUSUCHIDAE (NOTOSUCHIA, MESOEUCROCODYLIA) DA FORMAÇÃO ADAMANTINA, GRUPO BAURU, CRETÁCEO SUPERIOR.**

## Resumo

Grande parte dos tetrápodes fósseis são conhecidos a partir de um único espécime, impossibilitando o estudo de fontes de variação de forma como teratogêneses, deformações tafonômicas, dimorfismo sexual e ontogenia. Baurusuchidae, uma família de notossúquios predatórios que apresenta oreinirrostria e dentição zifodonte, são alguns dos materiais fósseis mais abundantes da Bacia Bauru, com múltiplos espécimes incluindo diferentes semaforontes. Nos últimos vinte anos, cerca de oito espécies adicionais de baurussuquídeos oriundas da Formação Adamantina foram formalmente descritas, porém poucos esforços foram direcionados na caracterização de suas trajetórias ontogenéticas, de suma importância para entender variações intraespecíficas. Esta tese de doutoramento procura, através da descrição anatômica de dois espécies juvenis e aplicação da morfometria geométrica, traçar as mudanças morfológicas que caracterizam membros desse grupo. O capítulo I apresenta uma revisão bibliográfica da literatura acerca dos crocodiliformes, inserindo os baurussuquídeos no seu contexto evolutivo. Os capítulos II e III são artigos descrevendo a osteologia e miologia de dois semaforontes de diferentes estágios: um indivíduo com cerca de um ano e outro juvenil mais próximo da maturidade esquelética. Por fim, o capítulo IV utiliza-se de análise morfométrica para melhor compreender mudanças nas proporções cranianas e, por consequência, a diferença entre os morfoespaços ocupados por adultos e juvenis. O trabalho levanta evidências que questionam os níveis de diversidade atualmente reconhecidas para o clado.

**Palavras-chave:** Crocodylomorpha; Bacia Bauru; Baurusuchidae; osteologia; ontogenia.

## Title

**OSTEOLOGY AND MORPHOMETRIC ANALYSIS OF ADULT AND JUVENILE BAURUSUCHID SPECIMENS (NOTOSUCHIA, MESOEUCROCODYLIA) FROM THE ADAMANTINA FORMATION, BAURU GROUP, LATE CRETACEOUS.**

## Abstract

The vast majority of fossil tetrapods are known single specimens, preventing studies on sources of variation such as teratogenesis, taphonomic deformations, sexual dimorphism, and ontogeny. Baurusuchidae, a family of oreinirostral predatory notosuchians with ziphodont dentition, are among the most abundant fossil materials in the Bauru Basin, with multiple specimens including different ontogenetic stages. In the past twenty years, about eight additional species of baurusuchids from the Adamantina Formation have been formally described, but few efforts were directed towards characterizing their ontogenetic trajectories, which is crucial for understanding intraspecific variations. This doctoral thesis aims to trace the morphological changes that characterize members of this group through the anatomical description of two juvenile specimens and the application of geometric morphometrics. Chapter I provides a literature review on crocodyliforms, placing baurusuchids in their evolutionary context. Chapters II and III are research articles describing the osteology and myology of two different ontogenetic stages: a yearling individual and another juvenile closer to skeletal maturity. Finally, Chapter IV uses morphometric analysis to better understand changes in cranial proportions and, consequently, the different morphospaces occupied by adults and juveniles. The work presents evidence that challenges the currently recognized levels of diversity within the clade.

**Keywords:** Crocodylomorpha; Bauru Basin; Baurusuchidae; osteology; ontogeny.

**Sumário**

# Capítulo I

## 1) – Introdução

Crocodylia, uma ordem atualmente composta por 27 espécies divididas em 3 famílias (Crocodylidae, Alligatoridae e Gavialidae), são predadores de topo, de hábitos semiaquáticos, e distribuídos em zonas tropicas e subtropicais ao redor do planeta (Grigg, 2015). Apesar de pouco especiosos, os crocodilianos são abundantes e desempenham papeis tróficos de extrema importância, sendo comumente classificados como *keystone species*, capazes de alterar a estrutura das cadeias tróficas, regulando a população de outros organismos e, por consequência, a saúde dos ecossistemas (Ashton, 2010; de Miranda., 2017; Mazotti *et al*., 2009; Palmer & Mazotti, 2004).

A escassez de espécies e a pouca variância no *blauplan* das formas atuais contrasta com o registro fóssil, que incluí formas relacionadas com as mais diversas adaptações alimentares para carnivoria, onivoria e, possivelmente, herbivoria, além planos corporais díspares para o preenchimento de nichos terrestres, marinhos e semiaquáticos continentais (Riff *et al*., 2012; Brochu, 2003).

A presente tese de doutoramento busca descrever a osteologia e, quando possível, a miologia craniana e pós-craniana de diferentes semaforontes de baurussuquídeos, identificando caracteres ontogenéticos com importantes implicações paleoecológicas e taxonômicas. Adicionalmente, procura-se aplicar a morfometria geométrica a família Baurusuchidae, de modo a qualificar sua trajetória de mudanças morfológicas atribuídas a ontogenia.

Para este fim, é preciso, primeiramente, apresentar ao leitor uma série de conceitos e seus históricos de pesquisa para que este faça melhor proveito dos capítulos que virão. A seguir, é apresentada uma breve revisão bibliográfica que insere Baurusuchidae (Price, 1945) dentro de seu contexto filogenético, começando pela origem dos arcossauros e dos primeiros crocodilomorfos e crocodyliformes durante o período Triássico, passando pelos clados mais abrangentes dentro de Mesoeucrocodylia (Notosuchia e Neosuchia) e culminando na definição da família Baurusuchidae, suas subfamílias Pissarrachampsinae e Baurusuchinae (Montefeltro *et al*., 2011), suas respectivas características morfológicas e sinapomorfias, e aspectos de sua ecologia.

### 1.1) – Histórico de pesquisa

O estudo formal dos crocodilianos, assim como de muitos outros clados, se inicia com a publicação do trabalho seminal *Systema naturæ* (1758), do pioneiro da classificação taxonômica Carolus Linnaeus. O trabalho de Lineu, sendo pré-gradista e muito anterior ao advento da sistemática filogenética, não classifica as formas com a intenção de gerar grupos naturais, ou seja, não leva em consideração processos evolutivos. Sendo assim, Crocodylia foi primeiramente agrupado à lagartos e cobras, formando o que Lineu chamou de 'Lacerta'.

Assim como será visto nos próximos tópicos, a postura do tipo *sprawling*, comumente utilizada por crocodilianos atuais, é na verdade uma condição derivada do estado plesiomórfico parasagital de Crocodylomorpha, levando muitos autores clássicos e, muitas vezes, o público em geral, a associar os mesmos aos Lepidosauromorfos.

O paleontólogo e anatomista britânico Richard Owen foi um dos primeiros a reconhecer a proximidade de algumas formas fósseis aos crocodilianos viventes e propor uma tentativa de classificação não-evolutiva desses táxons. Owen (1860), baseou-se na morfologia dos cótilos e côndilos das vértebras pré-sacrais, definindo os grupos Opisthocoelia, Amphicoelia e Procoelia. Huxley (1875), outro nome de referência da anatomia de vertebrados do século XIX, e um defensor ferrenho de Darwin, introduziu, pela primeira vez, o conceito evolutivo à classificação dos crocodilianos atuais e fósseis, criando uma série de 'grados', ou estágios evolutivos, sendo eles Parasuchia, Mesosuchia e Eusuchia.

Além dos caracteres vertebrais utilizados por Owen (1860), Huxley também se serviu da posição dos coanas e da morfologia dos coracóides para erguer seus grupos, observações que ainda se sustentam nas filogenias modernas. Apesar de incipiente, parte dos grados de Huxley, Mesosuchia e Eusuchia mais especificamente, se demonstraram monofiléticos, e mantiveram seus nomes mesmo após aplicação de técnicas sistemáticas modernas.

Já no começo do século XX, Brown (1930), com sua descrição de *Protosuchus richardsoni*, uma importante forma triássica de pequeno porte, reconhece um clado basal de crocodilomorfos e adiciona o grado 'Protosuchia' a antiga classificação de Huxley. A segunda metade de século XX, por sua vez, veria uma série de trabalhos clássicos empregando a sistemática filogenética (Hennig, 1966) ao estudo dos

crocodilomorfos fósseis e aos arcossauros em geral (Gauthier & Padian, 1985; Gauthier 1986).

Whetstone & Whybrown (1983), recuperam e erguem Mesoeucrocodylia, que une Mesosuchia e Eusuchia, enquanto Clark (1986) cunha o termo Crocodyliformes para o grupo que engloba protossuquídeos, mesossuquídeos e eussuquídeos. Estes são seguidos pela análise ampla de Benton & Clark (1988), que focou na linhagem dos pseudossúquios, inclusive incluindo arcossauros basais, culminando na definição de Metasuchia para mesoeucrocodilianos não-talatossuquídeos e Neosuchia para eussuquídeos e formas mais basais.

Atualmente, devido ao acúmulo de conhecimento e capacidades cada vez maiores de processamento e a aplicação dos mais variados métodos comparativos, diversos autores têm trabalhado com grandes bases de dados, gerando não só superárvores (Bronzati *et al*., 2015), como também mapeando transições evolutivas dos principais clados nas mesmas (Wilberg *et al*., 2019; Godoy *et al*., 2019; 2020).

### 1.2) – Archosauria

Os arcossauros, erguidos classicamente por Cope (1869), compõem um clado de vertebrados diápsidos que dominaram os ambientes terrestres durante a Era Mesozoica, sendo um grupo monofilético com um registro fóssil bastante especioso e díspare (Brusatte *et al*., 2008; 2010, Nesbitt, 2011).

A aplicação das técnicas da sistemática filogenética concebidas por Hennig (1966) nos estudos evolutivos dos arcossauros (Clark, 1986; Gauthier, 1986; Benton & Clark, 1988), resultou em cladogramas que sugerem que tal grupo é marcado por duas linhagens principais (**figura 1**), que surgiram e divergiram entre si no início do Período Triássico (Sereno, 1991). A linhagem dos Pseudosuchia (Gauthier, 1986), ou Crurotarsi (Sereno & Arcucci, 1991), deu origem aos crocodilomorfos e incluem formas fósseis mais proximamente aparentadas a estes. Os Avemetatarsália (Benton, 1999), por sua vez, incluem dinossauros (avianos e não-avianos), pterossauros e formas afins.

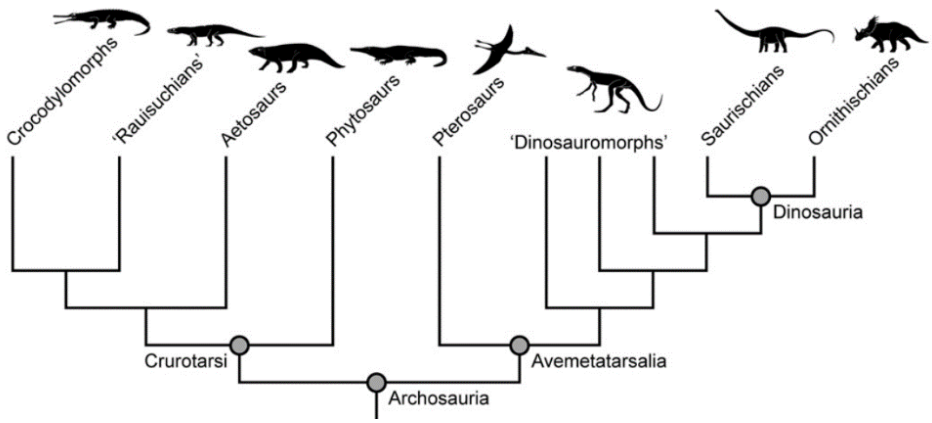


**Figura 1. Cladograma simplificado dos arcossauros mostrando suas duas principais linhagens, Crurotarsi e Avemetatarsália, em que estão inclusos os crocodilianos e as aves atuais, respectivamente. Durante o mesozóico, ambos grupos eram mais diversos que atualmente, tanto em disparidade de formas, como em número de espécies. Retirado de Brusatte *et al*., 2010.**

Os arcossauros já foram estabelecidos filogeneticamente utilizando-se de diferentes modos de definição de clado. Gauthier (1986), por exemplo, faz uso do conceito de grupo coronal, restringindo Archosauria ao último ancestral comum e exclusivo entre aves e crocodilianos e todos os seus descendentes, excluindo formas basais triássicas e renomeando-as Archosauromorpha e Archosauriformes, de acordo com seu grau de proximidade ao clado apical.

Resumidamente, as principais sinapomorfias que suportam a monofilia de Archosauria são: (1) presença de fenestra anteorbital entre as narinas e as órbitas; (2) desenvolvimento de fenestra mandibular; (3) dentes encaixados em soquetes (condição tecodonte) comprimidos lateralmente e com carenas serrilhadas e (4) um quarto trocânter do fêmur (Benton, 1999; 2005, mas ver Nesbitt, 2011).

Trabalhos iniciais focando na anatomia dos primeiros arcossauros já identificavam uma propensão evolutiva de algumas de suas linhagens ao bipedalismo, como uma tendência à redução dos membros anteriores, postura parasagital, com os membros situados abaixo do corpo, além de um desenvolvimento maior dos ossos que compõe a bacia, o ílio, ísquio e púbis, formando uma típica morfologia triradial de modo aumentar as áreas de inserção muscular para suporte das tensões geradas pelo movimento anteroposterior dos membros (Romer, 1956; Gower, 2003).

Uma das principais diferenças morfológicas estabelecida rapidamente após a divergência entre os grupos supracitados refere-se à disposição dos ossos tarsais (**figura 2**). Os Pseudosuchia são caracterizados por uma estruturação do tipo

crocodilo-normal (CN) ou *crurotarsal* (Sereno, 1991), onde os ossos tarsais proximais possuem tamanhos similares, e um processo cilíndrico do astrágalo se encaixa em uma fossa do calcâneo, conferindo maior flexibilidade e permitindo tanto uma postura parasagital como alastrada (Benton, 2004). Os Avemetatarsália, por outro lado, apresentam uma disposição do tipo *mesotarsal*, marcada por um astrágalo consideravelmente maior que o calcâneo, que envolve a tíbia e gera um único plano de articulação entre os tarsais proximais e os pés (Benton, 2004).

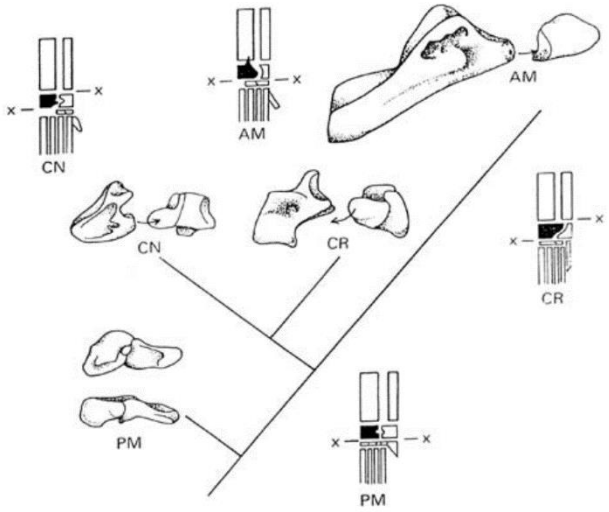


**Figura 2. Evolução do *tarsus* nos arcossauros. As morfologias observadas em Pseudosuchia e Avemetatarsália seriam derivadas da condição mesotarsal primitiva (PM), que teria se divergido ainda mais dentro do Pseudosuchia com a estruturação do tipo crocodilo-reversa (CR), presente em Ornithosuchidae. Ambas as disposições contribuíram para o desenvolvimento de postura parasagital nos arcossauros, contudo, a crocodilo normal (CN) é a única que permite também uma postura alastrada característica dos crocodilianos atuais. Retirada de Benton, 2004.**

Apesar dos primeiros arcossauromorfos datarem dos últimos instantes do Paleozoico, como membros do gênero *Archosaurus* Tatarinov 1960, do Permiano Tardio da Rússia e Polônia (Sennikov & Golubev, 2006), sua principal irradiação ocorreu somente após a vacância de nichos ecológicos deixada pela extinção Permo-Triássica, evoluindo rapidamente no início do Triássico em uma miríade de diferentes formas e divergindo nas duas linhagens citadas acima (Benton *et al*., 2014).

Os primeiros representantes dos Crurotarsi possuem registros já no Anisiano, Triássico Médio, com o já derivado *Arizonasaurus* (Nesbitt, 2003), membro da família Ctenosauriscidae, enquanto membros da linhagem aviana também têm seu registro

fóssil mais pretérito no Triássico Médio, com *Teleocrater rhadinus* (Nesbitt *et al*., 2017), pertencente ao clado Aphanosauria.

O grau de convergência e as similaridades entre as duas linhagens de arcossauros no início do Triássico, como as homoplasias entre alguns membros de Poposauroidea e Dinosauria (Gauthier *et al*., 2011), levantam dúvidas a respeito dos modelos que tentam explicar a emergência dos dinossauros como grupo de vertebrados terrestres dominantes durante o mesozóico (Brusatte *et al*., 2010). Uma visão tradicional postula que os dinossauros, com sua endotermia e postura ereta, possuíam metabolismos mais acelerados, conferindo maior rapidez e capacidade adaptativa em relação aos seus competidores (Bakker, 1968;1971; 1972; Charig, 1972).

Tal modelo, porém, foi classicamente questionado por Benton (1983; 1986ª, 1986b) que argumentou que as mudanças faunísticas durante o Triássico, incluindo o declínio de grupos abundantes como os rincossauros, teriam sido determinantes para a emergência dos dinossauros. O modelo tradicional também se tornar difícil de sustentar perante levantamentos recentes realizados por Brusatte e colaboradores (2008), que revelam que membros da linhagem crocodiliana eram mais diversos e díspares durante todo o período, dominando as faunas terrestres, enquanto os dinossauros compunham somente pequenas frações dos ecossistemas, inviabilizando, assim, uma visão de exclusão competitiva, e corroborando um caráter de contingência histórica.

O término da predominância dos pseudossuquídeos viria somente após a transição Triássico-Jurássico (T-J), marcada por um evento de extinção em massa de grandes proporções, que dizimou cerca de 80 % de todas as espécies viventes (Sepkoski, 1993), com autores estimando que até 42% de todos os tetrápodes terrestres tenham perecido (Olson *et al*., 1987). Ambos os grupos, dinossauros e pseudossuquídeos, sofreram perdas, porém este último foi particularmente atingido, com somente um único clado, os Crocodylomorpha, atravessando esse limite e diversificando-se no Jurássico e Cretáceo (Toljagic´& Butler, 2013; Irmis, Nesbitt & Sues, 2013; Sues, 2019).

### 1.3) – Crocodylomorpha

Os primeiros crocodilomorfos surgiram durante o Triássico Tardio, e têm como seu representante mais antigo conhecido o *Trialestes romeri* Reig 1963, da Formação

Ischigualasto, Carniano-Noriano da Argentina (Lecuona *et al*., 2016). Tais formas basais eram marcadas por seus esqueletos apendiculares gráceis, duas fileiras paramediais de osteodermos e postura graviportante (Parrish, 1987), sendo possivelmente faunívoros cursoriais, registrando uma aquisição gradual de características crocodilianas com táxons cada vez mais derivados (Benton, 2005; Irmis, Nesbitt & Sues, 2013).

Apesar da maior parte das formas descritas serem de pequeno porte, como *Dromicosuchus* (Sues *et al*., 2003) e *Sphenosuchus* (Walker, 1990), há registro de um táxon de grande porte, *Carnufex carolinensis* (Zanno *et al*., 2015), de pelo menos 3 metros de comprimento do Carniano da Carolina do Norte (EUA). Dentre as sinapomorfias mais comumente citadas para o clado estão: (1) a tendência de perda da cinese craniana, com a fusão dos ossos do basicrânio; (2) carpais e coracóides alongados; (3) deslocamento anterior das porções dorsais do quadrado e quadradojugal, de modo a contatar esquamosal, e (4) processo lateral do esquamosal suspenso sobre a região infratemporal (Clark *et al*., 2000; Clark *et al*., 2004; Benton, 2005; Pol *et al*., 2013) (**figura 3**).

Assim como definido por Sereno *et al*. (2005) e Nesbitt (2011), estabelecendo o grupo pelo ramo, Crocodylomorpha consiste do clado mais inclusivo que contém *Crocodylus niloticus* Laurenti 1768, porém não *Raiusuchus tiradentes* Huene 1942, *Poposaurus gracilis* Mehl 1915, *Gracilisuchus stipanicicorum* Romer 1972, *Prestosuchus chiniquensis* Huene 1942, ou *Aeotosaurus ferratus* Fraas 1877. Sendo assim, um grupo de crocodilomorfos basais denominados ‘Sphenosuchia’ (Bonaparte, 1972), não formariam um agrupamento natural, mas uma sucessão parafilética de táxons progressivamente mais derivados em relação à Crocodyliformes (Benton & Clark, 1988; Parrish, 1991; Clark *et al*., 2001; Clark & Sues, 2002; Clark *et al*., 2004; Nesbitt, 2011; Lecuona *et al*., 2016).

Algumas publicações, porém, ainda recuperam um Sphenosuchia monofilético (Sereno & Wild, 1992; Wu & Chatterjee, 1993; Sues *et al*., 2003). Curiosamente, tais formas basais persistiram até o Jurássico Médio, representadas por um táxon chinês denominado *Junggarsuchus sloani* Clark *et al*. 2004.

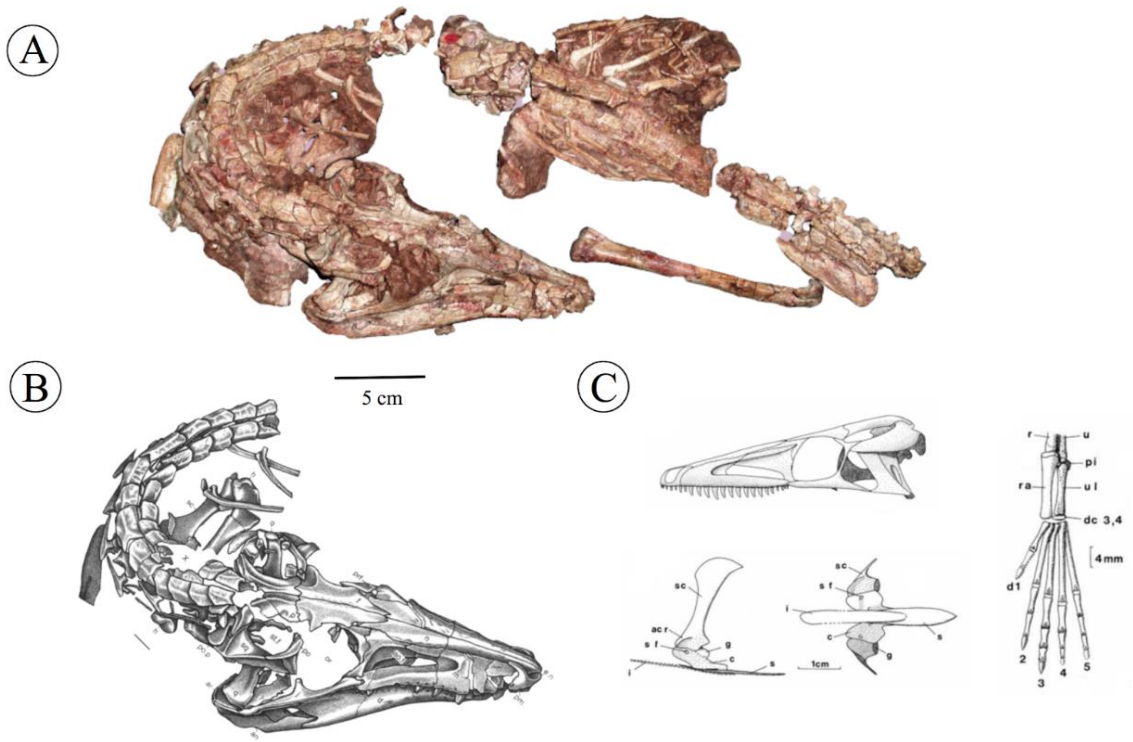


**Figura 3. A e B) – *Dromicosuchus grallator*, um crocodilomorfo não-crocodiliforme do Carniano dos EUA. Foto do holótipo e desenho esquemático representando a região dorsal anterior e crânio. Retirado de Sues et al. (2003). Notar fileira dupla parasagital de placas dérmicas, além de cabeça do fêmur ortogonal ao comprimento maior do mesmo, adaptação cursorial. C) – Desenho esquemático de *Terrestresuchus gracilis* Crush 1984, exemplificando o plano corporal grácil e outras características de membros basais de Crocodylomorpha. Sinapomorfias destacadas: (1) barra suspensa sobre a região temporal; (2) deslocamento anteroposterior do quadrado e quadradojugal, em detalhe à direita; (3) Coracóides longitudinalmente alongados e (4) Carpais (Ulnar e Radial) alongados. Adaptado de Crush (1984).**

### 1.4) – Crocodyliformes

Seguindo a definição de clado baseada no nó de Sereno *et al*. (2001), os crocodyliformes formam o clado mais inclusivo incluindo *Protosuchus richardsoni* Brown 1933, *Crocodylus niloticus* Laurenti 1768, seu ancestral em comum mais recente e todos os seus descendentes. As sinapomorfias que suportam os crocodyliformes estão concentradas no basicrânio, como a fusão e consolidação do crânio com um todo, que ganha um caráter cada vez mais acinético (Pol *et al*., 2013).

A formais mais basais de crocodiliformes juntas compõe o que Mook (1934) denominou de ‘Protosuchia’ (**figura 4**). Os protossúqueos, porém, foram repetidamente recuperados nas filogenias como parafiléticos (Pol *et al*., 2004; Fiorelli & Calvo, 2007; Clark, 2011; Buscalioni, 2017), e hoje são reconhecidas ao menos três famílias, Protosuchidae, Gobiosuchidae, Shartegosuchidae, além do gênero *Hsisosuchus*, que é grupo irmão deste último clado.

Protosuchidae representa, de fato, a primeira radiação de crocodiliformes, apresentando uma ampla distribuição geográfica, com táxons do Triássico da Patagônia e do Jurássico Inferior do Meio Oeste dos Estados Unidos (Brown, 1933; Martinez *et al*., 2019). Gobiosuchidae, apesar de basal, ocorre essencialmente no Cretáceo Tardio da Mongólia e Espanha (Buscalioni, 2017). Por fim, Shartegosuchidae é um clado Laurásico, ocorrendo no Jurássico e início do Cretáceo dos EUA, Rússia e Mongólia, enquanto que *Hsisosuchus* contém três espécies, todas chinesas (Young & Chow, 1953; Gao, 2001; Peng & Shu, 2005).

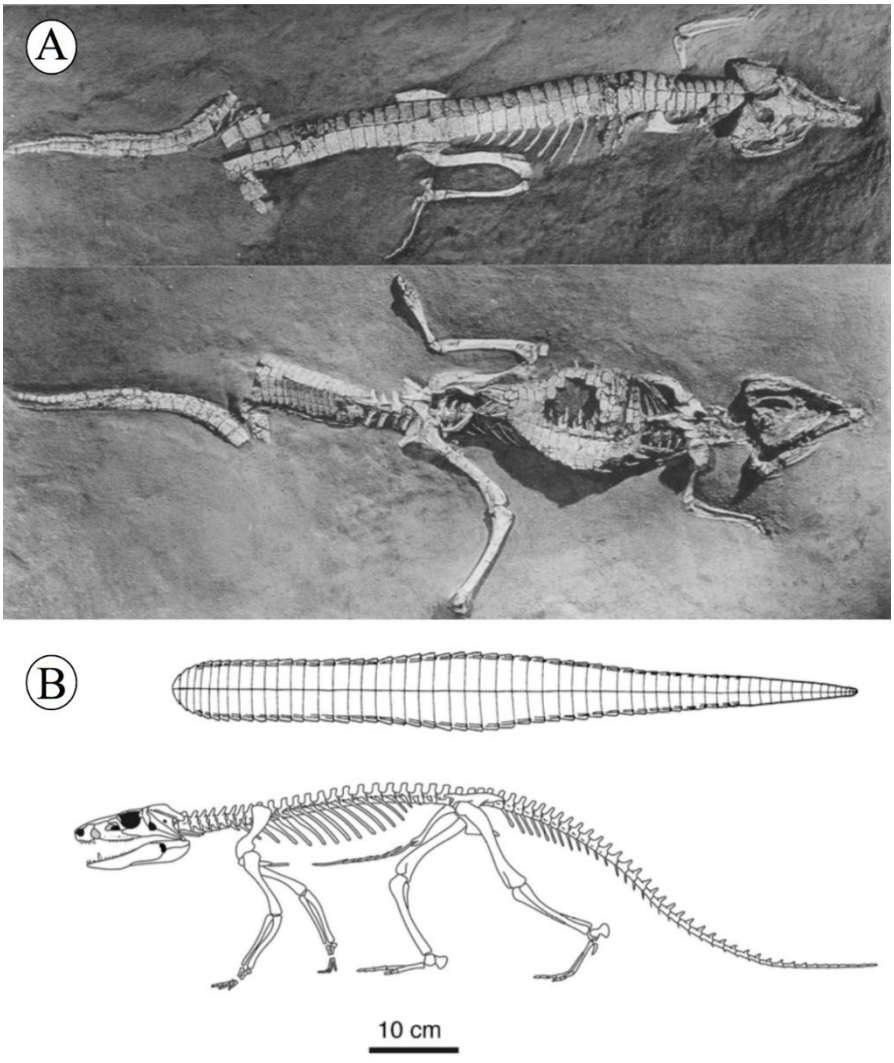


**Figura 4. Plano corporal de Protosuchidae, a primeira irradiação de crocodiliformes. A) – holótipo de *Protosuchus richardsoni*, retirado de Colbert & Mook (1951), em vista dorsal e ventral. B) - reconstrução do esqueleto articulado e em posição de vida, incluindo escudo dorsal de osteodermos. Retira de Sues (2019) e previamente adaptada de Frey (1988).**

Buscalioni (2017) revisou o que potencialmente são uma série de especializações de crocodiliformes basais, incluindo redução do tamanho corporal, um encurtamento do crânio atribuído a processos braquiocefálicos, ampliação do teto craniano, hiperdesenvolvimento de ossos dermais, além de modificações no pós-crânio que marcariam a transição para Mesoeucrocodylia.

### 1.5) – Mesoeucrocodylia

Excluindo as formas basais, o clado mais abrangente dentro de crocodiliformes é denominado Mesoeucrocodylia (**figura 5**), originalmente erguido por Whetstone & Whybrow (1983). A formação de um palato secundário extensivo, constituído pelos maxilares e palatinos, a presença de dois palpebrais bem desenvolvidos, teto craniano plano, quadrado pneumatizado e em contato dorsal com o lateroesfenóide, são algumas das novidades evolutivas citadas por Benton (2005) que diferenciam os membros de deste clado. Pol *et al*. (2013) ressaltam a importância da emergência do crânio completamente acinético em Mesoeucrocodylia, onde o palato, basicrânio, caixa craniana e quadrado estão inteiramente fusionados, o que poderia ter sido um passo evolutivo importante para o surgimento da grande disparidade morfológica vista durante o Mesozóico.

Um problema recorrente na filogenia dos Mesoeucrocodylia diz respeito ao posicionamento do clado de crocodilomorfos marinhos Thalattosuchia (Wilberg, 2015). Estes já foram recuperados em sua base, como uma primeira irradiação (Young & Andrade, 2009; Young *et al*., 2012), dentro de Neosuchia (Turner & Sertich, 2010), ou até mesmo fora de Crocodyliformes (Pol & Gasparini, 2009; Wilberg, 2015).

Dois grandes clados dentro de Mesoeucrocodylia dividem a evolução dos Crocodyliformes em uma dicotomia principal, que marca duas tendências evolutivas distintas, os Neosuchia, de onde se originaram os crocodilianos atuais, representados essencialmente por formas semiaquáticas, ou marinhas no caso dos Dyrosauridae, com crânios dorsoventralmente achatados e órgãos sensoriais dorsalmente posicionados, e os Notosuchia, grupo de crocodiliformes terrestres gondwânicos de pequeno a grande porte, que evoluíram uma alta disparidade de hábitos alimentares, com formas possivelmente hipercarnívoras e herbívoras (Gasparini, 1971). Tais grupos serão detalhados nas sessões seguintes.

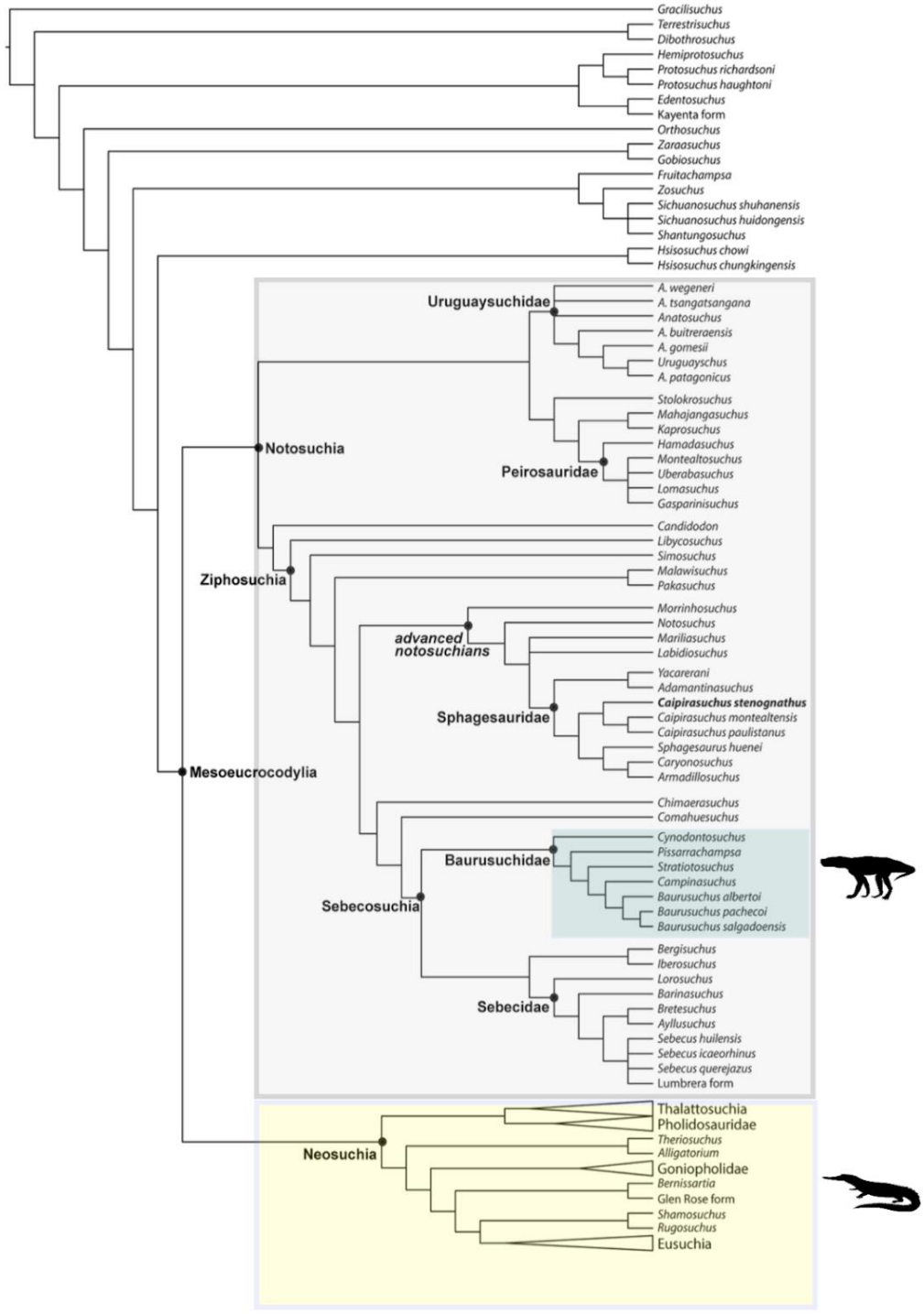


**Figura 5. Cladograma de consenso estrito de Crocodyliformes modificado de Pol e colaboradores (2014). Notar a duas principais linhagens de Mesoeucrocodylia, os Notosuchia (em cinza) e os Neosuchia (em amarelo). Baurusuchidae, objeto de estudo deste projeto, está destacado em azul.**

### 1.6) - Neosuchia

Os neossúquios integram todos os crocodiliformes mais proximamente aparentados com *Crocodylus niloticus* do que com *Notosuchus terrestris* (Sereno *et al*., 2001). Excluindo Thalattosuchia, uma irradiação marinha, as formas basais mais recorrentes nas filogenias de Neosuchia são os membros de Tethysuchia (**figura 6ª e B**) (Buffetaut, 1982). Estes possuem representantes no Jurássico e Cretáceo da África e América do Sul (Fortier, Perea & Schultz, 2011), e seus integrantes incluem a família Pholidosauridae, o gênero Sarcosuchus (para uma revisão detalhada, ver Souza *et al*., 2019), e os Dyrosauridae, que, além de marcar uma segunda migração ao ambiente marinho dentro de Crocodylomorpha, são um dos três clados deste último (juntamente com Sebecosuchia e Crocodylia) que sobreviveram ao evento K-Pg (Barbosa *et al*., 2008; Bronzati *et al*., 2015).

A transição de Neosuchia para o clado mais restrito e próximo dos crocodilianos atuais, denominado Eusuchia, é caracterizada pela evolução efetiva de hábitos semiaquáticos e de predação de emboscada, com algumas importantes exceções (Pristichampsidae, Brochu, 2013). Resumidamente, tal transição foi marcada pelo surgimento dos seguintes caracteres: (1) crânios platirostrais (achatados dorso-ventralmente); (2) desenvolvimento de vértebras procélicas; (3) segmentação do escudo parasagital, e (4) inclusão completa das coanas nos pterigoides (Benton, 2005; Salisbury *et al*., 2006).

Uma série de táxons relativamente completos, alguns descobertos recentemente, registram a evolução das características supracitadas e a aquisição gradual de caracteres classicamente associados ao grupo coronal Crocodylia. Os Goniopholididae, por exemplo, marcam uma família de neossúquios basais e possivelmente um grupo irmão de Tethysuchia (de Andrade *et al*., 2011; Souza *et al*., 2019), enquanto *Bernissartia fagesii* Dollo 1883, do Cretáceo Inferior da Laurásia, é considerado um neossúquio proximamente relacionado à Eusuchia, e superficialmente apresentaria anatomia muito próxima a estes.

As duas espécies de Susisuchus (Salisbury *et al*., 2003; Fortier & Schultz, 2009) e também o *Isisfordia duncani* (Salisbury *et al*., 2006) seriam os mais basais eussúquios já encontrados, apresentando morfologia extremamente similar aos membros do grupo coronal, porém ainda com um procelia incipiente e um escudo dorsal não totalmente desenvolvido. Imediatamente fora de Crocodylia, enfim, temos táxons como *Hylaeochampsa vectiana* Owen 1874, do Grupo Wealden, Cretáceo

Inferior de Ilha de Wight, Reino Unido. Este eussúquio já apresentava palato com a estruturação derivada das coanas (Clark & Norell, 1992) e evidencia um surgimento Laurásico para o grupo coronal.

As principais linhagens de crocodilianos atuais, sendo estas as três famílias viventes, já haviam se divergido ao final do Mesozóico (**figura 6C e D**), e seu registro não controverso mais pretérito consiste de *Portugalosuchus azenhae* (Mateus *et al*., 2019), e alligatoróides do Campaniano da América do Norte, como *Leidyosuchus canadensis* e *Brachychampsa sealeyi* (Williamson, 1996; Brochu, 1997; Brochu, 2003). *Brachychampsa* seria mais derivado que *Leidyosuchus*, sendo um gênero basal dentro de Caimaninae (Bona *et al*., 2018). O gênero *Deinosuchus* inclui formas de grande tamanho corporal e possivelmente predadores de topo do Campaniano da América do Norte, sendo de importante menção uma vez que já foram classificados como crocodilídeos e, mais recentemente, alligatoróides (Colbert & Bird, 1954; Brochu, 1999; Knight & Schwimmer, 2005).

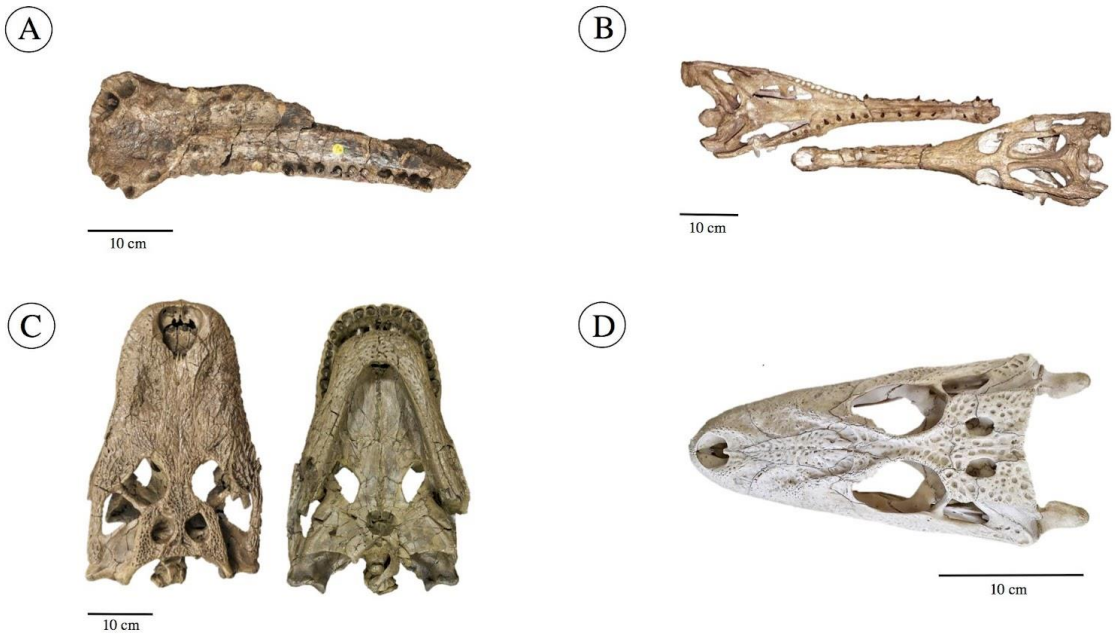


**Figura 6. Neossúquios representados por táxons mais basais (A e B) e mais derivados (C e D). A) – Sínfise mandibular de *Sarcosuchus hartti* (Tethysuchoideia) da Bacia do Recôncavo (Cretáceo Infeiror). Retirado e adaptado de Souza *et al*. (2019). B) – Crânio e mandíbula completos de *Guarinisuchus munizi*, um Dyrosaurídeo (Tethysuchoidea), coletado na Formação Maria Farinha, Bacia Paraíba (Paleoceno). Retirado de Barbosa *et al*. (2008). C) – *Brachychampsa montana* Gilmore (1911), um membro fóssil do grupo coronal Crocodylia (Alligatoroidea) do Cretáceo Superior do América do Norte (Campaniano – Maastrichtiano). Imagem © 2014 Dave Strauss. D) – Crânio de *Melanosuchus niger*, um caimaníneo moderno comum do norte da América do Sul. Foto pelo autor de espécime de coleção didática da FUP-UnB.**

Os Thoracosauria, antes considerados Gavialóides presentes no Maastrichtiano (Brochu, 2004), tiveram recentemente sua afinidade filogenética questionada, agora compreendidos por Lee & Yates (2018) como um grupo basal à Crocodylia e representando um exemplo extremo de convergência, o que corrobora uma radiação mais recente para Gavialidae. Por fim, os Crocodilóides têm um registo escasso no Cretáceo, de forma que somente *Prodiplocynodon langi* Mook 1941, da Formação Lance, Cretáceo tardio do Wyoming, seja conhecido.

A seguir, os crocodilianos propriamente ditos e sua história evolutiva são discutidos, com ênfase para Alligatoridae, uma vez que todas as seis espécies de uma de suas subfamílias, Caimaninae, ocorrem amplamente no território nacional (RAN/ICMBio).

### 1.6.1) – Crocodylia: Alligatoridae, Crocodylidae, Gavialidae

Contrariamente ao entendimento popular, os crocodilianos compõem um clado relativamente recente (Campaniano ao Holoceno), atualmente composto de três famílias (**figura 7**), que possui uma rica história evolutiva com cerca de cinco vezes mais táxons fósseis do que viventes (Brochu, 2003). Uma das principais divisões dentro de Crocodylia ocorre na separação entre os clados Gavialoidea e Brevirostres, este último, *sensu* Brochu (2003), é definindo como o último ancestral em comum de *Alligator mississippiensis*, *Crocodylus niloticus* e todos os seus descendentes, contendo, então, tanto Alligatoroidea quanto Crocodyloidea.

O gênero *Borealosuchus* é proximamente relacionado à Brevirostres, e ocorre do Cretáceo Superior ao Eoceno da América do Norte, exibindo uma morfologia craniana generalizada e plesiomórfica para o clado, caraterizada por um rostro relativamente curto, afinando anteriormente, presença de entalhe entre a pré-maxila e maxila, além de oclusão dos dentes do dentário medialmente em relação aos maxilares (Brochu, 2003). Deste padrão, evoluíram as diversas formas brevirostrinas e mesorostrinas que caracterizam a maioria dos alligatorídeos e crocodilídeos.

Alligatoridae é subdividida em duas subfamílias (Alligatorinae e Caimaninae), que abarcam todas as oito espécies viventes, sendo duas pertencentes ao gênero *Alligator* (*A. mississippiensis e A. sinensis*), presentes no sudeste dos E.U.A e no leste da China, dois caimaníneos do gênero *Paleosuchus* (*P. palpebrosus* e *P. trigonatus*), três do gênero *Caiman* (*C. crocodilus, C. yacare e C. latirostris*) e, por fim, *Melanosuchus niger*, que difere dos demais devido ao seu grande tamanho corporal.

Todos as seis espécies de caimaníneos viventes ocorrem no Brasil, e algumas delas estendem sua distribuição a outros países vizinhos, como Argentina, Paraguai, países amazônicos, e porção sul da América Central.


**Figura 7. Exemplos de membros viventes da ordem Crocodylia. A) – O aligatorídeo (Caimaninae) *Caiman crocodilus*, fotografado pelo autor no Zoológico de Brasília (Fundação Jardim Zoológico de Brasília). B) – Espécie de crocodilídeo recentemente reconhecida *Crocodylus halli*, da Nova Guiné. Retirado de Murray *et al*. (2019). C) – *Gavialis gangeticus*, única espécie remanescente da família Gavialidae. Foto de IUCN Red List (*International Union for Conservation of Nature*) – iNaturalist. D) – *Tomistoma schlegelii*, forma longirrostrina de afinidade incerta. Sua morfologia indica proximidade com crocodilídeos, enquanto dados moleculares apontam para Gavialidae. Retirado de ADW (*Animal Diversity Web*) – Jerry Gingerich.**

As sinapomorfias que sustentam as subfamílias supracitadas são discutidas em detalhe por Brochu (1999), e, para Alligatorinae, é possível destacar: (I) projeção anterodorsal dos nasais, eventualmente formando um septo completo no gênero *Alligator*; (II) dentário recurvado entre o terceiro e décimo alvéolos. Caimaninae, por sua vez, é suportado, dentre vários caracteres, por: (I) exclusão do esplenial da sínfise mandibular; (II) exoccipitais compondo as tuberosidades do basioccipital através do envio de processos ventrolaterais delgados; (III) exclusão do parietal da margem posterior do teto craniano.

Apesar de sua provável origem no hemisfério norte, a família Alligatoridae teve, e ainda retém, sua maior diversidade de espécies na América do Sul, através de sua

irradiação de cenozóica de caimaníneos, que incluiu desde pequenas espécies durófagas, que mantiveram o estado plesiomórfico de globidonta (clado que compreende formas mais basais e o último ancestral em comum entre caimaníneos e aligatoríneos), até os clássicos exemplos de gigantismo do Mioceno Amazônico como *Purussaurus* e *Mourasuchus* (Aguilera *et al*., 2006; Bona *et al*., 2018; Cidade *et al*., 2017; 2019; Souza-Filho *et a*l., 2019). Tais táxons possivelmente formavam uma complexa cadeia trófica no grande sistema lacustre-fluvial Pebas/Solimões (Salas-Gismondi *et al*., 2015).

Os crocodilóides, formas mais próximas de *Crocodylus niloticus* do que de *Alligator mississippiensis* e *Gavialis gangeticus*, após um registro pontual durante o Cretáceo, são comuns no Cenozóico do Hemisfério Norte, com membros do gênero *Asiatosuchus* ainda possuindo a morfologia geral dos Brevirostres (Brochu, 2003). A família Crocodylidae, clado apical dentro de Crocodyloidea, é definida como o ancestral em comum mais recente de *Crocodylus niloticus*, *Osteolaemus tetraspis* e *Tomistoma* schlegelii, sendo composta das subfamílias Tomistominae, hoje monoespecífica, Crocodylinae, e a recentemente reconhecida Osteolaeminae (Brochu, 1997; 2003; 2007). Esta última possivelmente inclui formas fósseis atípicas como *Voay robustos* e suas cristas protuberantes nos esquamosais, e *Euthecodon* (Brochu, 2017), excepcional devido a seu rostro alongado, diastemas grandes e alvéolos proeminentes (Brochu, 2007). Curiosamente, alguns membros fósseis do gênero *Crocodylus*, como *C. thorbjarnarsoni*, da Bacia Turkana (Plioceno-Pleistoceno) do Quênia, atingiram dimensões muitos superiores as formas viventes (Brochu & Storrs, 2012).

Crocodylidae é o clado mais especioso dentro de Crocodylia atualmente, com cerca de 15 espécies válidas (Grigg, 2015). Recentemente, estudos de genética de populações têm revelado uma diversidade velada de crocodilídeos onde previamente se reconhecia somente uma única espécie (Murray *et al*., 2019). Dentro do gênero *Mecistops*, por exemplo, foram reconhecidas duas espécies, *M. cataphractus* e *M. leptorhynchus*, separados geograficamente pela Linha vulcânica dos Camarões (Cameron Volcanic Line), marcando um possível evento de especiação alopátrica (Shirley *et al*., 2018).

Por fim, gavialóides e gavialídeos são representados no registro fóssil por uma miríade de formas que tinham uma distribuição geográfica bem mais ampla que nos dias atuais, começando no Maastrichtiano dos EUA (Brochu, 2004) e culminando nas

formas endêmicas da América do Sul durante o Mioceno, como os gigantescos membros do gênero *Gryposuchus* (Souza *et al*., 2018).

### 1.7) – Notosuchia

Outra linhagem principal dentro de Mesoeucrocodylia é formada pelo notossúquios, clado primeiramente erguido por Gasparini (1971), de modo a acomodar táxons gondwânicos de hábitos terrestres, contendo, originalmente, os gêneros *Notosuchus*, *Sphagesaurus*, *Uruguaysuchus* e *Araripesuchus*.

Com a descoberta de um número cada vez maior de espécies nas últimas duas décadas (Pol & Leardi, 2015), Notosuchia aumentou substancialmente de tamanho (Buckley *et al*., 2000; Carvalho & Bertini, 1999; Carvalho *et al*., 2004; 2007; Larsson & Sues, 2007; Martinelli *et al*., 2018; Nobre & Carvalho, 2006; O'connor *et al*., 2010; Sereno & Larsson, 2009, Montefeltro *et al*., 2011), e, nas filogenias mais recentes, engloba principalmente Uruguaysuchidae, Peirosauridade, "notossúquios avançados'' (Notosuchidae + Sphagesauridae), além de Baurusuchidae e Sebecidae (Pol *et al*., 2012; Iori *et al*., 2016; Martinelli *et al*., 2018).

Os notossúquios despertam a curiosidade científica principalmente por sua terrestrialidade e cursorialidade (Tavares *et al*., 2017), além de sua substancial variedade de hábitos alimentares, com adaptações cranianas e dentárias correspondentes (**figura 8**), com táxons possivelmente omnívoros/herbívoros e carnívoros de topo de cadeia (Pol *et al*., 2003; Riff & Kellner, 2011). Apesar de vários registros e espécies descritas em países como Argentina, Bolívia, Venezuela, Madagascar e Paquistão, o número de táxons e a disparidade dos mesmos na Bacia Bauru, no centro-sudeste do Brasil, amplamente supera seus pares internacionais, tornando esta região do país um *hotspot* de diversidade de crocodilomorfos durante o Neocretáceo (Riff *et al*., 2012).

Embora fragmentário, consistindo apenas de pré-maxila e a porção anterior do dentário esquerdo, *Razanandrongobe sakalavae* Sasso *et al*. 2017, do Jurássico Médio (Bathoniano) de Madagascar, compreende o registro mais antigo para Notosuchia (FAD), enquanto *Barinasuchus arveloi* Paolillo & Linares 2007, um sebecídeo do Mioceno da Venezuela, marca a última aparição para o clado (LAD). Os notossúquios irradiaram substancialmente durante o Eocretáceo, marcando uma diversificação de crocodilomorfos terrestres, em paralelo com a irradiação de neossúquios, que tem uma origem mais pretérita (Bronzati *et al*., 2015). Tais formas

do Eocretáceo incluem uruguayssuquídeos atípicos como o platirostral *Anatosuchus minor* (Sereno & Larsson, 2009), as espécies do gênero *Araripesuchus* (Price, 1959), pequenos zifossúquios basais com dentição heterodonte como *Pakasuchus* e *Malawisuchus*, além do Peirossaurídeo *Hamadasuchus rebouli* (Larsson & Sues, 2007).

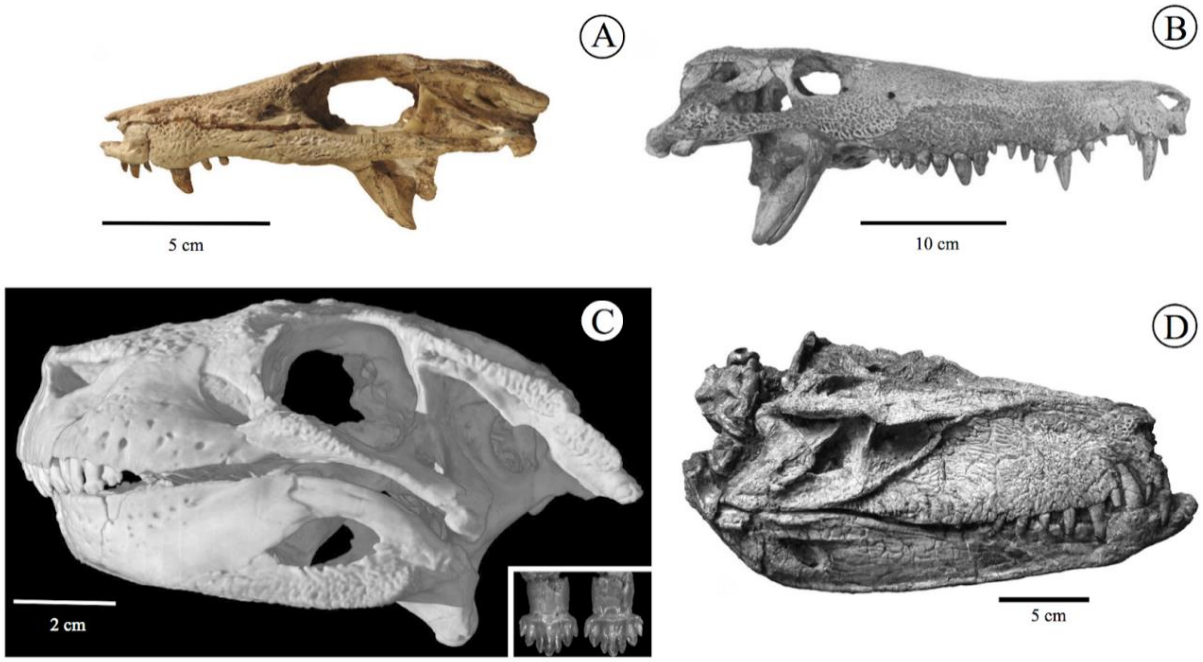


**Figura 8. Amostra da diversidade de notossúquios. A) – Crânio de *Araripesuchus wegeneri*, um Uruguaysuquídeo da Formação Elrhaz, Cretáceo Inferior da República do Níger. Adaptado de Sereno & Larsson (2009). B) – *Hamadasuchus rebouli*, pertencente ao clado Peirosauridae, em vista lateral direita. Coletado nas Kem Kem Beds (Albiano – Cenomaniano) do Marrocos. Retirado e adaptado de Larsson & Sues (2007). C) – Tomografia computadorizada de crânio e mandíbula de *Simosuchus clarki*, um zifossúquio basal altamente especializado, possivelmente herbívoro, com dentição multicuspidada (ver detalhe, canto inferior direito). Imagem de Digimorph.org, produzida por Kley e colaboradores (2010). D) – Espécime ainda não descrito de *Sebecus* sp., um sebecossuquídeo da Formação Lumbrera, Eoceno da Argentina.**

Ao final do Cretáceo encontramos a maior diversidade de notossúquios (Riff *et al*., 2012, Pol & Leardi, 2015), abrangendo grandes esfagessaurídeos com escudos dérmicos hiperdesenvolvidos, como *Armadillosuchus arrudai* (Marinho & Carvalho, 2009; Cunha *et al*., 2020), pequenos notossúquios avançados como *Mariliasuchus* e *Adamantinasuchus*, diversos peirossaurídeos como *Uberabasuchus*, *Montealtosuchus* e *Pepesuchus*, além das cerca de nove espécies de baurussuquídeos.

A coexistência de um alto número de espécies simpátricas de crocodilomorfos em uma única bacia, levanta uma série de perguntas relacionadas a estrutura trófica

de tal ecossistema, tendo em vista a falta de análogos modernos. Felizmente, evidências de relação de predação direta (Godoy *et al*., 2014) e promissoras novas técnicas de reconstrução de cadeias tróficas (Cardia *et al*., 2018) poderão dar luz a tal questão. Adicionalmente, o contexto idiossincrático da Bacia Bauru, com sua alta diversidade de crocodilomorfos, levou alguns autores a hipotetizar que os mesmos estariam se aproveitando da vacância de nichos ecológicos tradicionalmente preenchidos por dinossauros (Riff & Kellner, 2011; Bandeira *et al*., 2018).

As relações filogenéticas entre diferentes clados de notossúqueos, apesar da recuperação de uma série de topologias instáveis e variáveis, parece ter estabilizado em uma configuração padrão na maioria dos trabalhos mais recentes (Pol *et al*., 2012; 2014; Fiorelli *et al*., 2016; Martinelli *et al*., 2018). Contudo, diversas incertezas ainda persistem, principalmente aquelas relacionadas à posição de Peirosauridae, podendo ser mais próxima a linhagem de Neosuchia (Larsson & Sues, 2007) ou Notosuchia (Pol *et al*., 2014). A afinidade de formas como *Mahajangasuchus*, *Kaprosuchus* e outras aparentadas à *Trematochampsa* também é controversa (Buffetaut, 1991; Sereno & Larsson, 2009).

### 1.7.1) – Peirosauridae

Esta família de notossúquios predatórios de pequeno a médio porte erguida por Gasparini (1982) apresenta um rico registro com ampla distribuição geográfica (**figura 9**), ocorrendo do Albiano ao Maastrichtiano da África (Larsson & Sues, 2007; Sertich & O'connor, 2014), Argentina (Gasparini, Chiappe & Fernandez, 1991; Martinelli *et al*., 2012; Barrios *et al*., 2016; Lio *et al*., 2016; Filippi *et al*., 2018; Lamanna *et al*., 2019; Coria et al., 2019) e Brasil (Price, 1955; Carvalho et al., 2004; 2007; Campos *et al*., 2011).

Assim com outros crocodiliformes terrestres, possuíam uma postura parasagital, corroborada por estudos morfofuncionais (Tavares *et al*., 2017), além de um escudo dérmico bem desenvolvido (**figura 9B**), que se estendia até a região ventral e envolvia totalmente a cauda em algumas espécies (Fiorelli, 2010; Tavares *et al*., 2015). O caráter da preservação de alguns espécimes de peirossaurídeos, como o relativamente completo e articulado *Uberabasuchus terrificus*, levanta a possibilidade dos mesmos terem facilitado a sua preservação futura através de hábitos fossoriais ou pela construção de *gator holes* (Vasconcellos & Carvalho, 2006).

Segundo Gasparini, Chiappe & Fernandez (1991) e autores subsequentes, suas sinapomorfias incluem: (1) um processo maxilar em formato de cunha penetrando dorsoanteriormente a pré-maxila; (2) um pré-maxila curta em vista ventral; (3) 14 a 15 dentes na maxila com diferenciação, sendo os mais posteriores globulares; (4) dentes maxilares ultrapassam a margem anterior da fenestra suborbital; (5) nasais longos e uniformemente espessos ao longo do rostro; (6) crista medial e protuberâncias laterais proeminentes no basioccipital.

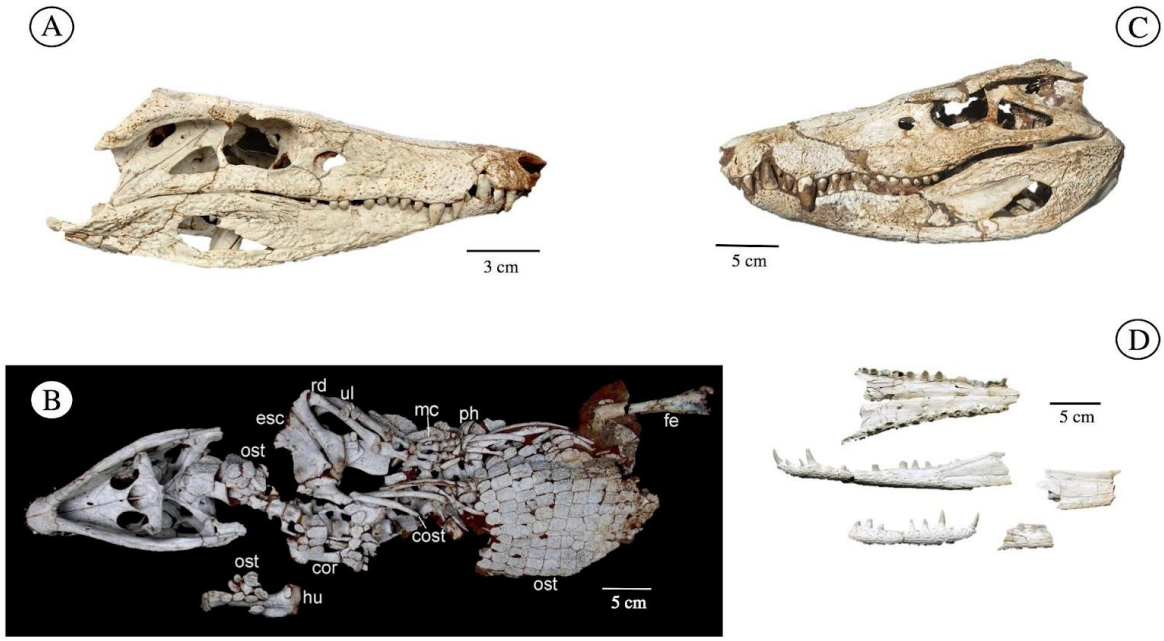


**Figura 9. Peirosauridae representada aqui por três táxons. A) – *Montealtosuchus arrudacamposi*, crânio em vista lateral direita. O contato em 'cunha' entre a pré-maxila e a maxila, típicos dos peirossaurídeos, pode ser observado. Foto cedida por Rodrigo Santucci (UnB). B) – Pós-crânio em vista ventral, com destaque para o escudo dérmico bem desenvolvido. Adaptado de Tavares *et al*. (2017). C) – Crânio e mandíbula completos de *Hamadasuchus rebouli* recentemente descobertos nas Kem Kem Beds (Cretáceo Inferior, Marrocos). Espécime não descrito, apresentado em Ibrahim *et al*. (2020). D) – *Pepesuchus deiseae*, rostro em vista palatal e porção anterior dos ramos direito e esquerdo dos dentários em vista lateral. Foto D obtida pelo autor.**

Desde sua proposição por Gasparini (1982), Peirosauridae não têm apresentado uma posição estável dentro das filogenias, contudo, utilizando-se a matriz de Pol *et al*. (2014), estes são posicionados como grupo irmão de Uruguaysuchidae, dentro de Notosuchia. Com resultados distintos, Geroto & Bertini (2018) obtiveram um posicionamento fora de Notosuchia, como grupo irmão da família Sebecidae, com formas como *Pepesuchus deiseae*, *Itasuchus jesuinoi, Caririsuchus*

*camposi* e *Barreirosuchus franciscoi* compondo uma subfamília denominada Pepesuchinae, com uma diagnose revisada disponibilizada para a família.

### 1.7.2) – Sphagesauridae

Os esfagessaurídeos formam um clado endêmico de notossúquios avançados de pequeno a médio porte da América do Sul, mais particularmente da Bacia Bauru, no sudeste brasileiro (Pol *et al*., 2003). Após a descrição de *Sphagesaurus huenei* por Price (1950), apesar da escassez do material, que consistia apenas de alguns dentes, ergueu-se uma família monotípica para o gênero (Sphagesauridae Kuhn, 1968). Hoje, após décadas de coleta, a diversidade e a disparidade morfológica conhecida para a família aumentou substancialmente, incluindo pequenos esfagessaurídeos como *Adamantinasuchus navae* (Nobre & carvalho, 2006), passando pelas quatro espécies do gênero *Caipirasuchus* (Andrade & Bertini, 2008; Iori & Carvalho, 2011: Pol *et al*., 2014; Martinelli *et al*., 2018), além de formas de grande porte e com escudos dérmicos muito desenvolvidos, como *Armadillosuchus arrudai* (Marinho & Carvalho, 2009).

Até a descoberta de *Yacarerani boliviensis*, um esfagessaurídeo do Cretáceo da Bolívia (Novas *et al*., 2009), pensava-se que estes notossúquios eram exclusivos da Bacia Bauru, Cretáceo Inferior do Brasil, tal descoberta, porém, em conjunto com outros táxons relacionados à sphagesauridae encontrados na África (O'connor *et al*., 2010), aumentou a distribuição do grupo. Este é um clado conhecido por sua heterodontia avançada, com a presença de dentes especializados incisiviformes, caniniformes e molariformes, por vezes multicuspidados (Novas *et al*., 2009; Montefeltro *et al*., 2009).

O padrão de oclusão dos dentes é peculiar ao clado e alguns táxons proximamente relacionados (ver *Notosuchus terrestris*, Fiorelli & calvo, 2008; Barrios *et al*., 2018), onde as carenas serrilhadas se desenvolvem distalmente nos molariformes maxilares, enquanto os mesmos no dentário possuem carenas mesiais (**Figura 10**).

Andrade & Bertini (2008) destacam, entre outras características únicas do clado, pré-maxilas reduzidas carregando pelo menos um par de caniniformes hipertrofiados, de seis a sete dentes maxilares, todos molariformes, e a implantação oblíqua dos mesmos. Em Pol e colaboradores (2014), o monofiletismo da família é suportado por sete sinapomorfias, algumas aqui ressaltadas: (1) superfície do esmalte

dos dentes maxilares e dentários posteriores é coberta por pequenas protuberâncias arredondadas; (2) os dentículos das carenas são unidos por uma crista apicobasal; (3) um vão entre os foramens neurovasculares anteriores e posteriores na superfície lateral da maxila. Outros caracteres são referentes a relação de contato entre elementos do basicrânio.

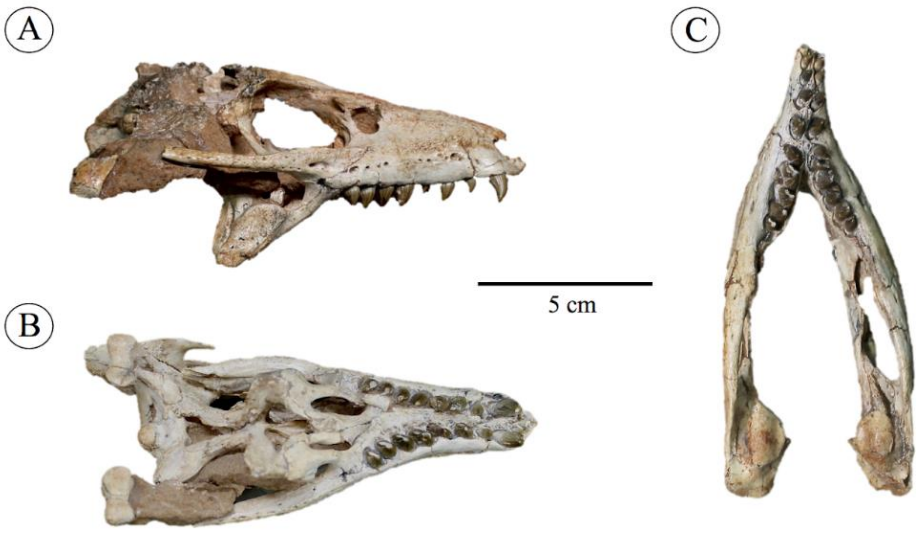


**Figura 10. *Caipirasuchus stenognathus*, um típico esfagessaurídeo da Formação Adamantina, Bacia Bauru, Brasil. Notar o padrão de oclusão oblíquo dos molariformes, onde as carenas serrilhadas do dentário e maxila apontam para direções opostas. Foto pelo autor (MZSP-PV 1390).**

Desde sua descoberta inicial por Price (1950), muito se especula a respeito da dieta dos esfagessaurídeos, inferindo-se, através de seu movimento propalinal de mastigação (Pol *et al*., 2003; Iori & Carvalho, 2018) e espessura da dentina (Ricart *et al*., 2019) uma dieta herbívora ou omnívora. Desdobramentos de técnicas geoquímicas recentemente desenvolvidas (Cardia *et al*., 2018), oferecem uma nova perspectiva de testar a herbivoria em esfagessaurídeos de maneira independente de dados morfológicos.

### 1.7.3) – Sebecidae / Sebecossúquios cenozóicos

Compreendendo o único clado de notossúquios remanescente após o evento K-Pg, (Pol *et al*., 2014; Kellner *et al*., 2014), os sebecídeos, assim como seu grupo irmão Baurusuchidae, são marcados por predadores de pequeno, médio e grande

porte, com rostros altos, achatados lateralmente, dentição zifodonte e grandes aberturas das narinas internas (coanas). Tal configuração peculiar levou Simpson (1937) a erguer a família Sebecidae baseando-se nos primeiros materiais de *Sebecus icaeorhinus*, representado por um crânio completo, porém desarticulado, coletado na Formação Sarmiento (Eoceno Médio), na província de Chubut, Argentina (Colbert, 1946).

*Sahitisuchus fluminensis*, do Paleoceno da Bacia do Itaboraí (Kellner *et al*., 2014), Estado do Rio de Janeiro, Brasil, é o registro mais antigo do clado, enquanto *Barinasuchus arveloi*, do Mioceno da Venezuela (Paolillo & Linares, 2007), seria sua última aparição. Apesar de se concentrarem na América do Sul (Simpson, 1937; Colbert, 1946; Gasparini, 1984; 1993; Busbey, 1986; Paolillo & Linares, 2007; Pol *et al*., 2011; 2012) (**figura 11**), sebecídeos apresentam distribuição geográfica mais ampla, tendo sido coletados tanto na Europa, com táxons como *Iberosuchus macrodon* e *Bergisuchus dietrichbergi* (Antunes, 1975; Kuhn, 1968; Ortega *et al*., 1996; Rossmann, *et al*., 2000; ver Martin *et al*., 2015), quanto na África (Buffetaut, 1982; 1986; 1989; Stefanic *et al*., 2020).

A monofilia dos sebecídeos é suportada por uma série de caracteres, que podem mudar de acordo com a matriz utilizada por cada trabalho, neste caso Pol e colaboradores (2011): (1) asas dos pterigóides anteroposteriormente curtas e dorsoventralmente desenvolvidas, em formato de ‘’barra’’; (2) mais de oito dentes maxilares; (3) quadradojugal alcançando a porção lateral dos côndilos articulares do quadrado; (4) maior eixo do quadrado direcionado posteroventralmente, porém defletido lateralmente em relação a região occipital; e (5) porção distal do quadrado lateromedialmente expandida e anteroventralmente achatada.

Gasparini *et al*. (1993), juntamente com a descrição de *Bretesuchus bonapartei*, também realizou um dos primeiros esforços cladísticos para os sebecídeos sul-americanos. É importante, então, citar algumas sinapomorfias que suportam tal clado, mas que não foram recuperadas por Pol *et al*. (2011): (1) nasal convexos; (2) tuberosidades no basioccipital; (3) basiesfenóide não exposto ventralmente; (4) dentes mandibulares procumbentes; (5) processo retroarticular bem desenvolvido; (6) borda ventral do angular ascendente; e (7) borda dorsal do surangular também ascendente.

Outras características importantes presentes em alguns sebecídeos cenozóicos, porém não em todos, incluem: (1) a ocorrência de fenestra antorbital em

táxons europeus (*Iberosuchus* e *Bergisuchus*, ver Rossmann *et al*., 2000); (2) a perda da fenestra mandibular, como em *Sahitisuchus fluminensis* (Kellner *et al*., 2014); (3) desenvolvimento de crista na margem ventral da mandíbula, percorrendo tanto o angular como o dentário (também presente em *Sahitisuchus fluminensis*) e (4) coanas grandes e semicirculares (ocorre na maioria dos táxons com exceção de *Zulmasuchus querejazus*, que, curiosamente, também não apresenta pterigóides anteroposteriormente curtos, ver Paolillo & Linares, 2007).

Assim como outros notossúquios, seu esqueleto pós-craniano apresenta diversas adaptações para a terrestrialidade (Pol *et al*., 2012; 2013). Contudo, alguns táxons como *Sahitisuchus* e *Lorosuchus* poderiam ser parcialmente semiaquáticos, cogitando-se até uma readaptação ao ambiente terrestre após o Paleoceno, com a volta da oreinirrostria (Pol & Powell, 2011; Kellner *et al*., 2014).

O posicionamento filogenético dos sebecídeos dentro de Mesoeucrocodylia têm duas hipóteses principais. Na primeira, estes formariam o clado Sebecia com os peirossaurídeos, porém na base da linhagem Neosuchia (Buffetaut & Marshall, 1991; Larsson & Sues, 2007), enquanto na segunda, formariam um grupo irmão de Baurusuchidae (Sebecosuchia) dentro de Notosuchia (Simpson, 1937, Pol *et al*., 2014). Apesar do compartilhamento de diversos caracteres entre Peirosauridae e Sebecidae, artigos mais recentes tendem a recuperar um sebecosuchia monofilético, enquanto Sebecia monofilético tende a surgir em topologias subótimas (Pol *et al*., 2011).

Por último, a presença continuada de crocodilomorfos terrestres nos faz reavaliar as relações ecológicas das faunas cenozóicas terrestres. A ocupação de nichos de predadores de topo e o gigantismo de alguns sebecídeos, como algumas de suas formas mais recentes como *Barinasuchus* e *Langstonia*, levou Molnar & Vasconcellos (2016) a revisitar a clássica narrativa de uma substituição rápida da fauna mesozóica durante a irradiação dos mamíferos ao longo do Paleógeno e Neógeno, postulando uma predominância continuada dos arcossauros na forma de Sebecídeos e Phorusrhacídeos.

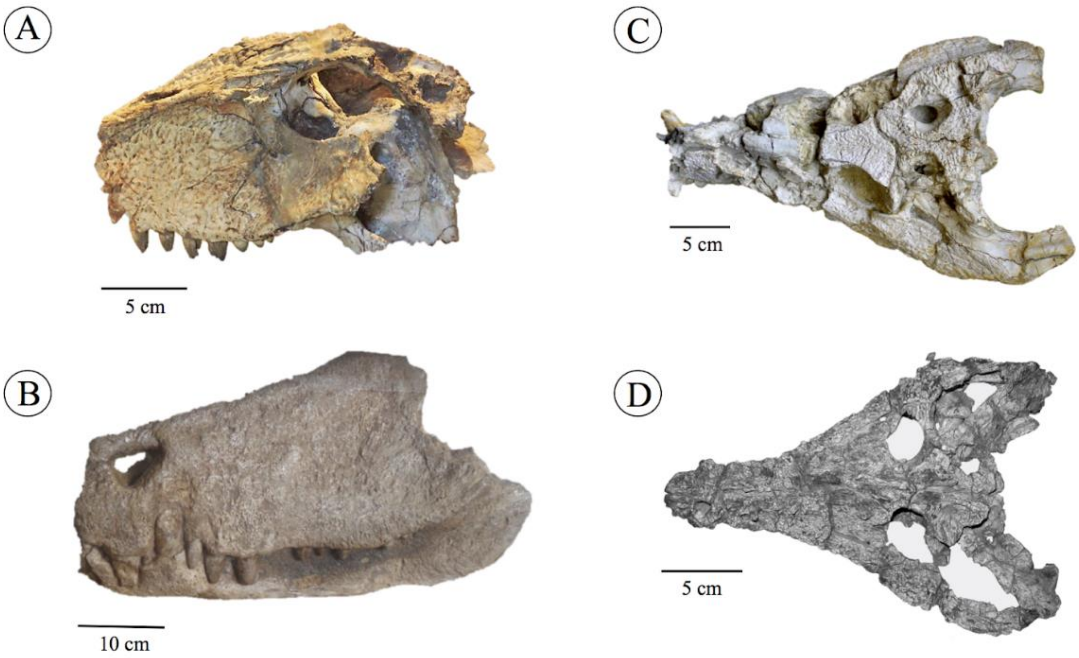


**Figura 11. Uma amostra de diversidade de Sebecídeos da América do Sul. A) – Crânio de *Zulmasuchus querejazus*, da Formação Santa Lucía (Paleoceno), Bolívia. Já foi referido como *Sebecus querejazus*, sendo subsequentemente renomeado por Paolillo & Linares, 2007. Imagem cedida por Javier Catala. B) – *Barinasuchus arveloi*, do Mioceno da Venezuela. Não somente um dos maiores crocodiliformes terrestres já encontrados, mas também seu registro mais recente (LAD). C) – *Sahitisuchus fluminensis*, da Bacia Itaboraí, Paleoceno Superior, em vista dorsal. Este é o sebecídeo mais completo descoberto no Brasil. Foto do holótipo pelo autor. D) – *Lorosuchus nodosus*, táxon da Formação Río Loro, Paleoceno da Argentina. Imagem adaptada de Pol & Powell (2011).**

### 1.7.4) – Baurusuchidae

A família de Baurusuchidae, primeiramente identificada por Price (1945), consiste em um grupo de predadores terrestres de médio a grande porte, do final Cretáceo, e de distribuição gondwânica. Seu crânio é caracterizado por rostro alto e achatado lateralmente, redução dentária, membros alongados, posicionados diretamente abaixo do corpo, em postura graviportante com o torso suspenso em relação ao chão, comprimento caudal similar ao comprimento pré-caudal, além de dupla fileira parasagital de osteodermos anteroposteriormente alongados (Riff & Kellner, 2011; Montefeltro, 2019).

Como a maior parte dos crocodiliformes fósseis, as principais sinapomorfias sustentando o clado estão concentradas no crânio (**figuras 12**), sendo estas: (1) oreinirrostria – rostros altos e achatados lateralmente (Riff & Kellner, 2011); (2) maxilares com redução dentária, apresentando somente cinco dentes (Riff, 2003); (3)

dentição zifodonte – dentes labiolingualmente achatados, com carenas mesiais e distais serrilhadas (dentição teropodomorfa, Nascimento, 2014); (4) processo anterior do jugal com crista infraorbital bem desenvolvida e depressão triangular em sua superfície lateral (Riff, 2003); (5) aproximação medial dos pré-frontais (Montefeltro et al., 2011; Godoy *et al*., 2014); (6) Pterigoides expandidos anteroposteriormente (Carvalho *et al*., 2011); (7) porção posterior dos esquamosais verticalizada (Riff, 2003) e (8) depressão semicircular na face lateral do quadrado (Riff, 2003).

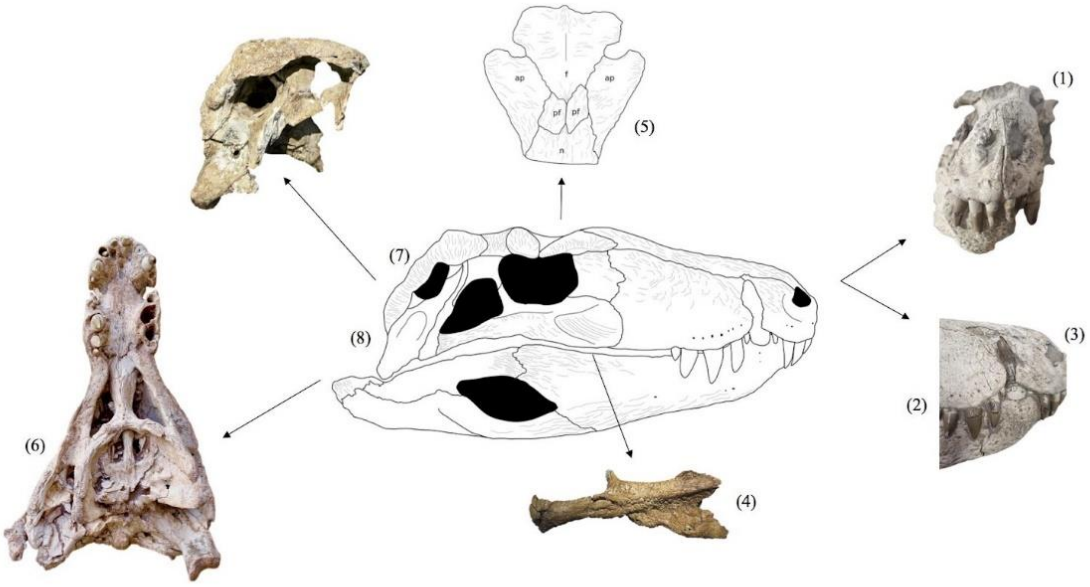


**Figura 12. Baurusuchidae, sua morfologia craniana geral e principais sinapomorfias enumeradas de acordo com o texto acima. (1,2,3) Vistas anterior e lateral direita do rostro de espécime de *Baurusuchus sp*, ressaltando a oreinirrostria, redução dentária e condição zifodonte; (4) morfologia do jugal em destaque, com visível depressão triangular no ramo anterior; (5) arranjo dos contatos da região anterior do teto craniano, com ênfase para a aproximação medial do pré-frontais; (6) espécime em vista palatal ressaltando os pterigóides anteroposteriormente expandidos; (7,8) porção anterior do esquamosal vertical e depressão semicircular na lateral do quadrado. Ap= palpebral anterior; f= frontal; n=nasal; pf=pré-frontal. Fotos tiradas pelo autor de uma série de espécimes para fins esquemáticos.**

Atualmente, existem nove espécies descritas em território brasileiro: *Baurusuchus pachecoi* Price, 1945, *Baurusuchus salgadoensis* Carvalho *et al*. 2005, *Baurusuchus albertoi* Nascimento & Zaher, 2010*, Stratiotosuchus maxhechti* Campos *et al*. 2001, *Pissarrachampsa sera* Montefeltro *et al*. 2011, *Campinasuchus dinizi* Carvalho *et al*. 2011, *Gondwanasuchus scabrosus* Marinho *et al*. 2013 *Aplestosuchus sordidus* Godoy *et al*. 2014, *Aphaurosuchus escharafacies*, Darlim *et al*., 2021 e

*Aphaurosuchus kaiju* Martins et al., 2023. *Cynodontosuchus rothi Woodward*, 1896, *Wargosuchus australis* Martinelli & Pais, 2008, e *Pabwehshi pakistanensis* Wilson *et al*. 2001, são outros três baurussuquídeos que completam a família, descritos a partir de espécimes provenientes da Argentina e Paquistão, respectivamente.

Montefeltro *et al*. (2011) e Godoy *et al*. (2014) forneceram as primeiras filogenias focadas na família Baurusuchidae, subdividindo-a em duas subfamílias principais, Baurusuchinae e Pissarrachampsinae, além das formas mais basais *Cynodonthosuchus rothi* e *Gondwanasuchus scabrosus*. A aproximação dos pré-frontais é a característica mais conspícua que divide as duas subfamílias (**figura 11-5**), com baurussuquíneos apresentando pré-frontais que se contatam ao longo de toda a sua superfície medial, enquanto os mesmos em pisarrachampsíneos somente se tocam em um único ponto medial, quase permitindo o contato entre frontal e nasal.

A maioria dos trabalhos que têm baurussuquídeos como seu objeto de estudo foca na descrição osteológica dos mesmos, principalmente de elementos cranianos, enquanto uma minoria se dedica ao pós-crânio (Riff, 2003; Nascimento & Zaher, 2010; Riff & Kellner, 2011; Cotts *et al*., 2016; Godoy *et al*., 2016). A tafonomia de uma ocorrência de pós-crânio articulado também foi alvo de investigação, destacando a ação de ressecamento e mumificação nos paleoambientes áridos da Bacia Bauru (de Araújo Júnior & Marinho, 2013).

Recentemente, novas linhas de pesquisa têm sido exploradas, incluindo histologia dentária e de ossos longos, que inferiu um crescimento determinado para *Baurusuchus* e Notosuchia em geral (Ricart *et al*., 2019). Adicionalmente, houve a descrição recente da morfologia dos osteodermos que compõe seu escudo parasagital (Montefeltro, 2019), além de reconstrução da neuroanatomia utilizando-se de dados de tomografia computadorizada, que revelou uma série de informações comportamentais e paleoecológicas, como a posição neutra no crânio e possíveis modos de forrageamento (Fonseca *et al*., 2020; Dumont *et al*., 2020). Análise de elementos finitos também foi recentemente aplicada para determinação da força de mordida de baurussuquídeos (Montefeltro *et al*., 2020), que, apesar de obter valores relativamente baixos, pode inferir uma adaptação para resistir à movimentos laterais associados a movimentação da presa.

Em contrapartida, pouco ainda é conhecido a respeito da ontogenia dos baurussuquídeos. Apesar de reportados previamente, foi somente com Oliveira *et al*. (2011), e subsequentemente com Marsola *et al*. (2016), que os ninhos e ovos de

crocodilomorfos da região de Jales-SP foram propriamente descritos nas escalas macro, micro e ultraestrutural. Oliveira e colaboradores (2011) ergueram um novo oogênero e espécie, *Bauruoolithus fragilis*, associando os mesmos aos restos esqueletais de *Baurusuchus*, frequentemente encontrados na proximidade das zonas de nidificação. Infelizmente, tais ocorrências não incluem material embrionário.

Existem poucos registros de estágios de desenvolvimento entre a eclosão e a fase adulta, e estes tendem a ser indivíduos menores que a maioria dos adultos coletados, porém já próximos a maturidade esquelética. Geroto & Bertini (2012) descreveram um rostro e sínfise mandibular do primeiro espécime reportadamente juvenil de *Baurusuchus*, osteologicamente similar ao holótipo de *Baurusuchus pachecoi*, porém menor, que apresenta um possível caráter ontogenético na forma da angulação da margem anterior da mandíbula, que ao contrário dos adultos, com sua disposição vertical, tem inclinação de 45º.

Godoy e colaboradores (2018), utilizando um crânio de juvenil bem preservado de *Pissarrachampsa sera*, fizeram uso da morfometria geométrica para avaliar se o desenvolvimento dos baurussuquídeos era influenciado por processos heterocrônicos peramórficos. Encontraram um bom suporte dos dados para tal, sugerindo então que as mudanças alimentares dos juvenis acompanhariam as mudanças ontogenéticas cranianas, eventualmente alcançando o nicho hipercarnívoro na fase adulta.

Estudos focando na ontogenia de crocodilianos atuais revelaram que os mesmos apresentam uma série de mudanças morfológicas, refletindo alterações na composição das presas, modo de forrageamento, até mesmo no padrão de nado (Tucker *et al*., 1996; Erickson *et al*., 2003; Seebacher *et al*., 2003). Dessa forma, é plausível inferir que bausuquídeos e outros notossúquios apresentavam mudanças osteológicas no crânio e pós-crânio que, de maneira similar, representavam partição de nicho entre adultos e juvenis. De modo a esclarecer quais mudanças seriam essas, novas investigações, explorando a osteologia de diferentes estágios de crescimento, se fazem necessárias.

### 1.8) – Considerações finais

A história evolutiva dos crocodilianos e, de maneira mais abrangente, dos crocodilomorfos, é rica e diversa, diferindo da percepção popular de uma linhagem evolutivamente estagnada (Brochu, 2003). O cretáceo do Brasil é particularmente rico

em formas fósseis, apresentando uma oportunidade única de estudo de um dos poucos ambientes terrestres não dominados por dinossauros durante o mesozóico.

Os baurussuquídeos, sendo predadores de topo, sinalizam um ecossistema continental complexo (Benton, 2003) e seu possível paralelismo com terópodos de médio porte (Riff & Kellner, 2011) é uma importante ocorrência de convergência evolutiva entre dois clados proximamente aparentados, porém morfologicamente díspares no registro fóssil, possibilitando uma melhor compreensão do surgimento dessas homoplasias (Losos, 2017).

A paucidade de espécimes juvenis e de estágios ontogenéticos iniciais de baurussuquídeos é uma lacuna a ser preenchida no estudo dos vertebrados da Bacia Bauru. Os capítulos a seguir apresentam, na forma de artigo, três trabalhos que buscam contribuir para o preenchimento de tal lacuna.

## Referências


**Aguilera, O.A., Riff, D. and Bocquentin-Villanueva, J., 2006**. A new giant Purussaurus (crocodyliformes, alligatoridae) from the upper Miocene Urumaco formation, Venezuela. *Journal of Systematic Palaeontology*, *4*(3), pp.221-232.

**Antunes, T., 1975**. Iberosuchus, crocodile Sebecosuchien nouveau, l'Eocene iberique au Nord de la Chaine Centrale, et l'origine du canyon de Nazare.

**Ashton, P.J., 2010**. The demise of the Nile crocodile (Crocodylus niloticus) as a keystone species for aquatic ecosystem conservation in South Africa: The case of the Olifants River. *Aquatic Conservation: Marine and Freshwater Ecosystems*, *20*(5), pp.489-493.

**Bakker, R.T., 1968**. *The superiority of dinosaurs*.

**Bakker, R.T., 1971**. Dinosaur physiology and the origin of mammals. *Evolution*, pp.636-658.

**Bakker, R.T., 1972**. Anatomical and ecological evidence of endothermy in dinosaurs. *Nature*, *238*(5359), pp.81-85.

**Bandeira, K. L., Brum, A. S., Pêgas, R. V., Cidade, G. M., Holgado, B., Cidade, A., & de Souza, R. G., 2018**. The Baurusuchidae vs Theropoda record in the Bauru Group (Upper Cretaceous, Brazil): a taphonomic perspective. *Journal of Iberian Geology*, *44*(1), 25-54.

**Barbosa, J.A., Kellner, A.W.A. and Viana, M.S.S., 2008**. New dyrosaurid crocodylomorph and evidences for faunal turnover at the K–P transition in Brazil. *Proceedings of the Royal Society B: Biological Sciences*, *275*(1641), pp.1385-1391.

**Barrios, F., Bona, P., Paulina-Carabajal, A., & Gasparini, Z., 2018**. Re-description of the cranio-mandibular anatomy of Notosuchus terrestris (Crocodyliformes, Mesoeucrocodylia) from the Upper Cretaceous of Patagonia. *Cretaceous Research*, *83*, 3-39.

**Barrios, F., Paulina-Carabajal, A., & Bona, P., 2016**. A new peirosaurid (Crocodyliformes, Mesoeucrocodylia) from the Upper Cretaceous of Patagonia, Argentina. *Ameghiniana*, *53*(1), 14-25.

**Benton, M. J., 2003**. *When life nearly died: the greatest mass extinction of all time*. Thames & Hudson.

**Benton, M., Forth, J. and Langer, M.C., 2014**. Models for the rise of the dinosaurs. Current Biology, 24(2), pp. R87- R95.

**Benton, M., 1999**. Scleromochlus taylori and the origin of dinosaurs and pterosaurs. Philosophical Transactions of the Royal Society of London B: Biological Sciences, 354(1388), pp.1423-1446.

**Benton, M.J. and Clark, J.M., 1988**. Archosaur phylogeny and the relationships of the Crocodylia. *The phylogeny and classification of the tetrapods*, *1*, pp.295-338.

**Benton, M.J., 1983**. Dinosaur success in the Triassic: a noncompetitive ecological model. *The Quarterly Review of Biology*, *58*(1), pp.29-55.

**Benton, M.J., 1986**. More than one event in the late Triassic mass extinction. *Nature*, *321*(6073), p.857.

**Benton, M.J., 1986**. The Late Triassic tetrapod extinction events. *The beginning of the age of dinosaurs; faunal change across the Triassic-Jurassic boundary*, pp.303-320.

**Benton, M.J., 2004**. Origin and relationships of Dinosauria. *The dinosauria*, *2*, pp.7-19.

**Benton, M.J., 2005**. Vertebrate Palaeontology. John Wiley & Sons.

**Bona, P., Ezcurra, M.D., Barrios, F. and Fernandez Blanco, M.V., 2018**. A new Palaeocene crocodylian from southern Argentina sheds light on the early history of caimanines. *Proceedings of the Royal Society B: Biological Sciences*, *285*(1885), p.20180843.

**Brandalise de Andrade, M., & Bertini, R. J., 2008**. A new Sphagesaurus (Mesoeucrocodylia: Notosuchia) from the upper cretaceous of monte alto city (Bauru Group, Brazil), and a revision of the Sphagesauridae. *Historical Biology*, *20*(2), 101-136.

**Brochu, C. A., & Storrs, G. W., 2012**. A giant crocodile from the Plio-Pleistocene of Kenya, the phylogenetic relationships of Neogene African crocodylines, and the antiquity of Crocodylus in Africa. *Journal of Vertebrate Paleontology*, *32*(3), 587-602.

**Brochu, C. A., 2017**. Pliocene crocodiles from Kanapoi, Turkana Basin, Kenya. *Journal of human evolution*.

**Brochu, C.A., 1997**. A review of "Leidyosuchus" (Crocodyliformes, Eusuchia) from the Cretaceous through Eocene of North America. *Journal of Vertebrate Paleontology*, *17*(4), pp.679-697.

**Brochu, C.A., 1999**. Phylogenetics, taxonomy, and historical biogeography of Alligatoroidea. *Journal of Vertebrate Paleontology*, *19*(S2), pp.9-100.

**Brochu, C.A., 2003**. Phylogenetic approaches toward crocodylian history. *Annual Review of Earth and Planetary Sciences*, *31*(1), pp.357-397.

**Brochu, C.A., 2004**. A new Late Cretaceous gavialoid crocodylian from eastern North America and the phylogenetic relationships of thoracosaurs. *Journal of Vertebrate Paleontology*, *24*(3), pp.610-633.

**Brochu, C.A., 2012**. Phylogenetic relationships of Palaeogene ziphodont eusuchians and the status of Pristichampsus Gervais, 1853. *Earth and Environmental Science Transactions of the Royal Society of Edinburgh*, *103*(3-4), pp.521-550.

**Bronzati, M., Montefeltro, F. C., & Langer, M. C., 2015**. Diversification events and the effects of mass extinctions on Crocodyliformes evolutionary history. *Royal Society open science*, *2*(5), 140385.

**Bronzati, M., Montefeltro, F.C. and Langer, M.C., 2012**. A species-level supertree of Crocodyliformes. *Historical Biology*, *24*(6), pp.598-606.

**Brown, B., 1933**. Na ancestral crocodile. American Museum Novitates 683:1-4.

**Brusatte, S.L., 2012**. *Dinosaur paleobiology*. John Wiley & Sons.

**Brusatte, S.L., Benton, M.J., Ruta, M. and Lloyd, G.T., 2008**. The first 50 Myr of dinosaur evolution: macroevolutionary pattern and morphological disparity. *Biology Letters*, *4*(6), pp.733-736.

**Brusatte, S.L., Nesbitt, S.J., Irmis, R.B., Butler, R.J., Benton, M.J. and Norell, M.A., 2010**. The origin and early radiation of dinosaurs. *Earth-Science Reviews*, *101*(1-2), pp.68-100.

**Buckley, G. A., Brochu, C. A., Krause, D. W., and Pol, D., 2000**. A pug-nosed crocodyliform from the Late Cretaceous of Madagascar. *Nature*, *405*(6789), 941-944.

**Buffetaut, E., and Marshall, L. G., 1991**. A new crocodilian, Sebecus querejazus, nov. sp. (Mesosuchia, Sebecidae) from the Santa Lucia formation (Early Paleocene) at Vila Vila, southcentral Bolivia. *Fósiles y Facies de Bolivia*, *1*, 545-557.

**Buffetaut, E., 1982**. A ziphodont mesosuchian crocodile from the Eocene of Algeria and its implications for 43steology43 dispersal. *Nature*, *300*(5888), pp.176-178.

**Buffetaut, E., 1986**. Na Mésosuchien 43steology dans l'Éoccne supérieurde La Livinicre (Hérault, France). *Geobios*, *19*(1), 101-113.

**Buffetaut, E., 1989**. A new ziphodont mesosuchian crocodile from the Eocene of Algeria. *Palaeontographica. Abteilung A, Paläozoologie, Stratigraphie*, *208*(1-3), 1-10.

**Busbey III, A.B., 1986**. New material of Sebecus cf. huilensis (Crocodilia: Sebecosuchidae) from the Miocene La Venta Formation of Colombia. *Journal of Vertebrate Paleontology*, *6*(1), pp.20-27.

**Buscalioni, Á.D., 2017**. The Gobiosuchidae in the early evolution of Crocodyliformes. *Journal of Vertebrate Paleontology*, *37*(3), p. e1324459.

**Campos, D. A., Oliveira, G. R., Figueiredo, R. G., Riff, D., Azevedo, S. A., Carvalho, L. B., and Kellner, A. W., 2011**. On a new peirosaurid crocodyliform from the Upper Cretaceous, Bauru Group, southeastern Brazil. *Anais da Academia Brasileira de Ciências*, *83*(1), 317-327.

**Campos, D., 2001**. Short note on a new Baurusuchidae (Crocodyliformes, Metasuchia) from the Upper Cretaceous of Brazil.

**Cardia, F. M. S., Santucci, R. M., Bernardi, J. V. E., de Andrade, M. B., and de Oliveira, C. E. M., 2018**. Mercury concentrations in terrestrial fossil vertebrates from the Bauru Group (Upper Cretaceous), Brazil and implications for 43steology43 paleontology. *Journal of South American Earth Sciences*, *86*, 15-22.

**Carvalho, I.S., Teixeira, V. D. P. A., Ferraz, M. L. D. F., Ribeiro, L. C. B., Martinelli, A. G., Neto, F. M., ... and Ferraz, P. F., 2011**. Campinasuchus dinizi gen. Et sp. Nov., a new Late Cretaceous baurusuchid (Crocodyliformes) from the Bauru Basin, Brazil. *Zootaxa*, *2871*(1), 19-42.

**Carvalho, I.S, Campos, A. D. C. A., and Nobre, P. H. 2005**. Baurusuchus salgadoensis, a new crocodylomorpha from the Bauru Basin (Cretaceous), Brazil. *Gondwana Research*, *8*(1), 11-30.

**Carvalho, I.S, and Bertini, R. J., 1999**. Mariliasuchus: um novo Crocodylomorpha (Notosuchia) do Cretáceo da Bacia Bauru, Brasil. *Geologia Colombiana*, *24*, 83-105.

**Carvalho, I.S, Ribeiro, L. C. B., and dos Santos Avilla, L., 2004**. Uberabasuchus terrificus sp. Nov., a new Crocodylomorpha from the Bauru Basin (Upper Cretaceous), Brazil. *Gondwana Research*, *7*(4), 975-1002.

**Carvalho, I.S, Vasconcellos, F.M and Tavares, S.A.S., 2007**. Montealtosuchus arrudacamposi, a new peirosaurid crocodile (Mesoeucrocodylia) from the Late Cretaceous Adamantina Formation of Brazil. *Zootaxa*, *1607*, 35-46.

**Charig, A.J., 1972**. The evolution of the 44steology 44steol and hindlimb: na explanation in functional terms. *Studies in 44steology44 evolution*, pp.121-155.

**Cidade, G.M., Solórzano, A., Rincón, A.D., Riff, D. and Hsiou, A.S., 2017**. A new Mourasuchus (Alligatoroidea, Caimaninae) from the late Miocene of Venezuela, the phylogeny of Caimaninae and considerations on the feeding habits of Mourasuchus. *PeerJ*, *5*, p. e3056.

**Cidade, G.M., Souza-Filho, J.P., Hsiou, A.S., Brochu, C.A. and Riff, D., 2019**. New specimens of Mourasuchus (Alligatoroidea, Caimaninae) from the Miocene of Brazil and Bolivia and their taxonomic and morphological implications. *Alcheringa: Na Australasian Journal of Palaeontology*, *43*(2), pp.261-278.

**Clark, J.M. and Norell, M., 1992**. The Early Cretaceous crocodylomorph Hylaeochampsa vectiana from the 44steolo of the Isle of Wight. American Museum 44steology; no. 3032.

**Clark, J.M. and Sues, H.D., 2002**. Two new basal crocodylomorph archosaurs from the Lower Jurassic and the monophyly of the Sphenosuchia. *Zoological Journal of the Linnean Society*, *136*(1), pp.77-95.

**Clark, J.M., 1986**. Phylogenetic relationships of the crocodylomorph archosaurs (Doctoral dissertation, University of Chicago, Department of Anatomy).

**Clark, J.M., 2011**. A new shartegosuchid crocodyliform from the Upper Jurassic Morrison Formation of western Colorado. *Zoological Journal of the Linnean Society*, *163*(suppl_1), pp. S152-S172.

**Clark, J.M., Sues, H.D. and Berman, D.S., 2001**. A new specimen of Hesperosuchus agilis from the Upper Triassic of New Mexico and the interrelationships of basal crocodylomorph archosaurs. *Journal of Vertebrate Paleontology*, *20*(4), pp.683-704.

**Clark, J.M., Xu, X., Forster, C.A. and Wang, Y., 2004**. A Middle Jurassic 'sphenosuchian'from China and the origin of the crocodylian skull. *Nature*, *430*(7003), p.1021.

**Colbert, E.H., Bird, R.T. and Brown, B., 1954**. A gigantic crocodile from the Upper Cretaceous beds of Texas. American Museum 44steology; no. 1688.

**Colbert, E.H., Simpson, G.G. and Williams, C.S., 1946**. Sebecus, representative of a peculiar suborder of fossil Crocodilia from Patagonia. Bulletin of the AMNH; v. 87, article 4.

**Cope, E. D., 1869**. Extinct Batrachia, Reptilia and Aves of North America. *Transactions of the American Philosophical Society*, *14*, 1-252.

**Coria, R. A., Ortega, F., Arcucci, A. B., and Currie, P. J., 2019**. A new and complete peirosaurid (Crocodyliformes, Notosuchia) from Sierra Barrosa (Santonian, Upper Cretaceous) of the Neuquén Basin, Argentina. *Cretaceous Research*, *95*, 89-105.

**Cotts, L., Pinheiro, A. E. P., da Silva Marinho, T., de Souza Carvalho, I., and Di Dario, F., 2017**. Postcranial skeleton of Campinasuchus dinizi (Crocodyliformes, Baurusuchidae) from the Upper Cretaceous of Brazil, with comments on the ontogeny and ecomorphology of the species. *Cretaceous Research*, *70*, 163-188.

**Cunha, G. O., Santucci, R. M., de Andrade, M. B., and de Oliveira, C. E. M., 2020**. Description and phylogenetic relationships of a large-bodied sphagesaurid notosuchian from the Upper Cretaceous Adamantina Formation, Bauru Group, São Paulo, southeastern Brazil. *Cretaceous Research*, *106*, 104259.

**Darlim, G., Montefeltro, F.C. and Langer, M.C., 2021**. 3D skull modelling and description of a new baurusuchid (Crocodyliformes, Mesoeucrocodylia) from the Late Cretaceous (Bauru Basin) of Brazil. *Journal of Anatomy*, *239*(3), pp.622-662

**de Andrade, M.B., Edmonds, R., Benton, M.J. and Schouten, R., 2011**. A new Berriasian species of Goniopholis (Mesoeucrocodylia, Neosuchia) from England, and a review of the genus. *Zoological Journal of the Linnean Society*, *163*(suppl_1), pp. S66-S108.

**De Araújo Júnior, H. I., and da Silva Marinho, T., 2013**. Taphonomy of a Baurusuchus (Crocodyliformes, Baurusuchidae) from the Adamantina Formation (Upper Cretaceous, Bauru Basin), Brazil: implications for preservational modes, time resolution and paleoecology. *Journal of South American Earth Sciences*, *47*, 90-99.

**De Miranda, E.B., 2017**. The plight of reptiles as ecological actors in the tropics. *Frontiers in Ecology and Evolution*, *5*, p.159.

**Erickson GM, Lappin AK, and Vliet KA., 2003**. The ontogeny of bite-force performance in American alligator (*Alligator mississippiensis*) *Journal of Zoology* 260:317-327.

**Filippi, L. S., Barrios, F., and Garrido, A. C., 2018**. A new peirosaurid from the Bajo de la Carpa Formation (Upper Cretaceous, Santonian) of Cerro Overo, Neuquén, Argentina. *Cretaceous Research*, *83*, 75-83.

**Fiorelli, L. E., 2010**. Predation bite-marks on a peirosaurid crocodyliform from the Upper Cretaceous of Neuquén Province, Argentina. *Ameghiniana*, *47*(3), 387-400.

**Fiorelli, L. E., Leardi, J. M., Hechenleitner, E. M., Pol, D., Basilici, G., and Grellet-Tinner, G., 2016**. A new Late Cretaceous crocodyliform from the western margin of Gondwana (La Rioja Province, Argentina). *Cretaceous Research*, *60*, 194-209.

**Fiorelli, L.E. and Calvo, J.O., 2008**. The first "protosuchian" (Archosauria: Crocodyliformes) from the Cretaceous (Santonian) of Gondwana. *Arquivos do Museu Nacional*, *65*(4), pp.417-459.

**Fonseca, P. H. M., Martinelli, A. G., da Silva Marinho, T., Ribeiro, L. C. B., Schultz, C. L., and Soares, M. B., 2020**. Morphology of the endocranial cavities of Campinasuchus dinizi (Crocodyliformes: Baurusuchidae) from the Upper Cretaceous of Brazil. *Geobios*.

**Fortier, D., Perea, D. and Schultz, C., 2011**. Redescription and phylogenetic relationships of Meridiosaurus vallisparadisi, a pholidosaurid from the Late Jurassic of Uruguay. *Zoological Journal of the Linnean Society*, *163*(suppl_1), pp. S257-S272.

**Fortier, D.C. and Schultz, C.L., 2009**. A new neosuchian crocodylomorph (Crocodyliformes, Mesoeucrocodylia) from the Early Cretaceous of north-east Brazil. *Palaeontology*, *52*(5), pp.991-1007.

**Gasparini, Z. B., 1971**. Los Notosuchia del Cretácico de América del Sur como na nuevo infraorden de los Mesosuchia (Crocodilia). *Ameghiniana*, *8*(2), 83-103.

**Gasparini, Z. D., 1982**. Na nueva 46steolo de cocodrilos 46steology cretácicos de América del Sur.

**Gasparini, Z.B., Chiappe, L. M., & Fernandez, M., 1991**. A new Senonian peirosaurid (Crocodylomorpha) from Argentina and a synopsis of the South American Cretaceous crocodilians. *Journal of Vertebrate Paleontology*, *11*(3), 316-333.

**Gasparini, Z.B., Fernandez, M., & Powell, J., 1993**. New tertiary sebecosuchians (Crocodylomorpha) from South America: phylogenetic implications. *Historical Biology*, *7*(1), 1-19.

**Gauthier, J., and Padian, K., 1985**. Phylogenetic, functional, and aerodynamic analyses of the origin of 46steo and their flight. *The Beginning of Birds. Freunde des Jura Museums, Eichstatt*, 185-197.

**Gauthier, J., 1986**. Saurischian monophyly and the origin of 46steo. *Memoirs of the California Academy of sciences*, *8*, pp.1-55. Joints. Neues Jahrbuch für Geologie und Paläontologie, Abhandlungen, 180(1), pp.21-52.

**Gauthier, J.A., Nesbitt, S.J., Schachner, E.R., Bever, G.S. and Joyce, W.G., 2011**. The bipedal stem crocodilian Poposaurus gracilis: inferring function in fossils and innovation in 47steology locomotion. *Bulletin of the Peabody Museum of Natural History*, *52*(1), pp.107-126.

**Geroto, C. F. C., and Bertini, R. J., 2012**. Descrição de um espécime juvenil de Baurusuchidae (Crocodyliformes: Mesoeucrocodylia) do Grupo Bauru (Neocretáceo): considerações preliminares sobre ontogenia. *Revista do Instituto Geológico*, *33*(2), 13-29.

**Godoy, P. L., Ferreira, G. S., Montefeltro, F. C., Vila Nova, B. C., Butler, R. J., and Langer, M. C., 2018**. Evidence for heterochrony in the cranial evolution of fossil crocodyliforms. *Palaeontology*, *61*(4), 543-558.

**Godoy, P. L., Montefeltro, F. C., Norell, M. A., and Langer, M. C., 2014**. Na additional baurusuchid from the Cretaceous of Brazil with evidence of interspecific predation among Crocodyliformes. *PloS one*, *9*(5).

**Godoy, P.L., 2020**. Crocodylomorph cranial shape evolution and its 47steology47rn47 with body size and ecology. *Journal of Evolutionary Biology*, *33*(1), pp.4-21.

**Godoy, P.L., Benson, R.B., Bronzati, M. and Butler, R.J., 2019**. The multi-peak adaptive landscape of crocodylomorph body size evolution. *BMC evolutionary biology*, *19*(1), p.167.

**Gower, D.J., 2003**. Osteology of the early archosaurian reptile Erythrosuchus africanus, Broom Publications, 379, pp. SP379-24.

**Grigg, G., 2015**. *Biology and Evolution of Crocodylians*. Csiro Publishing.

**Hennig, W., 1966**. Phylogenetic systematics. Urbana, IL. *IL: University of Illinois Press. [Google Scholar]*.

**Huxley, T. H., 1875**. On Stagonolepis robertsoni, and on the evolution of the Crocodilia. *Quarterly Journal of the Geological Society*, *31*(1-4), 423-438.

**Ibrahim, N., Sereno, P., Varricchio, D.J., Martill, D.M., Dutheil, D.B., Unwin, D.M., Baidder, L., Larsson, H.C.E., Zouhri, A.K., 2020**. Geology and paleontology of the Upper Cretaceous Kem Kem Group of eastern Morocco. *Zookeys*, 928: 1-216.

**Iori, F. V., and Carvalho, I. S., 2011**. Caipirasuchus paulistanus, a new sphagesaurid (Crocodylomorpha, Mesoeucrocodylia) from the Adamantina Formation (Upper Cretaceous, Turonian–Santonian), Bauru Basin, Brazil. *Journal of Vertebrate Paleontology*, *31*(6), 1255-1264.

**Iori, F. V., de Souza Carvalho, I., and da Silva Marinho, T., 2016**. Postcranial skeletons of Caipirasuchus (Crocodyliformes, Notosuchia, Sphagesauridae) from the Upper Cretaceous (Turonian–Santonian) of the Bauru Basin, Brazil. *Cretaceous Research*, *60*, 109-120.

**Iori, F.V. and de Souza Carvalho, I., 2018**. The Cretaceous crocodyliform Caipirasuchus: behavioural feeding mechanisms. *Cretaceous Research*, *84*, pp.181-187.

**Irmis, R.B., Nesbitt, S.J. and Sues, H.D., 2013**. Early Crocodylomorpha. Geological Society, London, Special.

**Kellner, A.W., Pinheiro, A.E. and Campos, D.A., 2014**. A new sebecid from the Paleogene of Brazil and the crocodyliform radiation after the K–Pg boundary. *PloS One*, *9*(1).

**Knight, T.K. and Schwimmer, D.R., 2005**, March. Anatomy of the skull and braincase of a new Deinosuchus rugosus specimen from the Blufftown Formation, Russell County, Alabama. In *Geological Society of America Abstracts with Programs* (Vol. 37, p. 12).

**Kuhn, O., 1968**. Die Vortzeitlichen Krokodile. Verlag Oeben, Krailing, Munchen, 124 pp.

**Lamanna, M. C., Casal, G. A., Ibiricu, L. M., and Martínez, R. D., 2019**. A New Peirosaurid Crocodyliform from the Upper Cretaceous Lago Colhué Huapi Formation of Central Patagonia, Argentina. *Annals of Carnegie Museum*, *85*(3), 193-211.

**Larsson, H. C., and Sues, H. D., 2007**. Cranial 48steology and phylogenetic relationships of Hamadasuchus rebouli (Crocodyliformes: Mesoeucrocodylia) from the Cretaceous of Morocco. *Zoological Journal of the Linnean Society*, *149*(4), 533-567.

**Lecuona, A., Ezcurra, M.D. and Irmis, R.B., 2016**. Revision of the early crocodylomorph Trialestes romeri (Archosauria, Suchia) from the lower Upper Triassic Ischigualasto Formation of Argentina: one of the oldest-known crocodylomorphs. *Papers in Palaeontology*, *2*(4), pp.585-622.

**Lee, M.S. and Yates, A.M., 2018**. Tip-dating and homoplasy: reconciling the shallow molecular divergences of modern gharials with their long fossil record. *Proceedings of the Royal Society B: Biological Sciences*, *285*(1881), p.20181071.

**Linnaeus, C., 1758**. *Systema naturae* (Vol. 1, No. Part 1, p. 532). Laurentii Salvii: Stockholm.

**Lio, G., Agnolín, F. L., Valieri, R. J., Filippi, L., and Rosales, D., 2016**. A new peirosaurid (Crocodilyformes) from the Late Cretaceous (Turonian–Coniacian) of Patagonia, Argentina. *Historical Biology*, *28*(6), 835-841.

**Losos, J.B., 2017**. *Improbable destinies: Fate, chance, and the future of evolution*. Penguin.

**Marinho, T. S., and Carvalho, I. S., 2009**. Na armadillo-like sphagesaurid crocodyliform from the Late Cretaceous of Brazil. *Journal of South American Earth Sciences*, *27*(1), 36-41.

**Marinho, T., Iori, F. V., de Souza Carvalho, I., and Vasconcellos, F. M., 2013**. Gondwanasuchus scabrosus gen. Et sp. Nov., a new terrestrial predatory crocodyliform (Mesoeucrocodylia: Baurusuchidae) from the Late Cretaceous Bauru Basin of Brazil. *Cretaceous Research*, *44*, 104-111.

**Marsola, J.C.A, Batezelli, A., Montefeltro, F. C., Grellet-Tinner, G., and Langer, M. C., 2016**. Palaeoenvironmental characterization of a crocodilian nesting site from the Late Cretaceous of Brazil and the evolution of crocodyliform nesting strategies. *Palaeogeography, Palaeoclimatology, Palaeoecology*, *457*, 221-232.

**Martin, J.E., 2015**. A sebecosuchian in a 49steol Eocene karst with comments on the dorsal 49steol in Crocodylomorpha. *Acta Palaeontologica Polonica*, *60*(3), pp.673-680.

**Martins, K.C., Queiroz, M.V., Ruiz, J.V., Langer, M.C. and Montefeltro, F.C.,** 2023. A new Baurusuchidae (Notosuchia, Crocodyliformes) from the Adamantina Formation (Bauru Group, Upper Cretaceous), with a revised phylogenetic analysis of Baurusuchia. *Cretaceous Research*, p.105680.

**Martinelli, A. G., and Pais, D. F., 2008**. A new baurusuchid crocodyliform (Archosauria) from the Late Cretaceous of Patagonia (Argentina). *Comptes Rendus Palevol*, *7*(6), 371-381.

**Martinelli, A. G., Marinho, T. S., Iori, F. V., and Ribeiro, L. C. B., 2018**. The first Caipirasuchus (Mesoeucrocodylia, Notosuchia) from the Late Cretaceous of Minas Gerais, Brazil: new insights on sphagesaurid anatomy and taxonomy. *PeerJ*, *6*, e5594.

**Martinelli, A. G., Sertich, J. J., Garrido, A. C., and Praderio, Á. M., 2012**. A new peirosaurid from the Upper Cretaceous of Argentina: Implications for specimens referred to Peirosaurus torminni Price (Crocodyliformes: Peirosauridae). *Cretaceous Research*, *37*, 191-200.

**Martínez, R.N., Alcober, O.A. and Pol, D., 2018**. A New Protosuchid Crocodyliform (Pseudosuchia, Crocodylomorpha) from the Norian Los Colorados Formation, Northwestern Argentina. *Journal of Vertebrate Paleontology*, *38*(4), pp.1-12.

**Mazzotti, F.J., Best, G.R., Brandt, L.A., Cherkiss, M.S., Jeffery, B.M. and Rice, K.G., 2009**. Alligators and crocodiles as indicators for restoration of Everglades ecosystems. *Ecological indicators*, *9*(6), pp. S137-S149.

**Molnar, R. E., and de Vasconcellos, F. M., 2016**. Cenozoic dinosaurs in South America-revisited. *Memoirs of Museum Victoria*, *74*.

**Mateus, O., Puértolas-Pascual, E. and Callapez, P.M., 2019**. A new eusuchian crocodylomorph from the Cenomanian (Late Cretaceous) of Portugal reveals novel implications on the origin of Crocodylia. *Zoological Journal of the Linnean Society*, *186*(2), pp.501-528.

**Montefeltro, F. C., 2019**. The 50steology50r of baurusuchid crocodyliforms (Mesoeucrocodylia, Notosuchia). *Journal of Vertebrate Paleontology*, *39*(2), e1594242.

**Montefeltro, F. C., Laurini, C. R., and Langer, M. C., 2009**. Multicusped crocodyliform teeth from the Upper Cretaceous (São José do Rio Preto Formation, Bauru Group) of São Paulo, Brazil. *Cretaceous Research*, *30*(5), 1279-1286.

**Montefeltro, F. C., Lautenschlager, S., Godoy, P. L., Ferreira, G. S., and Butler, R. J., 2020**. A unique predator in a unique ecosystem: 50steolog the apex predator within a Late Cretaceous crocodyliform-dominated fauna from Brazil. *Journal of Anatomy*.

**Montefeltro, F.C., Larsson, H.C. and Langer, M.C., 2011**. A new baurusuchid (Crocodyliformes, Mesoeucrocodylia) from the Late Cretaceous of Brazil and the phylogeny of Baurusuchidae. PloS One, 6 (7), p. e21916.

**Mook, C.C., 1941**. A new crocodilian from the Lance Formation. American Museum 50steology; no. 1128.

**Murray, C. M., Russo, P., Zorrilla, A., and McMahan, C. D., 2019**. Divergent Morphology among Populations of the New Guinea Crocodile, Crocodylus novaeguineae (Schmidt, 1928): Diagnosis of na Independent Lineage and Description of a New Species. *Copeia*, *107*(3), 517-523.

**Nascimento, P. M., 2014**. *Revisão da família Baurusuchidae e seu posicionamento filogenético dentro do clado Mesoeucrocodylia* (Doctoral dissertation, Universidade de São Paulo).

**Nascimento, P. M., and Zaher, H., 2010**. A new species of Baurusuchus (Crocodyliformes, Mesoeucrocodylia) from the Upper Cretaceous of Brazil, with the first complete 50steology50 skeleton described for the 50steol Baurusuchidae. *Papéis avulsos de Zoologia*, *50*(21), 323-361.

**Nesbitt, S.J., 2003**. Arizonasaurus and its implications for 50steology divergence. *Proceedings of the Royal Society of London. Series B: Biological Sciences*, *270*(suppl_2), pp. S234-S237.

**Nesbitt, S.J., 2011**. The early evolution of archosaurs: relationships and the origin of major clades. *Bulletin of the American Museum of Natural History*, *2011*(352), pp.1-292.

**Nesbitt, S.J., Butler, R.J., Ezcurra, M.D., Barrett, P.M., Stocker, M.R., Angielczyk, K.D., Smith, R.M., Sidor, C.A., Niedźwiedzki, G., Sennikov, A.G. and Charig,**

**A.J., 2017**. The earliest bird-line archosaurs and the assembly of the dinosaur body plan. *Nature*, *544*(7651), p.484.

**Nobre, P. H., and de Souza Carvalho, I., 2006**. Adamantinasuchus navae: a new gondwanan Crocodylomorpha (Mesoeucrocodylia) from the Late Cretaceous of Brazil. *Gondwana Research*, *10*(3-4), 370-378.

**Novas, F. E., Pais, D. F., Pol, D., Carvalho, I. D. S., Scanferla, A., Mones, A., and Riglos, M. S., 2009**. Bizarre notosuchian crocodyliform with associated eggs from the Upper Cretaceous of Bolivia. *Journal of Vertebrate Paleontology*, *29*(4), 1316-1320.

**O'Connor, P. M., Sertich, J. J., Stevens, N. J., Roberts, E. M., Gottfried, M. D., Hieronymus, T. L., ... and Temba, J., 2010**. The evolution of mammal-like crocodyliforms in the Cretaceous Period of Gondwana. *Nature*, *466*(7307), 748-751.

**Oliveira, C. E., Santucci, R. M., Andrade, M. B., Fulfaro, V. J., Basilio, J. A., and Benton, M. J., 2011**. Crocodylomorph eggs and eggshells from the Adamantina Formation (Bauru Group), Upper Cretaceous of Brazil. *Palaeontology*, *54*(2), 309-321.

**Olsen, P.E., Shubin, N.H. and Anders, M.H., 1987**. New Early Jurassic tetrapod assemblages constrain Triassic-Jurassic tetrapod extinction event. *Science*, *237*(4818), pp.1025-1029.

**Ortega, F., Buscalioni, A. D., and Gasparini, Z., 1996**. Reinterpretation and new denominationof Atacisaurus crassiproratus (Middle Eocene; Issel, France) as cf. Iberosuchus (Crocodylomorpha, Metasuchia). *Geobios*, *29*(3), 353-364.

**Owen, R., 1860**. *Palaeontology, or a systematic summary of extinct animals and their geological relations*. Adam and Charlos Black.

**Palmer, M.L. and Mazzotti, F.J., 2004**. Structure of Everglades alligator holes. *Wetlands*, *24*(1), pp.115-122.

**Paolillo, A., and Linares, O. J., 2007**. Nuevos cocodrilos sebecosuchia del cenozoico suramericano (Mesosuchia: Crocodylia). *Paleobiologia neotropical*, *3*, 1-25.

**Parrish, J.M., 1987**. The origin of crocodilian locomotion. *Paleobiology*, *13*(4), pp.396-414.

**Parrish, J.M., 1991**. A new specimen of na early crocodylomorph (cf. Sphenosuchus sp.) from the Upper Triassic Chinle Formation of Petrified Forest National Park, Arizona. *Journal of Vertebrate Paleontology*, *11*(2), pp.198-212.

**Peng, G. and Shu, C., 2005**. A new species of Hsisosuchus from the late jurassic of zigong, Sichuan, China. *Vertebrata Pal Asiatica*, *43*(4), pp.312-324.

**Pol, D. and Powell, J.E., 2011**. A new sebecid mesoeucrocodylian from the Rio Loro Formation (Palaeocene) of north-western Argentina. *Zoological Journal of the Linnean Society*, *163*(suppl_1), pp. S7-S36.

**Pol, D., and Leardi, J. M., 2015**. Diversity patterns of Notosuchia (Crocodyliformes, mesoeucrocodylia) during the cretaceous of Gondwana. *Publicación Electrónica de la Asociación Paleontológica Argentina*, *15*(1).

**Pol, D., 2003**. New remains of Sphagesaurus huenei (Crocodylomorpha: Mesoeucrocodylia) from the late Cretaceous of Brazil. *Journal of Vertebrate Paleontology*, *23*(4), 817-831.

**Pol, D., Ji, S.A., Clark, J.M. and Chiappe, L.M., 2004**. Basal crocodyliforms from the Lower Cretaceous Tugulu Group (Xinjiang, China), and the phylogenetic position of Edentosuchus. *Cretaceous Research*, *25*(4), pp.603-622.

**Pol D., Gasparini Z. 2009**. Skull anatomy of Dakosaurus andiniensis (Thalattosuchia: Crocodylomorpha) and the phylogenetic position of Thalattosuchia. *Journal of Systematic Palaeontology*, 7:163–197.

**Pol, D., Leardi, J. M., Lecuona, A., and Krause, M., 2012**. Postcranial anatomy of Sebecus icaeorhinus (Crocodyliformes, Sebecidae) from the Eocene of Patagonia. *Journal of Vertebrate Paleontology*, *32*(2), 328-354.

**Pol, D., Nascimento, P. M., Carvalho, A. B., Riccomini, C., Pires-Domingues, R. A., and Zaher, H., 2014**. A new notosuchian from the Late Cretaceous of Brazil and the phylogeny of advanced notosuchians. *PloS One*, *9*(4).

**Pol, D., Rauhut, O.W., Lecuona, A., Leardi, J.M., Xu, X. and Clark, J.M., 2013**. A new fossil from the Jurassic of Patagonia reveals the early basicranial evolution and the origins of Crocodyliformes. Biological Reviews, 88(4), pp.862-872.

**Price, L. I., 1950**. On a new crocodilian, Sphagesaurus, from the Cretaceous of the State of São Paulo, Brazil. *Anais da Academia Brasileira de Ciências*, *22*(1), 77-83.

**Price, L. I., 1955**. Novos crocodilídeos dos arenitos da Série Bauru. Cretáceo do Estado de Minas Gerais. *Anais da Academia brasileira de Ciências*, *27*(4), 487-498.

**Price, L. I., 1959**. “Sobre um 52steology52rn 52steology52r do Cretacico Brasileiro”. *Boletim Divisao de Geolgia e Mineralogia Rio de Janeiro*. **118**: 1–55.

**Price, L.I., 1945**. A new reptile from the Cretaceous of Brazil. Rio de Janeiro, Departamento Nacional da Produção Mineral, Notas preliminares e estudos, 8 p. Boletim, 25.

**Ricart, R.S.D., Santucci, R.M., Andrade, M.B., Oliveira, C.E.M., Nava, W.R. and Degrazia, G.F., 2019**. Dental histology of three notosuchians (Crocodylomorpha) from the Bauru Group, Upper Cretaceous, South-eastern Brazil. *Historical Biology*, pp.1-12.

**Riff, D. 2003**. Descrição morfológica do crânio e mandíbula de Stratiotosuchus maxhechti (Crocodylomorpha, Cretáceo Superior do Brasil) e seu posicionamento filogenético. *Unpublished Masters Dissertation, Museu Nacional da Universidade Federal do Rio de Janeiro*.

**Riff, D., and Kellner, A. W. A., 2011**. Baurusuchid crocodyliforms as theropod mimics: clues from the skull and 53steology53r morphology of Stratiotosuchus maxhechti (Upper Cretaceous of Brazil). *Zoological Journal of the Linnean Society*, *163*(suppl_1), S37-S56.

**Riff, D., Souza, R.G., Cidade, G.M., Martinelli, A.G. and Souza-Filho, J.P., 2012**. Crocodilomorfos: a maior diversidade de répteis fósseis do Brasil. *Terræ*, *9*(1/2), pp.12-40.

**Romer, A.S., 1956**. Osteology of the Reptiles.

**Rossmann, T., Rauhe, M. and Ortega, F., 2000**. Studies on Cenozoic crocodiles: 8. Bergisuchus dietrichbergi Kuhn (Sebecosuchia: Bergisuchidae n. fam.) from the Middle Eocene of Germany, some new systematic and 53steology53 conclusions. *PalZ*, *74*(3), p.379.

**Salas-Gismondi, R., Flynn, J.J., Baby, P., Tejada-Lara, J.V., Wesselingh, F.P. and Antoine, P.O., 2015**. A Miocene hyperdiverse crocodylian 53steology reveals peculiar trophic dynamics in proto-Amazonian mega-wetlands. *Proceedings of the Royal Society B: Biological Sciences*, *282*(1804), p.20142490.

**Salisbury, S.W., Frey, E., Martill, D.M. and Buchy, M.C., 2003**. A new crocodilian from the Lower Cretaceous Crato Formation of north-eastern Brazil. *Palaeontographica Abteilung A*, pp.3-47.

**Salisbury, S.W., Molnar, R.E., Frey, E. and Willis, P.M., 2006**. The origin of modern crocodyliforms: new evidence from the Cretaceous of Australia. *Proceedings of the Royal Society B: Biological Sciences*, *273*(1600), pp.2439-2448.

**Sasso, C., Pasini, G., Fleury, G., and Maganuco, S., 2017**. Razanandrongobe sakalavae, a gigantic mesoeucrocodylian from the Middle Jurassic of Madagascar, is the oldest known notosuchian. *PeerJ*, *5*, e3481.

**Seebacher, F., Elsworth, P. G., and Franklin, C. E., 2003**. Ontogenetic changes of swimming kinematics in a semi-aquatic reptile (Crocodylus porosus). *Australian Journal of Zoology*, *51*(1), 15-24.

**Sennikov, A.G. and Golubev, V.K., 2006**. Yazidi biotic assemblage of the terminal Permian. *Paleontological Journal*, *40*(4), pp. S475-S481.

**Sepkoski, J.J., 1993**. Na 53steo in the library: new data confirm 53steology53rn53al patterns. *Paleobiology*, *19*(1), pp.43-51.

**Sereno, P., and Larsson, H., 2009**. Cretaceous crocodyliforms from the Sahara. *ZooKeys*, *28*, 1.

**Sereno, P.C. and Arcucci, A.B., 1990**. The monophyly of crurotarsal archosaurs and the origin of bird and crocodile ankle joints. Neues Jahrbuch für Geologie und Paläontologie, Abhandlungen, 180(1), pp.21-52.

**Sereno, P.C. and Wild, R., 1992**. Procompsognathus: theropod, "thecodont" or both? *Journal of Vertebrate Paleontology*, *12*(4), pp.435-458.

**Sereno, P.C., 1991**. Basal archosaurs: phylogenetic relationships and functional implications. *Journal of Vertebrate Paleontology*, *11*(S4), pp.1-53.

**Sereno, P.C., 2005**. Stem Archosauria—Taxon Search. *URL http://www. Taxonsearch. Org/Archive/stem-archosauria-1.0. php*.

**Sertich, J. J., and O'Connor, P. M., 2014**. A new crocodyliform from the 54steol Cretaceous Galula Formation, southwestern Tanzania. *Journal of Vertebrate Paleontology*, *34*(3), 576-596.

**Shirley, M. H., Carr, A. N., Nestler, J. H., Vliet, K. A., and Brochu, C. A., 2018**. Systematic revision of the living African slender-snouted crocodiles (Mecistops Gray, 1844). *Zootaxa*, *4504*(2), 151-193.

**Simpson, G. G. 1937**. New reptiles from the Eocene of South America. American Museum Novitates no. 927: 1-3

**Souza-Filho, J.P., Souza, R.G., Hsiou, A.S., Riff, D., Guilherme, E., Negri, F.R. and Cidade, G.M., 2018**. A new caimanine (Crocodylia, Alligatoroidea) species from the Solimões Formation of Brazil and the phylogeny of Caimaninae. *Journal of Vertebrate Paleontology*, *38*(5), p. e1528450.

**Souza, R.G., Figueiredo, R.G., Azevedo, S.A., Riff, D. and Kellner, A.W., 2020**. Systematic revision of Sarcosuchus hartti (Crocodyliformes) from the Recôncavo Basin (Early Cretaceous) of Bahia, north-eastern Brazil. *Zoological Journal of the Linnean Society*, *188*(2), pp.552-578.

**Stefanic, C.M., Nestler, J.H., Seiffert, E.R. and Turner, A.H., 2020**. New crocodylomorph material from the Fayum Depression, Egypt, including the first occurrence of a sebecosuchian in African late Eocene deposits. *Journal of Vertebrate Paleontology*, p. e1729781.

**Sues, H.D., 2019**. *The Rise of Reptiles: 320 Million Years of Evolution*. JHU Press.

**Sues, H.D., Olsen, P.E., Carter, J.G. and Scott, D.M., 2003**. A new crocodylomorph 54steology from the Upper Triassic of North Carolina. *Journal of Vertebrate Paleontology*, *23*(2), pp.329-343.

**Tavares, S. A. S., Branco, F. R., de Souza Carvalho, I., and Maldanis, L., 2017**. The morphofunctional design of Montealtosuchus arrudacamposi

(Crocodyliformes, Upper Cretaceous) of the Bauru Basin, Brazil. *Cretaceous Research*, *79*, 64-76.

**Tavares, S. A. S., Ricardi-Branco, F., and de Souza Carvalho, I., 2015**. Osteoderms of Montealtosuchus arrudacamposi (Crocodyliformes, Peirosauridae) from the Turonian-Santonian (Upper Cretaceous) of Bauru Basin, Brazil. *Cretaceous Research*, *56*, 651-661.

**Toljagić, O. and Butler, R.J., 2013**. Triassic–Jurassic mass extinction as trigger for the Mesozoic radiation of crocodylomorphs. *Biology 55steolo*, *9*(3), p.20130095.

**Tucker, A. D., Limpus, C. J., McCallum, H. I., and McDonald, K. R., 1996**. Ontogenetic dietary partitioning by Crocodylus johnstoni during the dry season. *Copeia*, 978-988.

**Vasconcellos, F. M., and de Souza Carvalho, I., 2006**. Condicionante etológico na 55steology de Uberabasuchus terrificus (Crocodyliformes, Peirosauridae) da Bacia Bauru (Cretáceo Superior). *Geosciences= Geociências*, *25*(2), 225-230.

**Walker, A.D., 1990**. A revision of Sphenosuchus acutus Haughton, a crocodylomorph reptile from the Elliot Formation (late Triassic or early Jurassic) of South Africa. *Philosophical Transactions: Biological Sciences*, pp.1-120.

**Whetstone, K. N., and Whybrow, P. J., 1983**. *A" cursorial" crocodilian from the Triassic of Lesotho (Basutoland), southern Africa*. Museum of Natural History, University of Kansas.

**Wilberg, E. W., 2015**. What's in na outgroup? The impact of outgroup choice on the phylogenetic position of Thalattosuchia (Crocodylomorpha) and the origin of Crocodyliformes. *Systematic Biology*, *64*(4), 621-637.

**Wilberg, E.W., Turner, A.H. and Brochu, C.A., 2019**. Evolutionary structure and timing of major habitat shifts in Crocodylomorpha. *Scientific reports*, *9*(1), pp.1-10.

**Williamson, T.E., 1996**. Brachychampsa sealeyi, sp nov., (Crocodylia, Alligatoroidea) from the Upper Cretaceous (lower Campanian) Menefee Formation, 55steology55rn New Mexico. *Journal of Vertebrate Paleontology*, *16*(3), pp.421-431.

**Wilson, J. A., Malkani, M. S., and Gingerich, P. D., 2001**. New crocodyliform (Reptilia, Mesoeucrocodylia) from the Upper Cretaceous Pab Formation of Vitakri, Balochistan (Pakistan).

**Wu, X.C. and Chatterjee, S., 1993**. Dibothrosuchus elaphros, a crocodylomorph from the Lower Jurassic of China and the phylogeny of the Sphenosuchia. *Journal of Vertebrate Paleontology*, *13*(1), pp.58-89.

**Young, M. T., and de Andrade, M. B., 2009.**What is Geosaurus? Redescription of Geosaurus giganteus (Thalattosuchia: Metriorhynchidae) from the Upper

Jurassic of Bayern, Germany. *Zoological Journal of the Linnean Society*, *157*(3), 551-585.

**Young, M. T., Brusatte, S. L., De Andrade, M. B., Desojo, J. B., Beatty, B. L., Steel, L., and Schoch, R. R., 2012.** The cranial 56steology and feeding ecology of the metriorhynchid crocodylomorph genera Dakosaurus and Plesiosuchus from the Late Jurassic of Europe. *PloS One*, *7*(9).

**Young, C.C. and Chow, M.C., 1953**. New Mesozoic reptiles from Szechuan. *Acta Palaeontologica Sinica*, *1*, pp.87-109.

**Yu-Hui, G.A.O., 2001**. A new species of Hsisosuchus from Dashanpu, Zigong, Sichuan. *Vertebrata Palasiatica*, *39*, pp.177-184.

## Capítulo II

➔ Este capítulo foi publicado no periódico *Historical Biology*, da editora *Taylor & Francis*, sendo reproduzido no **apêndice** deste volume (ver final) como parte da tese de doutorado do presente candidato. Todos os direitos reservados.

➔ This chapter was published in the journal *Historical Biology* by *Taylor & Francis* and is reproduced here as part of the doctoral thesis of the present candidate. All rights reserved.

## Título

**Um pequeno semaforonte atribuído a Baurusuchidae (mesoeucrocodylia, Crocodyliformes) da Formação Adamantina, Grupo Bauru, Cretáceo Superior do Brasil.**

Daniel Martins dos Santos[1], Rodrigo Miloni Santucci[2], Carlos Eduardo Maia de Oliveira[3] e Marco Brandalise de Andrade[4].

1.Programa de Pós-Graduação em Zoologia, Instituto de Ciências Biológicas, Universidade de Brasília, Brasília, Brasil. 2.Universidade de Brasília, Campus Planaltina (FUP), Brasília, Brasil. 3.Instituto Federal de Educação, Ciência e Tecnologia de São Paulo, Campus Votuporanga (IFSP), Votuporanga, Brasil. 4. Pontifícia Universidade Católica do Rio Grande do Sul, Porto Alegre, Brasil.

## Resumo

Ocorrências de indivíduos jovens e imaturos, relativamente raros no registro fóssil, são importantes devido à grande quantidade de informações morfológicas e evolutivas que revelam sobre o desenvolvimento de uma linhagem. Embora os crocodilomorfos sejam os vertebrados terrestres mais abundantes encontrados na Bacia do Bauru, no sudeste do Brasil, superando em número até mesmo os materiais de dinossauros, muito ainda precisa ser compreendido sobre sua anatomia, ecologia e ontogenia. Fragmentos de ovos, ninhos e locais de nidificação atribuídos a *Baurusuchus* foram descritos anteriormente, mas infelizmente nenhum deles produziu restos de embriões ou filhotes. Aqui, descrevemos, pela primeira vez, material de um jovem notossúquio, recuperado da Formação Adamantina, com características

osteológicas consistentes com Baurusuchidae. Apresentamos e discutimos evidências osteológicas e histológicas de seu estágio ontogenético, revelando caracteres morfológicos distintos da maioria das formas adultas, incluindo lâminas centro-parapofisiais conspícuas e quilhas ventrais desenvolvidas. Dados de tomografia computadorizada também permitiram a identificação de ossificação incipiente e uma nova característica ontogenética na diminuição do volume das cavidades pneumáticas do frontal. Materiais semelhantes aumentarão nossa compreensão da ontogenia e diversidade de Notosuchia, exigindo que caracteres ontogenéticos sejam integrados às futuras filogenias.

**Palavras-chaves**: Crocodylomorpha, Notosuchia, Baurusuchidae, Ontogenia, Grupo Bauru.

## Conclusões

A descrição osteológica e a diversidade fóssil conhecida proveniente do local de coleta convergem para suportar uma afinidade baurussuquídea para este espécime. Adicionalmente, a análise histológica indica que se trata de um jovem precoce, provavelmente com menos de um ano de idade. Assumindo essa classificação taxonômica, várias características, com implicações ontogenéticas, são relevantes e merecem discussão e investigação adicionais:

Neonatos e jovens de crocodiliformes fósseis e crocodilianos modernos tendem a não apresentar fenestras supratemporais completamente desenvolvidas, que estão intimamente relacionadas à força de mordida, e mostram diferentes dietas e estratégias de forrageamento à medida que crescem (Tucker et al. 1996; Gignac e Erickson 2016; Vieira et al. 2018b; Drumheller et al. 2021). Portanto, considerando sua natureza completamente aberta em semaforontes precoces, o desenvolvimento das fenestras supratemporais pode ter ocorrido cedo na ontogenia.

No caso de IFSP-VTP/PALEO-0004 ser um baurussuquídeo, a presença de quilhas ventrais nas vértebras cervicais, lâminas centro-parapofisiais visíveis e a ausência de protuberâncias pré-zigapofisiais parecem ter uma forte influência ontogenética, uma vez que nenhuma dessas características é observada em

espécimes adultos e a primeira foi identificada como uma possível sinapomorfia pós-craniana para sebecossúquios (Pol et al. 2012).

Os ossos dérmicos cranianos, como o frontal, parecem exibir características ontogenéticas, como a diminuição do volume das recessos pneumáticos, o que pode contribuir para uma avaliação mais precisa da idade de possíveis espécimes juvenis, como o *Gondwanasuchus scabrosus* (Marinho et al. 2013), uma vez que propor novas espécies com base em indivíduos imaturos é inadequado.

As evidências osteológicas e histológicas observadas apontam para uma afinidade de um baurussuquídeo juvenil para este espécime. O material apresentado aqui é o primeiro exemplo de um estágio ontogenético precoce de notossúquio recuperado no registro fóssil e está espacialmente associado a locais de nidificação de *Bauroolithos fragilis* Oliveira et al. (2011) e ovos atribuídos a *Baurusuchus*. Curiosamente, o sedimento ao redor deste espécime é de natureza granulométrica e textural semelhante aos arenitos avermelhados associados a locais de nidificação encontrados na Formação Adamantina (Oliveira et al. 2011; Marsola et al. 2016).

Este semaforonte também forneceu informações sobre possíveis divergências osteológicas em relação a indivíduos adultos, incluindo a presença ou ausência de lâminas vertebrais, grau de pneumatização e ausência de ornamentação do esqueleto dérmico. Apesar da ausência de caracteres sinapomórficos totalmente desenvolvidos, a presença de características identificáveis em um estágio ontogenético tão precoce traz a esperança de que futuros espécimes possam ser devidamente atribuídos a clados conhecidos, permitindo possivelmente o estudo de séries de crescimento mais completas para outros grupos de notossúquios, que carecem de dados ontogenéticos.

Por fim, o recente interesse renovado em características pós-cranianas é bem-vindo (Pol et al. 2012; Leardi et al. 2015; Godoy et al. 2016), porém esforços adicionais são necessários, e tais informações aumentariam a probabilidade de avaliação adequada de descobertas futuras.

## Capítulo III

# CRANIAL AND POSTCRANIAL ANATOMY OF A BAURUSUCHID JUVENILE (NOTOSUCHIA, CROCODYLOMORPHA) AND THE TAXONOMICAL IMPLICATIONS OF ONTOGENY.


## Abstract

Baurusuchidae comprised a clade of top-tier terrestrial predators and are amongst the most abundant crocodyliform materials found in the Adamantina Formation, Bauru Basin, Brazil (Campanian-Maastrichtian). Although the preservation of juvenile individuals is somewhat rare in the fossil record, baurusuchid egg clutches, a yearling individual and larger, but skeletally immature specimens have also been reported, presenting a unique opportunity to track anatomical changes throughout their ontogenetic series. Here, we provide a detailed description of the cranial and postcranial osteology and myology of the most complete baurusuchid juvenile found to date. Its cranial anatomy was resolved with the aid of a three-dimensional model generated by the acquisition of CT data, and inferred adductor mandibular musculature was compared to mature specimens in order to assess possible ontogenetic shifts. A subsequent phylogenetic analysis also included the scoring of *Gondwanasuchus scabrosus*, the smallest baurusuchid species known to date, to evaluate its phylogenetic relationships relative to a known juvenile. We find considerable differences between juveniles and adults concerning skull ornamentation and muscle development, which might indicate ontogenetic niche partitioning, and also anatomical and phylogenetic evidence that supports *Gondwanasuchus* being based on a young semaphoront lacking mature cranial features.



**Key words:** Baurusuchidae; Notosuchia; ontogeny; anatomy; myology.

## 1. INTRODUCTION

Baurusuchidae (Price 1945) is a family of medium-sized predatory terrestrial crocodyliforms belonging to more inclusive notosuchian clade of likely Gondwanan origin (Gasparini 1971). Among other characters, these forms are mainly marked by the following commonly referred synapomorphies: (1) oreinirostral skulls with transversely expanded temporal regions (Riff & Kellner 2011); (2) a reduction in the number of teeth (Riff, 2003); (3) ziphodont dentition (Nascimento 2014); (4) high quadrate verticality (Nascimento & Zaher 2010; Riff 2003); (5) medial approximation of the prefrontals (Godoy *et al.* 2014; Montefeltro *et al.* 2011); (6) triangular, fan-like depression on the lateral surface of the jugal's anterior ramus (Riff 2003). In the past decade, several research efforts were directed towards their osteology, phylogeny, neuroanatomy and paleoecology, drawing from abundant fossil materials including cranial and postcranial remains, egg clutches and nesting sites, as well as coprolites (Cardia *et al.* 2018; Dumont Jr *et al.* 2020; Montefeltro *et al.* 2020; Nascimento & Zaher 2010; Oliveira *et al.* 2011, 2021).

Although most fossil finds are concentrated in the Campanian-Maastrichtian Adamantina Formation of the Bauru Basin, southeastern Brazil, fragmentary baurusuchid remains have also been recovered from both Argentina and Pakistan (Gasparini 1972; Martinelli & Pais 2008; Wilson *et al.* 2001). Currently, there are a total of ten valid species described in the Bauru Basin alone, them being: *Baurusuchus pachecoi* Price, 1945; *Baurusuchus salgadoensis* Carvalho *et al.* 2005; *Stratiotosuchus maxcheti* Campos, 2001; *Baurusuchus albertoi* Nascimento & Zaher 2010; *Pissarrachampsa sera* Montefeltro *et al.* 2011; *Campinasuchus dinizi* Carvalho *et al.* 2011; *Gondwanasuchus scabrosus* Marinho *et al.* 2013; *Aplestosuchus sordidus* Godoy *et al.* 2014; *Aphaurosuchus escharafacies* Darlim *et al.* 2021 and

*Aphaurosuchus kaiju* (Martins *et al.* 2023). Curiously, notwithstanding its relatively high diversity, the current composition of baurusuchidae displays no significant amount of morphological disparity, wherein most of its species, with the noticeable exception of *Gondwanasuchus*, represent sympatric high-tier predators of considerable size, thus constituting an ecological problematica.

Despite recent descriptions of postcranial materials (Cotts *et al.* 2017; Godoy *et al.* 2016; Nascimento & Zaher 2010), some well-known semi-complete skeletons remain undescribed (highly complete UFRJ DG 285-R, for instance, Vasconcellos & Carvalho 2010), and more is needed to increase overall anatomical knowledge beyond cranial features, with the potential to improve cladistic resolution. Moreover, important sources of morphological variation of cranial features, which could be mistakenly perceived as a taxon's autapomorphies, such as sexual dimorphism, teratogenesis, ontogeny and taphonomic deformation have not been assessed among the baurusuchid holotypes. These assessments have the potential to affect current baurusuchid taxonomy and need special attention.

Ever since the onset of modern studies into animal development, ontogeny was recognized as crucial for a comprehensive grasp of a species ecology and phylogeny (Gould, 1985). Several fossil archosaurian lineages, including crocodyliforms, have been shown to have undergone substantial morphological shifts throughout ontogeny, be it gradual or rapid (Carr 2020; Drumheller *et al.* 2021; Otero *et al.* 2019; Woodruff *et al.* 2018). Once better understood, these changes have constituted important challenges to proposed past diversity of these groups, potentially identifying recently erected taxons as semaphoronts of species described in the past (Horner & Goodwin 2006, 2009; Scannella & Horner 2010; Woodward *et al.* 2020).

The current work presents, for the first time, a detailed osteological description of a semi-complete baurusuchid juvenile (IFSP-VTP/PALEO-0003), histologically inferred have been around 4 years-old at the time of death (histology to be described in future publication). We provide a three-dimension reconstruction of its skull utilizing computerized tomographic imagery, modelling each bone independently, compare it to other baurusuchid specimens of different sizes, and perform a phylogenetic analysis with the inclusion of *Gonwanasuchus* in the Martinelli *et al*. (2018) data matrix to evaluate its behaviour as a putative juvenile. These analyses allowed for the identification of several ontogenetic changes, listed below, which could be used as a guide to identify skeletally immature baurusuchid individuals among known and undescribed specimens. These developments have important implications not only for baurusuchid taxonomy, but also for other notosuchian clades. Considering other sources of variability should thus be regarded as major line of evidence to support and substantiate novel taxa, impacting current perceptions of the diversity of past environments.

## 2. GEOLOGICAL SETTING

Baurusuchids, as well as a myriad of other notosuchian forms, are most abundant in the Bauru Basin (**Figure 1**), an Upper Cretaceous pelitic/psammitic sedimentary sequence, located in the southeastern part of Brazil, with an estimated outcropping area of roughly 370.000 km$^2$, covering the states of Goiás, Mato Grosso, Mato Grosso do Sul, Minas Gerais, Paraná and, mostly, São Paulo (Fernandes 2004). It is first comprised of one major stratigraphic division, the Caiuá e Bauru groups, the former of which is constituted by sandstone red beds of the Rio Paraná, Goio Erê and

Santo Anastácio formations, with their paleoenvironments interpreted as desert-like conditions which yield rare fossil sites, though that has been changing lately with intriguing archosaurian finds (Batezelli 2010; Fernandes & Coimbra 1996; Kellner *et al.* 2019; Manzig *et al.* 2014; de Souza *et al.* 2021).

The Bauru Group, in turn, is highly fossiliferous, and is classically composed of the Araçatuba Formation, marked by lacustrine, thinly laminated mudstones and siltstones; the Adamantina Formation, with its braided fluvial sandstones; and the high-energy alluvial fan deposits consisting of sandstones and conglomerates of the Uberaba and Marília formations (Batezelli 2010; Batezelli *et al.* 1999; Soares *et al.* 1980). Former age estimates have ranged between the Coniacian-Campanian to the Maastrichtian, with substantial overlap (Bertini 1993; Dias-Brito *et al.* 2001; Goldberg & Garcia 2000), while modern efforts utilizing radioisotopic methods have tended to yield ages towards the young end of the above range, between the Campanian-Maastrichtian (Castro *et al.* 2018; Dias *et al.* 2021). This is also supported by recently described Campanian palynomorphs found in Araçatuba Formation deposits (Arai & Fernandes 2023).

The specimen herein described was collected in 2006, in Adamantina Formation outcrops in the vicinities of the Fernandópolis municipality, State of São Paulo (**Figure 1**). It was embedded in oxidized, massive red sandstones (which may still be seen in the specimen, serving as its substrate after preparation) typical of the aforementioned unit, and, curiously, was also in close lateral proximity with a mostly complete but undescribed skeletally mature individual, which will be the target of future publications.

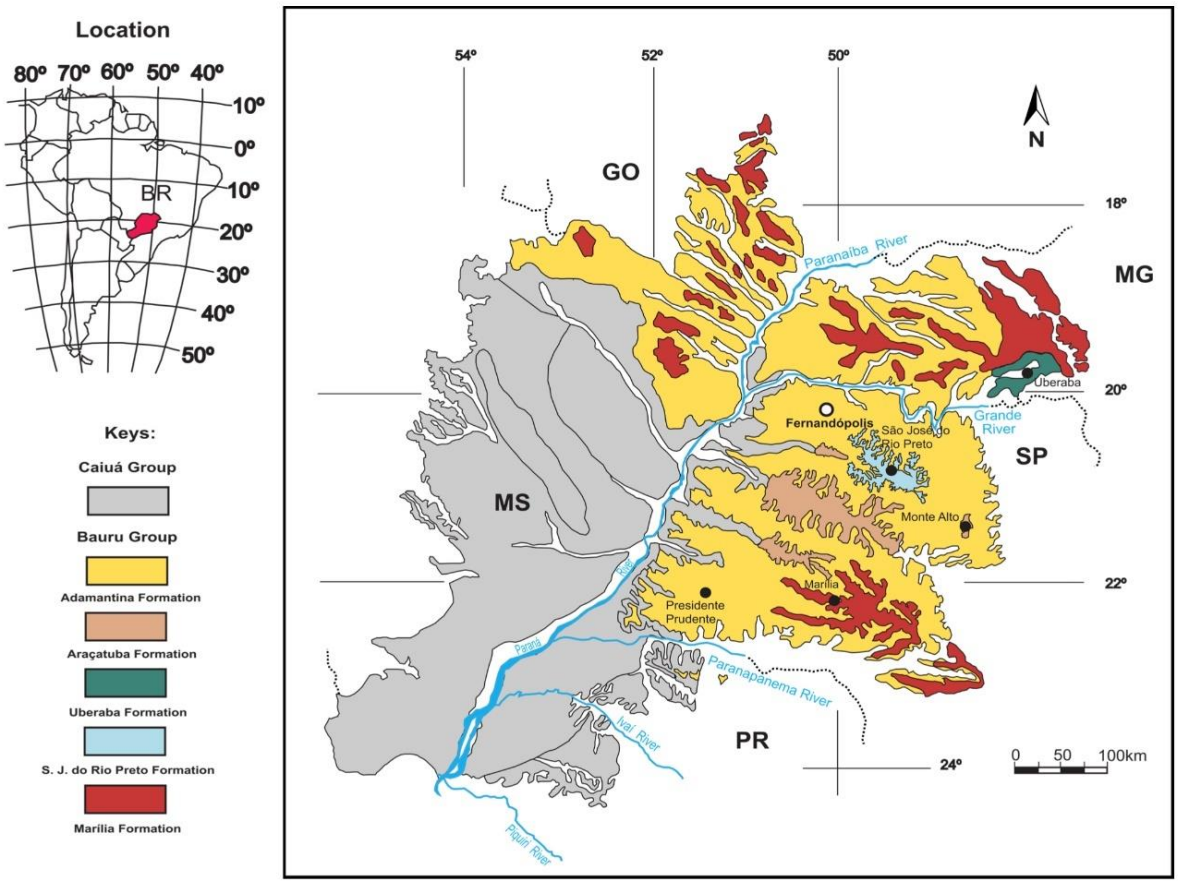


**Figure 1. Location of Bauru Basin within South America and its geological map. The Caiuá sequence is homogenized in grey, while stratigraphic units belonging the Bauru Group are highlighted in colour. The specimen was collected in the vicinities of Fernandópolis-SP municipality, marked in white.**

## 3. MATERIALS AND METHODS

Articulated cranial and postcranial remains were collected utilizing a combination of electrical and hand tools, later being transported from the field to the laboratory within a plaster jacket. Preparation employed a series of pneumatized hand jacks by Paleo Tools®. The specimen will be deposited in the vertebrate paleontology collection of the Federal Institute of Education, Science and Technology of São Paulo (Votuporanga, São Paulo, Brazil), under the number IFSP-VTP/PALEO-0003.

Given the varied nature of osteological and myological nomenclature utilized in the literature, the anatomical descriptions and muscular reconstruction inferences were

based on the preferred/most used terms in the literature, thus being drawed from multiple sources and respecting homologies (Bona & Desojo 2011; van Drongelen & Dullemeijer 1982; Holliday & Witmer 2007; Iordansky 2000). Cranial adductor musculature nomenclature, abbreviations and chosen colour schemes are after the work of Holliday *et al.* (2013) and Sellers *et al.* (2022). Comparisons focused mostly on morphological differences relating to muscular function, while the discussion of the cranial material is mostly focused on ontogeny, comparing it to adult forms. A list of taxa and specimens used for these comparisons is provided below (**Table 1**).

| Taxon and specimens | Source |
|---|---|
| *Baurusuchus sp.*<br>**FEF-PV-R-1/9**<br>**IFSP-VTP/PALEO 0002** | Dumont Jr et al. 2020 |
| *Baurusuchus pachecoi* | Price 1945 |
| *Baurusuchus salgadoensis* | Carvalho et al. 2005 |
| *Baurusuchus albertoi* | Nascimento and Zaher 2010; Nascimento 2014 |
| *Stratiotosuchus maxhechti* | Campos 2001; Riff 2003 |
| *Gondwanasuchus scabrosus* | Marinho et al. 2013 |
| *Aplestosuchus sordidus* | Godoy et al. 2014 |
| *Aphaurosuchus escharafacies* | Darlim et al. 2021 |
| *Campinasuchus dinizi*<br>***CPPLIP 1237***<br>***CPPLIP 1360*** | Carvalho et al. 2011 |
| *Pissarrachampsa sera*<br>**LPRP/USP 0049** | Godoy et al. 2018 |
| *Sebecus icaeorhinus* | Molnar 2010; Pol *et al.* 2012 |
| *Mariliasuchus amarali* | Nobre & Carvalho 2013 |
| *Araripesuchus tsangtsangana* | Turner 2006 |
| *Simosuchus clarki* | Georgi and Krause 2010; Kley et al. 2010; Sertich and Groenke 2010 |
| *Alligator mississippiensis* | Romer 1923; Witmer & Ridgely 2008 |
| *Melanosuchus niger* | Vieira et al. 2018a; Vieira et al. 2018b |

**Table 1. List of taxa and specimens mentioned in osteological and myological comparisons as well as their respective sources.**

### 3.1 Computerized tomography and processing

After mechanical preparation, the skull was separated from the skeleton for computerized tomography (CT) image acquisition using a Revolution EVO model at IMEB (Imagens Médicas de Brasília-DF), resulting in 392, 593, and 692 slices, respectively of 0.50 mm each, with resolution of 512 × 512 pixels, 140 kV, and 240 mA. Data was processed in the freely available software InVesalius® (Amorim *et al.* 2015), where manual segmentation and three-dimensional modelling of each skull bone was conducted. A yet undescribed adult baurusuchid skull, FEF-PV-R-1/9, has been scanned and modelled under the same conditions described above, and is further utilized below for myological reconstructions and comparisons.

### 3.2 Phylogenetic analysis

IFSP-VTP/PALEO-0003 was codified into the Martinelli *et al.* (2018) matrix, which is expanded upon and a more recent version of Pol *et al.* (2012, 2014) and Fiorelli *et al.* (2016), comprising 440 characters and 115 taxa. *Gondwanasuchus scabrosus*, the smallest known baurusuchid, was also codified and included in the analysis in order to compare and contrast its position relative to the juvenile herein described. Previously, this taxon had only been included in matrices encompassing only baurusuchids (Darlim *et al.* 2021b; Godoy *et al.* 2014; Montefeltro *et al.* 2011). The following series of 43 ordered characters were maintained from the work of Fiorelli *et al.* (2016): 1, 3, 6, 10, 23, 37, 43, 44, 45, 49, 65, 67, 69, 71, 73, 77, 79, 86, 90, 91, 96, 97, 105, 116, 126, 140, 142, 143, 149, 167, 182, 187, 193, 197, 226, 228, 279, 339, 356, 357 and 364.

The analyses utilized TNT software (Goloboff *et al.* 2008) and were run in two consecutive rounds to obtain the most parsimonious trees (MPTs). Similarly to previous

works that utilized this data matrix, an attempt to run the analyses including all 115 taxa derived poorly resolved topologies, making necessary the testing and pruning of specific group of species based on fragmentary materials (described below). The first round utilized tree bisection reconnection (TBR) swapping algorithm, resulting in 170 trees retained, followed by a second round of branch swapping which yielded 5568 MPTs, from which the strict consensus was obtained as a working hypothesis. Attempts utilizing the 'new technology' algorithm derived identical results.

## 4. RESULTS

### 4.1 Systematic paleontology

Crocodyliformes Hay, 1930, sensu Benton and Clark, 1988

Mesoeucrocodylia Whetstone and Whybrow, 1983

Notosuchia Gasparini, 1971

Baurusuchidae Price, 1945

### 4.2 State of preservation and taphonomy

The specimen consists of a semi-complete skeleton, including the skull, cervico-dorsal series with three preserved dorsal osteoderms, sacrum, shoulder and pelvic girdles, as well as appendicular elements, lacking only the tail. Most of the bones were found still articulated as they would have been in life, with zygapophyses still connected up to the 13$^{th}$ dorsal vertebra, glenohumeral condyle still attached to the scapular glenoid and femoral head within the acetabulum (**Figure 2a**). The right coracoid and humerus were dislocated and preserved parallel to each other. Posteriorly, the pelvic girdle displays a surprising level of articulation, with not only the three sacrals still in

place, but also the ischia and pubes. The latter remain articulated medially along the pubic symphysis and maintain contact posteriorly with the ischium along the pubic peduncle.

The skull preserves left-right symmetry when seen in both dorsal and palatal views, indicated by similar orbit size in addition to pterygoid and choanal morphology (**Figure 2b**). Considerable erosional damage removed most of the dorsal surface of the skull table, substantially altering the frontal, postorbitals, parietals, and squamosals. Fortunately, the left supratemporal fossa and fenestra were preserved. Sculpturing patterns of dermal bones are fully visible, being most conspicuous on the rostrum and symphysial portion of the dentary. There is evidence of dorsoventral flattening of the skull in the form of a fracture that runs ventroposteriorly through the dentary and infratemporal fenestra, displacing the anterior ramus of the jugal in relation to the posterior one, and also with the partial collapse of the temporal bar. The choanal septum and medial and lateral eustachian foramina are both preserved with minimum distortion.

Postcranial elements also display evidence of dorsoventral taphonomic flattening. The femora, for instance, are more laterally projected than expected, given that notosuchians (including baurusuchids) are suggested to have had a parasagittal gait (Riff & Kellner, 2011; Tavares *et al*., 2018). Ischia position also points to taphonomic compression due to their iliac blade not being ventromedially joined. A clear torsion of the axial skeleton can be observed as one follows the axial series posteriorly. Starting at the 14$^{th}$ dorsal, vertebrae positions vary from being laid on their left sides to a more vertical position, and, in addition to the decreasing level of rib articulation posteriorly, possibly reflects disarticulation of these elements while still embedded in soft tissues during decay. Lastly, all appendicular bones, with minor local

exceptions, could be accounted for, including anterior and posterior stylopods, zygopods and autopod elements. The flexion of the manus under the ulna and radius is common to other known baurusuchid skeletons (Vasconcellos & Carvalho 2010) and is suggested here to possibly represent a resting posture.

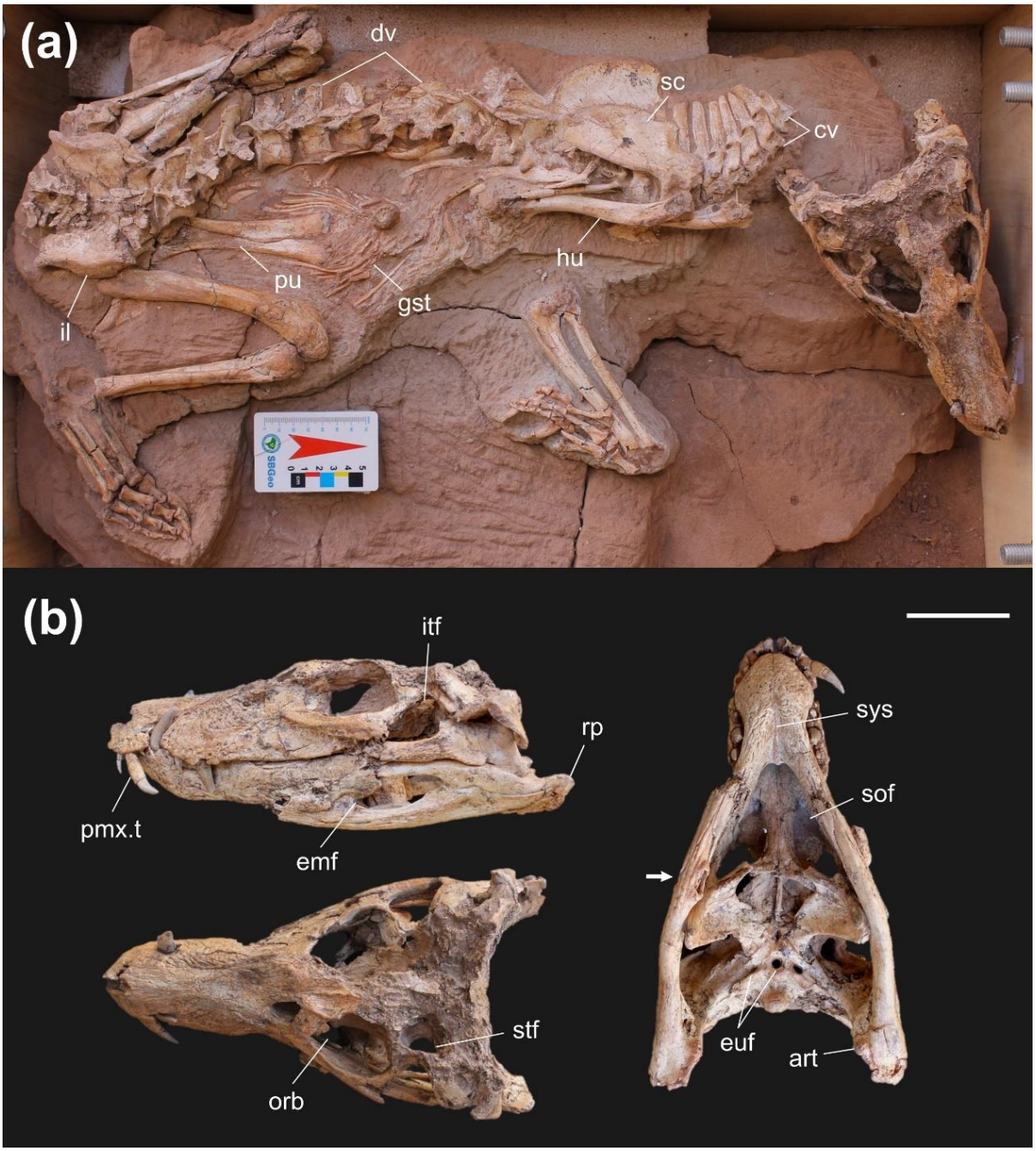


**Figure 2. General view of the specimen. (a) semi-complete, articulated skeleton after preparation; caudal series is lacking; (b) annotated cranium and mandibles in left lateral, dorsal and palatal views. Abbreviations: art, articular; emf, external mandibular fenestra; euf, eustachian foramina; itf, infratemporal fenestra; orb, orbit; pmx.t; premaxillary tooth; rp, retroarticular process; sof, suborbital fenestra; stf; supratemporal fenestra; sys, mandibular symphysis. Scale bar = 5 cm.**

### 4.3 Skull and mandibles

The skull material of IFSP-VTP/PALEO 0003 naturally concentrates the most conspicuous ontogenetic differences in relation to adult individuals. It is marked by relatively large orbits, that roughly divides it into two equal preorbital and postorbital lengths, shallower mandibular symphysis, more posterior-projecting retroarticular processes and incipient sculpturing of dermal bones. Most of its external surface is well preserved, except for the skull table (frontal, parietal, postorbitals and squamosals). The acquisition of computerized tomography allowed for the individual reconstruction of most bones (**Figure 3**), but unfortunately the internal structures of the basicranium are heavily distorted and/or fragmented, preventing modelling beyond their external profiles.

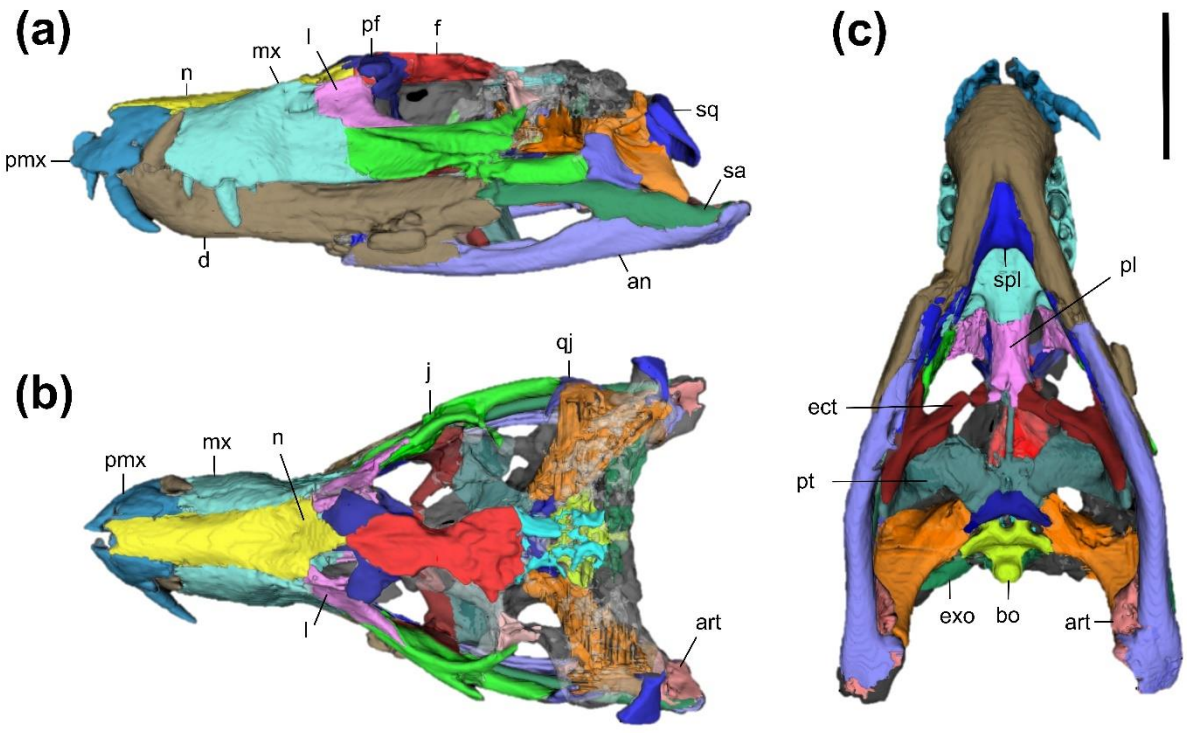


**Figure 3. Digital model of the complete, articulated cranium of IFSP-VTP/PALEO 0003 in (a) left lateral, (b) dorsal and (c) ventral views. Most bones were individually reconstructed, except for damaged elements of the basicranium and skull table. Abbreviations: an, angular; art, articular; bo, basioccipital; d, dentary; ect, ectopterygoid; exo, exoccipital; f, frontal; j, jugal; l, lacrimal; mx, maxilla; n, nasals; pf, prefrontal; pl, palatines; pmx, premaxilla; pt, pterygoids; q, quadrate; qj, quadratojugal; sa, surangular; spl, splenials; sq, squamosals. Scale bar = 5 cm.**

### 4.3.1 Premaxillae

These are paired elements that comprise the anteriormost portion of the rostrum, being anteroposteriorly longer than wide or tall, and possessing four premaxillary teeth. The premaxillae encircle the anteriorly facing external nares, contacting the nasals dorsally and the maxillae posteroventrally (**Figure 4a, b and c**). They display a trapezoidal outline in lateral view, marked by a vertical anteromedial margin, where counterparts meet collaterally, a straight dorsal edge as it contacts the nasals, and a convex ventrolateral alveolar border. In both dorsal and ventral views, it has a more triangular shape. Anteriorly, as left, and right elements contact, the premaxillae have an ascending, posterodorsal tubular process, which, as in other baurusuchids, contributed to the formation of the internarial bar, but here is fragmented at its base, leaving non-bisected open nares, which here is considered a taphonomic artifact. Nasals also contribute to the internarial bar formation, but their dorsal contribution is also missing.

External nares are ellipsoidal in anterior view, with a posterolateral major axis, and are surrounded by conspicuous semi-circular shallow depressions, the perinasal fossae (**Figure 4b**). In lateral aspect, the premaxillae meet the nasals and the maxillae posteriorly along a tapering ascending process, resulting in a wedge-like triple contact between these bones. Its posterior border is concave due to the formation of a well-defined notch between the premaxillary and maxillary bones for the insertion of a fourth, hypertrophied dentary tooth. The presence of the notch also obscures the premaxilla-maxilla suture, precluding a correct assessment of its conformation from this vantage point. Ventrolaterally, the premaxillae have shelves that emerge from the medial alveolar margins and are sutured to each other along the sagittal line, helping to form the anterior portion of the palate. Curiously, with the aid of computerized

imagery, it was possible to determine that cross-sectional shape of the premaxillary shelves is triangular, with clear, pneumatic tubular foramina running anteroposteriorly (**Figure 4a$_2$**). The premaxillary palatal surface is marked anteriorly by the *foramen incisivum*, a relatively large losangular-shaped opening, in addition to circular, alveolar-like fossae, between the first and second premaxillary teeth diastema, for the placement of the first procumbent dentary teeth.

Sculpturing is more pronounced dorsally, closer to the more heavily ornamented nasals, consisting of elongated shallow grooves, becoming smoother ventrally. Three, small circular nutrition foramina can be seen above the lateral alveolar margins of teeth two, three and four on the left side, while only two are present on the opposing side. A distinctive feature of these premaxillae, in comparison with more mature individuals, is the fact they mostly overhang the dentary symphysis anteriorly, resulting in the first two premaxillary teeth not coming into contact with the anterolateral surface of the dentary.

The premaxillae contain a total of four teeth set in a single wave, increasing in size up to the third tooth and then decreasing abruptly at the fourth alveolus, preceding the premaxillary-maxillary notch, as seen in anterolateral view. All teeth display mesio-distal serrated carinae, characterized by homogeneous denticles. The first premaxillary incisiviform tooth is marked by a somewhat symmetrical D-like cross-section (Hendrickx *et al.* 2015), with transversely shifted serrated carinae, while posteriorly teeth become more labio-lingually compressed with an elliptical sectional outline, a pattern that continues on the maxillary teeth series.

### 4.3.2 Maxillary bone

Comprising the majority of the lateral aspect of the rostrum, the maxillary bone displays a complex three-dimensional morphology, defined by a lateral process, which

is lateromedially compressed and nearly vertically oriented, contributing to the conspicuous oreinirostry characteristic of baurusuchids (Price 1945; Riff & Kellner 2011), as well as its palatal shelf, that meets medially with its counterpart to form an extensive portion of the secondary palate (**Figures 3 and 4a,b and c**). This element contacts the premaxilla anteriorly, the nasals dorsally, the lacrimals posterodorsally, the jugal posteriorly, and the ascending process of the pterygoid ventrally.

In lateral view, the maxillary bone possesses a trapezoidal profile that tapers anteriorly and forms the posterior margin of the premaxillary-maxillary notch, within which the fourth hypertrophied dentary tooth is allocated. Its ventral margin is marked by an anterior concavity, following the maxillary tooth row, transitioning to a more rectilinear aspect posteriorly towards the jugal (**Figure 4a-b**). As mentioned above, the lateral surface of the maxilla is more verticalized in comparison with other crocodylomorph clades, but it differs substantially from the sebecid condition, where the maxilla and the nasals meet to form a triangular cross-section of the rostrum, with a somewhat sharp dorsal end, while in baurusuchids their contact produces a rounder shape dorsally and laterally, due to both nasal and maxillary surface concavities (**Figure 3a-a$_1$**).

The internal anatomy of the palatal shelf could only be assessed with the aid of computerized tomography images, and the axial slices were particularly revealing (**Figure 3a$_1$**). The images show the palatal shelf in an orthogonal angle in relation to the lateral process of the maxilla, emerging as a thick, vertical wall, forming the medial margins of maxillary alveoli, and then proceeding as a transverse platform. The latter has a triangular cross-section, being dorsoventrally taller close to alveoli and tapering to a bony slate at the sagittal plane. Throughout its length, the maxilla displays a highly pneumatized palatal shelf, with most of its internal volume filled by recesses. These

openings occur in a similar position and might be homologous to maxillary sinuses described for the extant crocodylians, such as *Alligator mississippiensis* (Witmer & Ridgely 2008), and were also recently observed in adult *Campinasuchus* specimens (Fonseca *et al.* 2020). Due to taphonomic dorsoventral compression, some intricate bony laminae within the palatal recesses collapsed, precluding a correct assessment of its morphological complexity, although it is clear that, along some portions, the recesses were multichambered. Dorsally, the internal surface of the palatal shelf is concave, and is tenuously bisected by a sharp protuberance, defining left and right portions. Consequently, these structures define the ventral and lateral limits of the nasopharyngeal duct (sensu Witmer & Ridgley, 2008). Anteriorly, the duct is formed by the palatal shelf and nasal bones only, whereas posteriorly, as the maxillary bones deflect laterally, it is capped by the anterodorsal pterygoid extension, shaping a sigmoidal-shaped cavity.

Given the ziphodont condition of baurusuchid crocodyliforms, the alveoli here display an elliptical outline, being slightly lateromedially compressed. Moreover, these are divided by more conspicuous diastemas in comparison with adult forms, where alveoli are often confluent. Maxillary teeth, as shown by computerized tomography data (**Figure 4**), are deeply rooted within the maxilla, reaching the dorsal region, and thus creating visible bulges on its lateral surface. These are organized into a single wave, of which the third tooth is the largest, and like posterior premaxillary teeth have serrated carinae and display further labiolingual compression. With ontogenetic progression and the increasing robustness of the teeth, the aforementioned bulges become more marked, as seen in skeletally mature individuals. Sculpturing varies depending on the surface observed. The dorsolateral surface is more heavily ornamented than the lateral alveolar margin, bearing vermiform grooves and pits, at

the same time as the latter displays four neurovascular foramina along the third, fourth, and fifth maxillary teeth. In palatal view, it is possible to discern incipient sculpturing around the raised alveolar margins.

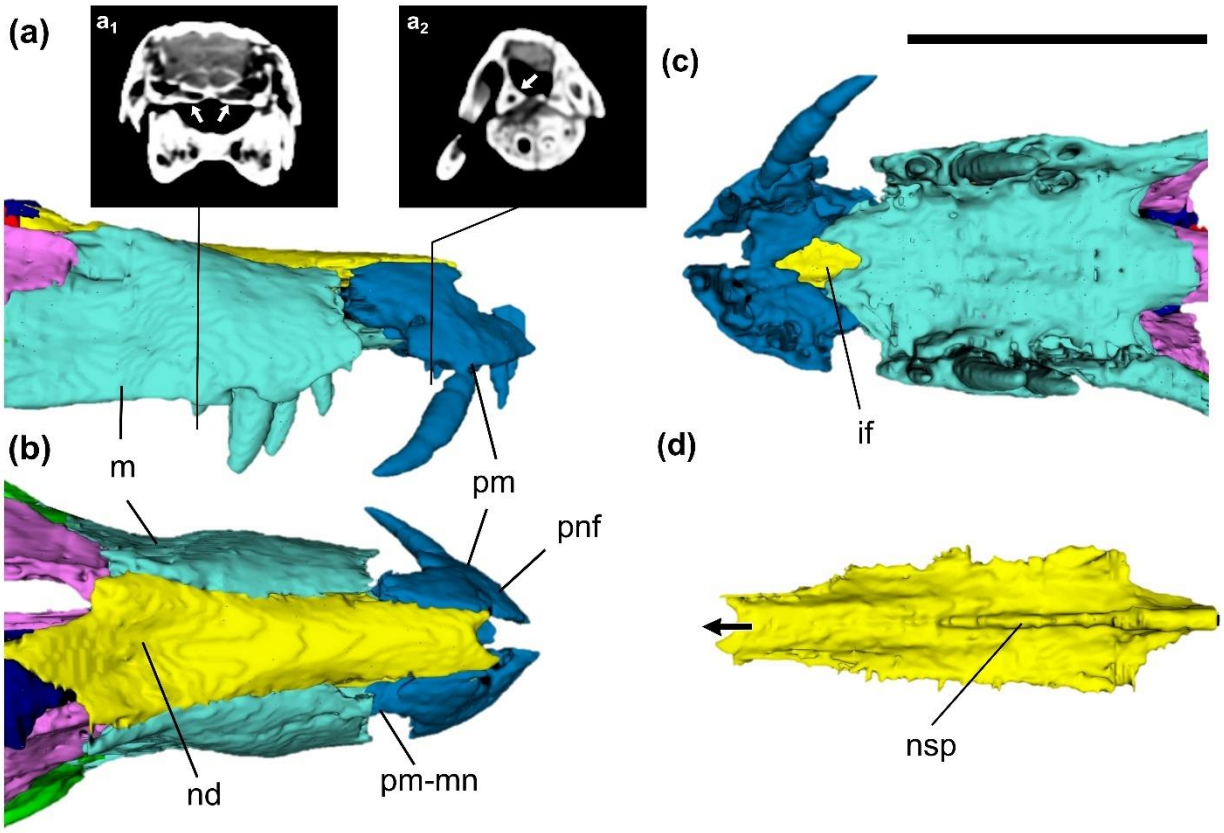


**Figure 4. Three-dimensional rostrum model of IFSP-VTP/PALEO 0003, highlighting individual bone morphology. (a) left-lateral view (reversed), showing premaxillary and maxillary alveolar margins and posterior (a1) and anterior (a2) transverse cross-sections. White arrows indicate pneumatic recesses. (b) rostrum in dorsal view. Note the posterior constrictions of the nasal and its wide depression. (c) Palatal view where a losangular-shaped incisivum foramen is observed. (d) Fused nasals in ventral view with well-developed nasal septum that reaches mid-length. Scale bar: 5 cm. Abbreviations: if, *foramen incisivum*; m, maxilla; nd, nasal depression; nsp, nasal septum; pm, premaxillae; pm-mn, premaxillary-maxillary notch.**

### 4.3.3 Nasal bone

The nasals are fused into a single bone making up the entire dorsal length of the rostrum (**Figure 4a-b**). It contacts the premaxilla anteriorly, the maxilla laterally, the prefrontals/frontals posteriorly, and the lacrimals posterolaterally. It is dorsoventrally flattened, having an elongated profile in dorsal view, where its length vastly exceeds

its width. The nature of its contacts with the surrounding bones varies. Anteriorly, it takes part in a triple wedge-like junction with the premaxilla and the maxilla, dorsomedially to the fourth dentary tooth notch, whereby laterally it is mostly overlapped by the maxilla (**Figure 3**). Unfortunately, the perinarial region of the nasal has been broken off, precluding the preservation of the internarial bar.

When seen from a dorsal perspective, the nasal shows relatively straight, parallel margins up to its mid-length, where it becomes slightly concave laterally, before it expands transversely as it approaches the prefrontals and the frontal. Additionally, the dorsal concavity and convexity also shift along its length, being mostly flat above the premaxilla, then developing a moderate concavity with a somewhat rhombic cross-section at the mid-rostrum segment, then finally forming a wide depression anterior to the nasal-frontal suture. As it widens posteriorly, the nasal takes part in the anterior palpebral attachment surface, an anteroposteriorly long facet that reaches the anterodorsal rim of the orbits. Ventrally, along its posterior half, it possesses an incipient septum that divides the nasal cavity into left-right portions (**Figure 4d**). Ornamentation consists of rectilinear grooves closer to the external nares and more randomly placed, vermiform grooves posteriorly. Minute rounded pits, that are common on the nasals of adult forms, are absent in this specimen.

4.3.4 Jugals

The jugals of IFSP-VTP/PALEO-0003, as in most crocodyliforms, make up the lateral cheek region of the skull and contact the maxillae anteriorly, the lacrimals anterodorsally, the ectopterygoids ventrally, the postorbitals posterodorsally and the quadratojugals posteriorly (**Figure 3a-b**). They are laterally flattened, substantially longer than tall, and their medial surfaces are concave, thus resulting in their anterior

and posterior ends curving slightly inwards. In lateral view, the jugals have a triradial architecture, marked by roughly equidistant anterior and posterior rami, in addition to an ascending posterodorsal process that, alongside the postorbitals, form the postorbital bar (**Figure 5**). The anterior ramus is formed by a dorsoventrally expanded projection that contributes to the ventral margin of the orbits. This border is gently concave along its length. It also contains a conspicuous infraorbital crest on its dorsolateral surface that tapers anteriorly, reaching the jugal-maxilla contact, and thickens posteriorly, merging with the posterior ramus. Ventral to the crest, a triangular depression develops, a common feature also observed in adult forms and a previously cited baurusuchid character (Montefeltro *et al.* 2011) (**Figure 5a-b**).

The posterior ramus is a rod-like projection (roughly circular cross-section) that meets the quadratojugal along a vertical, sutured contact. Furthermore, its dorsal surface forms the ventral border of the infratemporal fenestra. Internally, the jugals are characterized by their pneumatized nature. Along the posterior ramus runs a tubular-like recess that, as it extends to the anterior region, becomes dorsoventrally deeper and conforms to the internal morphology of the jugal. Axial and coronal CT scan slices, in addition to the presence of neurovascular foramina, suggests that there was external-internal connection between these structures. The ascending process adjoins with the postorbital descending equivalent in a planar contact, contributing to roughly half of the postorbital bar, which also forms the anterior border of the infratemporal fenestra.

Sculpturing varies throughout the jugal´s surface, with anteroventrally-inclined grooves predominating on the lateral triangular depression, alongside local foramina, while posteriorly, vermiform horizontal grooves are present, especially close to the jugal-quadratojugal contact. Medially, the surface is mostly smooth, with the exception

of neurovascular foramina that emerge close to the mid-length region, near the transition between anterior and posterior rami. The maxilla-jugal contact is marked by a sheet-like lateral overlap of the jugal over the maxilla, which is lateromedially thicker. Ventrally, these also constitute a triple contact with the ectopterygoid platform.

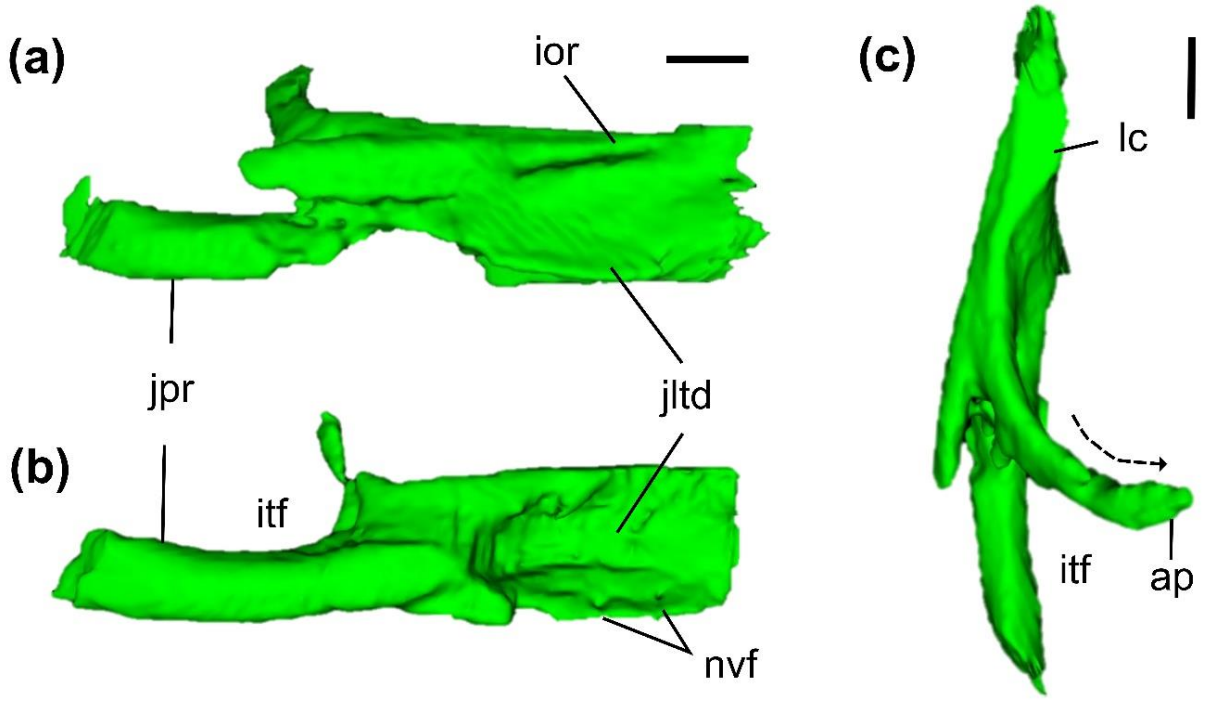


**Figure 5. Isolated (a) left (flipped) and (b) right jugals of IFSP-VTP/PALEO 0003. (c) left jugal in dorsal aspect showing a posteromedially inclined ascending process. The latter contributes to the postorbital bar. Abbreviations: ap, ascending process; itf, infraorbital fenestra; ior, infraorbital ridge; jpr, jugal posterior ramus; jtld, jugal triangular lateral depression; nvf, neurovascular foramina. Scale bar = 1 cm.**

4.3.5 Quadrate

Temporal and braincase bones display a substantial degree of fragmentation and erosion. The quadrates, in particular, have been affected by vertical compression, collapsing their dorsal process almost completely, including the otic cavity, and hampering an assessment of its arrangement with braincase elements. Distally, however, they are well-preserved, displaying ventroposteriorly oriented mandibular condyles (**Figure 6a-b**). As in other crocodyliforms, the quadrate and quadratojugal

are anterodorsally inclined, sharing a long contact with similar orientation. Its lateral surface bears a wide and shallow semi-circular depression, a baurusuchid synapomorphy (Riff 2003), that reaches the borders of the otic cavity as well as the quadratojugal's posterior margin. Posteriorly, it comes into contact with the squamosals along their posteroventral processes, which extend laterally and are still preserved. In occipital view, this suture becomes an acute, crest-like feature that divides the quadrate into lateral and medial surfaces.

The mandibular condyles are transversely oriented (perpendicular to the rostral-occipital axis) and well separated by a medial sulcus. The lateral hemicondyle is more robust and placed dorsally with respect to the medial one, while the latter is considerably more ventrally developed and narrower, thus generating a medially slopping condylar plane, following the observed superficial inclination of the articular. The quadrate's ventral surface is also moderately well-preserved, revealing a dorsomedial curvature of as they suture with ventral braincase elements, including the basioccipital, basisphenoid and pterygoids. This ventral facet is slightly concave and displays two tendon-fixating crests that composed the quadrate aponeurosis (**Figure 6a**). The first is a low-relief crest that borders the quadrate-quadratojugal suture and, consequently, the internal infratemporal fenestra, while the other is a more medially dislocated, robust, and sinuous crest, it curves towards the basisphenoid at a diverging angle from the former. These are, respectively, interpreted as homologous to crests A and B as seen in modern crocodylians, and are associated with the origins of mAMP and mAMES muscle groups (Holliday & Witmer 2007; Iordansky 2000).

### 4.3.6 Quadratojugal

Consists of a L-shaped, lateromedially thin bone, marked by an anterior and a dorsal process, making up the anterior infratemporal region of the specimen (**Figure 6a-b**). Its anterior process is short and thicker than other portions of the bone, inheriting the condition from the posterior jugal ramus, to which is firmly sutured along a vertical irregular contact close to the ventroposterior edge of the infratemporal fenestra. The dorsal process is a thin, anteroposteriorly short bony wall that ascends towards the temporal bar, forming most of the posterior limits of the aforementioned fenestra. Moreover, its dorsal end is slightly anterodorsally deflected. Its dorsalmost edge was not preserved enough for an assessment of its contacts. Posteriorly, it contacts the quadrate along an extensive suture that probably reached the ventral surface of the temporal bar. Its base is considerably anteroposteriorly longer than its apical region, forming a larger surface area that contributes to the lateral semi-circular depression of the quadrate. Its ventral border is convex up to the jugal contact, where a small gap between the skull and the mandible forms. The lateral surface displays noticeable striations and grooves, especially closer to the quadratojugal-jugal suture.

### 4.3.7 Prefrontals

These are paired, losangular-shaped elements in dorsal view, with limited medial approximation that does not prevent frontal-nasal contact (suggested as a baurusuchinae synapomorphy by Montefeltro et al., 2011). The prefrontals are bounded by the frontals posteromedially, the nasals anteriorly, the lacrimals ventrolaterally and the palatines and pterygoid ventrally. Along their lateral margins, which contribute to the anterodorsal border of the orbits, the prefrontals have a ventrally deflected surface for the attachment of the anterior palpebrals. This is an elliptical surface that extends into the nasals. Ventrally, the prefrontals are marked by lateromedially broad, and anteroposteriorly flattened pillars, clearly visible through the

orbits. Their surface curve outwards, reaching the medial surface of the orbital rim (**Figure 6c$_1$-c$_2$**). As the prefrontal pillars descend to contact the pterygoid anterior projection and the palatines, they seem to narrow into laminar processes, but their distal ends are still mostly embedded in sediment, hindering a description of their shape. The olfactory bulb passage is located dorsomedially at the contact with the ventral surface of the frontal, displaying a rounded outline. Ornamentation is only present on its dorsal surface and, contrasting adult forms, lacks deep grooves.

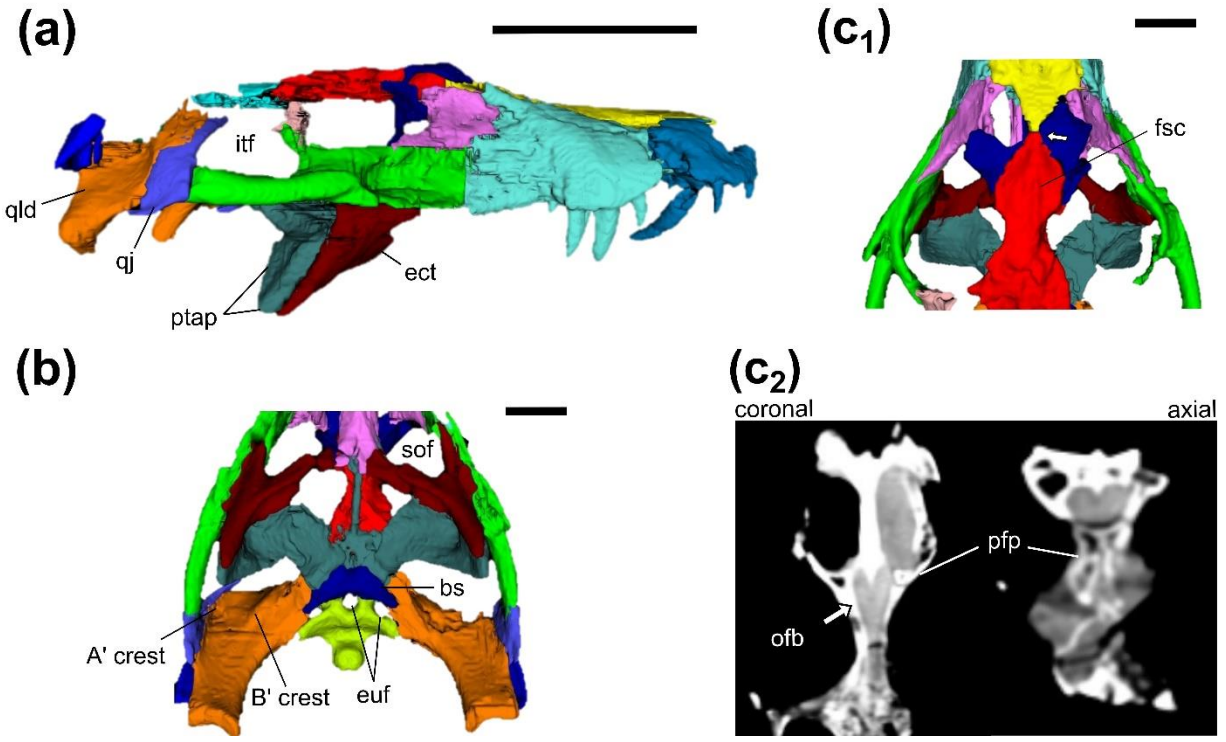


**Figure 6. Digitally reconstructed skull with quadrates and quadratojugals in ventral (a), and (b) lateral views. (c$_1$-c$_2$) shows in detail the medial approximation of the prefrontals, which do not prevent the contact between tapering nasal and frontal processes. Coronal and axial slices are also provided to illustrate the olfactory bulb cavity on the ventral surface of the frontal and the prefrontal's descending pillars, that come in contact with anterior end of the pterygoids. Abbreviations: bs, basisphenoid; ect, ectopterygoid; euf, eustachian foramina; fsc, frontal's saggital crest; itf, infratemporal fenestra; ofb, olfactory bulb; pfp, prefrontal pillars; ptap, pterygoid aponeurosis; qj, quadratojugal; qld, quadrate's lateral depression; sof, suborbital fenestra. Scale bars, (a) = 5 cm; (b-c$_1$) = 2 cm.**

### 4.3.8 Frontal

The frontal of IFSP-VTP/PALEO 0003, as most of its skull roof, is poorly preserved. Its dorsal surface is mostly eroded, lacking texture and ornamentation, in addition to being fragmented at lateral regions bordering the orbits, thus not representing the original shape *in vivo*. Nevertheless, it can be established, based on adult forms and other semaphoronts, that the frontal consisted of a trapezoidal element in dorsal view, contacting the parietal posteriorly along a transverse suture, the prefrontals anterolaterally and the nasals anteriorly (**Figure 6c$_1$-c$_2$**). The anterodorsal region is better preserved, bearing a somewhat sharp sagittal crest bound on both sides by anteroposteriorly long depressions. The crest seems to have originated posteriorly, tapering forwards, and failing to reach the frontal-nasal contact. Anteriorly, the frontal has a slender process that is laterally constricted by the prefrontals, reaching the nasals only at a single point. Ventrally, the frontal has medially inclined surfaces that meet at the longitudinal plane to form the concavity for the passage of the olfactory bulb. The internal structure, as revealed by CT data, is marked by lateral and medial recesses which volume in relation to cortical bone seem to be ontogenetically conditioned, with diminishing pneumatic openings being substituted by cortical bone (see Santos *et al*., 2021).

### 4.3.9 Postorbital

The postorbitals are major elements of the skull roof, bounding the supratemporal fenestra anterolaterally as well as forming the dorsal margins of the infratemporal fenestra. It is part of a complex arrangement of bones involving the skull roof, temporal region and the basicranium, contacting the frontal anteromedially, parietal posteromedially, squamosal posterolaterally, jugal anteroventrally,

quadratojugal posteroventrally and the laterosphenoid anteromedially. Due to the poor preservation state of the skull roof, the dorsal surface of the postorbital is mostly damaged, lacking the temporal bar and the original surface texture. What is preserved of the postorbital has a quadrangular shape in dorsal view, with a straight dorsal border, a concave anterior margin, part of the posterior orbital rim, and a sharp ventral concavity that delineates a triangular infratemporal fenestra. Dorsally, it displays a L-like shape, marked by a dorsoventrally compressed medial process. A descending anterior process contributes to the postorbital bar, having a more elliptical cross-section at its encounter with the jugal. There is also a laminar posterior process that is overlapped by the quadratojugal alongside the posterior edge of the infratemporal fenestra. The poorly preserved supratemporal region reveals a fully open fenestra, although proportionally smaller in comparison to adult individuals, with verticalized walls and incipient development of surrounding supratemporal fossae. No significant ornamentation was observed. The anterior insertion surface for the posterior palpebral was not preserved on neither side.

4.3.10 Lacrimals

The lacrimals comprise lateromedially compressed, laterally concave and vertically oriented elements with a quadrangular outline in lateral view. They are located on the posterolateral facet of the rostrum, contacting the maxilla anteriorly, nasals and prefrontals dorsally, frontal medially and jugals ventrally (**Figures 3 and 6**). Their anterior contact with the maxilla is convex in lateral view, being slightly anterodorsally inclined, while ventrally they possess a straight, horizontal contact with the jugals, extending posteriorly along a tapering process. Posteriorly, the lacrimals have a curved/concave margin that makes up the anterior rim of the orbital rim. A posterolateral view reveals that the dorsal region is medially deflect in respect to the

ventral one, thus resulting in its contact with the prefrontal pillars. In addition to the nasals and the prefrontals, the attachment surface for the anterior palpebral is also formed by the lacrimals. These constitute an auxiliary support surface that forms a dorsal platform. Despite the fact that a lacrimal canal is not visible externally, the CT data seems to indicate a posterodorsal emergence, with the main duct running anteroventrally along its length. The external surface lacks ornamentation, although the infraorbital crest reaches the lacrimal anteroventrally.

4.3.11 Palatines

These comprise paired bones of the palate that meet medially along the sagittal plane to form a single tube-like, anteroposteriorly long element. They contact the maxilla anteriorly, the pterygoids dorsally (composing the nasopharyngeal tract) and the ectopterygoids posterolaterally (**Figures 3 and 7**). Laterally, their surfaces are concave and slope ventromedially, creating shallow fossae bounding the medial edge of the suborbital fenestrae. In ventral view, the palatines become transversely expanded posteriorly, bifurcating to meet the ectopterygoids and forming a straight posterior margin that overhangs the choanal septum as it enters the tract. These lateral processes together form a visibly triangular area ventrally, bounded laterally by a relief change as it approaches the palatine's lateral surface. This region bears a relatively large pneumatic foramen at the medial plane. In cross-section, the palatines are crescent-shaped, composing the bottom half of the nasopharyngeal tract. Pneumatic cavities also mark the palatines close to their contact with the maxillary bones anteriorly. Superficially, the palatines are mostly smooth, not displaying any ornamentation or muscle scars.

4.3.12 Ectopterygoid-pterygoid complex

The pterygoid wings are the major components of the posterior palatal surface and here encircle and define the proportionally large and losangular choanae typical of baurusuchinae (Darlim *et al.* 2021a), forming their posterolateral margins (**Figure 7a-b**). Together, the ectopterygoid and pterygoid bones form large, triangular, wing-like structures surrounding the secondary nares that taper towards an end lateroventrally, being dorsoventrally flat but transversely wide, and tangentially contacting the medial surface of angular, close to its torose margin. The set was probably forced into an almost horizontal configuration due to dorsoventral compression of the cranium. In life, it would have had a more verticalized disposition, with a ventrolateral orientation, as seen in specimens that were not submitted to such distortion.

The ectopterygoid is formed by an ascending, laterally flattened process that culminates into an elliptical platform that sutures it to both the jugal and the maxilla, and also a narrow, tubiform, ventral projection that composes the pterygoid plate, thus sharing a log suture with the pterygoids. It also has a medial projection that meets the palatines along an almost anteroposterior contact plane. These, together, delimit the posterior margin of the suborbital fenestra. In palatal view, the ectopterygoid displays thickened anterior margins and a marked concavity bearing minute neurovascular foramina, contributing to the large perichoanal fossa encompassing the pterygoid plate. The pterygoids are the larger elements of the set, compose the choanae lateroposteriorly, the choanal septum itself and enclose a significant portion of the posterior nasopharyngeal tract. They contact the palatines and the ectopterygoids anteriorly, the prefrontals dorsally through their paramedial descending processes, the laterosphenoids posterodorsally, the basisphenoid posteroventrally and the quadrates posterolaterally. There is also a minor contact with the basioccipital close to quadrates. CT images reveal that, anteromedially, the pterygoids dorsal nasopharyngeal cap

forms a duct-like, dorsally convex arch, bounded ventrally by the palatines, that reach the nasal passages. This anterior process tapers to a point as it enters the aforementioned cavity.

A transverse cross-section (**Figure 7b$_1$-b$_2$**) shows a tall but laterally thin septum, attached to the dorsal surface of the conduct, that emerges anteriorly and has an extensive length, eventually emerging on the choanae as a thick rod that bisects the internal nares. The choanal opening itself displays thin bone walls (perichoanal lamina) surrounding the septum that possibly bounded the air flow, directing it into the pharynx. The pterygoid wings are distinctly concave ventrally, forming a wide perichoanal fossa, as mentioned previously. Their posterior edge is straight but curves markedly as the pterygoid narrows to meet the basisphenoid. This contact is roughly v-shaped in palatal view.

The pterygoid's lateral margin and distal end bear textures that might correlate with some known cranial musculature. For instance, when seen in lateral aspect the pterygoid buttress displays a shallow circular depression with porous surface texture dorsolaterally that might have been generated due to its contact with the *cartilage transiliens* (ct) in life (Iordansky 2000; Holliday *et al.* 2013). Ventral to this site there are longitudinal markings that may point to the passage of M. intramandibularis (mIRA) towards the mandibular adductor fossa, as inferred due to its attachment reliance on the ct sesamoid (Tsai & Holliday 2011). Dorsally, the pterygoid forms a wide concavity with a mostly smooth surface with only minor striations where the M. pterygoideus dorsalis (mPTd) would have passed, at the same time as ventrally, on its distal cojoined tip with the ectopterygoid, conspicuous deeper sulci indicate the origin site for the M. pterygoideus ventralis (mPTv).

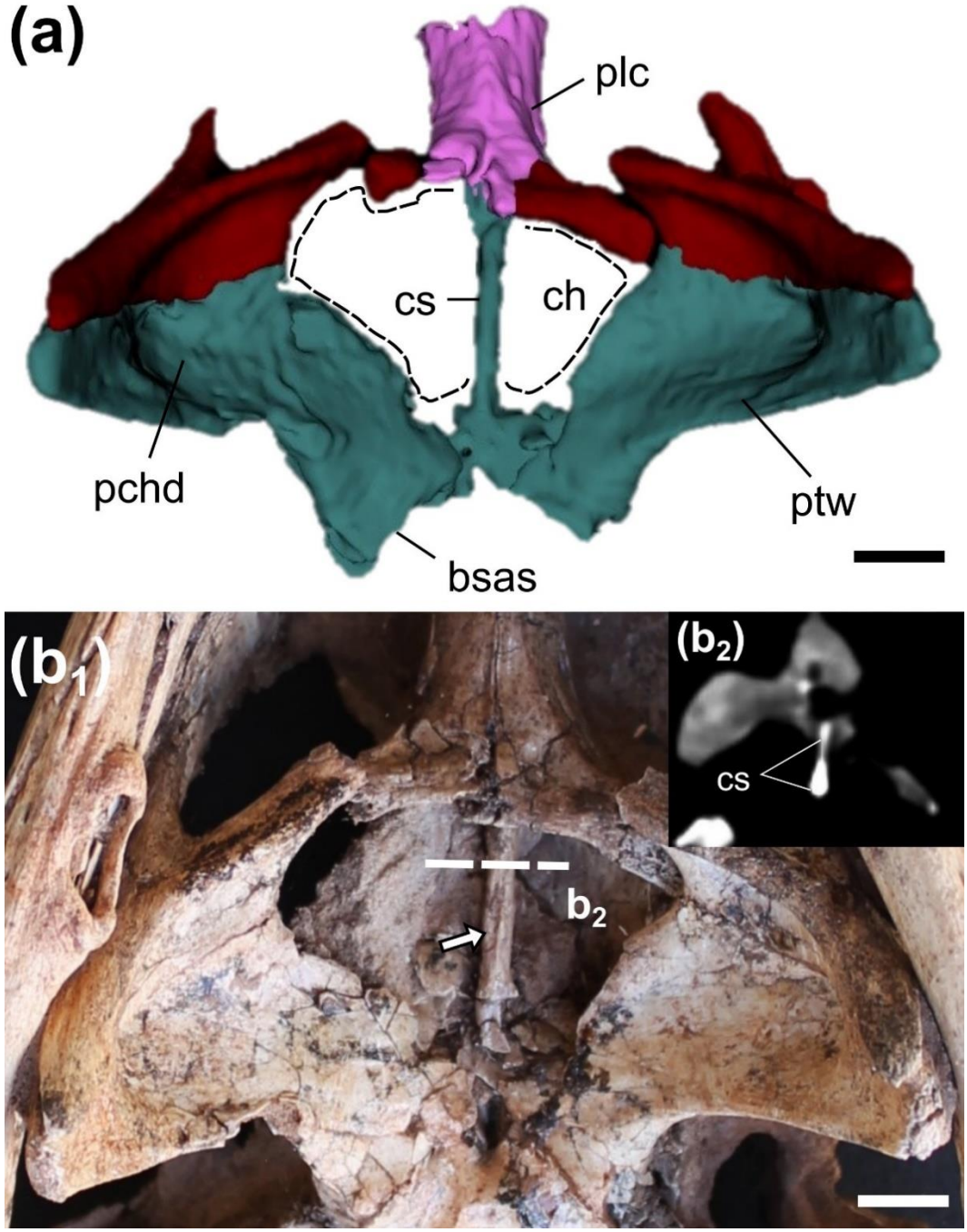


**Figure 7. Ectopterygoid-pterygoid complex. (a) digital model, including the palatines, in ventroposterior view. Note the relatively large and septate losangular choanae. ($b_1$-$b_2$) Photograph highlighting septum with minor longitudinal crest. Transverse cross-section reveals a laminar profile of septum. Abbreviations: bass, basisphenoid articular surface; ch, choanae; cs, choanal septum; pchd, parachoanal depression of pterygoid wings; plc, palatine medial constriction; ptw, pterygoid wing. Scale bars = 1 cm.**

4.3.13 Basisphenoid

Comprises a wedge-shaped/delta-shaped element of posteroventral basicranium, located between pterygoids anteriorly and the basioccipital posteriorly.

Its anterior ventral surface shares a strong depression with the posteroventral process of the pterygoids, with which shares a v-like suture (**Figure 6a**). Within this depression, at the same levels as the median eustachian foramen, but anterior to it, there is an additional large foramen, roughly at the limit between these two bones. Due to the mentioned depression, the anteroventral surface of the basisphenoid slopes anteriorly, yet, posteriorly, a squarish crest-like feature is present at its border with the basioccipital. The posterolateral basisphenoid projections also bear shallow depressions and reach the quadrate along a narrow contact. In term of surface texture, the basisphenoid is mostly smooth, lacking sculpturing and/or muscle striations. Given the poor preservation state of the dorsal portion of the basisphenoid, as well as some other basicranium bones, nor the endocranium floor, cultriform process or vasculary/nerve canals could be identified, even utilizing CT imagery.

4.3.14 Basioccipital

This element extends the occipital region of the skull as well as the ventral portion of the basicranium, contacting both otoccipitals dorsolaterally, quadrates ventrolaterally, the basisphenoid ventroanteriorly and, possibly, the prootic internally. It is comprised of an anteroposteriorly thin, but lateromedially expanded bone, with a roughly triangular shape in occipital view. Dorsally, it narrows and thickness to form its contribution to the occipital condyle, a robust, rounded process additionally formed by ventromedial projections of the exoccipital/otoccipitals, whilst ventrally it becomes increasingly transversely expanded, culminating in a fan-like process with an anteriorly convex contact with the basisphenoid (**Figure 6a**).

The occipital condyle is posteroventrally directed, being roughly rounded and marked by a vertical sagittal sulcus. Just ventral to the occipital condyle, three

diverging crests emerge: two adjacent lateral crests, thicker and ventrolaterally inclined, and a medial one, sharper and vertically oriented. They bound lateral depressions that encompass large areas of the wide ventral process of the basioccipital. These bear two minute neurovascular foramen bordering the midline, slightly ventral to the condyle and overhung by it. Each crest leads up to the basioccipital ventral border, where three conspicuous and rounded basal tubera emerge, making up the thickened margins surrounding the lateral and medial eustachian tubes. These foramina are placed at the interface between the basioccipital and basisphenoid and consist of elliptical lateral ones and a larger circular opening at the sagittal line. A ventral view exposes long sutures between these two basicranium elements, creating a sulcus where the eustachian tubes are located. The basioccipital external surface is mostly smooth with the noticeable exception of the basal tubera, that bear clear striations.

4.3.15 Skull roof and occiput

As previously mentioned, in addition to the dorsoventral compression that substantially affected the occipital region, flattening its components, the skull roof has also been exposed to weathering. The posterior end of the frontal, along with the parietal, the postorbitals and squamosals are all badly damaged, with almost all their dorsal surfaces obliterated. Fortunately, though, the rough outline of the left supratemporal fenestra is preserved, revealing a triangular shape, marked by somewhat rounded vertexes. One of the latter points medially, and no visible supratemporal fossae are preserved. Additionally, it is possible to discern that the fenestrae were relatively small in comparison to the skull roof area, not being nearly as developed as in adult individuals, where it becomes transversely wide, resulting in a narrowing of the parietals. Temporal bars have also collapsed, blocking a proper view

of the otic cavity. The inner ear anatomy was successfully recovered with the use of CT scanning, and detailed in Dumont Jr et al. (2020). As a result of dorsoventral compression, evidenced by the elliptical outline of the *foramen magnum*, and subsequent erosion, the supraoccipital and the exoccipitals are poorly preserved, represented only by fragments.

4.3.16 Dentary and splenials

The anterior and symphyseal regions of mandibular rami are composed by the dentary anterolaterally and the splenials posteromedially, respectively. Both elements contact each other anteriorly, along the symphysis and left-right mandibular rami, but also the angular and surangular posteriorly (**Figure 8a,b and c**). In ventral view, the mandibular symphysis is characterized by losangular-like shape, expanding transversely at mid length following the hypertrophied fourth dentary tooth and then tapering into a blunt anterior edge. Posterior to the fourth enlarged alveolus, the dentary develops a marked lateral compression, resulting in concavities that occlude lingually to the second and third maxillary teeth. The splenials make up about a third of the total symphyseal length posteriorly, forming a v-like anterior process as both counterparts meet along the sagittal plane to contact the dentaries, diverging from the longitudinal plane posteriorly to form the mandibular rami, assuming a verticalized and mediolaterally compressed aspect. Lateral to the medial suture, low-relief longitudinal crests develop close to its contact with the dentary ventrally, these are located within a wider triangular depression that reaches up to mid length. The sagittal suture of the symphysis is visibly thickened posteriorly, generating a conspicuous symphyseal torus which is locally surrounded by shallow depressions. It is noteworthy that its anterior symphyseal surface slopes into an oblique angle with respect to the horizontal plane, differing from the verticalized condition observed in mature semaphoronts.

In lateral view, the dentary has a somewhat rectangular shape, where both the dorsolateral and ventrolateral margins run in parallel, while ventrally form a wedge-like contact with the splenials and the angular's anterior process. Posterolaterally, the dentary becomes a thin vertical wall, slightly overlapping both angular and surangular, forming the mandibular fenestra's acute anterior edge. These elements together delimit the meckelian canal, the dentary laterally, and the splenials medially, respectively. The splenials, just posterior to the symphyseal torus, bear relatively large and elliptical anterior intermandibular foramina (*foramen intermandibularis oralis – fio*) (**Figure 8b$_2$**). These are slightly dorsally facing and are responsible for the local emergence of the mandibular nerve ($V_3$). The ornamentation is more developed and concentrated on the lateroventral surfaces of the mandibular symphysis, consisting of randomly distributed vermiform sulci. Laterally and posterolaterally, the dentary also displays less noticeable longitudinal sulci.

4.3.17 Angular

The angular composes the ventroposterior region of the mandibles, in this case making up more than half the ventral length of the latter (12 cm of a total of 22 cm, 54%). It is an anteroposteriorly elongated, but lateromedially narrow tubular-like bone with a convex outer surface and a concave medial one, forming a wide/open arch. A cross-section shows a characteristic U-shape, where a longitudinal sulcus, anteriorly contributing to the meckelian canal, is bounded by medial and lateral walls/laminae. Anteriorly, in ventral view, it is pinched to a point between the splenial and dentary, while posteriorly it becomes increasingly wide and dorsoventrally flat, forming a platform to receive the articular bone. In lateral view, it also contacts to the surangular posterolaterally along a roughly rectilinear suture that follows a tapering of both elements, reaching the retroarticular process of the articular posteriorly. Most

importantly, the angular makes up the ventral border of the external mandibular fenestra, where it develops a laminar dorsal process posteriorly (more robust in adult forms).

Midway along the mandibular adductor fossa, the medial wall of the angular becomes conspicuously taller than its lateral counterpart, giving rise to a noticeable protuberance (torose margin *sensu* Nascimento & Zaher 2010). This process takes the form of a thickened wall and topologically seems to have functioned as an attachment surface area for mandibular adductor musculature, most likely mAMP, which would over most of the external mandibular fenestra (**Figure 8b$_1$, but also see discussion and Figure 18**). A shallow, tear-drop-shaped depression for the lateral insertion of the mPTv is present close to the ventral margin of the mandibular fenestra, an intriguing baurusuchid feature not seen in other notosuchians, except for *Araripesuchus* (Sellers *et al.* 2022), although much less developed in this specimen than in adult forms. Deep carving grooves and pits can be seen on the anterolateral surface of the angular, whereas most of its remaining surface is smooth and ornament-free.

4.3.18 Surangular

A component of the posterior end of the mandibular ramus, the surangular comprises an anteroposteriorly long but mediolaterally compressed element that marks most of the external mandibular fenestra's dorsal edge. It contacts the dentary and the splenial anterolaterally and anteromedially, respectively, the angular posteroventrally and the articular posteromedially (**Figure 8a-b**). The surangular is marked by anterior narrowing process, fitting between the dentary and the splenial, forming a longitudinal sulcus where the mandibular branch of the trigeminal nerve ($V_3$) would fit, advancing anterodorsally through the meckelian canal. Along mid-length, this

element bulges faintly outwards, while ventrally is markedly concave, forming the dorsoposterior outline of the mandibular fenestra, with no visible fossa.

Posteriorly, it develops a tall but narrow process that bounds the articular bone laterally, and thus composing the lateral portion of the mandibular glenoid fossa. This process also further extends posteriorly, tapering in parallel with the angular to contribute to the retroarticular process. The contact between these two elements is straight, reaching the posterior margin of the articular. The surangular's mediodorsal surface is smooth and slightly depressed, serving as the attachment area for the mAMES that ran from the quadratojugal's concave ventral margin to the coronoid eminence (**Figure 8b$_1$**). The latter comprises a thickening on the surangular's anterior end, displaying a vertical medial wall adjacent to the pterygoid buttress, and consequently, the *cartilage transiliens* (ct). This surface likely served as an attachment facet for both mAMEM and mAMEP, but here lacks visible muscle scarring like those seen large adults such as in the *B.salgadoensis* holotype. Overall, the bone's surface is smooth externally, with the noticeable exception of the mandibular fenestra's posterior margin, displaying parallel striations where the mAMP likely bulged.

4.3.19 Articular

Fortunately, both left and right articulars are well-preserved, and despite being partially obscured by the articulation with the cranium itself, were reconstructed with the use of CT imagery. They contact the surangular laterally and the angular ventrally. The latter forms a wide platform onto which the articular rests upon. Overall, in dorsal view, the articular has a triangular outline, having an acute, tapering anterior process, wedged into the medial angular sulcus, and a wide restroarticular process posteriorly (**Figure 8b-c**). The glenoid fossa itself is located somewhat at the articular middle

section, having its deepest concavity laterally (for the reception of the quadrate lateral hemicondyle). The medial concavity is limited by a thickened and raised margin, followed by a vertical medial wall. In medial view it is possible to observe two distinct transverse crests that bound the glenoid fossa anteriorly and posteriorly, substantially limiting any fore-and-aft jaw movement. The anterior process slopes anteriorly as the element narrows, while posteriorly the articular contribution to the retroarticular process forms a wide and dorsoventrally flat sheet-like projection. This region reveals a medioventral inclination in occipital view. The ventromedial edge of the retroarticular process bears muscle insertion marks for the mPTv.

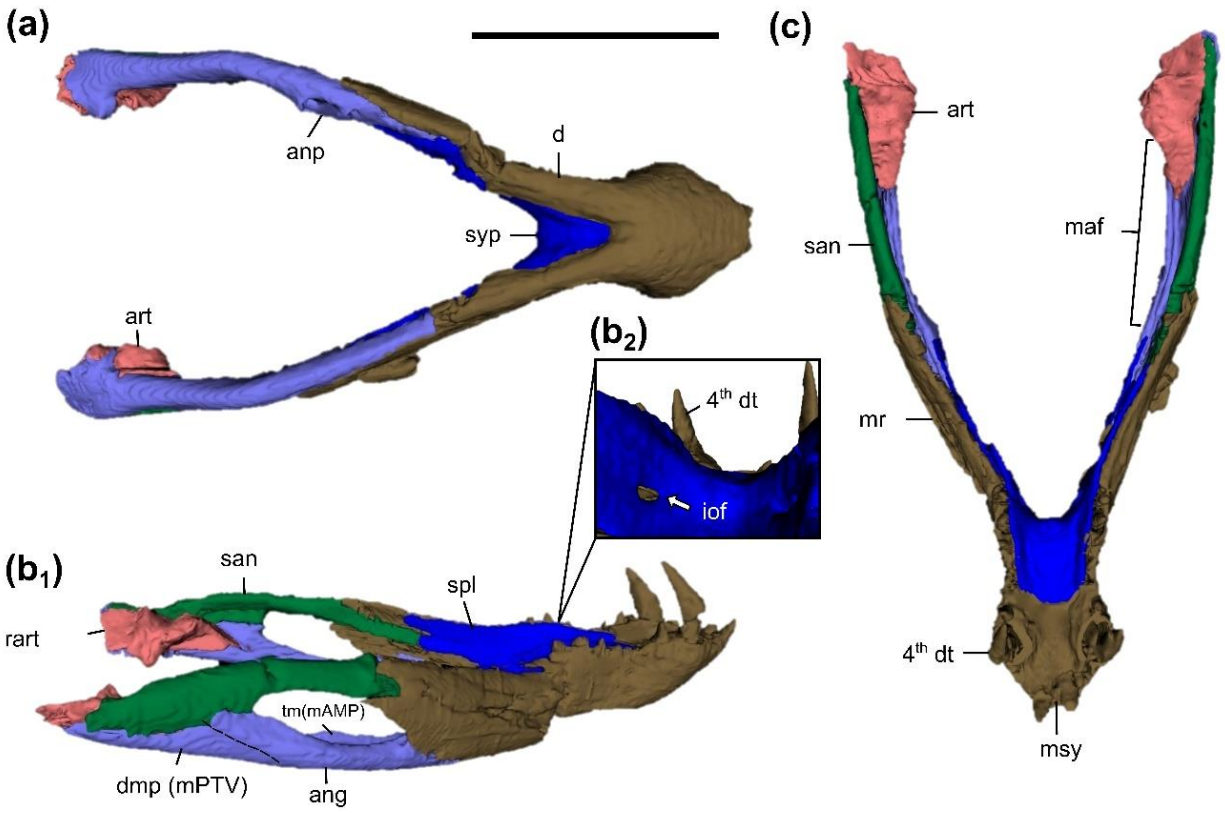


**Figure 8. Digital model of the mandibles of IFSP-VTP/PALEO 003 in (a) ventral, ($b_1$) dorsolateral, and (c) dorsal views. ($b_2$) is a detailed image of the mandibular ramus medial wall, formed by the splenials, and its elliptical oral intramandibular foramen (iof). Abbreviattions: ang, angular; anp, angular pathology; art, articular bone; d, dentary; dmp, depression for insertion of the *M. pterygoideus*; maf, mandibular adductor fossa; mr, mandibular ramus; msy, mandibular symphysis; san, surangular; spl, splenials; syp, symphyseal peg; 4th dt, fourth hypertrophied dentary tooth. Scale bar = 5 cm.**

4.3.20 Palpebrals

The specimen preserves a partial right anterior element and a complete set of left palpebrals. It follows a plesiomorphic crocodylomorph pattern of having two, anteroposterior articulating palpebrals, above each orbit, as seen in basal forms like protosuchids (Colbert *et al.* 1951; Dollman *et al.* 2019), and also derived notosuchians like *Araripesuchus* and *Simosuchus* (Kley *et al.* 2010; Turner 2006). This being a baurusuchid, the anterior palpebral is substantially larger than the posterior one, and both come into contact at discrete points medially and laterally, forming a large elliptical supraorbital fenestra (Carvalho *et al.* 2005; Nesbitt *et al.* 2012).

The anterior palpebral has a triangular outline in both dorsal and ventral views, tapering to a point and projecting posterolaterally at the horizontal plane above the eye socket (**Figure 9a**). Its lateral border is obliquely inclined with respect to the rostral-occipital length, while the posterior edge is mostly orthogonal to it and distinctively concave at the posterior palpebral level. Dorsally, the anterior palpebral develops a large shallow depression that encompasses most of its posteromedial area. It articulated with and was sutured to a lateral and elliptical facet formed marginally by the nasals, but mostly the prefrontal and frontal, where its medioventral process would fit.

The posterior palpebral, a small and triangular element, attached to an anterolaterally facing facet on the postorbital bone, protruding its lateral tip towards the anterior element (**Figure 9b**). This disposition, along with a visible concavity on its anterior margin, contributed to the formation of the supraorbital fenestra. Both palpebrals are substantially more sculptured when compared with the rest of the

dermocranium, bearing clear striations and sulci, as well as neurovascular foramina. Their ventral surfaces, however, are mostly smooth.

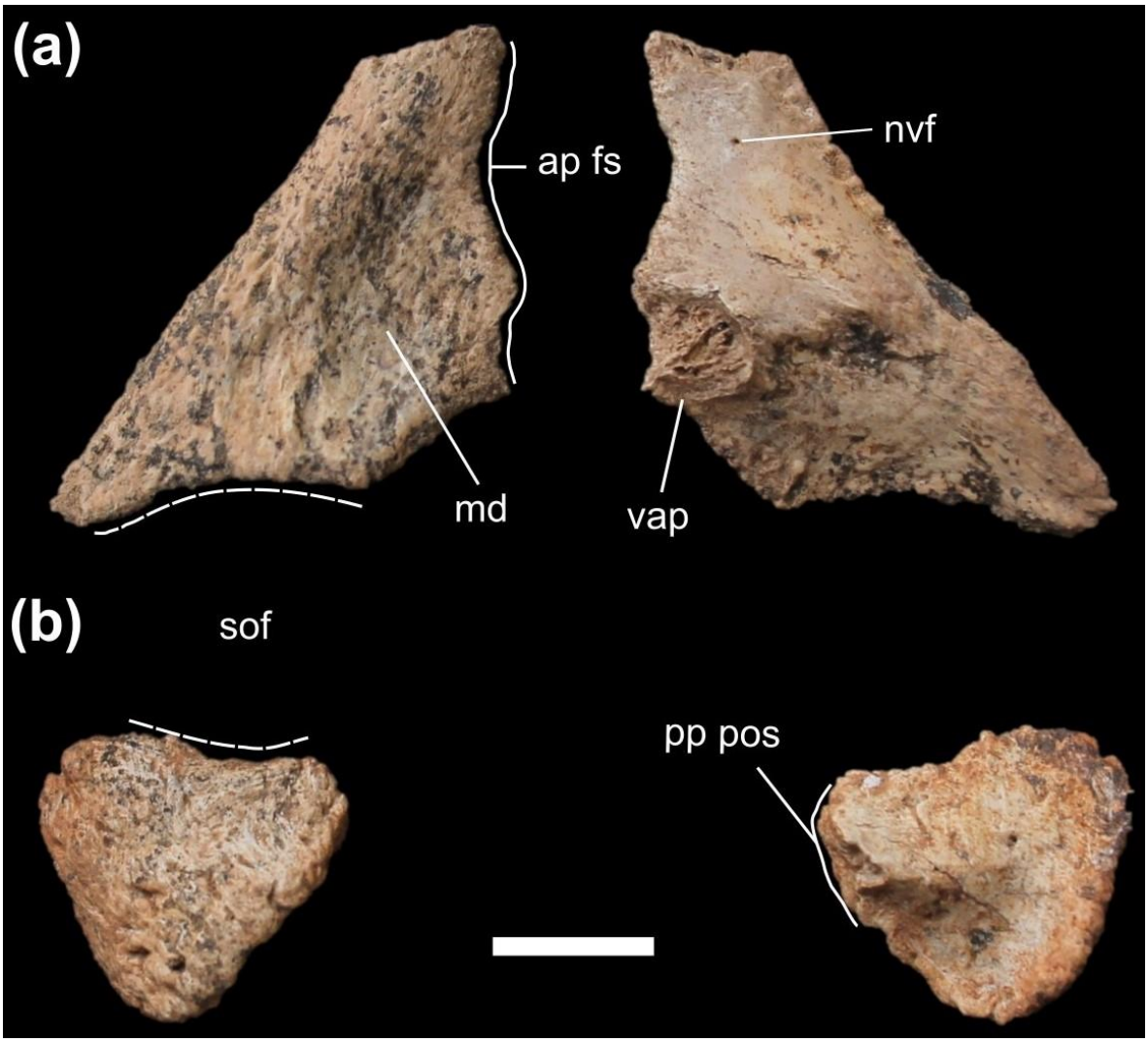


**Figure 9. Anterior (a) and posterior (b) palpebrals of IFSP-VTP/PALEO 0003 in dorsal (left) and ventral (right) views. Abbreviations: ap fs, anterior palpebral frontal suture; md, medial depression; nvf, neurovascular foramen; pp pos, posterior palpebral postorbital suture; sof, supraorbital fenestra; vap, ventral articular process. Scale bar = 1 cm.**

### 4.4 Axial skeleton

4.4.1 Atlas-axis complex.

The specimen herein described, IFSP-VTP/PALEO 0003, possesses the best preserved and most complete baurusuchid atlas-axis complex found to date, including

a proatlas with no substantial damage, both atlantal neural arches, intercentrum, odontoid process, which is fully sutured to the anterior articular surface of the axis, and, finally, the axial vertebra, with only minor signs of wear around the margins of the anterior and posterior articular surfaces (**Figure 10**). Evidently, this juvenile had a well-developed proatlas bridging the dorsal surfaces of the atlantal neural arches, and, along with *Baurusuchus albertoi* and *Campinasuchus dinizi* (Carvalho *et al.* 2011; Nascimento & Zaher 2010), it differs from advanced notosuchians like *Simosuchus clarki*, that show no signs of having possessed such an element (Georgi & Krause 2010).

The proatlas has an open v-like shape in both anterior and posterior views, and a straighter outline in dorsal view, being significantly wider (≃ 28 mm) than anteroposteriorly long (≃ 5 mm), as well as dorsoventrally flat. It is marked by two laterally-projecting processes that are cojoined dorsally, at an angle of roughly 120º as seen in anterior or posterior views (**figure 10b**). A major feature is a medial ridge that runs dorsally along a posteroventrally inclining slope, thus forming a sharp, anteriorly placed apical portion. In dorsal view, the lateral processes maintain a semi constant length up to their middle portions, where each expand anteroposteriorly and also mediolaterally, forming a widespread projection with rounded outer margins. Ventrally, these form roughly circular articular surfaces for the contact with corresponding surfaces of the planar process of the atlantal neural arches. Additionally, dorsally these lateral processes display transverse, low relief crests that are anteriorly shifted. These converge medially into the apical portion of the medial ridge and divide the proatlas upper surface in two distinct anteroposterior areas. The dorsal surface extends little anteriorly, transitioning rapidly into the ventral surface, while posteriorly this very plane forms a ventrally projecting triangular vertical wall. This wall's ventral margin forms a

medial knob and laterally merges into the edges of the articular processes. The element mostly lacks sculpturing, being smooth throughout its surface, except for the dorsolateral margins of the articular processes that show a rougher texture.

Ventral to the proatlas lies the atlas vertebra itself, composed of an intercentrum and left/right neural arches, in addition to the odontoid process, firmly fixed to the axis. The intercentrum morphology is in line with the general pattern seen in other extant and extinct crocodylomorphs for which it is available (e.g. Georgi & Krause 2010; Vieira *et al.* 2016), including baurusuchids (Cotts *et al.* 2017; Nascimento & Zaher 2010), being represented by a quadratic element in dorsal or ventral views, markedly broader than long, with a concave dorsal surface and a convex ventral one (**Figure 10a**). Its dorsal concavity inclines posteroventrally and provides a contact area for the odontoid process, while anteriorly it has a crescent-shaped, concave articular surface for the cranium´s occipital condyle (*fossa condyloidea* sensu Georgi & Krause 2010). Posteriorly, the intercentrum bifurcates into two posterolaterally oriented semi-circular processes for the articulation of the first pair of unpreserved unicapitate cervical ribs. These posterior atlantal ribs facets are slightly offset in relation to the anterior condyle, most likely due to its posterior contact with the odontoid process. There are moderately developed lateral constrictions that result in concave lateral margins and a visible depression. Posteriorly, between the atlantal rib facets, a trough develops, reaching mid length anteroposteriorly along the intercentrum. Texturally the bone lacks major markings, having only minor, shallow striations.

Dorsal to the intercentrum, and articulated to it, are the neural arches. These are separate paired elements, distinct due to their laterally curved, c-shaped outline in anterior/posterior views and their t-like shape in lateral or medial aspects (**Figure 10b**). These are formed by a dorsal, horizontal laminar process and the anteroventrally-

projecting pedicles (**Figure 10c**). The former is an anteroposteriorly elongated but dorsoventrally flattened laminar shelf that dorsally displays a shallow articular surface for the attachment of the proatlas and posteroventrally houses the postzygapophyses. Ventromedially, the postzygapophyses are visible as ovoid, low relief, mostly laterally facing surfaces. The horizontal laminar process also extends further posteriorly to meet the prespinal region of the axis in a tight fit. In lateral view, as it articulates with the axis, the neural arch concave posterior edge forms a vertically elliptical foramen with the anterior margin of the axial neural arch. Such foramen, as noted in previous works (Georgi & Krause 2010; Pol 2005), is responsible for the passage of the second cervical nerve (**Figure 10d-f**). Similarly, its concave anterior border also functions as passage, but for the first cervical nerve. The pedicles are projected anteroventrally by a laterally compressed process and display two articular areas set roughly 45º from each other. Anteriorly, there is the neural arch contribution to the cotyle that receives the occipital condyle, being an anteromedially directed half-moon-shaped surface, while posteriorly a triangular area forms for the proper articulation with the odontoid process. Despite the presence of a medial laminae emerging from the horizontal process, with clear ventrally inclining endings, the neural arches do not seem to meet along the sagittal plane, no preserved bony processes appear to bridge this gap.

The second cervical vertebra, the axis (**Figure 10d-f**), presents a trapezoidal centrum in lateral view, marked by a lateromedial compression that generates elliptical depressions on its surface, a common feature throughout the axial skeleton of notosuchians (Pol 2005). Ventrally, a conspicuous concavity develops, divided by a prominent sagittal keel, which anteriorly and posteriorly transition into ventral expansions, the latter being more pronounced than the former. Additionally, lateroventrally, centroparapophyseal laminae emerge, running along the centrum and

expanding anteriorly into the parapophyses. These are mostly ventrally facing. Firmly sutured to the anterior cotyle of the centrum is the odontoid process, characterized by a triangular profile in lateral view and a concave, half-moon-shaped outline in anterior view. The odontoid process is transversely expanded, having two anterolateral projections with horizontal platforms where the neural arches articulate. It is also marked by an anteriorly projecting medial ridge that fits the medial sulcus of the occipital condyle, likely limiting lateral movement of the skull. Ventrally the odontoid process is slightly convex for the reception of the intercentrum.

The atlas-axis complex articulates with two pairs of cervical ribs, the anteriormost being a unicapitate rib contacting the lateroventral atlantal rib facet of the intercentrum, and the posterior one a bicapitate element that attaches itself to two facets on the lateral surface of the odontoid process. These processes are separated by a local depression. Parapophyses seem to contribute with the atlantal rib facet, whereas there is no sign of the diapophyses playing a similar role regarding the axial ribs. The axial neural arch is distinctly tall, with slight lateral concavities, and extends the entire length of the centrum. It is visibly not fully fused with the centrum, having a partially open neurocentral suture. The pedicles, though being transversely expanded, still retain portions where the surface texture in contact with the centrum is relatively smooth. In anterior or posterior views, the rounded shape of the neural canal can be distinguished, in addition to an interesting feature that is also present on posterior cervical vertebrae, in the form of a longitudinal sulcus on the ventral wall of the neural canal. This sulcus possesses a rectangular cross-section and was observed to run medially along the canal.

Prezygapophyses are elliptical in shape and vertically positioned, facing anterolaterally. A low relief spinozygapophyseal lamina is present, laterally bounding a

prespinal lamina of the neural spine. The latter tapers ventrally, failing to reach the prespinal fossa. Differing from its anterior counterparts, the postzygapophyses are ventrolaterally inclined but share the presence of a spinopostzygapopheal lamina. This lamina, despite being partially damaged, can be determined to have been anteroposteriorly more stretched than anterior spinal lamina. The neural spine is a laterally compressed, posterodorsally inclined projection with a rectangular profile in lateral view. Moreover, its anteroposterior length decreases vertically.

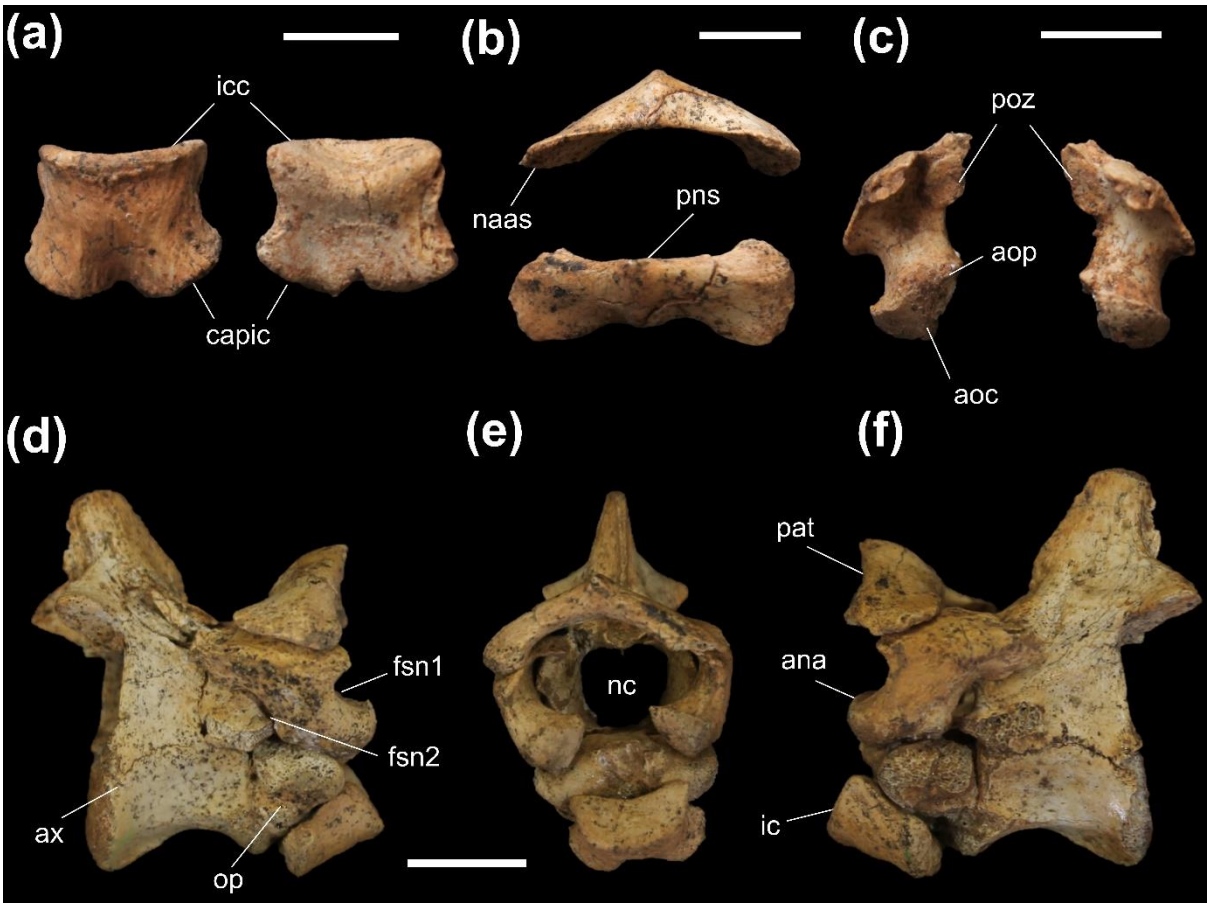


**Figure 10. Atlas-Axis complex of IFSP-VTP/PALEO-0003. (a) Intercentrum in ventral and dorsal views; (b) Proatlas, highlighting posterior and ventral views; (c) Right and left axial neural arches, respectively; (d-f) Complete articulated complex in right lateral, frontal and left lateral perspectives. Abbreviations: ax, axis vertebra; ana, axial neural arch; aoc, articular surface for the occipital condyle; aop, articular surface for odontoid process; capic, intercentrum capitular process; fsn1, spinal nerve foramen; fsn2, spinal nerve foramen 2; ic, intercentrum; icc, intercentrum cotyle; naas, articular surface for the neural arches; nc, neural canal; op, odontoid process; pat, proatlas; poz, postzygapophysis; pns, proatlas neural spine. Scale bars = 1cm.**

4.4.2 Post-axial vertebrae.

All of the post-axial vertebrae are articulated and exposed in right lateral view. Consistent with the specimen´s age at the time of death as estimated by previous histological work, both cervical and dorsal vertebrae show only partially closed neurocentral sutures (Brochu 1996), with clear signs of the onset of fusion between centrum and neural arch, but not fully sutured (**Figure 11a-b**).

The third cervical vertebra is characterized by a rectangular centrum, being longer than it is tall or wide, as well as a concave ventral facet, where an incipient ventral keel develops. Due to the ventral concavity, the latter noticeably thickens anteriorly and posteriorly into small protusions, despite maintaining a constant width along most of its length. The anterior protrusion is slightly more prominent, forming a bulge-like hypapophysis. A mediolateral compression of the centrum, a pattern that persists onto posterior vertebrae, produces a visible horizontal ovate depression on its lateral surface, bound anteriorly and posteriorly by the raised margins of the centrum's cotyles. Parapophyses are anterolaterally placed on the lateral facet of the centrum, close to its ventral limit, and display an elongated elliptical profile with a horizontal major axis. They are significantly larger than its counterparts on posterior vertebrae, occupying half the length of the centrum. The neural arch is taller than long, slightly anteriorly inclined in lateral view, mediolaterally compressed and runs the entire centrum. Prezygapophyses and diapophyses are connected by a robust lamina, which is not as conspicuous on posterior vertebrae. The articular surface of the diapophysis is rounded and points ventrolaterally. The prezygapophyses have a more acute angle, roughly 45º, than postzygapophyses, that are closer to the horizontal plane. Posteriorly, the neural arch shows a slight lateral compression for the accommodation of the prezygapophyses of succeeding vertebra. The neural canal is large, with a

circular cross section and a featureless, smooth inner surface. It is bound laterally by transversely expanded pedicles.

As expected, the neural spines form a laterally flattened vertical projection, having a rectangular shape with a rounded dorsal tip in lateral view, but much shorter than on posterior elements. It is somewhat centrally positioned on the neural arch and is bound laterally at its base by shallow depressions that extend anteroposteriorly between pre- and postzygapophyses, most likely corresponding to the attachment site for Mm. interarticulares (Tsuihiji 2005). The neural spine is also marked by prespinal and postspinal laminae, the former tapering into an anterior depression between prezygapophyses and the latter bisecting the postspinal fossa (pf). Additionally, there are well-defined prezygapophyseal and postzygapophyseal laminae that ascend and merge into the neural spine, running parallel to the abovementioned prespinal and postspinal laminae.

Cervicals four and five differ from the preceding vertebra by having anteroposteriorly shorter centra, thus more quadratic in lateral view, as well as more pronounced ventral keels. Anteriorly, these keels develop a low relief ventral projection treated here as hypapophyses. The articular surface of parapophyses undergo a significant change in form, reducing their length anteroposteriorly and expanding dorsoventrally, assuming an inverted D-like shape. Diapophyses become flatter and start to shift posteriorly, but still retain a posteroventral orientation, bordering the neurocentral suture. Here both zygapophyses are more horizontalized and, most importantly, anteriorly start to exhibit a clear prezygapophyseal bulge ventral to the articular facet, which might be related to M. longissimus group given its topology (Tsuihiji, 2007). Neural spines move posteriorly, their posterior edge now roughly

parallel to the posterior cotyle of the centrum. Furthermore, these become distinctly elongated with forward-inclining distal ends.

The remaining elements of the cervical series, the sixth and seventh cervical vertebrae have marginally longer centra anteroposteriorly, also deeper, more noticeable lateral depressions, which are bound dorsally by the diapophysis and the neurocentral suture and ventrally by the parapophysis. The latter increases the capitular articular area, at the same time maintaining the same outline as anterior elements. Ventrally, centra develop high relief longitudinal keels that transition anteriorly to rectangular-like hypapophysis in lateral view. Diapophyses continue to become more dorsoventrally compressed, assuming increasingly more dorsal positions on the neural arch, with their articular facets more posteriorly facing. Posterior cervicals also show a tendency to exhibit taller, anteroposteriorly shorter neural arches and more dorsally projecting prezygapophyses. These are also distinguished by the emergence of clear dorsoventral parallel muscle striations on the outer edges of their prezygapophyses, absent on anterior vertebrae. Neural spines, in addition to becoming taller up to the eighth cervical, gain substantially larger prespinal and postspinal laminae, that increase their superficial areas up to the middle section of the neural spine, giving it a convex aspect laterally but tapering dorsally. This is also seen in modern crocodylians and seems to represent increasing attachment surfaces for the intervertebral Mm. interspinales (Tsuihiji 2007; Vieira *et al.* 2016).

The last cervical vertebra of this series follows the general pattern described previously in *B. albertoi* (Nascimento & Zaher 2010), where the parapophyses gain a kidney-like shape in lateral view, differing sharply from anterior ones, but also markedly tall and anteroposteriorly more stretched neural spines with squarish dorsal ends in lateral view. The centrum seems to conserve their previous anteroposterior length and

typical lateral compression. Unfortunately, further details on this vertebra could not be properly assessed due to the scapula's position, which obscures most of its morphology.

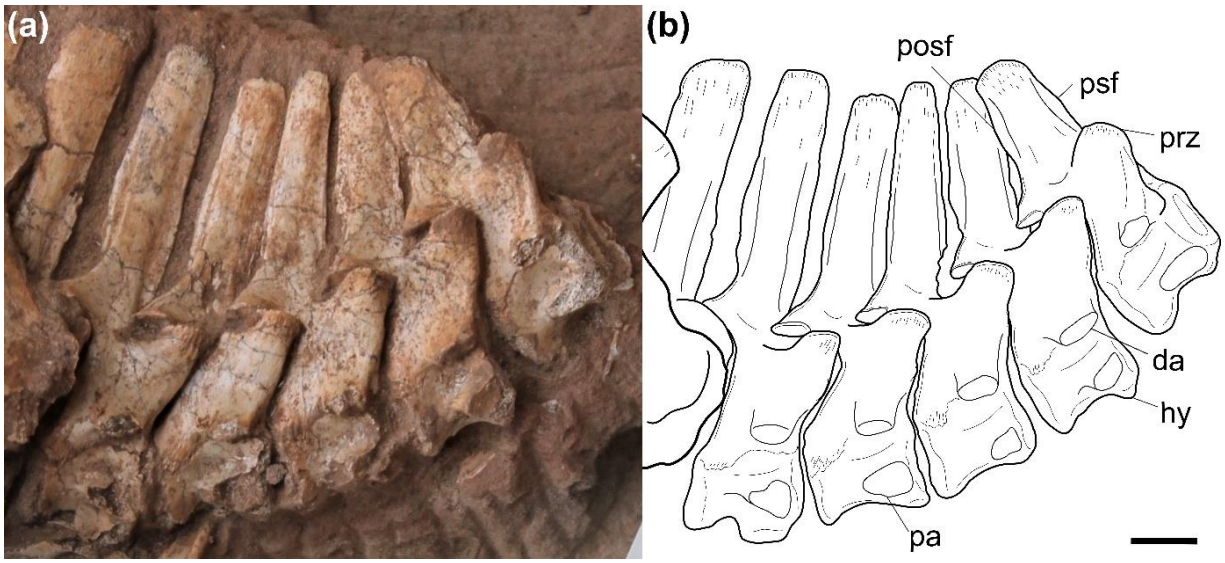


**Figure 11. Post-axial cervical series. Image of specimen in right lateral view (a), with line interpretation (b). Abbreviations: dia, diapophysis; hy, hypapophysis; pa, parapophysis; prz, prezygapophysis; ns, neural spine. Scale bar = 1 cm.**

### 4.4.3 Dorsal vertebrae

Comprised of fifteen vertebrae, the dorsal axial series is mostly articulated, with the exception of posterior lumbar vertebrae, where centrum cotyles do not seem to come into contact with each other. These elements are preserved in a similar fashion to the cervical ones, being exposed in right lateral view (**figure 12a-b**). Despite being partially concealed by the right scapular bone, it is still possible to discern the general morphology of the first two dorsal vertebrae. Their centra retain a cervical aspect of having a squarish profile in lateral view, being anteroposteriorly longer than tall or wide, as well as having characteristic kidney-like parapophysis. The dorsal migration of the latter is noticeable as its dorsal margin surpassed the neurocentral suture, partially reaching the lateral surface of the pedicles. The diapophysis reach the same plane of

the zygapophysis on the second dorsal, but are not confluent with these, with a laterally facing concavity separating these structures. Zygapophyses have elliptical articular surfaces, and are still inclined on a steep angle, but increasingly become horizontalized on posterior elements. As in cervical vertebrae, neural spines are tall, laterally flattened and anteroposteriorly short.

Posteriorly, the series is marked by anteroposteriorly stretched and laterally compressed centra, assuming a classic spool-like shape (Pol 2005), with smooth and concave lateral and ventral surfaces. Parapophyses have fully migrated to the neural arch, being integrated with the diapophyses into the transverse process, where a small lateral concavity separates the two. Despite still being somewhat ventromedially placed on anterior dorsal vertebrae, the parapophyses gradually shift dorsolaterally, eventually reaching the same level as the diapophyses. Neural arches become stretched anteroposteriorly, conforming to centra, and running their lengths.

Mid and posterior dorsal vertebrae also have mediolaterally flattened and rectangular neural spines in lateral view, as well as robust spinopostzygapophyseal lamina, that merges into the spinal body itself, attenuating as it extends anterodorsally on its lateral facet. Well-developed postspinal fossae are also present, being bisected by a conspicuous vertical postspinal lamina. Zygapophyseal articular facets here now face dorsally anteriorly and ventrally posteriorly, roughly parallel to the horizontal plane.

### 4.4.4 Sacral vertebrae

The specimen possesses three sacral vertebrae, a common character state for notosuchians (Martinelli *et al.* 2018; Nascimento & Zaher 2010), but distinct from extant crocodylians, which only have two (Ristevski 2019; Vieira *et al.* 2016). Unfortunately,

the neural arches and spines display substantial erosional damage, almost completely obliterating the superficial features of the second/middle element.

All sacral vertebrae are characterized by spool-shaped centra, wide and horizontally stretched neural arches, as well as robust, laterodorsally projecting sacral ribs. Attesting to the skeletal immaturity of the specimen, the latter had not fully fused to the ilium's medial wall at the time of the animal's death. The first two sacrals attach at a more anterior position with respect to the third, that is posteriorly shifted toward the end of the postacetabular process. The first sacral vertebra generally resembles the lumbar morphology, with elliptical zygapophyseal facets set at roughly an 45º inclination and anteriorly shifted neural spines with prominent prespinal laminae. Its ribs emerge anterolaterally and have posteromedially inclined attachment surfaces that conform to the medial wall of the preacetabular process, resulting in a triangular shape in dorsal view.

The middle elements have the largest and more robust set of sacral ribs, marked by an hourglass-like shape with markedly concave anterior and posterior margins. It attaches itself to a more ventromedial position in relation to its anterior counterpart. The attachment/sutural expansion is substantially anteroposteriorly longer, encompassing a wider area of the ilium's medial surface. The third sacral vertebra shares a similar rib morphology with the first element, with more slender ribs, except these are posteriorly inclined towards the postacetabular process medial wall.

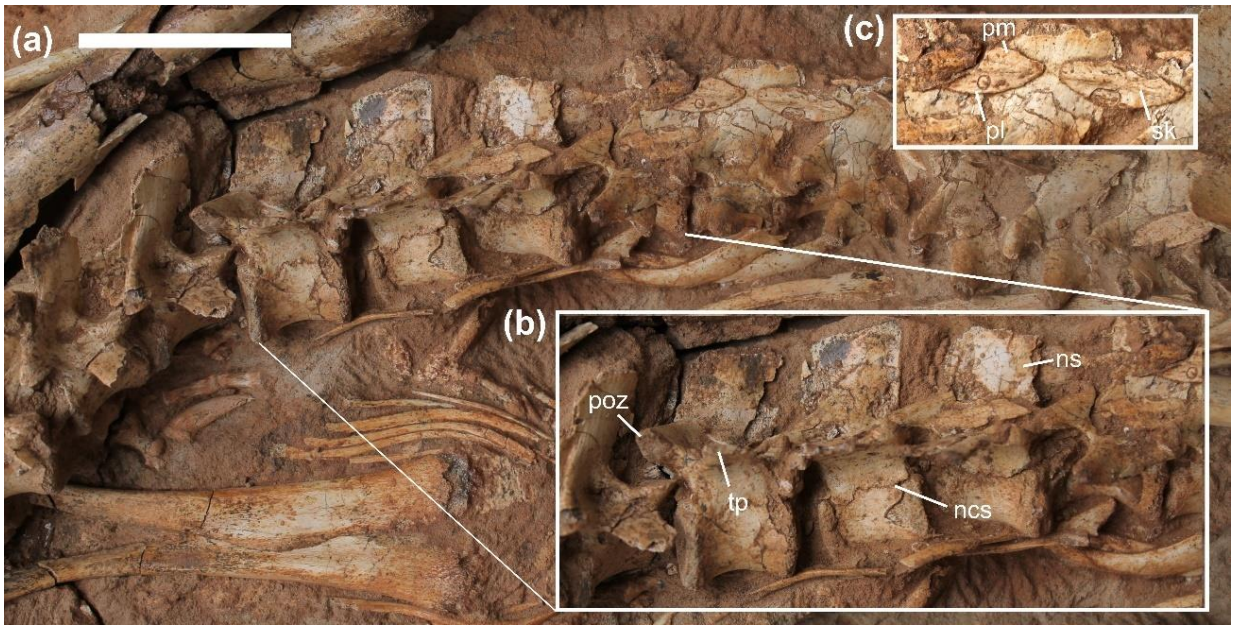


**Figure 12. Complete dorsal series in (a) lateroventral view. Pubes and gastralia can be seen in the lower left corner. (b) Tenth, eleventh and twelfth dorsal vertebrae in detail. (c) close up of a sequence of thin and poorly sculptured dorsal osteoderms. Abbreviations: pm, *pars mediale*; poz, postzygapophyses; pl, *pars laterale*; ncs, neurocentral suture; ns, neural spine; sk, sagittal keel. Scale bar = 5 cm.**

### 4.4.5 Ribs

Out of eight cervical vertebrae, only two right-side ribs have been preserved, while the dorsal series is mostly complete and semi-articulated, excluding the terminal lumbar vertebrae, which lack ribs. The cervical rib has the recurrent plow-shaped form observed in other archosaurs (Romer, 1956), with an anteroposteriorly stretched shaft orthogonal to bifurcating articular processes. The tuberculum is more dorsally positioned than the capitulum, both being of similar length and roughly aligned. The latter is slightly thicker and displays a larger articular facet, due to the larger parapophyses. Posteriorly, the tubercular process is additionally connected to the shaft by a visible lamina that extends the latter's surface dorsally. The capitular process is slightly inset in relation to the medial margin, where an ill-developed longitudinal flange is present. Externally, the shaft's outer martin is mostly straight, with only minor

undulations, while medially it is marked by a strong, channel-like concavity. The shaft extends substantially further posteriorly than anteriorly, with both tapering to a point at their ends.

Naturally, dorsal rib morphology changes as the parapophyses migrate dorsally towards the transverse process, thus shifting the disposition of the costovertebral articulation. Capitula and tubercula now gradually start to emerge and bifurcate roughly out of the same plane, with the processes of the former being longer and more robust than the latter. Shafts become substantially more elongate, shifting from an anteroposteriorly orientation to a more posteroventral position. These are comprised of dorsoventrally stretched but lateromedially compressed projections that bow outwards at mid length, being main components of the thorax. As the series progresses, the articular processes become less projected, the incisure that separates the capitulum and tuberculum decreases, and eventually both assume a cojoined aspect posteriorly. The shafts of anterior dorsal ribs are very characteristic, due to greater size and the presence of large anterior semi-lunate lamina that taper distally. Posterior elements have shorter and more strongly bowed shafts, culminating at the last rib, which is rod-like.

## 4.5 Forelimb

### 4.5.1 Scapula

Both left and right elements of the pectoral girdle are preserved, with scapulae and coracoids, yet only right-side components could be thoroughly described given the mode of preservation, where the left counterparts are totally or partially obscured by the cervical vertebrae and the right girdle itself. The dorsal outer edge of the scapular

blade has been damaged, lacking fragments on its posterior and anterodorsal regions, while its distal process has minor erosional loss on the coracoidal and glenoid surfaces The scapular blade has also been partially perforated by a dorsal vertebra's neural spine, evidence of substantial taphonomic compression. In general terms, the scapula is a proximodistally tall, but lateromedially flat component of the pectoral girdle, with three major anatomical portions: the fan-shaped, anteroposteriorly expanded scapular blade, marked by a conspicuous rounded dorsal edge; the short and anteroposteriorly constricted scapular shaft; and the distal process, characterized anteriorly by the scapulocoracoid suture (scs), as well as the glenoid fossa and the scapular buttress (sb) (**Figure 13**).

In right lateral view, the scapular blade is posteriorly shifted in respect to its distal portions, resulting in an anterodorsally inclined bone. The scapular blade displays a straight posterior margin while the anterior one is markedly concave, especially at the transition towards the shaft. Its broad, lateral surface displays three major depressions, separated by anterior and median ridges, with muscle scars on the dorsal edge of the blade for each of these regions.

The anteriormost sulcus is a slightly curved, dorsoventrally elongated, and thin depression, bound anteriorly by the edge of the scapular blade and posteriorly by the low relief anterior ridge (ar). It is thus inferred to have been the insertion area for the trapezoidal muscle, as well as the M. levator scapulae. Posterior to the latter is a large trapezoidal depression where the M. deltoideus scapularis originates, bound posteriorly by the median ridge, and followed by the slanted and triangular-shaped depression for the M. teres major (**figure 13**). The slightly deflected posterior margin is marked by the insertion of M. serratus ventralis thoracis (svt) dorsally and the origin region of the medial scapulosternal ligament ventrally (mssl). The scapular shaft and

distal ends are marked by a deep excavation which is topologically consistent with the origination of the M. coracobrachialis brevis.

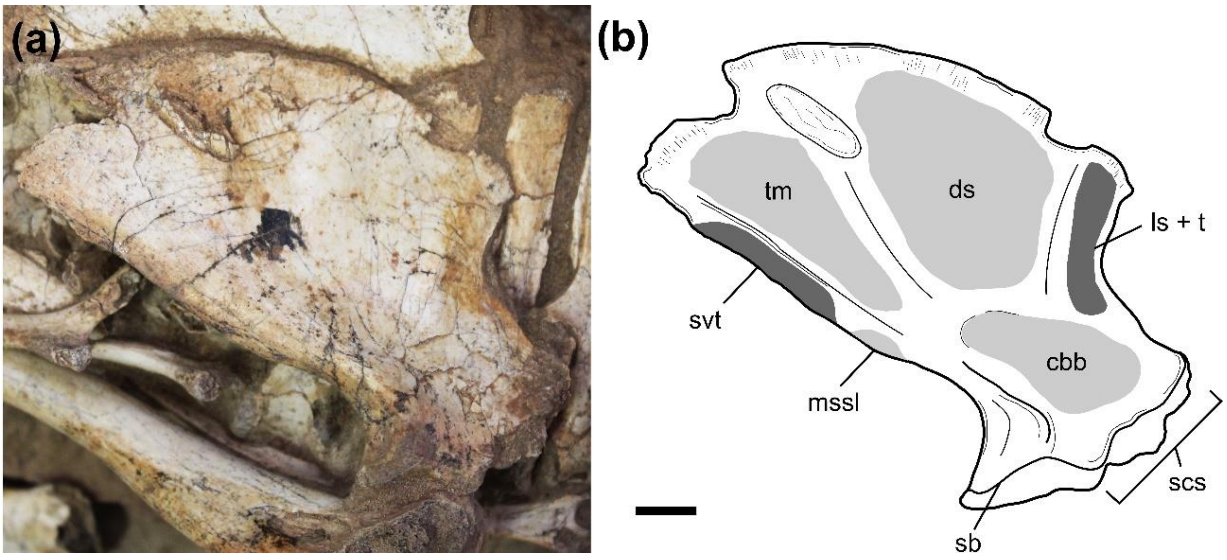


**Figure 13. Left scapula in lateral view (a) and schematic drawing with inferred muscle origination (light grey) and insertion (dark grey) areas. Abbreviations: cbb, M. coracobrachialis brevis; ds, M. deltoideus scapularis; ls + t, M. levator scapulae and M. trapezius; mssl, medial scapulosternal ligament; sb, scapular butress; scs, scapulocoracoid suture; svt; M serratus ventralis thoracis; tm, M. teres major. Scale bar = 1 cm.**

### 4.5.2 Coracoid

The coracoid composes the lower half of the shoulder girdle, contributing to the glenoid fossa (**Figure 14a-d**). Proximally, it is marked by a robust and blocky epiphysis, with a large semi-circular depression on its lateral side perforated by a prominent coracoid foramen (cf), located close to the eroded glenoid facet. The latter depression provided an origination site for M. supracoracoideus (sc) muscle. The irregular suture/synchondrosis edge with the scapula is found dorsally, bound posteriorly by the posterolaterally slopping glenoid surface. When articulated with the scapula, the coracoid was posteroventrally inclined towards the torso's midline and the non-preserved sternum. The shaft is elongated, somewhat laterally compressed, and visibly outwardly arched, with concave anterior and posterior margins. Just ventral to

the glenoid's pendulous facet, a deep fossa develops as an attachment site for the medial scapulosternal ligament.

Distally, along the posterior margin of the shaft, a sulcus forms, similarly to the insertion for the M. costocoracoideus superficialis in extant and fossil crocodyliforms (Meers 2003; Sertich & Groenke 2010). Midway along this same surface, the coracoid origination site for the triceps muscle manifests as a small circular rugosity. The distal fan-shaped expansion bears vertical muscle scarring on its medial side, corresponding to origin of the M. coracocrachialis brevis ventralis that then fixates on the anterior end of the humerus proximal epiphysis.

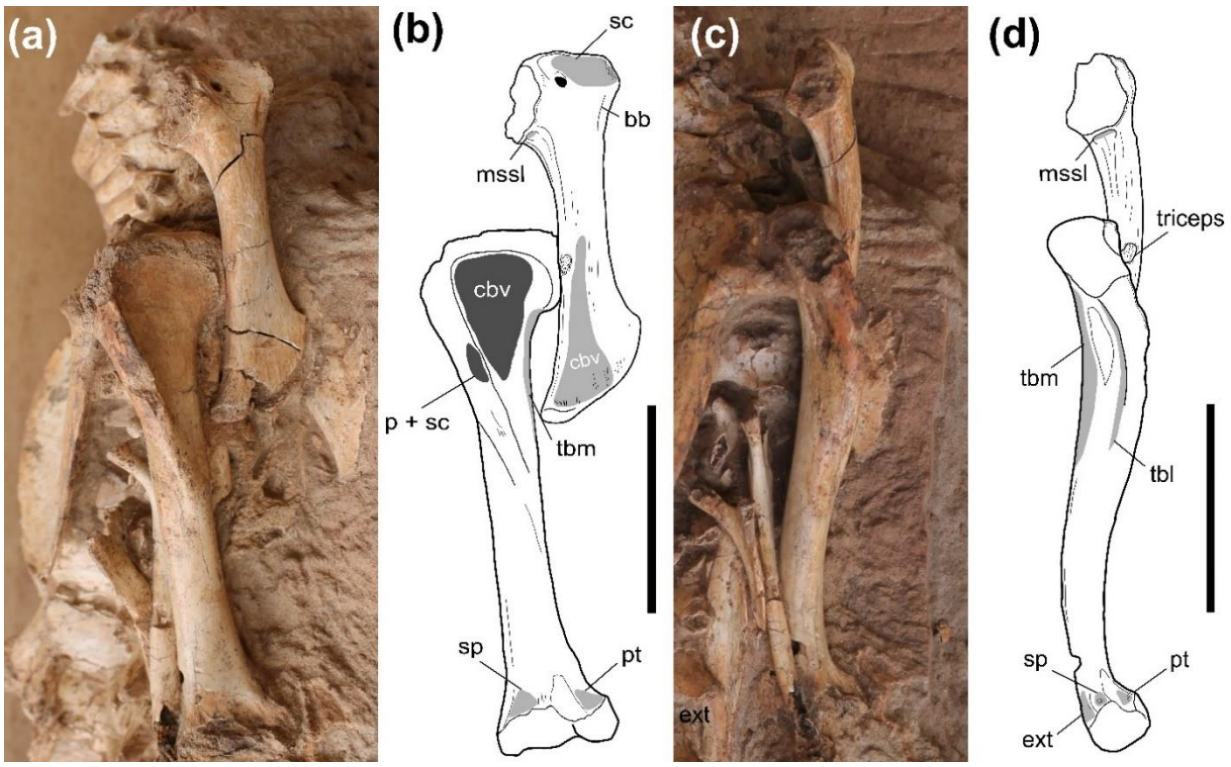


**Figure 14. Right humerus and coracoid with myological interpretations of origination (light grey), and insertion sites (dark grey) based on osteological correlates. (a-b) Humerus in anterolateral and coracoid in ventrolateral view. (c-d). Abbreviations: bb, M. biceps branchii; ext, distal extensors; mssl, medial scapulosternal ligament; p + sc, M. pectoralis and M. supracoracoideus; pt, M. pronator teres; tbl, M. triceps branchii caput laterale; tbm, M. triceps branchii caput mediale; sc. M supracoracoideus; sp, M. supinator. Scale bar = 5cm.**

4.5.3 Stylopodium (humerus)

The humerus follows a similar pattern previously observed in other notosuchian taxa (Pol *et al.* 2012; Tavares *et al.* 2017), with the exception of *Simosuchus clarki* (Sertich & Groenke 2010), which seems to be an outlier in some regards. It is an elongate element, marked by a transversely expanded, anteroposteriorly flattened proximal end, a straight shaft in anterior view, and prominent distal condyles, with little rotation between proximal/distal epiphysis and the diaphysis (**Figure 14a-d**). In lateral or medial views, the articular end of the proximal epiphysis curves posteriorly, while the distal metaphysis, alongside the distal epiphyses, bends anteriorly, seemly giving the distal condyles an anterior projection. The proximal epiphysis is characterized by a wide/broad, trapezoidal outline in anterior or posterior views, possessing distinct medial and lateral tubercles adjacent to the medial glenohumeral condyle. The articular condyle is straight and horizontalized, extending considerably posteriorly, while the medial tubercle displays a pronounced rounded margin and the lateral one a sharper, lateroventrally inclining edge. There seems to be no clear depressions separating the glenohumeral condyle from lateral and medial tubercles anteriorly, forming a somewhat continuous humeral proximal surface.

Anteriorly, the proximal end presents a large triangular-shaped depression with a rounded dorsal margin for the insertion of the M. coracobrachialis brevis ventralis (cbv; **figure 14b**), limited dorsally by the glenoid protuberance and laterally by the deltopectoral crest, along with muscle scars on its medial edge, where Triceps brevis medialis (tbm) would originate, extending distally along the shaft. The pectoral crest emerges lateroventrally from the lateral humeral protuberance, reaching maximum width at its mid length, where anterolaterally an insertion area is found for both M. pectoralis and M. supracoracoideus (p + sc), then further tapering distally as it

integrates into the shaft. Its distal portion is visibly medially shifted and extensive, thus resulting in the pectoral crest extending roughly half the total humeral length. Its proximolateral surface has, dorsal to the pectoralis and coracoideus, two successive, vertical circular depressions: the smaller one likely for the M. deltoideus scapularis (ds) and a larger more elliptical one, with vertical striations interpreted as the muscle scars of M. deltoideus scapularis (dc). Ventral to both abovementioned muscles, with a more posterolateral position in relation to the deltoid crest, there is a large negative relief area, roughly vertical, and limited medially by the Triceps brevis cranialis crest, that possibly marks the origination of the humeroradialis.

Due to the preserved exposure of the right humerus, the depression for the M.scapulohumeralis cannot be clearly distinguished, though its presence is inferred by the presence of the laterally preceding crest occupied by the Triceps brevis. Lateromedially, there is a small vertical crest medial to the pectoral crest which might be a marker for the Triceps brevis cranialis. The distal condyles are transversely expanded and markedly asymmetrical in both anterior and posterior views, where the radial lateral condyle is substantially larger than the ulnar medial one. These are separated by a narrow trough that extends into the anterior region. Additionally, just dorsal to the condyles proper (anteriorly), a wide depression forms, separating lateral and medial ramifications. In anterior view the radial condyle is lateromedially wide and elliptical in shape, whereas the ulnar is more rounded. A medial or lateral aspect suggests an anterior extension of the articular surfaces and a somewhat limited backwards movement between stylopodium and zygopodium. Muscle scars in the form of vertical and oblique striations indicate origin sites for M. pronator teres dorsal to ulnar condyle and M. supinator above the radial articular surface. The supinator seems

to be separated from the extensor group by a vertical change in surface relief, giving rise to a more verticalized origination area for the latter (**Figure 14c and d**).

4.5.4 Zygopodium (ulna and radius)

This section of the forelimb is mostly complete with both ulna and the radius well-preserved and articulated close to what it would have been in life (**figure 15**). Their metaphysis and diaphysis are marked by a few longitudinal but mainly transverse fractures. The distal epiphyses of both elements are not preserved due to a fracture that also damaged the carpals. The ulna is an elongated and laterally flattened element, with a convex lateral surface and a concave medial one, resulting in a noticeable medial bend of the diaphysis. The element is considerably anteroposteriorly taller and transversely thicker proximally than distally, mostly owing to the development of the humeral and radial articular surfaces in addition to the olecranon process.

The proximal glenoid facet is marked by a semi-lunate anterior surface with two distinct lobi, a lateral and a medial one, for the respective articulation of the humeral condyles. Additionally, ventral to these lobi, there is also a slightly ventrally deflected edge where the proximal head of the radius would rest. Laterally, the most prominent humeral articular facet overhangs the outer surface and is more proximodistally developed than the medial one. In lateral view, it is possible to observe a partial erosion of the olecranon process, which would not have extended substantially posterior to the proximal articular region. Its posteroventral margin is somewhat rounded and bears muscle insertion marks for the M. triceps branchii (tbb), whilst proximally the olecranon process is a mediolaterally compressed posterior expansion, roughly aligned with the ulnar major axis.

The diaphysis displays an anterior, low relief ridge that tapers distally and most likely limited the extension of the M. pronator quadratus (pq) onto the dorsolateral facet of the humerus. A lateral aspect reveals an additional longitudinal ridge, now running mostly along the diaphysis mid-section, as well as a similarly oriented sulcus closer to the proximal metaphysis. The ulnar surface of IFSP-VTP/PALEO-0003 also displays some distinct regions that correlate with known muscle origins or insertions. Ventral to the glenoid articular facet, in lateral view, there is a shallow depression that extends distally and is consistent with the origination area of M. extensor carpi radialis (erg). Running parallel to the longitudinal sulcus, and ventral to it, yet another elongated depression is observed, here interpreted as the insertion area for the M flexor ulnaris (fu), due to its proximodistal disposition.

A medial view of the proximal end of the humerus reveals addition muscle attachment sites (**figure 15b$_2$**), including a large, triangular depression, encompassing the medial surface of the olecranon process, followed distally by a narrow sulcus that runs the diaphyseal length. These represent the M. pronator quadratus (pq) and the M. flexor digitorum longus (fdl), respectively.

The radius, the second zygopodium element, comprises a rectilinear, gracile, and elongated bone where the diaphysis retains a somewhat constant thickness throughout its length. A slight ventrolateral flexure of the proximal metaphysis is present but does not propagate distally. The shaft and epiphysis also display a slight anteroposterior compression. Its proximal and distal articular regions, although not fully preserved, lacking articular facets, are marked by clear mediolateral expansions, and bear visible striations for muscle attachments. As expected, the radius shares musculature with the ulna, and osteological markings for these are present. The shaft bears an anterior ridge that emerges anterolaterally on the proximal process and then

shifts anteriorly, and also a sinuous, lateral ridge which becomes visible on the proximal metaphysis and then gradually curves dorsally/anteriorly as it approaches the distal epiphysis. The area in-between ridges delimitates the origination surface of M. extensor carpi radialis brevis (ecrb), while dorsally the anterior ridge marks the lateral boundaries of the M. supinator, that runs anteriorly. Ventral to the lateral edge, and located mostly ventrally along the shaft, there is the radial contact for the M. pronator teres muscle. Unfortunately, the medial facet of the radius could not be described due to the surrounding matrix and fragility that prevented further preparation.

4.5.5 Autopodium

The specimen preserves an almost complete and semi-articulated right manus, including proximal carpals (ulnar and pisiform), except for the radial, likely lost to the erosional fracture surrounding this region (this feature was also responsible for the loss of the distal extremities of the ulna and radius). The manus itself is exposed in palmar view (**figure 15a-b**), owing to a strong taphonomic outwards inflexion. This dynamic also partially disarticulated and dislocated metacarpals II and V, while MC I, III and IV in close association with their respective sequence of phalanges. Fortunately, digits I, II, III and IV retained a high degree of cohesiveness, and the full extent of their phalangeal formulas could be determined: 2-3-4-4-?. In light of previously published work by Nascimento & Zaher (2010), which established a phalangeal formula of 2-3-4-4-3 for *B.albertoi*, and given the lack of digit V phalanges in the current specimen, it was deemed likely that these were indeed missing, due to a fragmented MC V, and despite considerable phalangeal number variability in modern crocodylians, even amongst closely related species (Gregorovičová *et al.* 2018).

Generally, the metacarpals of IFSP-VTP/PALEO 0003 have mediolaterally expanded proximal epiphysis that are slightly dorsoventrally compressed, with distinct articulation edges where the adjacent element would rest. The shafts of MC I and II are markedly robust, becoming longer and more gracile laterally in the series, with the MC IV being the longest. Distally they display well-developed and rounded trochleae whose articular edge extends ventrally. These and the phalanges, with the exception of the distal ones, bear circular pits on the lateral surface of their trochleae, an attachment site for M. interosseus muscle group (Meers, 2003). The shaft of the MC I and II display concave lateral margins, contrasting a more rectilinear medial one, as well as slight lateral inflexion of their distal articular ends. The trochleae of MC III and IV are also well-developed but present a straighter orientation. Their diaphysis become visibly narrower at mid length, gradually thickening again towards the distal end. The phalanges of digits I and II are sturdier and mostly proximodistally shorter, with distinctly concave ventral surfaces and well developed trochleae marked by deeper intercondylar fossae. Lateromedially compressed, claw-like ungual phalanges of decreasing sizes are present only on digits I, II and III, a recurrent condition among fossil crocodyliforms and modern crocodylians (Colbert *et al.* 1951; Grigg 2015; Nascimento & Zaher 2010; Sertich & Groenke 2010). These articulated with their posterior phalanges in a slightly laterally inclined manner and bear triangular lateral neurovascular sulci. Digit IV displays a series of four morphologically similar phalanges that diminish in size distally. These are characterized by tapering, less developed thochleae.

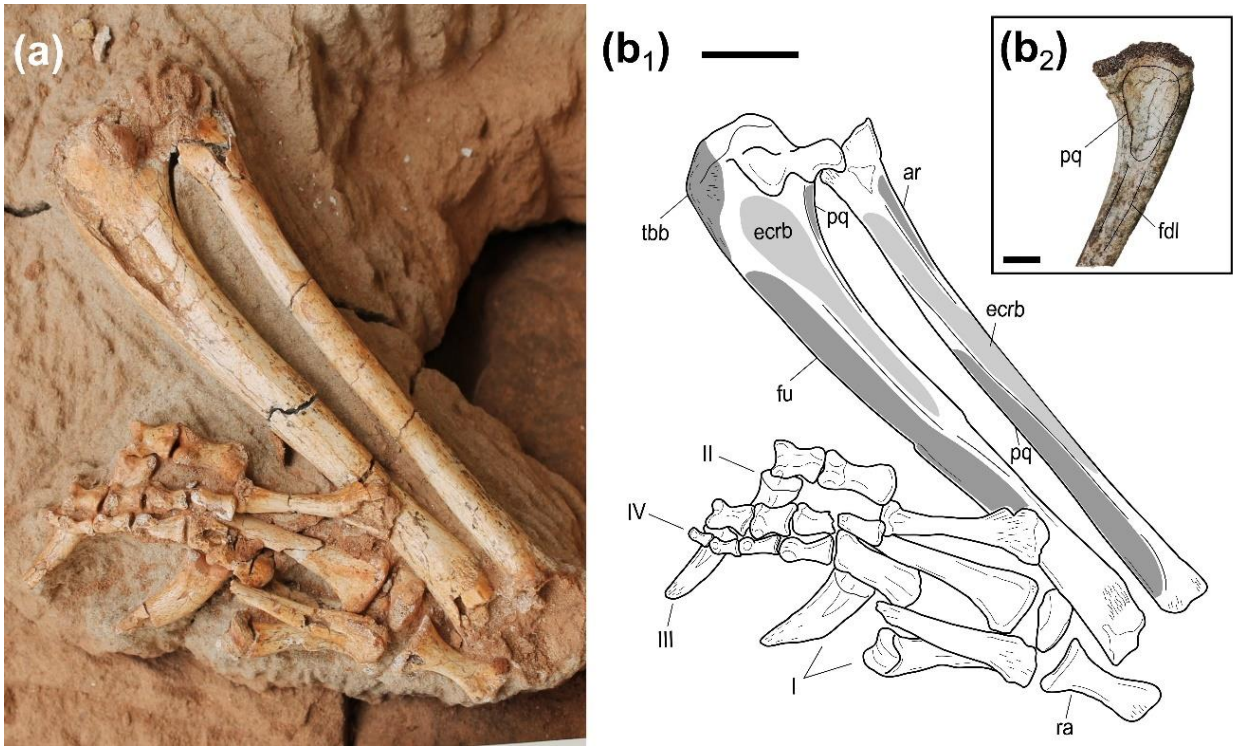


**Figure 15. Right ulna and radius in lateral view with myological interpretations of origination (light grey) and insertion sites (dark grey), as well as all preserved autopodium elements. (a -$b_1$) photograph with line interpretation and; ($b_2$) detail of medial facet of ulnar proximal epiphysis. Abbreviations: ar, anterior ridge; ecrb, M. extensor carpi radialis brevis; fdl, M. flexor digitorum longus; fu, M. flexor ulnaris; pq, M. pronator quadratus; tbb, M. triceps branchii. Scale bars: $b_1$ = 2 cm; $b_2$ =1 cm.**

### 4.6 Hindlimb

All elements of the pelvic girdle are present and relatively well-preserved, despite the visible dorsoventral compression to which the entire set was submitted. Both ilia are still found to be medially sutured to two sacral vertebrae, through their transversely expanded ribs, that fused at anteromedial and medioventral positions, respectively. Ischia were laterally deflected due to taphonomic forces, but their proximal ends are properly connected with the ilia, enclosing the acetabulum, to which both femora are articulated. The pubes were also preserved close to what their position

would have been in life, being anteroposteriorly oriented and meeting along their medial edge, with a clear articular relationship towards the gastralia.

### 4.6.1 Ilium

The ilium´s morphology is distinct due to the short, anteriorly tapering preacetabular process, a strong ventral deflection of the supracetabular process and an anteroposteriorly developed, postacetabular process, that makes up more than half the length of the entire element (**Figure 16**). In anterior/posterior view, the acetabular wall is medially set in respect to the acetabular roof, thus resulting is an inverted I-like shape. These features generate a sigmoidal shape in lateral view, where the ventral border of the iliac blade is sharply convex anteriorly, whilst acutely concave posteriorly, along the postacetabular process. The dorsal margin follows the opposite concavity/convexity pattern. In dorsal view, the ilia are also marked by a substantial lateromedial expansion, resulting in highly developed acetabular roof, that laterally obscures and overhangs the deeply inset acetabular wall, which could not be observed due to the articulated femora. This gives the ilia a somewhat trapezoidal shape dorsally. As mentioned previously, the preacetabular process tapers towards the anterior end, but reaches roughly the same level as the anterior margin of the first sacral prezygapophyses. It is medially accompanied by a similar anterior projection, thus creating an anteriorly concave margin.

Dorsally, the iliac blade has a conspicuous depression that runs its length and is bounded laterally by the thickened edge of the supracetabular crest. The lateral surface of the latter bulges outwards, especially directly above the acetabulum, and possesses a few osteological cues for muscle insertions/originations. A lateral view

reveals a dorsal margin marked by continuous local rugosities which seem to merge anteriorly with the laterally depressed precetabular process, which itself displays vertical and longitudinal striations. Together, these likely marked the origination of anteriormost M. iliotibialis (it – **Figure 16**). The highest rugosity density consisting of vertical sulci and striations may be found on the surface of the supracetabular crest, which is consistent with the insertion of the M. iliofemoralis (if), given similar configurations in basal and extant pseudosuchians (Liparini & Schultz 2013; Romer 1923). These are followed posteriorly, along the transition towards the postacetabular process, by fewer rugosities and a shallow and somewhat oblique elliptical depression where the M. iliofibularis (ilfb) would originate from. The postacetabular process has a clear posteroventral deflection on its posteriormost end, forming a lateroventral surface with oblique muscle scars, the site where M. flexor tibialis internus fascia (fti) would attach. It is here inferred, given the described pelvic anatomy, that the inset nature of the acetabular wall and the verticality of the supracetabular crest would strongly hinder the abduction motion of the femur, thus constantly forcing a 'pillar-erect' parasagittal gait (Bates & Schachner 2011), where most of the weight of region would rest on the proximal end of the femur, mostly limiting it to fore-and-aft movements.

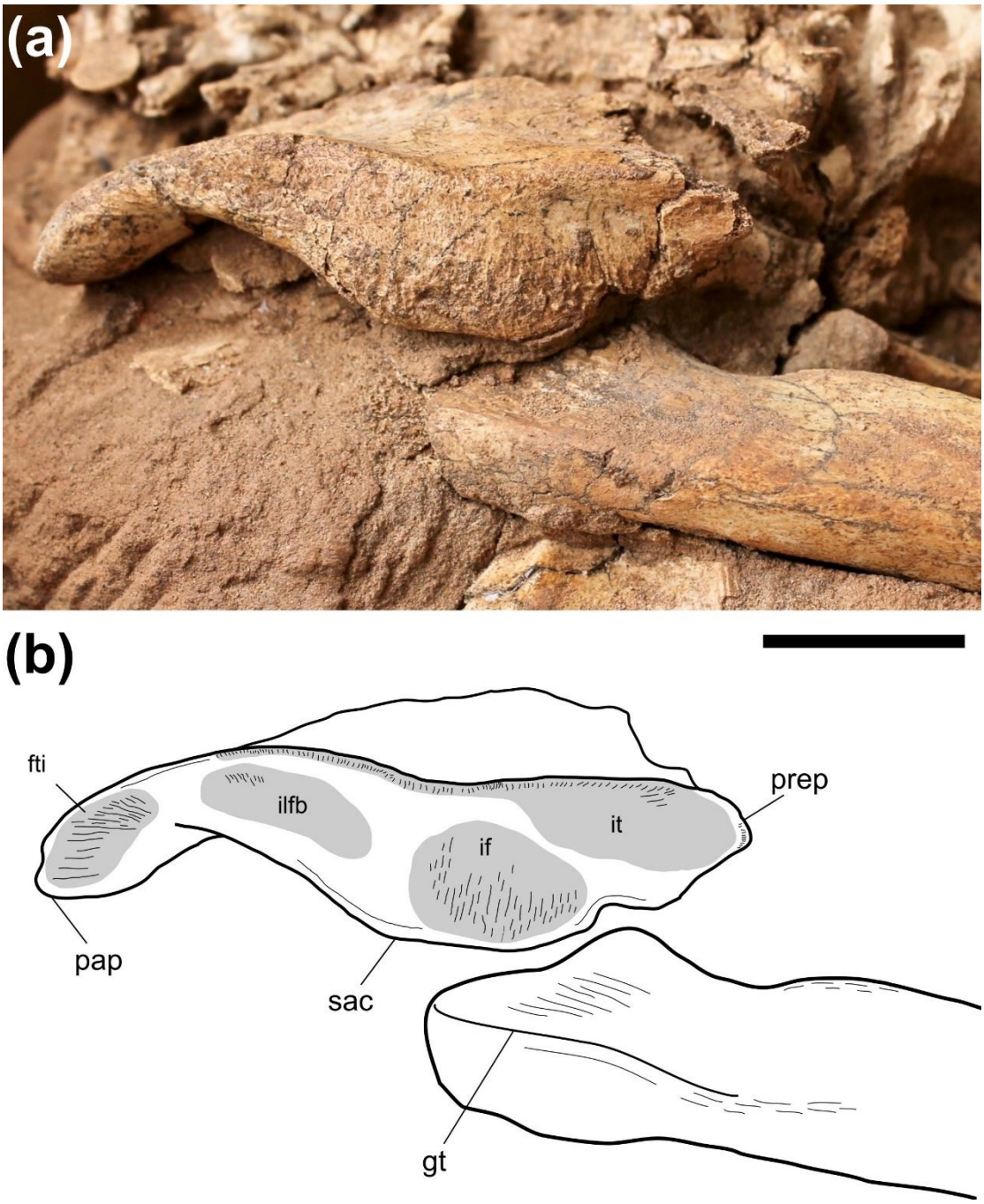


**Figure 16. Ilium in right lateral view (a), and inferred muscle origins (light grey) and insertions (dark grey) (b). Abbreviations: fti, M. flexor tibialis internus fascia; gt, great trochanter; if, M. iliofemoralis; iflb, M. iliofibularis; it, M. iliotibialis; pap, precetabular process; prep, postacetabular process; sac, supracetabular crest. Note ventrally inclined supracetabular crest and possible abduction of femur. Scale bar = 2cm.**

### 4.6.2 Pubis

These are the anteriormost elements of the pelvic girdle and both sides are preserved in their full extend in this specimen. The pubic bones are exceptionally elongated, reaching the same level as the tenth dorsal vertebrae anteriorly, and have two distinct processes separated by a long shaft (**Figure 11**). The posterior pubic head (ph) is transversely narrow and has a verticalized articular surface that attaches to the ischium pubic pedicle, whereas anteriorly the tubular shaft becomes wider as it reaches the distal pubic blade (pb), forming a tabular-like (squarish shaped margin in dorsal view), dorsoventrally flattened anterior end. There is a clear rotation between these two distinct regions of the pubis, as recognized in other baurusuchids (Godoy *et al.* 2016), with the shaft transitioning from a dorsomedial orientation posteriorly to a horizontal disposition anteriorly.

In dorsal view the pubis is clearly bent medially, generating laterally inclining ends as well as a medial pubic symphyseal margin (psm) at mid length, where counterparts come into contact. This region is characterized by the development of a pronounced medial lamina, with a shallow elliptical depression on its dorsal surface. The shaft surface is mostly smooth, whereas the pubic blade displays anteroposterior striations and muscle insertion marks on its distalmost edge. Given this surface would have faced medially in life, it is thus interpreted as insertion scars for the M. pubioischiofemoralis externus 1 (PIFE 1 *sensu* Romer 1923).

### 4.6.3 Ischium

Owing to the way the pelvic girdle was preserved, the left ischium is not available for description since it is still embedded within the surrounding sandstone, while the right element, although visible, is partially obstructed by the right femur, precluding a

more detailed description of its proximal region. Here the ischium follows the general crocodyliform shape seen in other clades (Colbert *et al.* 1951; Pol *et al.* 2012; Romer 1923; Vieira *et al.* 2016), as a quadrangular, mediolaterally compressed iliac blade (ib) with strongly and slightly concave posterior and anterior edges, respectively.

In lateral view, the iliac blade bears a conspicuous proximodistal ridge close to the posterior border but is separated from it by a similarly shaped negative relief region. Anterior to it, a large, depressed surface emerges, comprising most of the iliac blade´s lateral surface area. Additionally, there is a posteroventrally tapering process, which gives the blade an anteriorly inclining aspect in lateral view. Although muscle insertions left less conspicuous markings on the ischium surface as compared to adult forms, there are clear muscle scars for the Adductor muscle 1 on the anteroventral edge of the blade, and similar striations on the anteroventral and posteroventral regions of the iliac ridge, possibly for M. pubioischiofemoralis 3 (PIFE 3) and Adductor 2.

4.6.4 Stylopodium

The specimen preserves both left and right femora, yet the left element is mostly unavailable for description, due to its poor state of preservation. The right femur is displayed in anterolateral view, still articulated with the pelvic girdle, close to what it would have been in life. It is a slender and elongate bone, slightly longer than the tibia and fibula, set apart by a somewhat straight shaft, an only marginally expanded proximal epiphysis with a medially inturned femoral head, and a transversely expanded condylar distal end (**figure 17a-b**). The proximal epiphysis is marked by being only slightly thicker than the diaphysis and mediolaterally flattened, bearing a circular depression laterally. Within this depression there are proximodistal striations marking the passage and attachment of M. puboischiofemoralis internus (pifi 2), which extends

posterodistally ventral to the great trochanter. Posterolaterally, the great trochanter manifests as a raised proximodistal crest that displays shallow depressions and striations posteriorly and anterolaterally to it, where the M. puboischiofemoralis externus (pife) and the aforementioned second extension of M. puboischiofemoralis internus (pifi 2) would attach (Klinkhamer *et al.* 2017; Romer 1923).

Anterolaterally, the proximal metaphysis bears an undeveloped anterior flange (af), where longitudinal muscle scars for the anterior extension of M. pubioischiofemoralis would attach (pifi 1). Although mostly straight, the diaphysis is also slightly anteriorly curved, generating a concave posterior surface and an anterior convex one, but substantially less so than the more sigmoidal eusuchian condition (Romer, 1956).

In anterolateral view, the proximal metaphysis bears an elongated and shallow tear-drop shaped depression, anteriorly bound by an oblique and low relief crest, near to the anterior flange. These represent, respectively, the insertion site for the M.iliofemoralis (if) and for its auxiliary fixation crest (cif). Anteriorly, along the distal half of the diaphysis, the femorotibialis ridge (ftr) runs as a thin crest on its anterior convexity, limited distally by the intercondylar fossa (if). Making use of the opposite concavity, the posterior adductors attach (add 1+2, Romer, 1923; or M. adductor femoris sensu Sertich et al., 2010), having originated on the ischium. Distally, both the metaphysis, lateral and medial condyles rotate outwards from the proximal plane, being approximately orthogonal to it. The distal epiphysis is comprised by the mediolaterally expanded condyles, which posteroventrally bear the tibial articular surfaces. The lateral condyle is visibly larger, more ventrally developed and forward leaning with respect to the medial one and both are separated anteriorly by an intercondylar fossa, emerging on the proximal metaphysis and then becoming

increasingly deeper and wider ventrally. The ventrolateral margin of the lateral condyle possesses a crescent-shaped articular surface for the fibula, also known as the fibular condyle. Above it, clear markings for the origination of M. gastrocnemius (gc) and M. extensor digitorum communis (edc) are present.

4.6.5 Zeugopodium

Composing the middle section of the hindlimbs are the epipodials, the tibia and fibula, both preserved on either side (**Figure 17b$_1$-b$_2$**). The tibia is a robust and thick long bone with a much-expanded proximal epiphysis and a roughly circular diaphyseal cross-section. Proximally, the articular surface is somewhat triangular and flattened, accommodating both distal femoral condyles in a hinge-like articulation. Just anterior from the proximal articular surface there is a low relief cnemial crest (*quadriceps femoris* insertion). The *tibial shaft arches outwards/laterally along its middle portion, resulting in a confluence of* both tibia and fibula proximally, while distally there is a clear gap between the two.

Distally the tibia develops wide lateral and medial condyles which articulate with the proximal tarsals, mostly the astragalus. While the medial condyle contacts the fibula, the lateral one extends even further distally, also being laterally inclined, creating an oblique articular surface. The tibia articulates laterally with the fibula, a gracile and elongate bone distinguished by a mediolateral compression along its length in addition to a posteriorly curved and anteroposteriorly stretched proximal epiphysis. Its shaft is mostly straight, maintaining a constant thickness, and culminates into a distal expansion, bearing the tarsal articular surface ventrally as well as the distal hook medially that extends to contact the medial tibial condyle.

A depression and vertical striations on the proximal end's lateral surface correspond to the attachment of the long external lateral ligament (lell), whilst anteroproximally the *iliofibularis* trochanter (ilft) develops as a thickened and swollen crest. Medial to the latter, a depression for the *flexor digitorum longus* is visible.

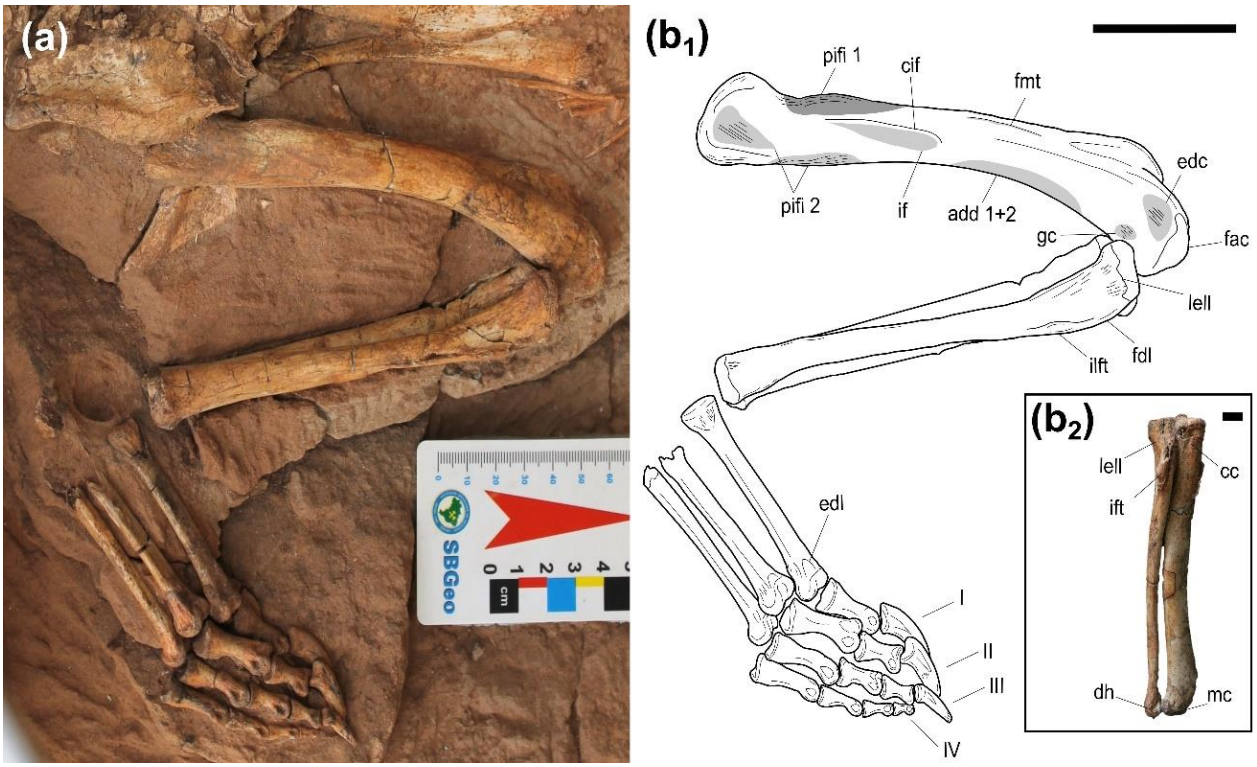


**Figure 17. Articulated hindlimb in detail. (a-$b_1$)-photograph followed by schematic drawing with highlighted features and musculature insertions (dark grey) and origins (light grey) based on textural correlates. ($b_2$)-tibia and fibula in anterior view. Abbreviations: add 1+2, M. adductor femoris 1 and 2; cc, cnemial crest; cif, crest for the insertion of the M. iliofemoralis; dh, distal hook of fibula; edc, M. extensor digitorum communis; M. extensor digitorum longus; fac, fibular articular facet of the femur; fdl, M. flexor digitorum longus; fmte, M. femorotibialis externus; gc, M. gastrocnemius; if, M. Iliofemoralis; ift, M. iliofemoralis trochanter; lell, external lateral ligament; pifi 1, M. puboischiofemoralis internus 1; pifi 2, M. puboischiofemoralis internus 2. Scale bar equals to 5cm in $b_1$ and 1 cm in $b_2$.**

*Tarsus*. A single right astragalus is the only well-preserved proximal tarsal element in this specimen. It is in good condition, in spite of an oblique fracture affecting mostly the medial distal roller. In both anterior and posterior views, it displays an hourglass-like shape, being wider than tall but also anteroposteriorly narrow, with distinct concave dorsal and ventral margins (**Figure 18**). Dorsally, the astragalus is

marked by the v-shaped tibial articular facet (tbf), where a larger and posteriorly extending depression would receive the tibial medial condyle, and the laterodorsal and elongate shallow elliptical fossa, the lateral one. These facets are somewhat orthogonal to each other and delimited medially by the astragalar fossa.

Anteromedially, the astragalus is dominated by a large, semi-circular surface that bulges outwards, the medial distal roller, where the first metatarsal usually articulate. By contrast, the lateral end bifurcates into a fibular articular facet dorsally, and the calcaneal peg ventrally. The latter fits into the calcaneal socket at the astragalus-calcaneum interface.

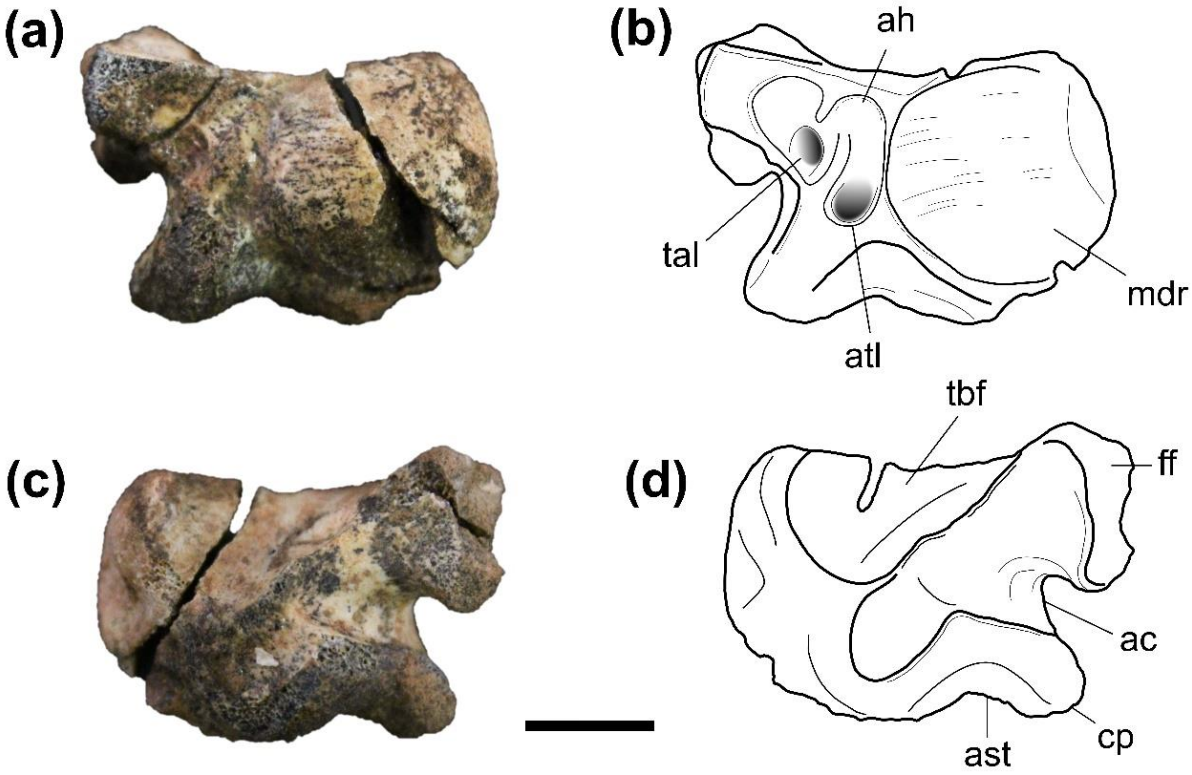


**Figure 18. Right astragalus and corresponding line interpretation in anterior (a) and posterior (b) views. Abbreviations: ac, articulation channel; ah, anterior hollow; ast, astragalar trochlea; atl, astragalar tarsale ligament pit; cp, calcaneal peg; ff, fibular facet; mdr, medial distal roller; tal, tibial-astragalar ligament pit; tbf, tibial articular facet. Scale bar = 1 cm.**

A visible anterior hallow develops anterolaterally, defined by a shallow triangular depression which is bisected by a conspicuous crest. The medial fossa corresponds to the astragalar-tarsale ligament attachment (atl), at the same time as the rounded lateral one represents the tibial astragalar ligament pit (tal). Posterolaterally, between the fibular articular facet and the calcaneal peg, the astragalar articulation channel (ac) develops as a deep sulcus, bounded ventrally by the astragalar trochlea.

### 4.6.6 Autopodium

The right pes is articulated and mostly complete, only missing the fourth metatarsal, the proximal articular ends of MT II and III, and also the smaller MT V (**Figure 17a-b**). Noticeably, these were preserved with shafts parallel and near to each other, with minimum spread, and at an oblique angle to phalangeal plane. The metatarsals are similar and share a common morphology comprised of an elongated and dorsoventrally compressed element, with proximally and distally expanded epiphysis, and a straight shaft with a uniform thickness and elliptical cross-section. Their proximodistal lengths increase, with MT I being the shortest and MT III being the longest. The latter, consequently, also yields the most prolonged digit. Distally, they exhibit transversely wide and strongly rounded trochleae with shallow intercondylar sulci. Anterodistally, the metaphysis, just dorsal to articular end, bear conspicuous semi-circular depressions.

Curiously, the articular surfaces of trochleae ascend anterodorsally towards the distal metaphysis, possibly allowing for increased dorsiflexion/hyperextension of the metatarsophalangeal joint, as evidenced by manual articulation (**figure 16**). This feature is present on all three preserved metatarsals. The pedal phalangeal formula,

not encompassing the fifth digit is the following: 2-3-4-4. The proximal phalanges of digits I and II are visibly more robust and stout than the more lateral ones, which are more gracile. They display well-developed proximal concavities for articulation with the metatarsals, straight dorsal surfaces, and strongly concave ventral ones, giving them an arch-like aspect. Deep lateral and medial pits for ligament insertions are present on all observed phalanges. Distal phalanges decrease in size preserving their general morphology, and digits I, II and III terminate in laterally compressed claw-like unguals, that articulate with a noticeable lateral inclination. Similarly, digit IV contains four sequential phalanges that diminish in size.

### 4.7 Osteoderms

The two parallel sagittal rows of osteoderms typical of baurusuchids are poorly preserved here and only three individual plates were found associated with the skeleton. However, these are sequential, and rest upon the neural spines of the thirteenth and fourteenth dorsal vertebrae, respectively, suggesting preservation close to their position in life.

The osteoderms of IFSP-VTP/PALEO-0003 are highly elliptical and symmetrical in superficial view, being substantially anteroposteriorly longer than wide, with convex lateral and medial margins and a tapering anterior articular surface (*facies articularis externa* - fae) (**Figure 11c**). There is also a slightly medially shifted longitudinal keel (lk) that reaches the posterior end but fails to invade the anterior one. Consequently, the marginally inset position of the keel creates a larger area of the *pars laterale* in respect to the *pars mediale*. The keel itself is low relief, not raising substantially above the overall external surface. These osteoderms also lack the thickness/robustness and

dorsal deflection of anterior and posterior ends observed in adult forms, being instead mostly flat and dorsoventrally thin, almost sheet-like. Sculpturing patters of pits and sulci are also absent and/or incipient at most. Despite not being imbricated, the presence of a *facies articularis externa* indicates that they might have been so in life, or, perhaps, gained progressively increasing ,imbrication as the animal grew. No suture marks were observed on the medial edge of the osteoderms, pointing to a looser parallel arrangement at this life stage.

### 4.8 Phylogenetic systematics

An initial analysis that included all 115 taxa resulted in a poorly resolved topology typified by several polytomies. These affected the relationships of both basal crocodyliforms as well as more derived clades, diminishing the intended informative power and thus making it not adequate as a working hypothesis. Following the procedures of Martinelli *et al.* (2018) and subsequent work based on the same character matrix, such as Cunha *et al.* (2020), a set of five unstable taxa were pruned from the following attempt (Pehuenquesuchus, Neuquensuchus, Microsuchus, Pabhwehshi and Coringasuchus), yielding a much improved phylogeny, with the strict consensus of a total of 5568 MPTs with 1729 steps, presented below (**Figure 19**).

As expected, it recovers the main dichotomy within Mesoeucrocodylia, characterized by Neosuchia, a mainly semi-aquatic lineage, and the terrestrial and ecologically diverse Notosuchians. Nevertheless, the obtained inner relationships of major notosuchian clades have changed significantly from previous works (Fiorelli *et al.* 2016; Martinelli *et al.* 2018; Pol *et al.* 2012). The monophyly of Sebecosuchia, originally erected by Colbert (1946) to encompass superficially similar oreinirostral and

ziphodont forms, *Sebecus icaeorhinus* and *Baurusuchus pachecoi*, is no longer supported, and sebecids now counterintuitively emerge as the basal most notosuchian clade, implying a substantial ghost lineage, in spite of recent finds of Cretaceous materials with likely sebecid affinities (Rabi & Sebők 2015; Sellés *et al.* 2020). Sebecidae is then followed by a divergence between Peirosauridae (excluding *Stolokrosuchus*) and a new clade uniting Uruguaysuchidae and a larger group containing the so-called "advanced notosuchians" (sensu Pol, 2005) plus Baurusuchidae.

Although there is some uncertainty regarding the positioning of *Chimaerasuchus*, the internal relationships of Sphagesauridae and related forms are similar to previous works, marked by small-bodied genus *Caipirasuchus* and the much larger *Sphagesaurus* and *Armadillosuchus* (Cunha *et al.* 2020). Curiously, *Comahuesuchus*, an enigmatic taxon known from a fragmentary skull (Martinelli, 2003), is recovered as closely related to Baurusuchidae, sharing with them a more recent common ancestor then with any other notosuchians. The latter, in accordance to recent baurusuchid-focused phylogenies (Darlim *et al.* 2021b; Godoy *et al.* 2014; Montefeltro *et al.* 2011), is comprised of the Pissarrachampsine and Baurusuchinae subfamilies, with the noticeable difference of *Cynodontosuchus*, which now is a more derived member of the clade and sister taxon to *Stratiotosuchus*. The newly codified specimens, IFSP-VTP/PALEO-0003 and *Gondwanasuchus*, sit sequentially as the second most and most basal baurusuchid, respectively. We interpret that the basal position of the former, considering its immature semaphoront condition, has important implications that are discussed further in the coming section.

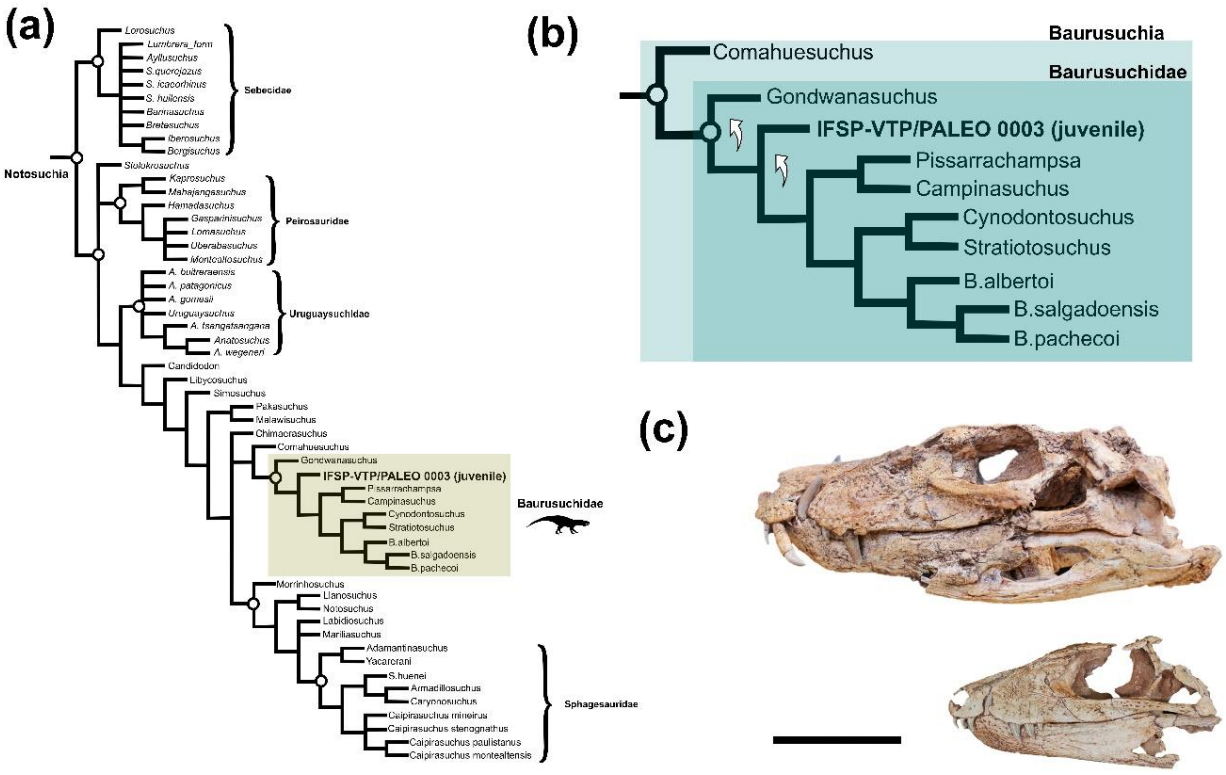


**Figure 19. Results of phylogenetic analysis. (a) Strict consensus tree of 5568 MPTs obtained as a working hypothesis. The neosuchian branch within mesoeucrocodylia is not shown. Bremer supports are shown for each node. (b) Detailed internal relationships of Baurusuchidae, showing the tendency of both IFSP-VTP/PALEO 003 and Gondwanasuchus to emerge as basal terminals. (c) Skulls shown in left lateral view to highlight size differential. Scale bar = 5cm.**

## 5. DISCUSSION

The skull of IFSP-VTP/PALEO-0003 differs considerably from adult individuals. Differences in proportion, ornamentation and development of individual bones are made sharper by a side-by-side comparison (**Figure 20, 21 and 22**). The in-depth description above allowed for more detailed comparisons with other baurusuchid semaphoronts (table below), which resulted in the identification of several osteological characters, mostly cranial, that show substantial morphological shifts with ontogeny.

These may be divided into characters relating to: (1) dermatocranium development; and (2) hypertrophy of jaw adductors. As with modern and fossil

crocodyliforms (Drumheller *et al.* 2021; Salas-Gismondi *et al.* 2015; Staniewicz *et al.* 2018; Tucker *et al.* 1996), as well as other non-related archosaurian lineages (Frederickson *et al.* 2020; Holtz 2021), ontogeny plays an important role in the trophic structures of both intraspecific and interspecific communities. Given its inferred position as filling the top predator guild by anatomical, biomechanical, and tentative geochemical evidence (Cardia *et al.* 2018; Montefeltro *et al.* 2020; Riff & Kellner 2011), it is important to assess the predatory capabilities of immature baurusuchid specimens in order to better understand their paleoecology, as well as make a critical assessment of previously proposed trophic interrelationships for this taxon in the Bauru Basin (Godoy *et al.* 2014; Klock *et al.* 2022).

### 5.1 Dermatocranium development

In both extant and fossil crocodylians, post-hatching growth is characterized by substantial development of the sculpturing patterns and relief structures of dermatocranium bones (de Buffrénil *et al.* 2015; Grigg, 2015), which have a history of being used to assess growth stages (Griffin *et al.* 2021). Juveniles, such as the present specimen IFSP-VTP/PALEO-0003, in line with what is also observed in the ontogenetic series of modern crocodylians, and *Melanosuchus niger* is used here as an example (**Figure 20**), show only incipient ornamentation with respect to larger specimens.

Sculpturing is concentrated on the rostral region, mostly on the nasal and dorsolateral surfaces of the maxilla, being marked by shallow and incipient vermiform grooves, whereas other regions retain mostly smooth or smoother external surfaces. Ornamentation on much larger and skeletally mature baurusuchid specimens, on the other hand, such as MPMA 62-0001- 02 and DGM 1477-R (Carvalho *et al.* 2005; Riff 2003; Riff & Kellner 2011), develop further, encompassing the entire cranium, with the

noticeable exception of the quadrate, which is part of the splanchnocranium (of distinct embryonic origin). It becomes a network of more densely concentrated grooves and pits, also heavily concentrated on skull roof elements, that may obliterate or complicate the identification of sutures, resulting in a more robust overall aspect of the skull. Congruently with IFSP-VTP/PALEO-0003, incipient ornamentation or its absence are also observed in both LPRP/USP 0049, a *Pissarrachampsa* juvenile (Godoy *et al.* 2018), and *Gondwanasuchus*, the smallest known baurusuchid.

The mandibles seem to closely follow the pattern above, where juveniles like IFSP-VTP/PALEO-0003 and LPRP/USP 049, in addition to *Gondwanasuchus*, while already possessing symphyseal sculpturing marked by pitting, present mostly smooth lateral surfaces of mandibular rami, at the same time as adults expanded ornamentation to these areas, reaching the anterior border of the external mandibular fenestrae, and also the surangular's lateral surface in the case of *B.salgadoensis*.

Another tentative ontogenetic shift linked with the dermatocranium relates to cranial crests. As previously hinted by Santos *et al.* (2021), IFSP-VTP/PALEO-0003 displays more clearly visible and high-relief sagittal crests on frontal's dorsal surface compared to adult forms, where this feature becomes proportionately less raised with respect to surrounding surfaces, especially as a wide frontal depression develops (Carvalho *et al.* 2005; Price 1945; Riff 2003).

The development of dense sculpturing adjacent to the crest might be a contributing factor, as it helps to obscures other features. This general pattern is followed by members of *Baurusuchus* genus within baurusuchinae plus *Aphaurosuchus escharafacies* Darlim *et al.* (2021), but not by *Aplestosuchus sordidus* (Godoy *et al.* 2014). Similarly to the latter, *P.sera* seems to have retained a high-relief

frontal crest into maturity as well (Montefeltro *et al.* 2011, fig 3B). Additionally, the immature specimens IFSP-VTP/PALEO-0003 and LPRP/USP 0049 also share a protruding infraorbital crest that overhangs the jugal's anterior ramus. Such feature seemed to get reabsorbed into the jugal lateral surface as the animal matured, resulting in a less distinct, but still noticeable crest that, together with the development of the ventral margin of the jugal, resulted in the fan-shaped lateral depression shared by baurusuchids (Godoy *et al.* 2014).

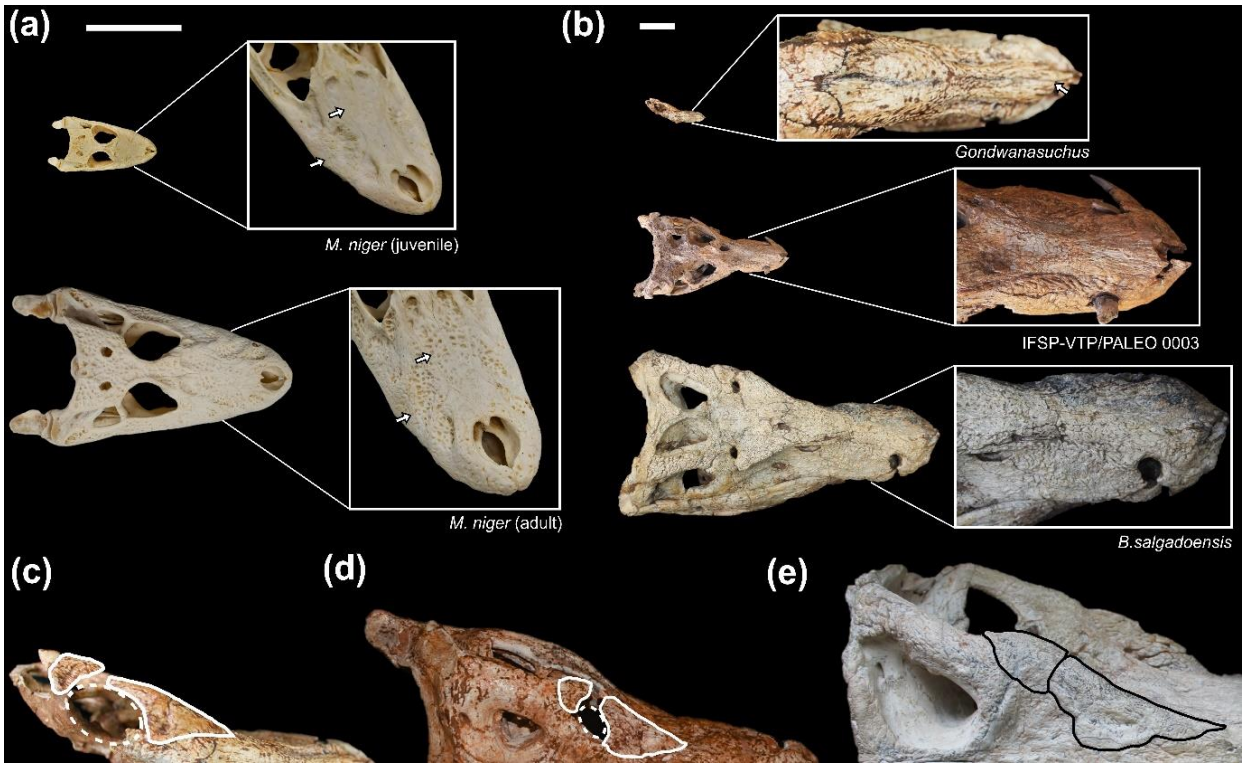


**Figure 20. Ontogenetic development of dermal bone ornamentation in *Melanosuchus niger* and Baurusuchidae. (a) juvenile and adult *M. niger* showing increasing sculptured rostra. (b) Rostral sculpturing development in *Gondwanasuchus*, IFSP-VTP/PALEO 0003 and *B. salgadoensis*. Note the size differential and unfused nasals in *Gondwanasuchus*. (c-e) Levels of fusion between palpebrals in different baurusuchid semaphoronts. (d) is a juvenile *Pissarrachampsa* (Godoy et al., 2018). Scale bars, a = 10 cm, b = 5 cm.**

Lastly, juvenile individuals display slender, less ornamented palpebrals that form proportionally larger elliptical supraorbital fenestrae. Comparisons with mature individuals reveals the gradual closure of such opening, with gradual fusing occurring

along the frontal's lateral margin (**Figure 20c-e**). Specimens assumed to have been adult forms generally have reduced supraorbital openings that shifted to ellipses with lateromedially oriented major axis. Curiously, *Stratiotosuchus maxcheti* Campo et al. 2001, the largest baurusuchid skull ever found, is marked by palpebrals that have fully fused to each other, completely closing these fenestrae. Together, it seems likely that these differences constitute the complete ontogenetic series, starting with relatively large circular openings, reaching a smaller elliptical phase in adulthood as palpebrals become more robust, and eventually culminating in total closure in older adults.

## 5.2 Hypertrophy of jaw adductors

Considering the nature of preservation of most vertebrate fossil remains, myological reconstructions and comparisons are commonly achieved by the observation of osteological correlatives of muscle origins and insertions in the form of surface textures, like muscle scarring and crest-like features (Bona & Desojo 2011). These crests and tuberosities, in the context of extant homologies, may thus be inferred to have marked where the known crocodylian jaw musculature aponeurosis and tendons inserted (Iordansky 1964, 2000).

Overall, the osteological correlates for jaw adductor musculature present in IFSP-VTP/PALEO-0003 closely follow the living crocodylian architecture (Bona & Desojo 2011; van Drongelen & Dullemeijer 1982; Iordansky 2000; Schumacher 1973), despite differences in positioning and size, that are mostly attributable to the platyrostral condition characteristic of neosuchians (Sellers *et al.* 2022). Nevertheless, it was possible to determine that IFSP-VTP/PALEO 0003 exhibits significant size and development deviations from adult individuals within baurusuchidae (**figure 21 and**

**22**). These may be ascribed to muscle growth in association with their origin and insertion sites. Considering the ecological relevance of bite force and the subsequent ontogenetic shift in muscle arrangement and development in modern crocodylians (Erickson *et al.* 2003; Gignac & Erickson 2016a; Sellers *et al.* 2017), the description of such changes in baurusuchidae is made necessary to better grasp their post-hatching ecology.

In agreement with the findings of Gignac & Erickson (2016), and also Sellers et al. (2022), the ontogenetic hypertrophy and lateral insertion of the M. pterygoideus ventralis (mPTv) seemed to also have played a similar role in the bite force of the altirostral baurusuchids. In the IFSP-VTP/PALEO-0003 juvenile and LPRP/USP 049, the distal ends of pterygoids and ectopterygoids are roughly subequal, both contributing to form the origination area for mPTv, whereas in adults the ectopterygoid fails to reach the distal tip, and the pterygoid aponeurosis is dominated by the distal pterygoid flange (**Figures 21a-b and 22a-b**). As expected, based on modern crocodylian cranial mandibular myology (Bona & Desojo 2011), the mPTv would proceed to envelop the angular's ventral edge as it reached for its lateral surface, where it inserted to a depression that bounds the external mandibular fenestrae (dmp, depression for the insertion of the M. pterygoideus ventralis).

Comparisons with medium-sized and large adults revealed that this tear-drop-shaped depression developed to encompass not only a larger area but also became substantially deeper as the mPTV enlarged with growth (**figures 21 and 21 $a_1$-$a_3$**). Its shallowness and limited posterodorsal reach in IFSP-VTP/PALEO-0003, marginally extending above the angular-surangular suture, contrasts with the much deeper and broader depression in adults, that extends almost to the dorsal edge of the surangular (**figure 21$a_3$, white arrow)**. It is bound by an oblique crest that borders the posterior

margin of the external mandibular fenestra that also develops further, going from a low relief feature to a thick torus-like crest, limiting the mPTV anteriorly.

There is also evidence for pennate muscle fibers in the form of parallel striations that rapidly shift to an oblique orientation on the posterolateral surface of the angular, reaching the retroarticular process in lateral view. These striations, marking the growth of the ventral M. Pterygoideus, are lacking in the juveniles IFSP-VTP/PALEO-0003 and LPRP/USP 049, and may attest to an increasing reliance on bite-force as the animals grew, as the pennate configuration yields larger cross-sections and, consequently, enhanced tensions (Gignac & Erickson 2016a; Holliday *et al.* 2022; Sellers *et al.* 2017, 2022).

The dorsal surfaces of the pterygoid wings also display increased muscle scarring with ontogeny. While the dorsal facet of the pterygoid in juvenile are mostly smooth and featureless, larger specimens have numerous thin parallel sulci that pervade this surface extending anteriorly into the closed caviconchal fossa, in similar fashion to modern crocodylians (Holliday *et al.* 2013; Witmer 1997). These represent osteological evidence of the passage and development of the mPTd in adult stages, a muscle responsible for the largest percentages of total bite-force in the pseudosuchian lineage (Sellers *et al.* 2022).

Another related ontogenetic cranial difference is found in the general aspect of the retroarticular processes (**Figures 21 and 22 $a_1$-$a_3$**). While in juveniles like IFSP-VTP/PALEO-0003 these are laminar, more rectangular, and anteroposteriorly longer processes with a shallow incline to the horizontal plane, resulting in a straight profile that extends much further back relative to mandibular rami, adults develop comparably shorter, deeper, and more robust paddle-shaped retroarticular processes. Their lateral

flange transitions from a thin, dorsoventrally flattened aspect to a more vertically oriented and dorsally ascending state, gaining a rounded posterior margin, further expanding, and reorienting the retroarticular aponeurosis where the mPTv partially attaches to (**Figure 21a1**). The medial flange of the retroarticular process somewhat conserves its orientation to the horizontal plane, maintaining a sharp oblique lamina that connects its posterior end to the medial margin, where a ventromedial pendant protuberance becomes more robust and pronounced, further projecting towards the sagittal plane as an orthogonal process, that both increases the surface area for the attachment of mPTd and limits in posterior reach (**figures 21-22 $a_2$**).

Additionally, osteological correlatives for posterior adductor muscle groups were also observed to undergo changes with ontogeny. As described above, ventrally the IFSP-VTP/PALEO-0003 displays a medially curving elongate crest running parallel and close to the quadrate-quadratojugal ventromedial contact, bordering the infratemporal fenestra. Somewhat oblique to the latter, an additional, but substantially thicker and high-relief crest is found, bordering the contact between the quadrate and the basioccipital, and conforming to the quadrate's shape as it bends towards the sagittal plane in ventral view (**Figure 21 and 22 $b_1$-$b_2$**). Considering their position on the ventral surface of the quadrate's distal process, they were thus inferred to be homologous to the crests described by Iordansky (1964; 2000) for modern crocodylians that support tendon's A and B, respectively. These comprised and were encompassed by the quadrate aponeurosis, which could be divided into lateral and medial sheets (van Drongelen and Dullemeyer, 1982). The lateral edge of the A' crest would be the origination site of most of mAMES, whereas external portions of mAMP would attach to its medial border, with its deepest bundles emerging from anteromedial B' crest (van Drongelen & Dullemeijer 1982; Holliday & Witmer 2007; Iordansky 1964).

There is substantial development in terms of relief and thickness of both these adductor crests from juveniles to adult forms, in line with observations of the *M. niger* ontogenetic series. While the A' crest gains relief above the quadrate surface, becoming more pronounced and rugose, it is the B' crest that displays the largest shifts, becoming more robust, slightly sinuous, and anteriorly developing into a hook-like projection with medially concave and laterally convex facets (**Figure 22b$_2$**). Similarly shaped features on the B-crest were only found in the largest of *M.niger* specimens, such as UF Herp 5600.

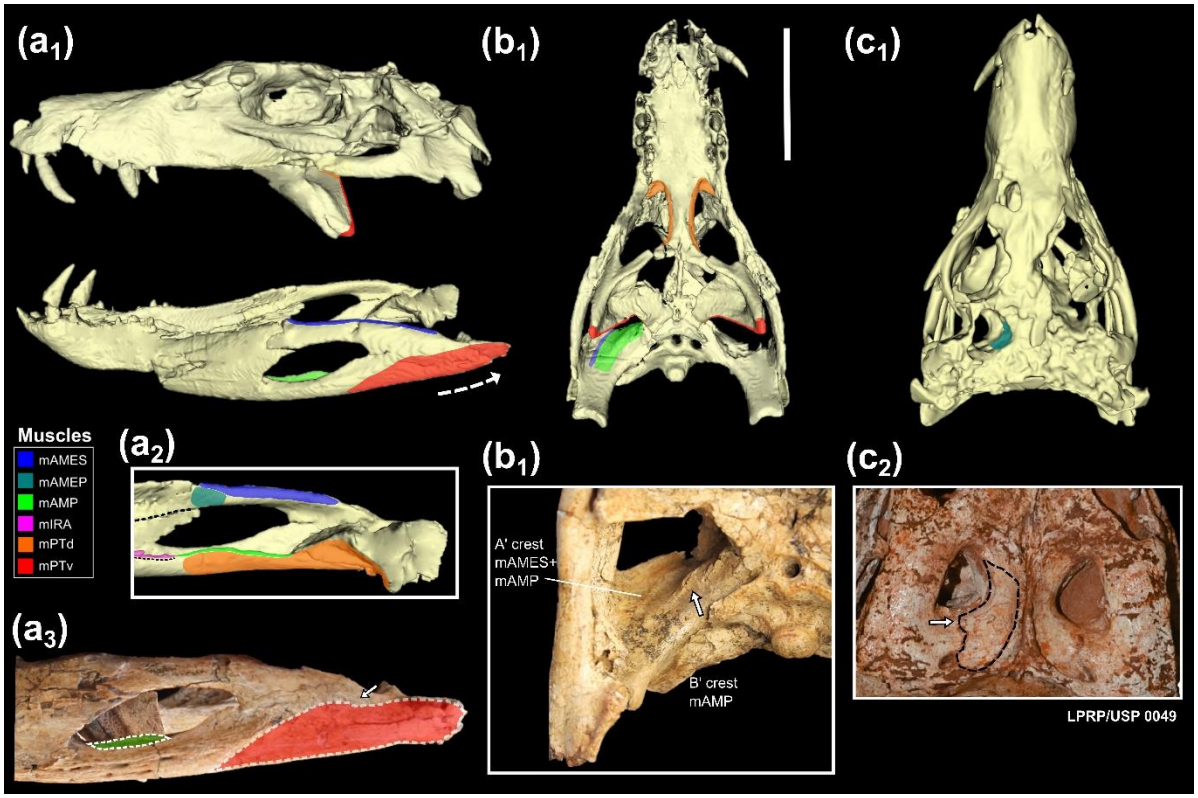


**Figure 21. Digital reconstruction of adductor musculature for IFSP-VTP/PALEO 0003 in lateral, medial, palatal, and dorsal views ($a_1$-$a_2$, $b_1$ and $c_1$). An annotated photograph of its left posterior mandibular ramus and quadrate aponeurosis are also shown ($a_3$ and $b_2$). A *Pissarrachampsa* juvenile, LPRP/USP 0049, is shown to highlight the origination site for mAMEP in the dorsotemporal fossa ($c_2$). Abbreviations: mAMES, M. adductor mandibulares externus superficialis; mAMEP, M. adductor mandibularis externus profundus; mAMP, M. adductor mandibularis posterior; mIRA, M. intramandibularis; mPTd, M. pterygoideus dorsalis; mPTv, M. pterygoideus ventralis. Scale bar $a_1$-$b_1$-$c_1$ = 5 cm**

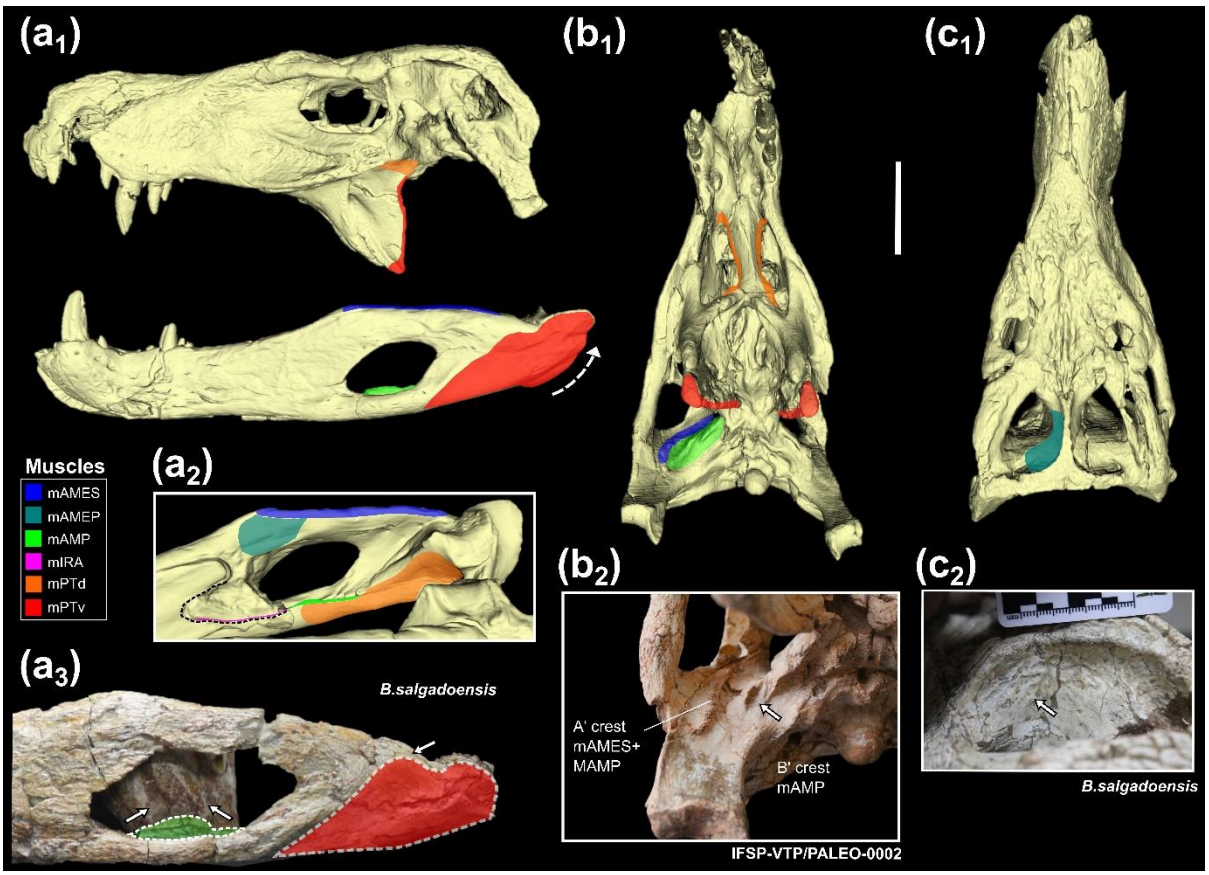


**Figure 22. Digital adductor musculature reconstruction for FEF-PV-R-1/9, and adult baurusuchid in lateral, medial, palatal, and dorsal views ($a_1$-$a_2$, $b_1$ and $c_1$). Both *B. salgadoensis* ($a_3$ and $c_2$) and IFSP-VTP/PALEO 0002 ($b_2$) are shown to highlight origination and insertion sites. Abbreviations: mAMES, M. adductor mandibulares externus superficialis; mAMEP, M. adductor mandibularis externus profundus; mAMP, M. adductor mandibularis posterior; mIRA, M. intramandibularis; mPTd, M. pterygoideus dorsalis; mPTv, M. pterygoideus ventralis. Scale bar $a_1$-$b_1$-$c_1$ = 5 cm**

Corresponding changes were also observed on the insertion sites of the aforementioned muscle groups. The mAMP ventrally attaches to the angular bone, covering most of the external mandibular fenestrae (emf), and fixating on the lateral surface of the angular's medial process (torose margin *sensu* Nascimento & Zaher, 2010; Darlim *et al*., 2021), inserting itself within the meckelian groove and being anteriorly bound by the mIRA (M. intermandibularis) (**Figures 21-22 $a_2$**). The latter enters the meckelian canal itself attaching to its medial wall at the intramandibular aponeurosis (Iordansky, 2000; Bona & Desojo, 2011).

The angular's medial process varies from an undeveloped, more rectilinear shape in IFSP-VTP/PALEO-0003 and *Pissarrachampsa*, to a dorsally ascending, thickened and torose aspect in adult specimens (**Figures 21 and 22 a$_3$**), reflecting an exacerbated development of mAMP. Curiously, as notosuchians lack a coronoid bone (Bona *et al.* 2022), which in crown crocodylians is partially responsible for the attachment surface of both mAMP and mIRA and the closure of the caudal intermandibular foramen (Holliday et al., 2013; Sellers et al., 2021, Appendix A), we hypothesize that such exacerbated enlargement of the angular medial process through ontogeny might have evolved as a compensatory structure for larger adductor attachment in Baurusuchidae.

Also related to the development of the A' crest and the M. adductor mandibulae externus group, whose origin sites of the deepest bundles are not preserved in IFSP-VTP/PALEO-0003, a substantial ontogenetic development of the surangular bone is noted. Its gains dorsoventral depth at the same time as its coronoid prominence becomes more raised above the surangular's dorsal margin (**Figures 21 and 22 a$_1$-a$_3$**). The mAMES inserts dorsomedially on the surangular and is limited by the posteroventral projection of the quadratojugal posteriorly and the coronoid prominence anteriorly, setting it above the external mandibular fenestrae in lateral view. A medial view comparison reveals a shorter coronoid prominence with a smoother medial surface in IFSP-VTP/PALEO-0003, thus possessing proportionally smaller insertion areas for both mAMEM and mAMEP in respect to larger specimens (**Figures 21 and 22 a$_2$)**. Area increase is accompanied in skeletally mature indivuduals by conspicuous anteroposterior muscle scarring at these sites.

A medial view of both juvenile and adult mandibular rami allow for the recognition of further differences involving the mandibular adductor fossa (maf). The

lack of a coronoid bone results in an anteriorly open-ended fossa, marked by the absence of a caudal intermandibular foramen (FIC), not constrained by ossifications (Bona *et al.* 2022). Their anterior margins are formed by the surangular dorsally, the dentary anteromedially and the angular ventrally, producing a rounded profile, which is somewhat anteriorly tapered in IFSP-VTP/PALEO-0003 but dorsoventrally expanded in larger specimens (**Figures 21 and 22 $a_2$)**.

Unfortunately, the poor preservation of the dorsotemporal fenestra and basicranium elements, such as laterosphenoid, hinders comparisons of origination sites for deep and external adductors like mPST and mAMEM. Still, we would like to call attention to the holotype of *B. salgadoensis*, consisting of a large adult skull (ROL = 43cm) that displays substantial muscle scarring in the form of a network of irregular anastomosed pits and vertical striations on the lateral wall of the parietal, within its dorsotemporal fossae (**Figure 22$c_2$**). Considering the pennation of its dorsal portion with respect to the distal one, they are here interpreted to represent the cross-section of individual bundles of mAMEP as it inserted on parietal walls (Holliday *et al.* 2022).

The fact that other smaller adult skulls lack such features (such as LPRP/USP 049, **Figures 21-22 c1-c2**), points to increased development of such muscle throughout life, an important ontogenetic indicator, and perhaps a higher degree of dependency on its functions for mature individuals. Moreover, the absence of additional muscle correlatives outside of the parietal lateral surfaces and dorsotemporal fossae supports the Holliday *et al.* (2020) model for supratemporal fenestra function, where mAMEP would be the only adductor to reach the dorsotemporal fossa, whereas the frontoparietal fossa would house vasculature, fatty tissues and serve a thermoregulatory role.

Size and wear discrepancies between the exposed teeth IFSP-VTP/PALEO-0003 and adult specimens are also revealing. None of the premaxillary and maxillary teeth in the former display any wear facets and/or apical spalled surfaces which were found in more than one adult specimen collected at the same site (**Figure 23a-d**). The third premaxillary tooth, in fact, despite showing minimal wear, was preserved as it was being pushed down by a replacement tooth (**Figure 23e-f**), exposing an attached long root projecting ventrolaterally. The spalled surfaces of baurusuchid teeth are remarkably similar to the ones large tyrannosaurids exhibit due to flaking from tooth and food contact (Schubert & Ungar 2005). The osteophagy, which likely caused the observed wear, is also corroborated in tyrannosaurs by abundant bone fragments found in coprolites, puncture marks and bite force modelling (Chin *et al.* 1998, 2003; Erickson & Olson 1996; Gignac & Erickson 2017; Rayfield 2004). Similarly, in addition to tooth flaking, rare stomach contents showed *Aplestosuchus* to have consumed bone fragments of a small sphagesaurid (Godoy *et al.* 2014), and the recent analysis of coprolites assigned to baurusuchidae, including X-ray diffraction, also points to osteophagy (Oliveira *et al.* 2021), despite finite element modelling indicating a weaker than expected bite force (Montefeltro *et al.* 2020).

In line with the ontogenetic niche shifts observed in modern crocodylians with increases in size and bite forces (Erickson *et al.* 2012; Gignac & Erickson 2015, 2016b; Tucker *et al.* 1996), also inferred for fossil crocodyliforms (Drumheller *et al.* 2021), and considering the presented differences between juveniles and adults, we suggest baurusuchid semaphoronts of distinct ages and sizes similarly occupied distinct trophic levels. Altogether, these changes attest to baurusuchids undergoing considerable ontogenetic development of cranial adductor muscles between the late juvenile stages

and skeletal maturity, which likely reflected on bite forces, prey size and shifting patterns of tooth wear (Erickson, 2003; Gignac & Erickson, 2016; Holliday et al., 2013).

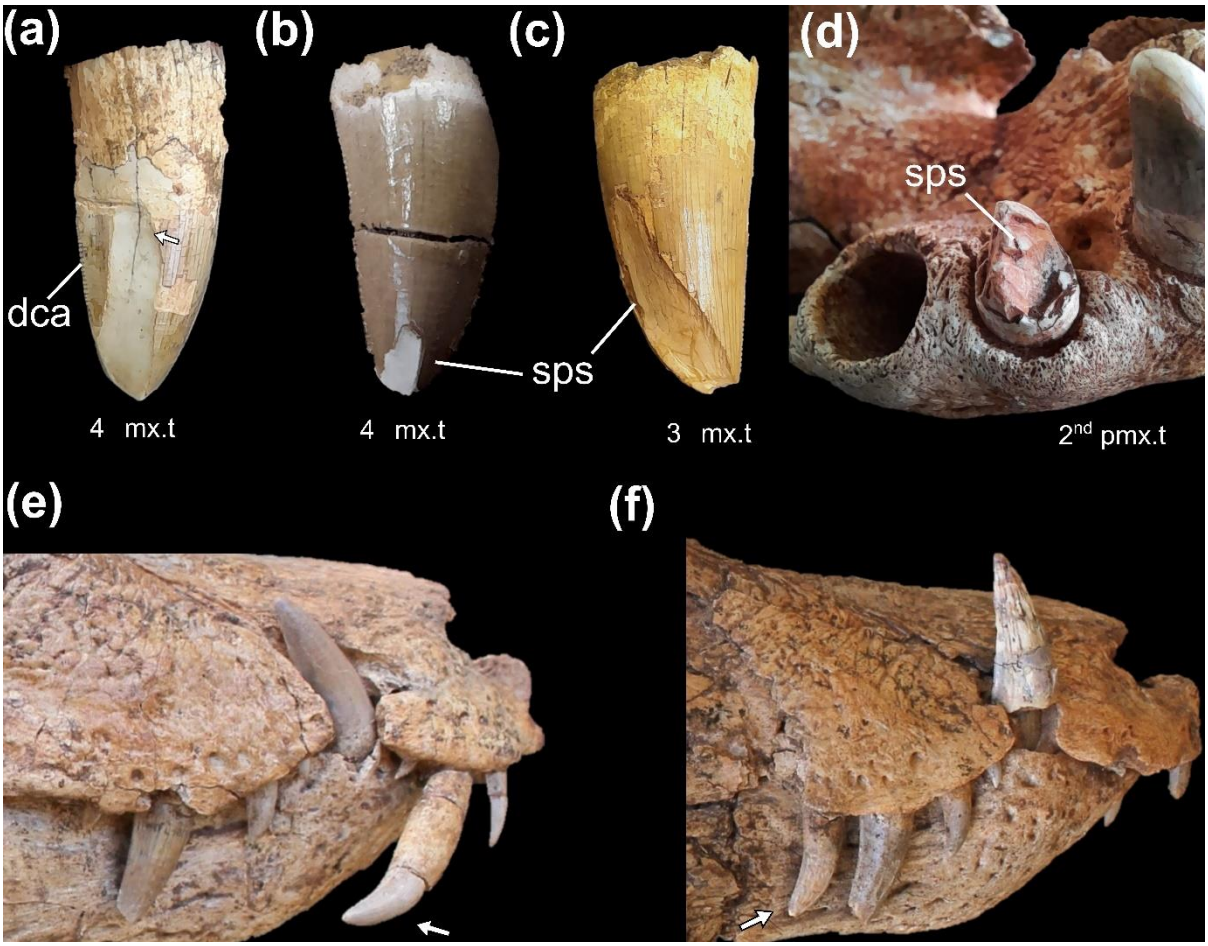


**Figure 23. Patterns of tooth wear in Baurusuchidae. (a-d) adults repeatedly preserve spalled enamel surfaces resulted from tooth-prey contact, similar to some tyrannosaurs, while a smaller juvenile such as IFSP-VTP/PALEO 0003 (e-d) replaced teeth with little to no damage. Abbreviations: dca, distal carina; sps, spalled surface. Not to scale.**

### 5.3 Comments on postcranial anatomy

*Pelvic girdle*. Considering that the sizable majority of phylogenetically relevant characters on current matrices are concentrated on cranial features, and given the paucity of comprehensive postcranial notosuchian materials, the completeness of the present specimen provides an opportunity for comparisons with members of distinct

notosuchian clades in order to continue to elucidate the disparity levels of their axial and appendicular skeletons.

As expected, the ilium of IFSP-VTP/PALEO-0003 resembles closely the overall morphology of more derived ziphosuchians with known complete postcrania, as those of sphagesaurids like *C.mineirus* (Martinelli et al., 2018), and differs most substantially from more distantly related forms such as *A*. *tsangatsangana* (Turner, 2006), and extant crocodylians, including *A. mississippiensis* and *M. niger* (Romer 1923; Vieira et al., 2016). Those morphological discrepancies arise mainly from the poorly developed precetabular process found in these forms, represented by minor projections on the anterior margins of the iliac blades, as well as the configuration of their supracetabular crests. The latter taxa tend to have medially dislocated precetabular processes in respect to supracetabular crests, thus not composing a continuous, lateral-projecting surface as seen in this juvenile specimen.

They also share laterally open and dorsoventrally tall iliac blades, where the acetabular wall is only slightly dislocated from the lateral surface of a poorly developed supracetabular crest with no strong abduction-limiting ventral inflexion. Pelvic girdles materials attributable to sebecids are not common, the best case being an ilium belonging to *S.icaeorhinus* (Pol et al., 2012), which is similar to the overall notosuchian condition, including mature baurusuchids, but also lacks, for instance, the ventral inflexion of the supracetabular crest.

Curiously, known adult baurusuchid ilia generally mirror the discrepancies highlighted above when compared to IFSP-VTP/PALEO-0003 (Nascimento & Zaher, 2010; Cotts et al., 2016), with the noticeable of exception of UFRJ DG 285-R (*B.*

*salgadoensis*), that displays a more pronounced and acute precetabular process and ventrally deflected supracetabular crest (Vasconcellos & Carvalho, 2010).

The configuration of Iliotibialis 1, a knee extensor, originating from a laterally facing and wide preacetabular process could potentially indicate distinct biomechanical requirements for this muscle group particular to this group of baurusuchids. Likewise, the ventral inflection of the supracetabular crest, where the Iliofemoralis would attach, an important muscle that raises the limb above the substrate (Gatesy, 1997; Klinkhamer et al., 2017), besides suggesting a pillar-erect pelvic joint morphology, the ancestral condition for pseudosuchians (Parrish, 1987; Demuth et al., 2020), would also substantially hinder the abduction capacity of the femur, making a sprawling-like stance highly unlikely, forcing a parallel orientation to the sagittal plane. Femur morphology seems congruent with this inference, given the roughly orthogonal angle formed between the proximal and distal epiphysis (Nascimento & Zaher, 2010; Godoy et al., 2016), that seems optimized for anteroposterior movement.

Although it is possible the differences cited may relate to ontogeny, taphonomic deformation must also be considered, given that the preservation of IFSP-VTP/PALEO-0003 involved dorsoventral compression, which could have distorted the original morphology of the ilium. It is important to highlight that a yet undescribed skeletally mature individual recovered from the same site as IFSP-VTP/PALEO-0003 closely matches its iliac anatomy, raising the possibility that, at least regionally, these differences were not due to growth.

The pubes of IFSP-VTP/PALEO-0003, and Baurusuchidae in general (Cotts *et al.* 2017; Godoy *et al.* 2016), are very distinct, characterized by their anteroposterior elongation and a long medial symphysis, contrasting the proportionately shorter,

paddle-shaped morphology found in living crocodylians (Romer, 1923; Vieira et al., 2016; Klinkhamer et al., 2017). Curiously, similar lateromedial, fan-shaped expansions on the anterior ends of the pubes together with limited medial contact between counterparts is also observed in notosuchians like *A. Tsangatsangana*, *M. amarali* and *Y. boliviensis* (Turner, 2006; Nobre & Carvalho, 2013; Leardi et al., 2015). These distinctions should be informative of myological specializations and biomechanical requirements. Considering the pubes as origination sites for the Pubo-ischio-femoralis externus 1 and 2 (PIFE) and Ambiens muscle groups, acting as hip adductors and knee extensors respectively (Allen et al., 2015; Klinkhamer et al., 2017), it is possible that the overly elongated, rod-like pubes could stabilize their inferred parasagittal gaits and represent a specialized adductor attachment configuration optimized for fore-and-aft motion, which is intriguing in the light of recent neuroanatomical data suggesting baurusuchids as active predators, contrasting the ambush, sit-and-wait foraging strategies of modern taxa (Dumont et al., 2021).

Biomechanical and muscle activation EMG data acquired during the "high walk" locomotion of living crocodylians indicated high levels of activity of ventral pelvic adductors during the swing phases, which is consistent with reducing hindlimb abduction and thus elevating the body above the substrate (Gatesy 1997; Reilly & Blob 2003). Adducted hindlimb postures are generally used by crocodylians for more extended excursions and are thus related to low muscular stress (Wiseman et al., 2021). Interestingly, the transverse processes of the last two lumbar vertebrae on UFRJ DG 285-R are anteriorly inclined, suggesting a forward shift to counteract the forces exerted by M. puboischiofemoralis internus 2 (PIFI 2). As previously reported by Gatesy (1997), both PIFI 2 and PIFE 2 act to protract the femur during swing phase, with the latter also adducting the limb to oppose abduction forces by the iliofemoralis.

In extant forms, the employment of such postures are likely not optimal in terms of muscle moment arms and increases tensions over the ankle and femur (Reilly & Blob, 2003; Wiseman *et al.* 2021).

## 5.4 Phylogenetics and ontogeny

The notosuchian internal relationships here obtained constitute one of the most divergent topologies derived from the Pol *et al.* (2014) character matrix. While sebecids being recovered as basal notosuchians seems strange in light of their abundance and diversity in Cenozoic terrestrial environments, especially in South America (Cidade *et al.* 2019), their position here underpins the possibility that their shared morphological characters with baurusuchidae are in fact homoplasies, thus making the status of Sebecosuchia (Colbert, 1946) questionable.

Larsson & Sues (2007), in their description and scoring of *Hamadasuchus rebouli*, originally erected a clade uniting sebecids and peirosaurids, named Sebecia, which has been finding support amongst recently published results (Pinheiro *et al.* 2021; Ruiz *et al.* 2021). The present placement of peirosaurids, emerging after Sebecidae, does not support Sebecia, but we find some morphological similarities between the two clades intriguing nonetheless, such as choanae anatomy, their anteroposteriorly thin pterygoid flanges compared to baurusuchids, their upturned retroarticular processes, and, more strikingly, the shared configuration of their posterior mandibular rami (Carvalho *et al.* 2004; Powell *et al.* 2011, pg. 356, fig 3D), including: (1) a tear drop-shaped external mandibular fenestrae with a medially inset and acute posterior dentary process; (2) heavily sculptured and thick ventrolateral margin of angular; (3) bulged dorsolateral torus of surangular; (4) lack of lateral insertion of M. pterygoideus ventralis.

Furthermore, the oreinirostral and ziphodont conditions utilized to unite sebecids and baurusuchids are only marginally similar. Baurusuchids display a more abrupt transition from their skull roofs to their rostra in dorsal view, and also a more rounded dorsal surface along the latter, resulting in a roughly c-shaped cross-section, whereas sebecids generally display a more gradual transition and a distinct v-shaped profile (Colbert *et al.* 1946; Molnar 2010). Sebecid teeth are also generally smaller and more numerous, hence contrasting the reduced number of more incrassate, hypertrophied teeth observed in baurusuchids (Bravo *et al.* 2021; Colbert *et al.* 1946), with the noticeable exception of *Barinasuchus* and *Dentaneosuchus*, some of the largest terrestrial crocodyliforms found to date (Martin *et al.* 2022; Paolillo & Linares 2007). Altogether, and in the light of myological inferences presented here and elsewhere for *Sebecus icaeorhinus* (Molnar 2012), we find plausible that these two forms had distinct ecologies, despite being considered top-tier terrestrial predators, and so could have arrived at superficially similar morphologies along different character transformation sequences.

Yet another interesting aspect of the phylogeny presented is its overall level of topological convergence with the results by Ruiz *et al.*(2021), itself derived from the previous revision and combination of several other matrices (Montefeltro *et al.* 2013). The monophyly of the minimally defined clade Eunotosuchia is corroborated in detriment of the commonly recovered Ziphosuchia Ortega *et al.* 2000, which, as recently recovered, contained "advanced notosuchians" and sebecosuchians (Cunha *et al.* 2020; Martinelli *et al.* 2018; Pol *et al.* 2014).

Likewise, eunotosuchians are comprised of Uruguaysuchidae plus Sphagesauridae and Baurusuchia, the latter two sharing a more recent common ancestor, and albeit some internal relationships are distinct from the original proposition. For instance, "the least inclusive clade containing *Sphagesaurus huenei* Price, 1950, and *Baurusuchus pachecoi*

Price, 1945…" advanced to define xenodontosuchia, herein does not exclude *Morrinhosuchus luzie* Iori & Carvalho, 2009, but would *Pakasuchus kapilimai* O'Connor *et al.* 2010, preventing the support of the original proposition.

The phylogenetic affinities of Baurusuchidae reaffirms previous works in their main recovered dichotomy (Darlim *et al.* 2021b; Godoy *et al.* 2018; Montefeltro *et al.* 2011), with the exception *Cynodontosuchus rothi* Woodward, 1896, which emerges as a sister taxon to *Stratiotosuchus* within Baurusuchinae. As previously mentioned, the main objective of the analysis was to codify the juvenile specimen IFSP-VTP/PALEO-0003 in order to observe its systematic placement with respect to adult baurusuchids, testing the degree to which the ontogeny of phylogenetically relevant characters affect the topology and the problematic inclusion of juvenile specimens (Hennig 1966; Sharma *et al.* 2017). Similarly to Campione *et al.* 2013, we also sought to compare its behaviour with *Gondwanasuchus scabrosus*, a putative juvenile and the smallest baurusuchid species known (Marinho *et al.* 2013), by codifying it in this character matrix for the first time.

Our results show that both *Gondwanasuchus* and the juvenile baurusuchid behaved similarly and were recovered as sequential terminal taxa at the base of Baurusuchidae, outside the derived subfamilies Pissarrachampsine and Baurusuchinae, with *Gondwanasuchus* being the basalmost form.

The anatomical description here provided allowed for the identification of several differences between IFSP-VTP/PALEO-0003 and skeletally mature baurusuchids (details above), including characters relating to dermocranium development and muscle aponeurosis and attachment sites, accumulating evidence for extensive ontogenetic changes in different crocodyliform lineages (Drumheller *et al.* 2021; Godoy *et al.* 2018; Watanabe & Slice 2014).

The resulting systematic placement of this specimen, though likely invalid, is in line with similar effects attested by the inclusion of juveniles in other archosaur groups, whereby immature individuals of known derived taxa tend to fall outside their clades, like in Hadrosauridae and Tyrannosauridae (Campione *et al.* 2013; Tsuihiji *et al.* 2011). This migration effect to a more basal position in the tree by juveniles, coupled with its size and morphology, is compelling indication of the immature state of the *Gondwanasuchus* holotype, highlighted by the states of characters with ontogenetic influence ( see supplemental material). With this in mind, and in the light of recent controversies regarding the validity of putative juveniles described as new taxa (Carr 2020; Horner & Goodwin 2006, 2009; Larson 2013; Woodward *et al.* 2020), more time should be devoted towards the placement of a given specimen in its ontogenetic context when possible, especially when substantial discrepancies in size, proportion and anatomy are present.

### 5.5 Implications for Baurusuchidae diversity.

Whilst such revision is beyond the scope of this paper, and the aim of future work, the detailed osteological description and ontogenetic characters here provided can be applied to known species to better assess their validity. The minimum anatomical threshold necessary to disentangle one species from another, and the very species concept itself, are controversial topics (Boyd 1999; De Queiroz 2007; Mayr 1996, 2000; Simpson 1951), and there seems to be no consensus (Wheeler & Meier, 2000). This is a particularly difficult issue in paleontology since one rarely has lines of evidence beyond bone anatomy available. Modern practices (e.g. morphometric and molecular evidence, Balaguera-Reina *et al.* 2020; Murray *et al.* 2019) and integrative taxonomy are making considerable strides towards increasing the robustness of

proposed discrete evolutionary entities (Dayrat 2005; Padial *et al.* 2010; Yeates *et al.* 2011), but the lack of genomic, behavioural, and ecological data must not necessarily prevent putative fossil species from being corroborated with additional investigations. When possible, the combined diagnostic characters should account for possible teratogenic, sexual dimorphic, ontogenetic and taphonomic biases and discrepancies in order to increase the longevity and stability of named taxa.

### 5.5.1 *Stratiotosuchus maxchetii*

A didactic example of how these criteria could be applied within Baurusuchidae is *Stratiotosuchus maxcheti* (Campos et al., 2001). We hold that the rectangular outline of the orbits, the distorted external nares, the elliptical *foramen magnum*, together with a fragmented posterior palate, are robust indicators of dorsoventral taphonomic compression, indicating the specimen was not preserved in its original form. Additionally, a supposedly unique character of *Stratiotosuchus*, the presence of only three premaxillary teeth (all other baurusuchids have four)(Riff & Kellner 2011), could be explained by non-phylogenetic processes like an ontogenetic shift in tooth count, as observed in modern crocodylids, where some individuals were found to loose premaxillary teeth (Brown *et al.* 2015). As mentioned above, *Stratiotosuchus* also lacks a supraorbital fenestra between palpebrals, which, as herein inferred, showed to tendency to reduce in size with increases in body size and dermal ornamentation. If its noticeable large size, in this proposed taphonomic and ontogenetic context, could challenge the validity of this taxon is now an open question. Further comparisons, long bone histology and application of geometric morphometrics might come a long way towards resolving these questions.

### 5.5.2 *Gondwanasuchus scabrosus*

Baurusuchid semaphoronts have been identified and described previously without the necessity of erecting new species (Geroto & Bertini 2012; Godoy *et al.* 2018). The influence of ontogeny on their cranial anatomy, and the changes herein described, make it possible to determine that the vast majority of baurusuchid name-bearing types were skeletally mature individuals, with the noticeable exception of *Gondwanasuchus*. This taxon consists of a partially complete skull, with a rostral-occipital length of just ≅ 12cm, just about 1/3 the average length of other holotypes, which range between 30 and 40 cm. In fact, this is substantially smaller even when compared with the currently described juvenile (20 cm).

Naturally, size alone would not suffice to demonstrate a young age for the *Gondwanasuchus* holotype, since small-bodied forms could have existed, but the skull also lacks the proportions, morphology, and sculpturing characteristic of adult individuals (**Figure 18c and 19**), sharing character states with IFSP-VTP/PALEO 0003, a now known juvenile, and also sharing with it migration to a more basal position in the tree. Most of the unique features provided for the diagnoses of *Gondwanasuchus* may now be reinterpreted as ontogenetic. For instance, both an overbite, where premaxillary teeth overhang the mandibular symphysis, and slender jugals, can also be found in the juvenile here described and on LPRP/USP 0049. Consequently, the original diagnoses seems outdated, and fails to demonstrate that *Gondwanasuchus* falls outside the expected range of morphological variation for the ontogenetic series of previously known baurusuchid species. It is here thus considered to be an invalid name, with the additional consideration that it should be further treated as a *nomem dubium*, given it could not yet be firmly attributed to semaphoront series of other species.

The discovery of further specimens may yield new information that allows for its placement into firmly stablished species, most likely within the *Baurusuchus* genus, due to proximity to the sites where *B. Salgadoensis* and *B. albertoi* were collected. Comparisons with other known juveniles will also contribute to better constrain ontogenetic character variation within the clade. Even though the apicobasal sulci and ridges present on the teeth *Gonwanasuchus* may be perceived as the most autapomorphic feature present, it is not sufficient to sustain this taxon, considering that dental morphology varies substantially throughout ontogeny in other archosaur lineages (Therrien *et al.* 2021; Voris *et al.* 2021; Woodruff *et al.* 2018), shifting its morphofunctional properties as the animal grew.

Similar features might be common in juveniles of basal theropod *Coelophysis* (Buckley & Currie 2014), for instance, and longitudinal enamel ridges were described to become less prominent with increasing tooth size in the neosuchian *Deltasuchus*, which was also suggested to have exhibited ontogenetic niche partitioning (Drumheller *et al.* 2021). Apicobasal ridges are a common feature amongst taxa that fed on aquatic environments and could be related to the capture of pliable prey (McCurry *et al.* 2019). If longitudinally ridged crowns truly pertain to development, it might then be another important indicative of ontogenetic niche partitioning in Baurusuchidae.

This may be resolved in the future with the use of modern tools such as mercury geochemistry and bite force estimates for juveniles (Cardia *et al.* 2018; Montefeltro *et al.* 2020). Ultimately, for the reasons expressed above, a thorough taxonomic revision of Baurusuchidae is made necessary. All holotypes must be examined not only for atypical and ontogenetic features, but also their diagnoses must be revised in search for the influences of taphonomic deformation in their listed autapomorphies.

## 6. Conclusions

We sought to better understand baurusuchid ontogeny by providing an osteomyological description of the most complete baurusuchid juvenile known to date, deepening our knowledge of the group's anatomy. Comparisons with adult baurusuchids and other taxa allowed for the listing of several ontogenetic anatomical shifts, including the degree of sculpturing of dermal bones, the development of origin and attachment sites of mandibular adductor musculature, as well as distinct tooth wear patterns that could work as a framework to better fit other crocodyliform specimens in their post-hatching developmental context.

A phylogenetic analysis including both the new semaphoront and the small baurusuchid *Gondwanasuchus* yielded both as basal baurusuchids, with the latter as the basalmost within the clade. This was interpreted as a shift towards the base also seen in other phylogenies which include immature individuals. In the light of the ontogenetic characters here described, their dimensions and phylogenetic placement, we conclude that *Gondwanasuchus* most likely constituted an immature individual, perhaps younger than IFSP-VTP/PALEO-0003 at the time of death, whereas the exceptionally large *Stratiotosuchus* exhibits tentative signs of being an older individual. Consequently, we propose the former henceforth should be considered as a *nomem dubium* and suggest that a future taxonomic revision for Baurusuchidae should account for both ontogenetic and taphonomic sources of morphological variation in order to improve the stability of proposed taxonomic units.

**Acknowledgements**

This study was financed in part by the Coordenação de Aperfeiçoamento de Pessoal de Nível Superior – Brasil (CAPES) – Finance Code 001.

The authors would like to thank the Brazilian funding agencies CAPES and CNPq, for the financial support of DMS and the sponsoring of this project. We would also like to extend our gratitude to Dr. Julia Klaczo and Dr. Angele Martins of the Zoology department of the University of Brasília, who kindly provided materials to support anatomical descriptions and comparisons.

## Conflict of interest statement

No conflicts were reported by the authors.

## References

Amorim, P., Moraes, T., Silva, J. & Pedrini, H. (2015) InVesalius: An Interactive Rendering Framework for Health Care Support. In: G. Bebis, R. Boyle, B. Parvin, D. Koracin, I. Pavlidis, R. Feris, T. McGraw, M. Elendt, R. Kopper, E. Ragan, Z. Ye, and G. Weber (Eds), *Advances in Visual Computing*. Lecture Notes in Computer Science. Springer International Publishing, Cham, pp. 45–54.

Arai, M. & Fernandes, L.A. (2023) Lower Campanian palynoflora from the Araçatuba Formation (Bauru Group), Southeastern Brazil. *Cretaceous Research* 150, 105586. https://doi.org/10.1016/j.cretres.2023.105586

Balaguera-Reina, S.A., Vargas-Ramírez, M., Ordóñez-Garza, N., Hernández-González, F. & Densmore, L.D. (2020) Unveiling the mystery: assessing the evolutionary trajectory of the Apaporis caiman population (Caiman crocodilus apaporiensis, Medem 1955) via mitochondrial molecular makers. *Biological Journal of the Linnean Society* 131, 163–171.

Bates, K. & Schachner, E. (2011) Disparity and convergence in bipedal archosaur locomotion. *Journal of the Royal Society, Interface / the Royal Society* 9, 1339–53. https://doi.org/10.1098/rsif.2011.0687

Batezelli, A. (2010) Arcabouço tectono-estratigráfico e evolução das Bacias Caiuá e Bauru no Sudeste brasileiro. *Revista Brasileira de Geociências* 40, 265–285.

Batezelli, A., Perinotto, J.D.J., Etchebehere, M.D.C., Fulfaro, V.J. & Saad, A.R. (1999) Redefinição litoestratigráfica da unidade Araçatuba e da sua extensão regional na Bacia Bauru, Estado de São Paulo, Brasil. *Simpósio sobre o Cretáceo do Brasil* 5, pp.195-200.

Benton, M.J. & Clark, James.M. (1988) Archosaur phylogeny and the relationships of the Crocodylia. *The Phylogeny and Classification of the Tetrapods, Volume 1: Amphibians, Reptiles, Birds* 1, 295–338.

Bertini, R.J. (1993) Paleobiologia do Grupo Bauru, Cretáceo Superior continental da Bacia do Paraná, com ênfase em sua fauna de amniotas. Universidade Federal do Rio de Janeiro, Rio de Janeiro.

Bona, P. & Desojo, J.B. (2011) Osteology and cranial musculature of Caiman latirostris (crocodylia: Alligatoridae). *Journal of Morphology* 272, 780–795. https://doi.org/10.1002/jmor.10894

Bona, P., Fernandez Blanco, M.V., Ezcurra, M.D., von Baczko, M.B., Desojo, J.B. & Pol, D. (2022) On the homology of crocodylian post-dentary bones and their macroevolution throughout Pseudosuchia. *The Anatomical Record* 305, 2980–3001. https://doi.org/10.1002/ar.24873

Boyd, R. (1999) Homeostasis, species, and higher taxa. *Species: New interdisciplinary essays* 141, 185.

Bravo, G.G., Pol, D. & García-López, D.A. (2021) A new sebecid mesoeucrocodylian from the Paleocene of northwestern Argentina. *Journal of Vertebrate Paleontology* 41, e1979020. https://doi.org/10.1080/02724634.2021.1979020

Brochu, C.A. (1996) Closure of neurocentral sutures during crocodilian ontogeny: Implications for maturity assessment in fossil archosaurs. *Journal of Vertebrate Paleontology* 16, 49–62. https://doi.org/10.1080/02724634.1996.10011283

Brown, C.M., VanBuren, C.S., Larson, D.W., Brink, K.S., Campione, N.E., Vavrek, M.J. & Evans, D.C. (2015) Tooth counts through growth in diapsid reptiles: implications for interpreting individual and size-related variation in the fossil record. *Journal of Anatomy* 226, 322–333.

Buckley, L.G. & Currie, P.J. (2014) 63 *ANALYSIS OF INTRASPECIFIC AND ONTOGENETIC VARIATION IN THE DENTITION OF COELOPHYSIS BAURI (LATE TRIASSIC), AND IMPLICATIONS FOR THE SYSTEMATICS OF ISOLATED THEROPOD TEETH: Bulletin 63*. New Mexico Museum of Natural History and Science.

de Buffrénil, V., Clarac, F., Fau, M., Martin, S., Martin, B., Pellé, E. & Laurin, M. (2015) Differentiation and growth of bone ornamentation in vertebrates: A comparative histological study among the Crocodylomorpha. *Journal of Morphology* 276, 425–445. https://doi.org/10.1002/jmor.20351

Campione, N.E., Brink, K.S., Freedman, E.A., McGarrity, C.T. & Evans, D.C. (2013) “Glishades ericksoni”, an indeterminate juvenile hadrosaurid from the Two Medicine Formation of Montana: implications for hadrosauroid diversity in the latest Cretaceous (Campanian-Maastrichtian) of western North America. *Palaeobiodiversity and Palaeoenvironments* 93, 65–75. https://doi.org/10.1007/s12549-012-0097-1

Campos, D.A. (2001) Short note on a new Baurusuchidae (Crocodyliformes, Metasuchia) from the Upper Cretaceous of Brazil. *Museu Nacional*.

Cardia, F.M.S., Santucci, R.M., Bernardi, J.V.E., Andrade, M.B. de & Oliveira, C.E.M. de (2018) Mercury concentrations in terrestrial fossil vertebrates from the Bauru Group (Upper Cretaceous), Brazil and implications for vertebrate paleontology. *Journal of South American Earth Sciences* 86, 15–22. https://doi.org/10.1016/j.jsames.2018.06.006

Carr, T.D. (2020) A high-resolution growth series of Tyrannosaurus rex obtained from multiple lines of evidence. *PeerJ* 8, e9192. https://doi.org/10.7717/peerj.9192

Carvalho, I. de S., Arruda Campos, A. de C. & Henrique Nobre, P. (2005) Baurusuchus salgadoensis, a New Crocodylomorpha from the Bauru Basin (Cretaceous), Brazil. *Gondwana Research* 8, 11–30. https://doi.org/10.1016/S1342-937X(05)70259-8

Carvalho, I. de S., Borges Ribeiro, L.C. & Avilla, L. dos S. (2004) Uberabasuchus terrificus sp. nov., a New Crocodylomorpha from the Bauru Basin (Upper Cretaceous), Brazil. *Gondwana Research* 7, 975–1002. https://doi.org/10.1016/S1342-937X(05)71079-0

Carvalho, I.D.S., Teixeira, V.D.P.A., Ferraz, M.L.D.F., Ribeiro, L.C.B., Martinelli, A.G., Neto, F.M., Sertich, J.J.W., Cunha, G.C., Cunha, I.C. & Ferraz, P.F. (2011) Campinasuchus dinizi gen. et sp. nov., a new Late Cretaceous baurusuchid (Crocodyliformes) from the Bauru Basin, Brazil. *Zootaxa* 2871, 19–42. https://doi.org/10.11646/zootaxa.2871.1.2

Castro, M.C., Goin, F.J., Ortiz-Jaureguizar, E., Vieytes, E.C., Tsukui, K., Ramezani, J., Batezelli, A., Marsola, J.C.A. & Langer, M.C. (2018) A Late Cretaceous mammal from Brazil and the first radioisotopic age for the Bauru Group. *Royal Society Open Science* 5, 180482. https://doi.org/10.1098/rsos.180482

Chin, K., Eberth, D.A., Schweitzer, M.H., Rando, T.A., Sloboda, W.J. & Horner, J.R. (2003) Remarkable preservation of undigested muscle tissue within a Late Cretaceous tyrannosaurid coprolite from Alberta, Canada. *Palaios* 18, 286–294.

Chin, K., Tokaryk, T.T., Erickson, G.M. & Calk, L.C. (1998) A king-sized theropod coprolite. *Nature* 393, 680–682. https://doi.org/10.1038/31461

Cidade, G.M., Fortier, D. & Hsiou, A.S. (2019) The crocodylomorph fauna of the Cenozoic of South America and its evolutionary history: a review. *Journal of South American Earth Sciences* 90, 392–411. https://doi.org/10.1016/j.jsames.2018.12.026

Colbert, E.H., Mook, C.C. & Brown, B. (1951) The ancestral crocodilian Protosuchus. Bulletin of the AMNH ; v. 97, article 3.

Colbert, E.H., Simpson, G.G., Williams, C.S. & Expedition 1930-1931), S.P. (1946) Sebecus, representative of a peculiar suborder of fossil Crocodilia from Patagonia. Bulletin of the AMNH ; v. 87, article 4.

Cotts, L., Pinheiro, A.E.P., da Silva Marinho, T., de Souza Carvalho, I. & Di Dario, F. (2017) Postcranial skeleton of Campinasuchus dinizi (Crocodyliformes, Baurusuchidae) from the Upper Cretaceous of Brazil, with comments on the ontogeny and ecomorphology of the species. *Cretaceous Research* 70, 163–188. https://doi.org/10.1016/j.cretres.2016.11.003

Cunha, G.O., Santucci, R.M., Andrade, M.B. de & Oliveira, C.E.M. de (2020) Description and phylogenetic relationships of a large-bodied sphagesaurid notosuchian from the Upper Cretaceous Adamantina Formation, Bauru Group, São Paulo, southeastern Brazil. *Cretaceous Research* 106, 104259. https://doi.org/10.1016/j.cretres.2019.104259

Darlim, G., Carvalho, I. de S., Tavares, S.A.S. & Langer, M.C. (2021a) A new Pissarrachampsinae specimen from the Bauru Basin, Brazil, adds data to the understanding of the Baurusuchidae (Mesoeucrocodylia, Notosuchia) distribution in the Late Cretaceous of South America. *Cretaceous Research* 128, 104969. https://doi.org/10.1016/j.cretres.2021.104969

Darlim, G., Montefeltro, F.C. & Langer, M.C. (2021b) 3D skull modelling and description of a new baurusuchid (Crocodyliformes, Mesoeucrocodylia) from the Late Cretaceous (Bauru Basin) of Brazil. *Journal of Anatomy* n/a. https://doi.org/10.1111/joa.13442

Dayrat, B. (2005) Towards integrative taxonomy. *Biological Journal of the Linnean Society* 85, 407–417. https://doi.org/10.1111/j.1095-8312.2005.00503.x

De Queiroz, K. (2007) Species Concepts and Species Delimitation. *Systematic Biology* 56, 879–886. https://doi.org/10.1080/10635150701701083

Dias, A.N.C., Chemale, F., Candeiro, C.R.A., Lana, C.C., Guadagnin, F. & Sales, A.S.W. (2021) Unraveling multiple tectonic events and source areas in the intracratonic Bauru Basin through combined zircon geo and thermochronological studies. *Journal of South American Earth Sciences* 106, 103061. https://doi.org/10.1016/j.jsames.2020.103061

Dias-Brito, D., Musachio, E.A., Castro, J.C., Maranhão, M.S.A.S., Suarez, J.M. & Rodrigues, R. (2001) Bauru Group: a continental Cretaceous unit in Brazil - Concepts based on micropaleontological, oxygen isotope and stratigraphic data. *Rev. paléobiol* 20, 245–304.

Dollman, K.N., Viglietti, P.A. & Choiniere, J.N. (2019) A new specimen of Orthosuchus stormbergi (Nash 1968) and a review of the distribution of Southern African Lower Jurassic crocodylomorphs. *Historical Biology* 31, 653–664. https://doi.org/10.1080/08912963.2017.1387110

van Drongelen, W. & Dullemeijer, P. (1982) The feeding apparatus of Caiman crocodilus: A functional-morphological study. *Anatomischer Anzeiger* 151, 337–66.

Drumheller, S.K., Adams, T.L., Maddox, H. & Noto, C.R. (2021) Expanded Sampling Across Ontogeny in <I>Deltasuchus motherali</I> (Neosuchia, Crocodyliformes): Revealing Ecomorphological Niche Partitioning and

Appalachian Endemism in Cenomanian Crocodyliforms. *Elements of Paleontology*. https://doi.org/10.1017/9781009042024

Dumont Jr, M.V., Santucci, R.M., Andrade, M.B. de & Oliveira, C.E.M. de (2020) Paleoneurology of Baurusuchus (Crocodyliformes: Baurusuchidae), ontogenetic variation, brain size, and sensorial implications. *The Anatomical Record* n/a. https://doi.org/10.1002/ar.24567

Erickson, G.M., Gignac, P.M., Steppan, S.J., Lappin, A.K., Vliet, K.A., Brueggen, J.D., Inouye, B.D., Kledzik, D. & Webb, G.J.W. (2012) Insights into the Ecology and Evolutionary Success of Crocodilians Revealed through Bite-Force and Tooth-Pressure Experimentation. *PLOS ONE* 7, e31781. https://doi.org/10.1371/journal.pone.0031781

Erickson, G.M., Lappin, A.K. & Vliet, K.A. (2003) The ontogeny of bite-force performance in American alligator (Alligator mississippiensis). *Journal of Zoology* 260, 317–327. https://doi.org/10.1017/S0952836903003819

Erickson, G.M. & Olson, K.H. (1996) Bite marks attributable to Tyrannosaurus rex: preliminary description and implications. *Journal of Vertebrate Paleontology* 16, 175–178.

Fernandes, L.A. (2004) Mapa litoestratigráfico da parte oriental da Bacia Bauru (PR, SP, MG), escala 1: 1.000. 000. *Boletim Paranaense de Geociências* 55.

Fernandes, L.A. & Coimbra, A.M. (1996) A Bacia Bauru (Cretáceo Superior, Brasil). *Anais da Academia Brasileira de Ciências* 68(2), pp.195-206.

Fiorelli, L.E., Leardi, J.M., Hechenleitner, E.M., Pol, D., Basilici, G. & Grellet-Tinner, G. (2016) A new Late Cretaceous crocodyliform from the western margin of Gondwana (La Rioja Province, Argentina). *Cretaceous Research* 60, 194–209. https://doi.org/10.1016/j.cretres.2015.12.003

Fonseca, P.H.M., Martinelli, A.G., Marinho, T. da S., Ribeiro, L.C.B., Schultz, C.L. & Soares, M.B. (2020) Morphology of the endocranial cavities of Campinasuchus dinizi (Crocodyliformes: Baurusuchidae) from the Upper Cretaceous of Brazil. *Geobios* 58, 1–16. https://doi.org/10.1016/j.geobios.2019.11.001

Frederickson, J.A., Engel, M.H. & Cifelli, R.L. (2020) Ontogenetic dietary shifts in Deinonychus antirrhopus (Theropoda; Dromaeosauridae): Insights into the ecology and social behavior of raptorial dinosaurs through stable isotope analysis. *Palaeogeography, Palaeoclimatology, Palaeoecology* 552, 109780. https://doi.org/10.1016/j.palaeo.2020.109780

Gasparini, Z.B. de (1971) Los Notosuchia de Cretacico de America del Sur como un nuevo infraodern de los mesosuchia (crocodilia). *Ameghiniana* 8, 83–103.

Gasparini, Z.B. de (1972) LOS SEBECOSUCHIA (CROCODILIA) DEL TERRITORIO ARGENTINO. CONSIDERACIONES SOBRE SU “STATUS” TAXONÓMICO. 9, 23–34.

Gatesy, S.M. (1997) An electromyographic analysis of hindlimb function in Alligator during terrestrial locomotion. *Journal of Morphology* 234, 197–212.

Georgi, J.A. & Krause, D.W. (2010) Postcranial axial skeleton of Simosuchus clarki (Crocodyliformes: Notosuchia) from the Late Cretaceous of Madagascar. *Journal of Vertebrate Paleontology* 30, 99–121. https://doi.org/10.1080/02724634.2010.519172

Geroto, C.F.C. & Bertini, R.J. (2012) Descrição de um espécime juvenil de Baurusuchidae (Crocodyliformes: Mesoeucrocodylia) do Grupo Bauru (Neocretáceo): considerações preliminares sobre ontogenia. *Revista do Instituto Geológico* 33, 13–29. https://doi.org/10.5935/0100-929X.20120007

Gignac, P.M. & Erickson, G.M. (2015) Ontogenetic changes in dental form and tooth pressures facilitate developmental niche shifts in American alligators. *Journal of Zoology* 295, 132–142. https://doi.org/10.1111/jzo.12187

Gignac, P.M. & Erickson, G.M. (2016a) Ontogenetic bite-force modeling of Alligator mississippiensis: implications for dietary transitions in a large-bodied vertebrate and the evolution of crocodylian feeding. *Journal of Zoology* 299, 229–238. https://doi.org/10.1111/jzo.12349

Gignac, P.M. & Erickson, G.M. (2016b) Ontogenetic bite-force modeling of Alligator mississippiensis: implications for dietary transitions in a large-bodied vertebrate and the evolution of crocodylian feeding. *Journal of Zoology* 299, 229–238. https://doi.org/10.1111/jzo.12349

Gignac, P.M. & Erickson, G.M. (2017) The Biomechanics Behind Extreme Osteophagy in Tyrannosaurus rex. *Scientific Reports* 7, 2012. https://doi.org/10.1038/s41598-017-02161-w

Godoy, P.L., Bronzati, M., Eltink, E., Marsola, J.C. de A., Cidade, G.M., Langer, M.C. & Montefeltro, F.C. (2016) Postcranial anatomy of Pissarrachampsa sera (Crocodyliformes, Baurusuchidae) from the Late Cretaceous of Brazil: insights on lifestyle and phylogenetic significance. *PeerJ* 4, e2075. https://doi.org/10.7717/peerj.2075

Godoy, P.L., Ferreira, G.S., Montefeltro, F.C., Nova, B.C.V., Butler, R.J. & Langer, M.C. (2018) Evidence for heterochrony in the cranial evolution of fossil crocodyliforms. *Palaeontology* 61, 543–558. https://doi.org/10.1111/pala.12354

Godoy, P.L., Montefeltro, F.C., Norell, M.A. & Langer, M.C. (2014) An Additional Baurusuchid from the Cretaceous of Brazil with Evidence of Interspecific Predation among Crocodyliformes. *PLOS ONE* 9, e97138. https://doi.org/10.1371/journal.pone.0097138

Goldberg, K. & Garcia, A.J.V. (2000) Palaeobiogeography of the Bauru Group, a dinosaur-bearing Cretaceous unit, northeastern Parana Basin, Brazil. *Cretaceous Research* 21, 241–254. https://doi.org/10.1006/cres.2000.0207

Goloboff, P.A., Farris, J.S. & Nixon, K.C. (2008) TNT, a free program for phylogenetic analysis. *Cladistics* 24, 774–786. https://doi.org/10.1111/j.1096-0031.2008.00217.x

Gould, S.J. (1985) *Ontogeny and phylogeny*. Harvard University Press.

Gregorovičová, M., Kvasilová, A. & Sedmera, D. (2018) Ossification Pattern in Forelimbs of the Siamese Crocodile (Crocodylus siamensis): Similarity in Ontogeny of Carpus Among Crocodylian Species. *The Anatomical Record* 301, 1159–1168. https://doi.org/10.1002/ar.23792

Griffin, C.T., Stocker, M.R., Colleary, C., Stefanic, C.M., Lessner, E.J., Riegler, M., Formoso, K., Koeller, K. & Nesbitt, S.J. (2021) Assessing ontogenetic maturity in extinct saurian reptiles. *Biological Reviews* 96, 470–525. https://doi.org/10.1111/brv.12666

Grigg, G. (2015) *Biology and Evolution of Crocodylians*. Csiro Publishing, 671 pp.

Hay, O.P. (1930) Second bibliography and catalogue of the fossil vertebrata of North America.

Hendrickx, C., Mateus, O. & Araujo, R. (2015) A proposed terminology of theropod teeth (Dinosauria, Saurischia). *Journal of Vertebrate Paleontology* 35, e982797. https://doi.org/10.1080/02724634.2015.982797

Hennig, W. (1966) *Phylogenetic Systematics*. University of Illinois Press.

Holliday, C.M., Porter, W.R., Vliet, K.A. & Witmer, L.M. (2020) The Frontoparietal Fossa and Dorsotemporal Fenestra of Archosaurs and Their Significance for Interpretations of Vascular and Muscular Anatomy in Dinosaurs. *The Anatomical Record* 303, 1060–1074. https://doi.org/10.1002/ar.24218

Holliday, C.M., Sellers, K.C., Lessner, E.J., Middleton, K.M., Cranor, C., Verhulst, C.D., Lautenschlager, S., Bader, K., Brown, M.A. & Colbert, M.W. (2022) New frontiers in imaging, anatomy, and mechanics of crocodylian jaw muscles. *The Anatomical Record* 305, 3016–3030. https://doi.org/10.1002/ar.25011

Holliday, C.M., Tsai, H.P., Skiljan, R.J., George, I.D. & Pathan, S. (2013) A 3D Interactive Model and Atlas of the Jaw Musculature of Alligator mississippiensis | PLOS ONE. *PLOS ONE*. Available from: https://journals.plos.org/plosone/article?id=10.1371/journal.pone.0062806 (October 6, 2022)

Holliday, C.M. & Witmer, L.M. (2007) Archosaur adductor chamber evolution: Integration of musculoskeletal and topological criteria in jaw muscle homology. *Journal of Morphology* 268, 457–484. https://doi.org/10.1002/jmor.10524

Holtz, T.R. (2021) Theropod guild structure and the tyrannosaurid niche assimilation hypothesis: implications for predatory dinosaur macroecology and ontogeny in later Late Cretaceous Asiamerica1. *Canadian Journal of Earth Sciences* 58, 778–795. https://doi.org/10.1139/cjes-2020-0174

Horner, J.R. & Goodwin, M.B. (2006) Major cranial changes during Triceratops ontogeny. *Proceedings of the Royal Society B: Biological Sciences* 273, 2757–2761. https://doi.org/10.1098/rspb.2006.3643

Horner, J.R. & Goodwin, M.B. (2009) Extreme Cranial Ontogeny in the Upper Cretaceous Dinosaur Pachycephalosaurus. *PLOS ONE* 4, e7626. https://doi.org/10.1371/journal.pone.0007626

Iordansky, N.N. (1964) The jaw muscles of the crocodiles and some relating structures of the crocodilian skull. *Anatomischer Anzeiger* 115.

Iordansky, N.N. (2000) Jaw muscles of the crocodiles: structure, synonymy, and some implications on homology and functions. *Russian Journal of Herpetology*, 41–50.

Iori, F.V. & Carvalho, I.D.S. (2009) Morrinhosuchus luziae, um novo Crocodylomorpha Notosuchia da Bacia Bauru, Brasil. *Revista Brasileira de Geociências* 39, 717–725. https://doi.org/10.25249/0375-7536.2009394717725

Kellner, A.W.A., Weinschütz, L.C., Holgado, B., Bantim, R. a. M. & Sayão, J.M. (2019) A new toothless pterosaur (Pterodactyloidea) from Southern Brazil with insights into the paleoecology of a Cretaceous desert. *Anais da Academia Brasileira de Ciências* 91, e20190768. https://doi.org/10.1590/0001-3765201920190768

Kley, N.J., Sertich, J.J.W., Turner, A.H., Krause, D.W., O'Connor, P.M. & Georgi, J.A. (2010) Craniofacial morphology of Simosuchus clarki (Crocodyliformes: Notosuchia) from the Late Cretaceous of Madagascar. *Journal of Vertebrate Paleontology* 30, 13–98. https://doi.org/10.1080/02724634.2010.532674

Klinkhamer, A.J., Wilhite, D.R., White, M.A. & Wroe, S. (2017) Digital dissection and three-dimensional interactive models of limb musculature in the Australian estuarine crocodile (Crocodylus porosus). *PLOS ONE* 12, e0175079. https://doi.org/10.1371/journal.pone.0175079

Klock, C., Leuzinger, L., Santucci, R.M., Martinelli, A.G., Marconato, A., Marinho, T.S., Luz, Z. & Vennemann, T. (2022) A bone to pick: stable isotope compositions as tracers of food sources and paleoecology for notosuchians in the Brazilian Upper Cretaceous Bauru Group. *Cretaceous Research* 131, 105113. https://doi.org/10.1016/j.cretres.2021.105113

Larson, P. (2013) The case for Nanotyrannus. *Tyrannosaurid paleobiology*, 15–53.

Larsson, H.C.E. & Sues, H.-D. (2007) Cranial osteology and phylogenetic relationships of Hamadasuchus rebouli (Crocodyliformes: Mesoeucrocodylia) from the Cretaceous of Morocco. *Zoological Journal of the Linnean Society* 149, 533–567. https://doi.org/10.1111/j.1096-3642.2007.00271.x

Liparini, A. & Schultz, C.L. (2013) A reconstruction of the thigh musculature of the extinct pseudosuchian Prestosuchus chiniquensis from the Dinodontosaurus Assemblage Zone (Middle Triassic Epoch), Santa Maria 1 Sequence, southern Brazil. *Geological Society, London, Special Publications* 379, 441–468. https://doi.org/10.1144/SP379.20

Manzig, P.C., Kellner, A.W.A., Weinschütz, L.C., Fragoso, C.E., Vega, C.S., Guimarães, G.B., Godoy, L.C., Liccardo, A., Ricetti, J.H.Z. & Moura, C.C. de (2014) Discovery of a Rare Pterosaur Bone Bed in a Cretaceous Desert with Insights on Ontogeny and Behavior of Flying Reptiles. *PLOS ONE* 9, e100005. https://doi.org/10.1371/journal.pone.0100005

Marinho, T. da S., Iori, F.V., Carvalho, I. de S. & de Vasconcellos, F.M. (2013) Gondwanasuchus scabrosus gen. et sp. nov., a new terrestrial predatory crocodyliform (Mesoeucrocodylia: Baurusuchidae) from the Late Cretaceous Bauru Basin of Brazil. *Cretaceous Research* 44, 104–111. https://doi.org/10.1016/j.cretres.2013.03.010

Martin, J.E., Pochat-Cottilloux, Y., Laurent, Y., Perrier, V., Robert, E. & Antoine, P.-O. (2022) Anatomy and phylogeny of an exceptionally large sebecid (Crocodylomorpha) from the middle Eocene of southern France. *Journal of Vertebrate Paleontology* 42, e2193828. https://doi.org/10.1080/02724634.2023.2193828

Martinelli, A.G. (2003) Comahuesuchus brachybuccalis (Archosauria, Crocodyliformes) from the Late Cretaceous of Río Negro Province (Argentina). 40, 559–572.

Martinelli, A.G., Marinho, T.S., Iori, F.V. & Ribeiro, L.C.B. (2018) The first Caipirasuchus (Mesoeucrocodylia, Notosuchia) from the Late Cretaceous of Minas Gerais, Brazil: new insights on sphagesaurid anatomy and taxonomy. *PeerJ* 6, e5594. https://doi.org/10.7717/peerj.5594

Martinelli, A.G. & Pais, D.F. (2008) A new baurusuchid crocodyliform (Archosauria) from the Late Cretaceous of Patagonia (Argentina). *Comptes Rendus Palevol* 7, 371–381. https://doi.org/10.1016/j.crpv.2008.05.002

Martins, K.C., Queiroz, M.V., Ruiz, J.V., Langer, M.C. & Montefeltro, F.C. (2023) A new Baurusuchidae (Notosuchia, Crocodyliformes) from the Adamantina Formation (Bauru Group, Upper Cretaceous), with a revised phylogenetic analysis of Baurusuchia. *Cretaceous Research*, 105680. https://doi.org/10.1016/j.cretres.2023.105680

Mayr, E. (1996) What is a species, and what is not? *Philosophy of science* 63, 262–277.

Mayr, E. (2000) The biological species concept. *Species concepts and phylogenetic theory: a debate*, 17–29.

McCurry, M.R., Evans, A.R., Fitzgerald, E.M.G., McHenry, C.R., Bevitt, J. & Pyenson, N.D. (2019) The repeated evolution of dental apicobasal ridges in aquatic-feeding mammals and reptiles. *Biological Journal of the Linnean Society* 127, 245–259. https://doi.org/10.1093/biolinnean/blz025

Meers, M.B. (2003) Crocodylian forelimb musculature and its relevance to Archosauria. *The Anatomical Record Part A: Discoveries in Molecular, Cellular, and Evolutionary Biology* 274A, 891–916. https://doi.org/10.1002/ar.a.10097

Molnar, R.E. (2010) A new reconstruction of the skull of Sebecus icaeorhinus (Crocodyliformes: Sebecosuchia) from the Eocene of Argentina. *Brazilian Geographical Journal: Geosciences and Humanities research medium* 1, 314–330.

Molnar, R.E. (2012) Jaw musculature and jaw mechanics of Sebecus icaeorhinus Simpson, 1937 (Mesoeucrocodylia, Sebecosuchia). *Earth and Environmental Science Transactions of The Royal Society of Edinburgh* 103, 501–519. https://doi.org/10.1017/S1755691013000285

Montefeltro, F.C., Larsson, H.C.E., de França, M.A.G. & Langer, M.C. (2013) A new neosuchian with Asian affinities from the Jurassic of northeastern Brazil. *Naturwissenschaften* 100, 835–841. https://doi.org/10.1007/s00114-013-1083-9

Montefeltro, F.C., Larsson, H.C.E. & Langer, M.C. (2011) A New Baurusuchid (Crocodyliformes, Mesoeucrocodylia) from the Late Cretaceous of Brazil and the Phylogeny of Baurusuchidae. *PLOS ONE* 6, e21916. https://doi.org/10.1371/journal.pone.0021916

Montefeltro, F.C., Lautenschlager, S., Godoy, P.L., Ferreira, G.S. & Butler, R.J. (2020) A unique predator in a unique ecosystem: modelling the apex predator within a Late Cretaceous crocodyliform-dominated fauna from Brazil. *Journal of Anatomy* 237, 323–333. https://doi.org/10.1111/joa.13192

Murray, C.M., Russo, P., Zorrilla, A. & McMahan, C.D. (2019) Divergent morphology among populations of the New Guinea crocodile, Crocodylus novaeguineae (Schmidt, 1928): diagnosis of an independent lineage and description of a new species. *Copeia* 107, 517–523.

Nascimento, P.M. (2014) Revisão da família Baurusuchidae e seu posicionamento filogenético dentro do clado Mesoeucrocodylia. text. Universidade de São Paulo.

Nascimento, P.M. & Zaher, H. (2010) A new species of Baurusuchus (Crocodyliformes, Mesoeucrocodylia) from the Upper Cretaceous of Brazil, with the first complete postcranial skeleton described for the family Baurusuchidae. *Papéis Avulsos de Zoologia* 50, 323–361. https://doi.org/10.1590/S0031-10492010002100001

Nesbitt, S.J., Turner, A.H. & Weinbaum, J.C. (2012) A survey of skeletal elements in the orbit of Pseudosuchia and the origin of the crocodylian palpebral. *Earth and Environmental Science Transactions of The Royal Society of Edinburgh* 103, 365–381. https://doi.org/10.1017/S1755691013000224

Nobre, P.H. & Carvalho, I. de S. (2013) Postcranial Skeleton of Mariliasuchus amarali Carvalho and Bertini, 1999 (Mesoeucrocodylia) from the Bauru Basin, Upper Cretaceous of Brazil. *Ameghiniana* 50, 98–113. https://doi.org/10.5710/AMGH.15.8.2012.500

O'Connor, P.M., Sertich, J.J.W., Stevens, N.J., Roberts, E.M., Gottfried, M.D., Hieronymus, T.L., Jinnah, Z.A., Ridgely, R., Ngasala, S.E. & Temba, J. (2010)

The evolution of mammal-like crocodyliforms in the Cretaceous Period of Gondwana. *Nature* 466, 748–751. https://doi.org/10.1038/nature09061

Oliveira, C.E.M., Santucci, R.M., Andrade, M.B., Fulfaro, V.J., Basílio, J. a. F. & Benton, M.J. (2011) Crocodylomorph eggs and eggshells from the Adamantina Formation (Bauru Group), Upper Cretaceous of Brazil. *Palaeontology* 54, 309–321. https://doi.org/10.1111/j.1475-4983.2010.01028.x

Oliveira, F.A. de, Santucci, R.M., Oliveira, C.E.M. de & Andrade, M.B. de (2021) Morphological and compositional analyses of coprolites from the Upper Cretaceous Bauru Group reveal dietary habits of notosuchian fauna. *Lethaia*. https://doi.org/10.1111/let.12431

Ortega, F., Gasparini, Z., Buscalioni, A.D. & Calvo, J.O. (2000) A new species of Araripesuchus (Crocodylomorpha, Mesoeucrocodylia) from the lower Cretaceous of Patagonia (Argentina). *Journal of Vertebrate Paleontology* 20, 57–76. https://doi.org/10.1671/0272-4634(2000)020[0057:ANSOAC]2.0.CO;2

Otero, A., Cuff, A.R., Allen, V., Sumner-Rooney, L., Pol, D. & Hutchinson, J.R. (2019) Ontogenetic changes in the body plan of the sauropodomorph dinosaur Mussaurus patagonicus reveal shifts of locomotor stance during growth. *Scientific Reports* 9, 7614. https://doi.org/10.1038/s41598-019-44037-1

Padial, J.M., Miralles, A., De la Riva, I. & Vences, M. (2010) The integrative future of taxonomy. *Frontiers in Zoology* 7, 16. https://doi.org/10.1186/1742-9994-7-16

Paolillo, A. & Linares, O.J. (2007) Nuevos cocodrilos sebecosuchia del cenozoico suramericano (Mesosuchia: Crocodylia). *Paleobiologia Neotropical* 3, 1–25.

Pinheiro, A.E.P., Souza, L.G.D., Bandeira, K.L.N., Brum, A.S., Pereira, P.V.L.G.C., Castro, L.O.R.D., Ramos, R.R.C. & Simbras, F.M. (2021) The first notosuchian crocodyliform from the Araçatuba Formation (Bauru Group, Paraná Basin), and diversification of sphagesaurians. *Anais da Academia Brasileira de Ciências* 93, e20201591. https://doi.org/10.1590/0001-3765202120201591

Pol, D. (2005) Postcranial remains of Notosuchus terrestris Woodward (Archosauria: Crocodyliformes) from the upper Cretaceous of Patagonia, Argentina. *Ameghiniana* 42, 21–38.

Pol, D., Leardi, J.M., Lecuona, A. & Krause, M. (2012) Postcranial anatomy of Sebecus icaeorhinus (Crocodyliformes, Sebecidae) from the Eocene of Patagonia. *Journal of Vertebrate Paleontology* 32, 328–354. https://doi.org/10.1080/02724634.2012.646833

Pol, D., Nascimento, P.M., Carvalho, A.B., Riccomini, C., Pires-Domingues, R.A. & Zaher, H. (2014) A New Notosuchian from the Late Cretaceous of Brazil and the Phylogeny of Advanced Notosuchians. *PLOS ONE* 9, e93105. https://doi.org/10.1371/journal.pone.0093105

Powell, J., Babot, J., García-López, D., Deraco, V. & Herrera, C. (2011) Eocene vertebrates of northwestern Argentina: annotated list. In: , p. 458.

Price (1945) A new reptile from the Cretaceous of Brazil. *Rio de Janeiro, Departamento Nacional da Produção Mineral, Notas preliminares e estudos* Boletim 25.

Rabi, M. & Sebők, N. (2015) A revised Eurogondwana model: Late Cretaceous notosuchian crocodyliforms and other vertebrate taxa suggest the retention of episodic faunal links between Europe and Gondwana during most of the Cretaceous. *Gondwana Research* 28, 1197–1211. https://doi.org/10.1016/j.gr.2014.09.015

Rayfield, E.J. (2004) Cranial mechanics and feeding in Tyrannosaurus rex. *Proceedings of the Royal Society of London. Series B: Biological Sciences* 271, 1451–1459.

Reilly, S.M. & Blob, R.W. (2003) Motor control of locomotor hindlimb posture in the American alligator (Alligator mississippiensis). *Journal of Experimental Biology* 206, 4327–4340.

Riff, D. (2003) Descrição morfológica do crânio e mandíbula de Stratiotosuchus maxhechti (Crocodylomorpha, Cretáceo Superior do Brasil) e seu posicionamento filogenético. *Masters dissertation*.

Riff, D. & Kellner, A.W.A. (2011) Baurusuchid crocodyliforms as theropod mimics: clues from the skull and appendicular morphology of Stratiotosuchus maxhechti (Upper Cretaceous of Brazil). *Zoological Journal of the Linnean Society* 163, S37–S56. https://doi.org/10.1111/j.1096-3642.2011.00713.x

Ristevski, J. (2019) Crocodilia Morphology. In: J. Vonk and T. Shackelford (Eds), *Encyclopedia of Animal Cognition and Behavior*. Springer International Publishing, Cham, pp. 1–22.

Romer, A.S. (1923) Crocodilian pelvic muscles and their avian and reptilian homologues. Bulletin of the AMNH ; v. 48, article 15.

Ruiz, J.V., Bronzati, M., Ferreira, G.S., Martins, K.C., Queiroz, M.V., Langer, M.C. & Montefeltro, F.C. (2021) A new species of Caipirasuchus (Notosuchia, Sphagesauridae) from the Late Cretaceous of Brazil and the evolutionary history of Sphagesauria. *Journal of Systematic Palaeontology* 19, 265–287. https://doi.org/10.1080/14772019.2021.1888815

Salas-Gismondi, R., Flynn, J.J., Baby, P., Tejada-Lara, J.V., Wesselingh, F.P. & Antoine, P.-O. (2015) A Miocene hyperdiverse crocodylian community reveals peculiar trophic dynamics in proto-Amazonian mega-wetlands. *Proceedings of the Royal Society B: Biological Sciences* 282, 20142490. https://doi.org/10.1098/rspb.2014.2490

dos Santos, D., Santucci, R., Andrade, M. & Oliveira, C.E.M. (2021) A baurusuchid yearling (Mesoeucrocodylia, Crocodyliformes), from the Adamantina Formation, Bauru Group, Upper Cretaceous of Brazil. *Historical Biology*. https://doi.org/10.1080/08912963.2021.2001807

Scannella, J.B. & Horner, J.R. (2010) Torosaurus Marsh, 1891, is Triceratops Marsh, 1889 (Ceratopsidae: Chasmosaurinae): synonymy through ontogeny. *Journal*

*of Vertebrate Paleontology* 30, 1157–1168. https://doi.org/10.1080/02724634.2010.483632

Schubert, B.W. & Ungar, P.S. (2005) Wear facets and enamel spalling in tyrannosaurid dinosaurs. *Acta Palaeontologica Polonica* 50.

Schumacher, G.H. (1973) The head muscles and hyolaryngeal skeleton of turtles and crocodilians. *Biology of the Reptilia* Volume 4 Morphology D, 101–199.

Sellers, K.C., Middleton, K.M., Davis, J.L. & Holliday, C.M. (2017) Ontogeny of bite force in a validated biomechanical model of the American alligator. *Journal of Experimental Biology* 220, 2036–2046. https://doi.org/10.1242/jeb.156281

Sellers, K.C., Nieto, M.N., Degrange, F.J., Pol, D., Clark, J.M., Middleton, K.M. & Holliday, C.M. (2022) The effects of skull flattening on suchian jaw muscle evolution. *The Anatomical Record* 305, 2791–2822. https://doi.org/10.1002/ar.24912

Sellés, A.G., Blanco, A., Vila, B., Marmi, J., López-Soriano, F.J., Llácer, S., Frigola, J., Canals, M. & Galobart, À. (2020) A small Cretaceous crocodyliform in a dinosaur nesting ground and the origin of sebecids. *Scientific Reports* 10, 15293. https://doi.org/10.1038/s41598-020-71975-y

Sertich, J.J.W. & Groenke, J.R. (2010) Appendicular skeleton of Simosuchus clarki (Crocodyliformes: Notosuchia) from the Late Cretaceous of Madagascar. *Journal of Vertebrate Paleontology* 30, 122–153. https://doi.org/10.1080/02724634.2010.516902

Sharma, P.P., Clouse, R.M. & Wheeler, W.C. (2017) Hennig's semaphoront concept and the use of ontogenetic stages in phylogenetic reconstruction. *Cladistics* 33, 93–108. https://doi.org/10.1111/cla.12156

Simpson, G.G. (1951) The species concept. *Evolution* 5, 285–298.

Soares, P.C., Landim, P.M.B., Fúlfaro, V.J. & Neto, A.F.S. (1980) ENSAIO DE CARACTERIZAÇÃO ESTRATIGRÁFICA DO CRETÁCEO NO ESTADO DE SÃO PAULO: GRUPO BAURU. *Revista Brasileira de Geociências* 10, 177–185.

de Souza, G.A., Soares, M.B., Weinschütz, L.C., Wilner, E., Lopes, R.T., de Araújo, O.M.O. & Kellner, A.W.A. (2021) The first edentulous ceratosaur from South America. *Scientific Reports* 11, 22281. https://doi.org/10.1038/s41598-021-01312-4

Staniewicz, A., Behler, N., Darmansyah, S. & Jones, G. (2018) Niche partitioning between juvenile sympatric crocodilians in Mesangat Lake, East Kalimantan, Indonesia. *The Raffles Bulletin of Zoology* 66, 528–537.

Tavares, S.A.S., Branco, F.R., Carvalho, I. de S. & Maldanis, L. (2017) The morphofunctional design of Montealtosuchus arrudacamposi (Crocodyliformes, Upper Cretaceous) of the Bauru Basin, Brazil. *Cretaceous Research* 79, 64–76. https://doi.org/10.1016/j.cretres.2017.07.003

Therrien, F., Zelenitsky, D.K., Voris, J.T. & Tanaka, K. (2021) Mandibular force profiles and tooth morphology in growth series of Albertosaurus sarcophagus and Gorgosaurus libratus (Tyrannosauridae: Albertosaurinae) provide evidence for an ontogenetic dietary shift in tyrannosaurids1. *Canadian Journal of Earth Sciences* 58, 812–828. https://doi.org/10.1139/cjes-2020-0177

Tsai, H.P. & Holliday, C.M. (2011) Ontogeny of the Alligator Cartilago Transiliens and Its Significance for Sauropsid Jaw Muscle Evolution. *PLOS ONE* 6, e24935. https://doi.org/10.1371/journal.pone.0024935

Tsuihiji, T. (2005) Homologies of the transversospinalis muscles in the anterior presacral region of Sauria (crown Diapsida). *Journal of Morphology* 263, 151–178. https://doi.org/10.1002/jmor.10294

Tsuihiji, T. (2007) Homologies of the longissimus, iliocostalis, and hypaxial muscles in the anterior presacral region of extant diapsida. *Journal of Morphology* 268, 986–1020. https://doi.org/10.1002/jmor.10565

Tsuihiji, T., Watabe, M., Tsogtbaatar, K., Tsubamoto, T., Barsbold, R., Suzuki, S., Lee, A.H., Ridgely, R.C., Kawahara, Y. & Witmer, L.M. (2011) Cranial osteology of a juvenile specimen of Tarbosaurus bataar (Theropoda, Tyrannosauridae) from the Nemegt Formation (Upper Cretaceous) of Bugin Tsav, Mongolia. *Journal of Vertebrate Paleontology* 31, 497–517. https://doi.org/10.1080/02724634.2011.557116

Tucker, A.D., Limpus, C.J., McCallum, H.I. & McDonald, K.R. (1996) Ontogenetic Dietary Partitioning by Crocodylus johnstoni during the Dry Season. *Copeia* 1996, 978–988. https://doi.org/10.2307/1447661

Turner, A.H. (2006) Osteology and phylogeny of a new species of Araripesuchus (Crocodyliformes: Mesoeucrocodylia) from the Late Cretaceous of Madagascar. *Historical Biology* 18, 255–369. https://doi.org/10.1080/08912960500516112

Vasconcellos, F.M. & Carvalho, I.S. (2010) Paleoichnological assemblage associated with Baurusuchus salgadoensis remains, a Baurusuchidae Mesoeucrocodylia from the Bauru Basin, Brazil (Late Cretaceous). *Bulletin of the New Mexico Museum of Natural History and Science* 51, 227–237.

Vieira, L.G., Lima, F.C., Mendonôa, S.H.S.T., Menezes, L.T., Hirano, L.Q.L. & Santos, A.L.Q. (2018a) Ontogeny of the Postcranial Axial Skeleton of Melanosuchus niger (Crocodylia, Alligatoridae). *The Anatomical Record* 301, 607–623. https://doi.org/10.1002/ar.23722

Vieira, L.G., Santos, A.L.Q., Hirano, L.Q.L., Menezes-Reis, L.T., Mendonça, J.S. & Sebben, A. (2018b) Ontogeny of the skull of the Black Caiman (Melanosuchus niger) (Crocodylia: Alligatoridae). *Canadian Journal of Zoology*. https://doi.org/10.1139/cjz-2018-0076

Vieira, L.G., Santos, A.L.Q., Lima, F.C., Mendonça, S.H.S.T., Menezes, L.T. & Sebben, A. (2016) Osteologia de *Melanosuchus niger* (Crocodylia: Alligatoridae) e a evidência evolutiva. *Pesquisa Veterinária Brasileira* 36, 1025–1044. https://doi.org/10.1590/S0100-736X2016001000018

Voris, J.T., Zelenitsky, D.K., Therrien, F., Ridgely, R.C., Currie, P.J. & Witmer, L.M. (2021) Two exceptionally preserved juvenile specimens of Gorgosaurus libratus (Tyrannosauridae, Albertosaurinae) provide new insight into the timing of ontogenetic changes in tyrannosaurids. *Journal of Vertebrate Paleontology* 41, e2041651. https://doi.org/10.1080/02724634.2021.2041651

Watanabe, A. & Slice, D.E. (2014) The utility of cranial ontogeny for phylogenetic inference: a case study in crocodylians using geometric morphometrics. *Journal of Evolutionary Biology* 27, 1078–1092. https://doi.org/10.1111/jeb.12382

Wheeler, Q.D. & Meier, R. (2000) *Species concepts and phylogenetic theory: a debate*. Columbia University Press.

Whetstone, K.N. & Whybrow, P.J. (1983) A cursorial crocodilian from the Triassic of Lesotho (Basutoland) southern Africa. *Occasional papers of the Museum of Natural History, the University of Kansas.* 106, 1–37.

Wilson, J.A., Malkani, M.S. & Gingerich, P.D. (2001) NEW CROCODYLIFORM (REPTILIA, MESOEUCROCODYLIA) FROM THE UPPER CRETACEOUS PAB FORMATION OF VITAKRI, BALOCHISTAN (PAKISTAN). *Contributions from the Museum of Paleontology*.

Wiseman, A.L.A., Bishop, P.J., Demuth, O.E., Cuff, A.R., Michel, K.B. & Hutchinson, J.R. (2021) Musculoskeletal modelling of the Nile crocodile (Crocodylus niloticus) hindlimb: Effects of limb posture on leverage during terrestrial locomotion. *Journal of Anatomy* 239, 424–444. https://doi.org/10.1111/joa.13431

Witmer, L.M. (1997) The Evolution of the Antorbital Cavity of Archosaurs: A Study in Soft-Tissue Reconstruction in the Fossil Record with an Analysis of the Function of Pneumaticity. *Journal of Vertebrate Paleontology* 17, 1–76. https://doi.org/10.1080/02724634.1997.10011027

Witmer, L.M. & Ridgely, R.C. (2008) The Paranasal Air Sinuses of Predatory and Armored Dinosaurs (Archosauria: Theropoda and Ankylosauria) and Their Contribution to Cephalic Structure. *The Anatomical Record* 291, 1362–1388. https://doi.org/10.1002/ar.20794

Woodruff, D.C., Carr, T.D., Storrs, G.W., Waskow, K., Scannella, J.B., Nordén, K.K. & Wilson, J.P. (2018) The smallest diplodocid skull reveals cranial ontogeny and growth-related dietary changes in the largest dinosaurs. *Scientific Reports* 8, 1–12.

Woodward, A.S. (1896) On two mesozoic crocodilians Notosuchus (genus novum) and Cynodontosuchus (genus novum) from the red sandstones of the territ ory of Neuquen (Argentine republic)= Sobre dos cocodrilos mesozoicos Notosuchus (genus novum) y Cynodontosuchus (genus novum) de las areniscas rojas del territorio del Neuquen (República Argentina). *(No Title)*.

Woodward, H.N., Tremaine, K., Williams, S.A., Zanno, L.E., Horner, J.R. & Myhrvold, N. (2020) Growing up Tyrannosaurus rex: Osteohistology refutes the pygmy “Nanotyrannus” and supports ontogenetic niche partitioning in juvenile

Tyrannosaurus. *Science Advances* 6, eaax6250. https://doi.org/10.1126/sciadv.aax6250

Yeates, D.K., Seago, A., Nelson, L., Cameron, S.L., Joseph, L. & Trueman, J.W.H. (2011) Integrative taxonomy, or iterative taxonomy? *Systematic Entomology* 36, 209–217. https://doi.org/10.1111/j.1365-3113.2010.00558.x

**Supplementary information S.1**

# CRANIAL AND POSTCRANIAL ANATOMY OF A BAURUSUCHID JUVENILE (NOTOSUCHIA, CROCODYLOMORPHA) AND THE TAXONOMICAL IMPLICATIONS OF ONTOGENY

Daniel Martins dos Santos[1]*, Rodrigo Miloni Santucci[2], Joyce Celerino de Carvalho[2], Carlos Eduardo Maia de Oliveira[3] and Marco Brandalise de Andrade[4].

[1]Zoology Graduate Program, Institute of Biological Sciences, University of Brasília, DF, Brazil; *Corresponding author e-mail: danielmartinsantos@hotmail.com

[2]University of Brasília, Planaltina Campus (FUP), DF, Brazil;

[3]Federal Institute of Education, Science and Technology of São Paulo, Votuporanga Campus (IFSP), Votuporanga-SP, Brazil;

[4]Pontifical Catholic University of Rio Grande do Sul, Porto Alegre-RS, Brazil.

## 1. Introduction

Below we provide the original sequence of additive characters and the scoring for both IFSP-VTP/PALEO 0003, the specimen described in the paper, and *Gondwanasuchus scabrosus* Marinho et al. 2013, the first time it is scored in this data matrix, derived from Pol et al. (2012), Fiorelli et al. (2016) and Martinelli et al. (2018).

## 2. Additive characters

The following characters should be set as additive in TNT in order for the presented results to be replicated: 1, 3, 6, 10, 23, 37, 43, 44, 45, 49, 65, 67, 69, 71, 73, 77, 79, 86, 90, 91, 96, 97, 105, 116, 126, 140, 142, 143, 149, 167, 182, 187, 193, 197, 226, 228, 279, 339, 356, 357 and 364. Please note that, due to counting

differences, in the TNT environment this sequence starts at 0, so the subsequent characters should also be subtracted by 1.

### 3. Scoring of IFSP-VTP/PALEO 0003

100?000132010011l0??11??11?????????32110110l???1?011?1000????1??3?
2?111101011111?111021?02?0000102?00?20210321O?1012?110111010111?0
011101011021O?00?1110000?12000000?2?01???1?1?001?[01]0001?010010101
?0100011?10010000000??000??0?00100011111000000300?01???10?001100?0
?1????00?111000010?00?01?00001100111?1111000?110111?01????11????
1????0?1011?102????00?000???1??1100?00011100010??2100??00[01]100?00
???000?1101?110?01??0111??11?0?0010??00?1100??00

### 4. Scoring of *Gondwanasuchus scabrosus*

100000?1320100?110?01???11?011??????2?????????????????????????????30
1??1???00?1[01]1?????????????????????????12??113??0??????11011101?1111
0?01?00101?0210????????01??12000000?2?0??1?1???0?1??0000?0?0??0?0?
??10?0????20?0???000??0??????0?10001???1000000???00????1???00????0
???????????0?0010??0???000?01?00?????????????????????????????????
?????????????????????0????0???????100?000????0????????0??01110??00??
??0??110??11??00?????????????????????????????

# CAPÍTULO IV

## DISENTANGLING ONTOGENETIC VARIATIONS WITHIN BAURUSUCHIDAE (CROCODYLOMORPHA, NOTOSUCHIA) USING GEOMETRIC MORPHOMETRICS


### Abstract

The incompleteness of the fossil record often precludes research assessments of variation within a clade due to most species being known from single specimens. Baurusuchidae are a rare exception, with abundant materials, including different ontogenetic stages, being recovered from the Adamantina Formation, Late Cretaceous of Brazil. Here, we attempt to distinguish and characterize specimens in distinct places along a possible growth series using geometric morphometrics. A tight relationship between size and shape is demonstrated, with adult individuals displaying a cohesive collection of characteristics and proportions in comparison to juveniles. An ontogenetic signal amongst the vast majority of baurusuchid specimens is identified, opening the possibility that the diagnostic characters of some species could be explained by ontogenetic development, not evolutionary divergence. Collection biases and ecological inconsistencies also point to a possible overestimation of baurusuchid diversity. Finally, a taxonomic revision of the family and suggestions to restrict the proposals of diagnostic characters are pointed as possible improvements that may support a reduction in the number of valid baurusuchid species.



**Keywords:** Baurusuchidae; morphometrics; ontogeny; taxonomy; Bauru Basin.


### 1. Introduction

Allometry, the relationship between size and shape, whether of phylogenetic or ontogenetic variation, is of crucial importance to improve our understanding of evolutionary, developmental, and ecological aspects of organisms (Gould 1966). Sources of shape variation in fossil vertebrates, whether teratogenic, taphonomic, sexual dimorphic or ontogenetic are often difficult to assess due to the scarcity specimens (Mariani and Romano 2017), with most species known from a single

individual. Nevertheless, whenever possible, attention to variability and its mechanisms, especially ontogeny, allows for more precise assessments of the past diversity of clades (Horner and Goodwin 2006; Horner and Goodwin 2009; Scannella and Horner 2010; Woodward et al. 2020; Carr 2020).

Baurusuchids were predatory notosuchians from Upper Cretaceous deposits of Gondwana with remarkable adaptations for hypercarnivory, including oreinirostral snouts and ziphodont dentition (Price 1945; Riff and Kellner 2011). Their remains are amongst the most common tetrapod materials recovered in the Adamantina Formation, Bauru Basin, Brazil, with several articulated skeletons and well-preserved skulls yielding a total of nine local species (Price 1945; Campos 2001; Carvalho et al. 2005; Carvalho et al. 2011; Montefeltro et al. 2011; Marinho et al. 2013; Godoy et al. 2014; Darlim, Montefeltro, et al. 2021; Martins et al. 2023). Despite this relative abundance, and a pioneering study by Godoy et al. (2018) identifying heterochronic processes in the skull evolution of Baurusuchidae, there has been no attempt to apply modern morphometric methods to the holotypes and additional baurusuchid specimens in order to establish if these indeed occupy distinct morphospaces or if their differences are attributable to ontogenetic processes and/or taphonomic alterations.

Using geometric morphometrics, this study aims to search for the presence of immature individuals within Baurusuchidae by testing whether known specimens fall under an ontogenetic series. In spite of the significant sample size gap between paleontology and neontology, these techniques have the potential to contribute to important taxonomic and ecological discussions, as is demonstrated by the recent unveiling of hidden crocodylian diversity (Angulo-Bedoya et al. 2019; Murray et al. 2019), the clear distinction of ontogenetic series (Watanabe and Slice 2014; Foth et al.

2015; Foth et al. 2018), and relationship between form and function (Drumheller and Wilberg 2020).

## 2. Materials and Methods

In order to conduct the morphometric analyses of both lateral and dorsal views of the skull, an assessment of both the quantity and quality of available baurusuchid specimens needed to be made, which is summarized in the table below (**Table 1**). We found at least sixteen partial, semi-complete and complete skulls, in various stages of preservation and, most importantly, belonging to different ontogenetic stages. The data encompasses 14 skulls analysed in lateral view and 13 in dorsal aspect. There is almost total overlap between the two data sets, with the exception of *Aplestosuchus sordidus* (Godoy et al. 2014), which could only be utilized in dorsal view due to strong dorsoventral compression, and the recently published *Campinasuchus dinizi* CPPLIP 1360 specimen (Fonseca et al. 2020), which is the opposite case, not having an adequate-enough dorsal profile.

Skulls of a total of eight brazilian baurusuchid species (**Figure 1a**), whether holotypes or paratypes, were included in the analysis, encompassing the basal taxon *Gondwanasuchus scabrosus* (Marinho et al. 2013), and members of the subfamilies Pissarrachampinae and Baurusuchinae (Montefeltro et al. 2011; Darlim, Montefeltro, et al. 2021). Three putative juvenile specimens are also considered, one most likely attributable to the *Baurusuchus* genus itself, IFVP-VTP/PALEO 0003, described in detail in dos Santos *et al*. (2023) (chapter III), a *Pissarrachampsa sera* semaphoront LPRP/USP 0049 (Godoy et al. 2018), and an immature *Campinasuchus dinizi* CPP 1237 (Carvalho et al. 2011). The fragmentary nature of the Pakistani *Pabwehshi*

*pakistanensis* (Wilson et al. 2001), Argentinian species *Cynodontosuchus rothi* (Woodward 1896) and *Wargosuchus australis* (Martinelli and Pais 2008), as well as *Baurusuchus albertoi* (Nascimento and Zaher 2010) and the recently discovered *Aphaurosuchus kaiju* (Martins et al. 2023), precluded their addition in the present study.

| ***Taxon and specimen*** | **Lateral profile Missing landmarks (n)** | **Dorsal profile Missing landmarks (n)** |
|---|---|---|
| *Baurusuchus sp.* **IFSP-VTP/PALEO-0002** | ✓(0) | ✓(1) |
| *Baurusuchus sp.* **FEF- Pv-R-1/9** | ✓(1) | ✓(2) |
| *Baurusuchus sp.* ***FUP-Pv 000020*** | ✓(0) | ✓(1) |
| *Baurusuchus sp* ***FUP-Pv 000022*** | ✓(3) | ✓(1) |
| *Baurusuchus sp.* (juvenile) **IFSP – VTP/PALEO 0003** | ✓(1) | ✓(5) |
| *Baurusuchus pachecoi* **DGM-299 R** | ✓(2) | ✗ |
| *Gondwanasuchus scabrosus* **UFRJ DG 408-R** | ✓(4) | ✓(10) |
| *Baurusuchus albertoi* **MZSP-PV 140** | ✗ | ✗ |
| *Baurusuchus salgadoensis* ***MPMA 62-0001-02*** | ✓(0) | ✓(0) |
| *Aplestosuchus sordidus* ***LPRP/USP 0229a*** | ✗ | ✓(0) |
| *Stratiotosuchus maxhechti* ***DGM 1477-R*** | ✓(1) | ✓(0) |
| *Campinasuchus dinizi* **CPPLIP 1360** | ✓(4) | ✗ |
| *Campinasuchus dinizi* (juvenile) **CPP 1237** | ✓(2) | ✓(1) |
| *Pissarrachampsa sera* ***LPRP/USP 0019*** | ✓(4) | ✓(3) |
| *Pissarrachampsa sera* (juvenile) ***LPRP/USP 0049*** | ✓(0) | ✓(0) |
| *Aphaurosuchus escharafacies* ***LPRP 0697*** | ✓(0) | ✓(0) |
| *Aphaurosuchus kaiju* **LPRP/USP 0634** | ✗ | ✗ |

**Table 1. List of utilized specimens. Number of missing landmarks estimated in each view is shown.**

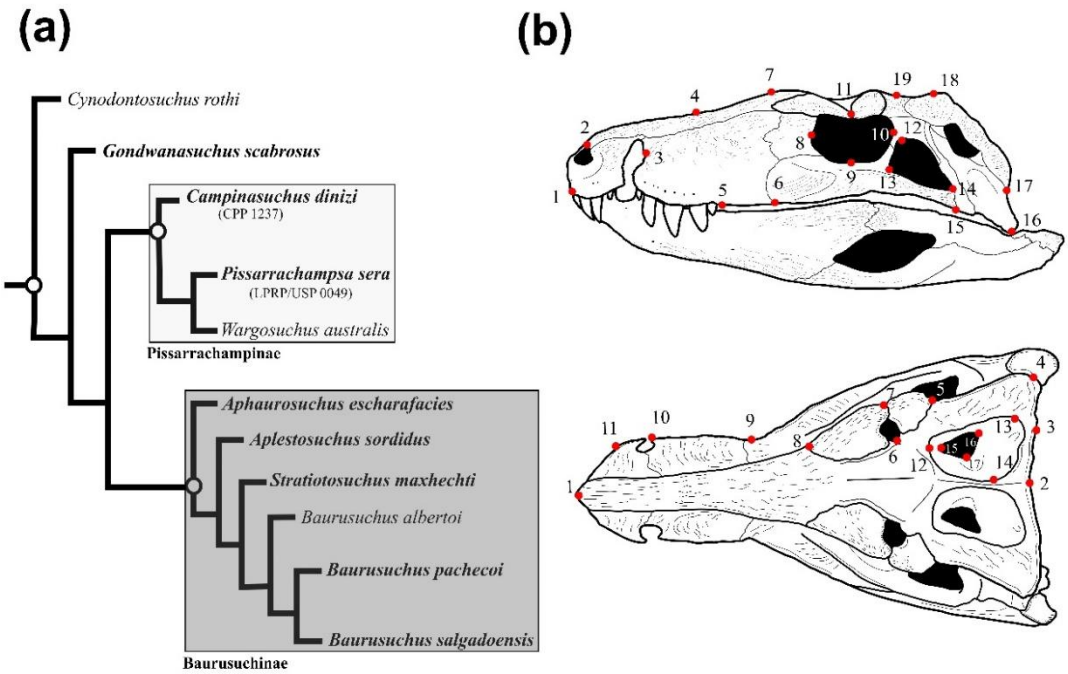


**Figure 1. (a) phylogenetic tree of Baurusuchidae, adapted from Darlim et al. (2021), showing the basal form *Gondwanasuchus*, followed by the dichotomy between Pissarrachampinae and Baurusuchinae. Taxa utilized in the analyses are highlighted in bold. *Campinasuchus* and *Pissarrachampsa* juveniles were also included, and their referred specimen numbers are shown. (b) Schematic drawing of generalized baurusuchid skulls in left lateral (top), and dorsal (bottom) views, with chosen landmark arrangement.**

| LANDMARK NUMBER | DESCRIPTION |
|---|---|
| 1 | Alveolar margin of the premaxillary's first teeth |
| 2 | Dorsal margin of internarial bar |
| 3 | Posterodorsal edge of pmx-mx notch |
| 4 | Inflexion point of rostrum's dorsal margin |
| 5 | Distal edge of fifth maxillary teeth alveolus |
| 6 | Ventral margin of the maxillary-jugal contact |
| 7 | Dorsalmost point of the preorbital rise |
| 8 | Orbit's anteriormost point |
| 9 | Orbit's ventralmost point |
| 10 | Orbit's posteriormost point |
| 11 | Orbit's dorsalmost point |
| 12 | Dorsal vertex of itf |
| 13 | Anterior vertex of itf |
| 14 | Posterior vertex of itf |
| 15 | Ventral margin of the jugal-quadratojugal contact |
| 16 | Ventral point of the quadrate's lateral condyle |
| 17 | Quadrate-squamosal lateral contact point |
| 18 | Anterodorsal point of squamosal |
| 19 | Dorsal edge of postorbital |

**Table 2. Brief topological description of landmarks as seen in lateral view (see figure 1b). Abbreviations: itf, infratemporal fenestra; mx, maxillary bone; pmx, premaxillary bone;**

| LANDMARK NUMBER | DESCRIPTION |
|---|---|
| 1 | Anteriormost tip of nasals |
| 2 | Point where parietals meet at occipital margin |
| 3 | Occipital edge of temporoorbital foramen of stf |
| 4 | Posterolateral point of squamosal flange |
| 5 | Posterolateral vertex of posterior palpebral |
| 6 | Medial point of suborbital fenestra |
| 7 | Lateral point of suborbital fenestra |
| 8 | Anterior vertex of anterior palpebral |
| 9 | Concavity inflexion point of lateral margin of skull |
| 10 | Posterior edge of pmx-mx notch |
| 11 | Concavity inflexion point of pmx lateral margin |
| 12 | Anterior vertex of dtf |
| 13 | Lateral vertex of dtf |
| 14 | Medial vertex of dtf |
| 15 | Anterior vertex of infratemporal fossa |
| 16 | Lateral vertex of infratemporal fossa |
| 17 | Medial vertex of infratemporal fossa |

**Table 3. Brief topological description of landmarks as seen in dorsal view (see figure 1b). Abbreviations: dtf, dorsotemporal fenestra; mx, maxillary bone; pmx, premaxillary bone; stf, supratemporal fenestra.**

### 2.1 Data acquisition

Most specimens were photographed during visits by the authors, utilizing a Canon® 1100D camera, while others were included using the profiles seen in their original publications (**Table 1**). The analysis of their lateral views comprised 19 landmarks (**Table 2**), comprising the rostrum, orbital rim, infratemporal fenestra, quadrate condyles and temporal bar, whereas the dorsal views encompassed 17 landmarks along the rostrum, palpebrals and supraorbital fenestra, dorsotemporal fenestra (sensu Holliday et al. 2020), and occipital margin (**Figure 1b**, but also see **Table 3** for landmark description). Landmarks digitization was conducted using *tpsDig* (Rohlf, 2009), and missing landmarks were assigned an "NA" on both axes. The resulting data files were further processed and analysed using the *Geomorph* R package (Collyer and Adams 2018; Baken et al. 2021; Adams et al. 2023).

Landmarks rested upon non-preserved portions of the skull were reconstructed using the *estimate.missing* function under the TPS method, which estimates positions based on a complete reference specimen to interpolate landmarks using a thin-plate spline (Gunz et al. 2009). Despite assumed assumptions and uncertainties of landmark reconstruction methods, work by Arbour and Brown (2014) has shown that larger data sets with reconstructed specimens are preferrable and better correspond shape variation than smaller sets comprised of only complete specimens. TPS performance is on pair with other methods when well-preserved complete reference specimens are present, taxonomic diversity is low and landmark numbers are high, although in most other cases its accuracy might lag behind alternatives (Gunz et al. 2009; Arbour and Brown 2014). It has also recently outperformed other methods when applied to the study of extant caimans (Blanco et al. 2018). Given that analyses included only members of a small, low disparity clade with only 3 to 4 specimens requiring landmark reconstruction, TPS seemed the most logical fit.

### 2.2 Geometric morphometrics and ontogenetic patterns

The disposition of landmarks was aligned with a standard Procrustes function, which minimises sources of variation such as size and orientation (Rohlf and Slice 1990), and their mean positions were plotted against variations for each specimen (**see supplementary materials**). The procrustes was followed by the generation of a covariance matrix and a Principal Component Analysis (PCA) to assess shape variation between data points. In order to aid shape change visualization, the results of PC1 and PC2, which explained the vast majority of variation, are presented as scatterplots, and linked transformation grid graphs for the most positive(+) and most

negative(-) specimens along both axes were generated to assess particulars about proportion variation of cranial structures and major vectors of taphonomic deformation.

As a means to test the relationship between shape and size, a regression for Procrustes shape variables/Procrustes ANOVA was performed prior to the plotting of the multivariate regression of shape (y axis) as the independent variable, and size (x axis) in the form of log centroid size as the dependant variable. R-squared and *P*-values were utilized as parameters to assess the statistical significance of the possible presence of an ontogenetic signal for both vistas. Additionally, not to solely rely on the above to infer relationship between shape and size, a Partial Least Squares (PLS) regression (Rohlf and Corti 2000), with 1000 random permutations, independently tested the covariance between the two, and its *P*-value similarly compared to statistical confidence thresholds.

## 3. Results

Most of the variance in shape in the lateral profile analysis was accounted for by PC1(56.85%) (**Figure 2**) while the first three PCs together explain more than 76% (PC2=11.45%, PC3=8.5%). Scatterplot distribution may be divided into three distinct groupings, with no observed superposition of morphospaces: (1) a cluster of 10 specimens on the negative end of PC1, with relatively small scattering along the PC2 axis (between -0.02 to 0.02); (2) 3 specimens aligned in the middle of the PC1

sequence (0.07) but displaying high vertical variance on PC2; and (3) a single specimen at the more positive end of PC1.

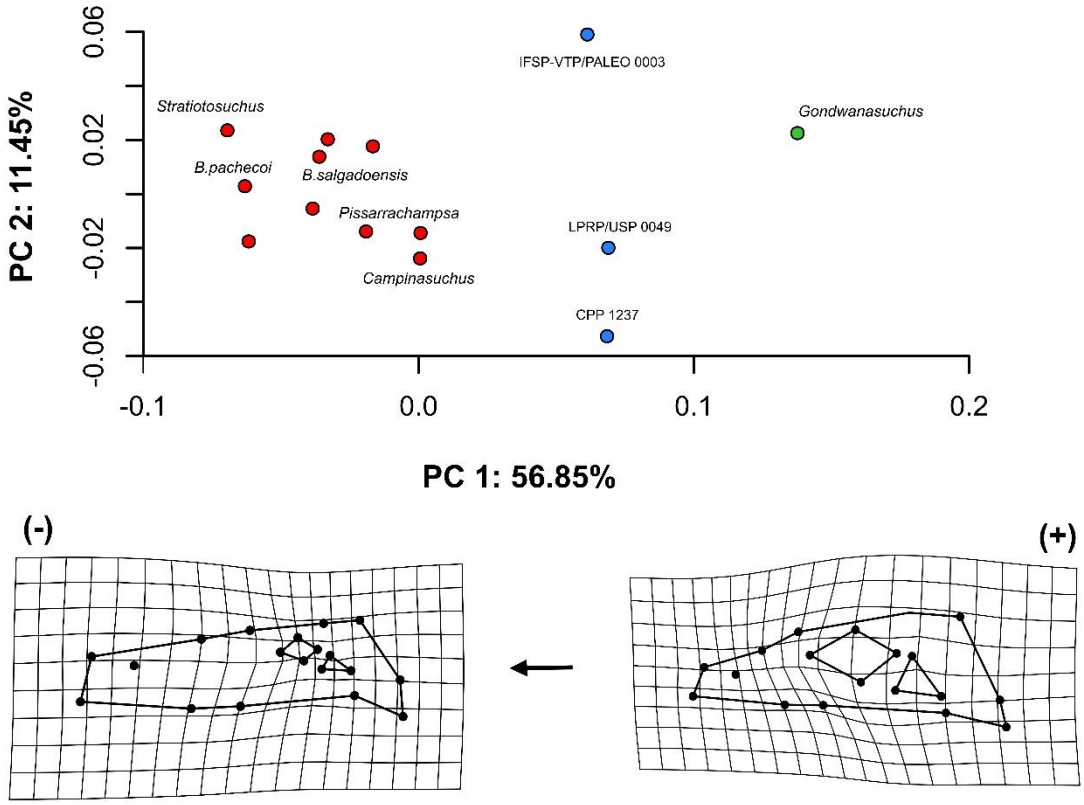


**Figure 2. Lateral view PCA scatterplot and associated transformation grids of the most positive and negative data points. PC1 accounts for the majority of shape variance, despite considerable vertical scattering of some specimens. Note the significant change in overall outline and proportions along the series. Red circles are comprised of larger skulls, while blue and green ones represent intermediate and small skulls, respectively.**

PC1 is more intimately linked with horizontal variation of skull length, which consequently alters the overall profile shape and proportions, while we interpret that PC2 is related to dorsoventral compression vectors. Linked transformations grids of both the most positive and negative ends of PC1 reveals a significant shape and relative proportions change between these groupings, going from a skull form with roughly equal preorbital and postorbital lengths, shorter rostrum and proportionally large orbits and infratemporal fenestra, to forms with hyperdeveloped and deep rostra

that far exceed postorbital (skull table) length, relatively smaller skull openings and more verticalized quadrate condyles (**Figure 2**)

Data point distribution and clustering on the PC1 axis seems to be strongly related with the respective ontogenetic stage of each specimen, separating the specimens widely regarded and previously described as skeletally mature individuals on the negative end, while juveniles fall on the right side of the graph. The isolation of *Gondwanasuchus*, and its association with a profile displaying features commonly found in extant and extinct young crocodyliform individuals (Foth et al. 2015; Foth et al. 2018; Blanco et al. 2018; Drumheller et al. 2021), is noteworthy and consistent with the great size discrepancy in relation to other baurusuchid material included in the analysis.

Multivariate regression of shape to log centroid size yielded very strong support against the null hypothesis, with a *p*-value of 0.002, well below a 0.05 threshold for statistically significant associations, indicating that size indeed has a significant effect on shape, and supporting the presence of an ontogenetic signal (**Figure 4**).

A substantial effect size (z) value of 2.67 was also found, and the R-squared value of 0.3957 translates to 39.57% of changes in shape being explained by variations in size. The PLS results also support this covariance, with a p-value of 0.01.

As expected, adults concentrate on the upper right side of the distribution, with *Stratiotosuchus maxcheti* as its most mature representative, later stage juveniles in the mid-section, and *Gondwanasuchus* as the youngest semaphoront in the series, with a noticeable separation towards the others.

The dorsal view PCA produced a similar, but not as widely separated clustering of data points (**Figure 3**). PC1 alone accounts for 45.14% of shape variance, whereas

PC2 also displays significant explanatory potential at 24.59%. PC1 through PC4(PC3=13.94%;PC4=7.02%) together explain 90.69% of change. Skulls of skeletally mature individuals, with the exception of *Pissarrachampsa*, groups closer to the 0.0 mark on the PC1 axis, with little vertical dispersion. In accordance with the previous analysis, juveniles display high PC2 variance, but IFSP-VTP/PALEO 0003 falls within the adult morphospaces. *Gondwanasuchus* persists as an isolated data point, on the more positive side of PC1. The scatterplot distribution also suggests separation along ontogenetic lines, although less so then on the lateral PCA. The horizontal axis, PC1, describes a differential elongation of the rostrum, accompanied by a lateromedial compression characteristic of the oreinirostral condition typical of baurusuchids, at the same time as PC2 is interpreted to account for lateral compression and shear forces to which the specimens were submitted.

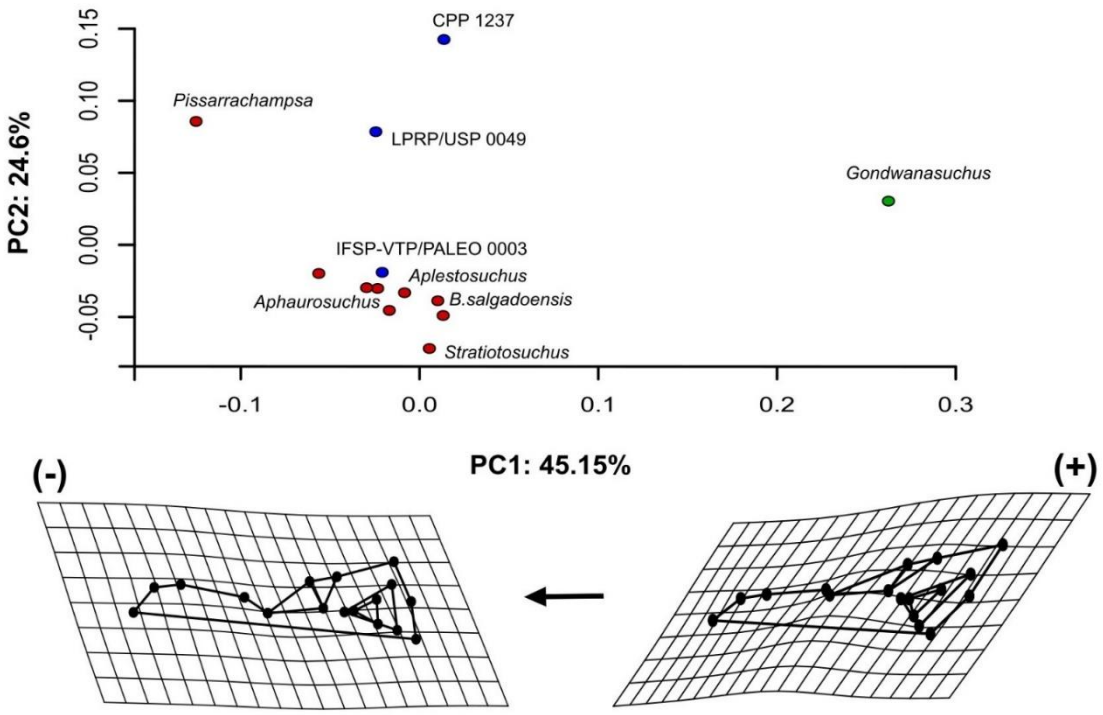


**Figure 3. Dorsal view PCA scatterplot with corresponding transformations grids showing shape variation along PC1 and PC2. In a similar manner to the lateral view analysis, PC1 accounts mostly for the heterochronic development of the rostrum throughout ontogeny. Red circles are comprised of larger skulls, while blue and green ones represent intermediate and small skulls, respectively.**

Regression of shape *vs.* log centroid size resulted in moderate to strong support against the null hypothesis, with a p-value of 0.02, below the 0.05 significance benchmark, and R-squared values of 0.2449 yields a 24.49% of shape change being explained by size differences. PLS analysis produced effect size (z) values of 1,62 and p-value of 0.043, marginally below the confidence level. An ontogenetic signal has similarly been detected (**Figure 4**), but with lower statistical confidence, most likely due to this view being more substantially affected by taphonomic deformation.

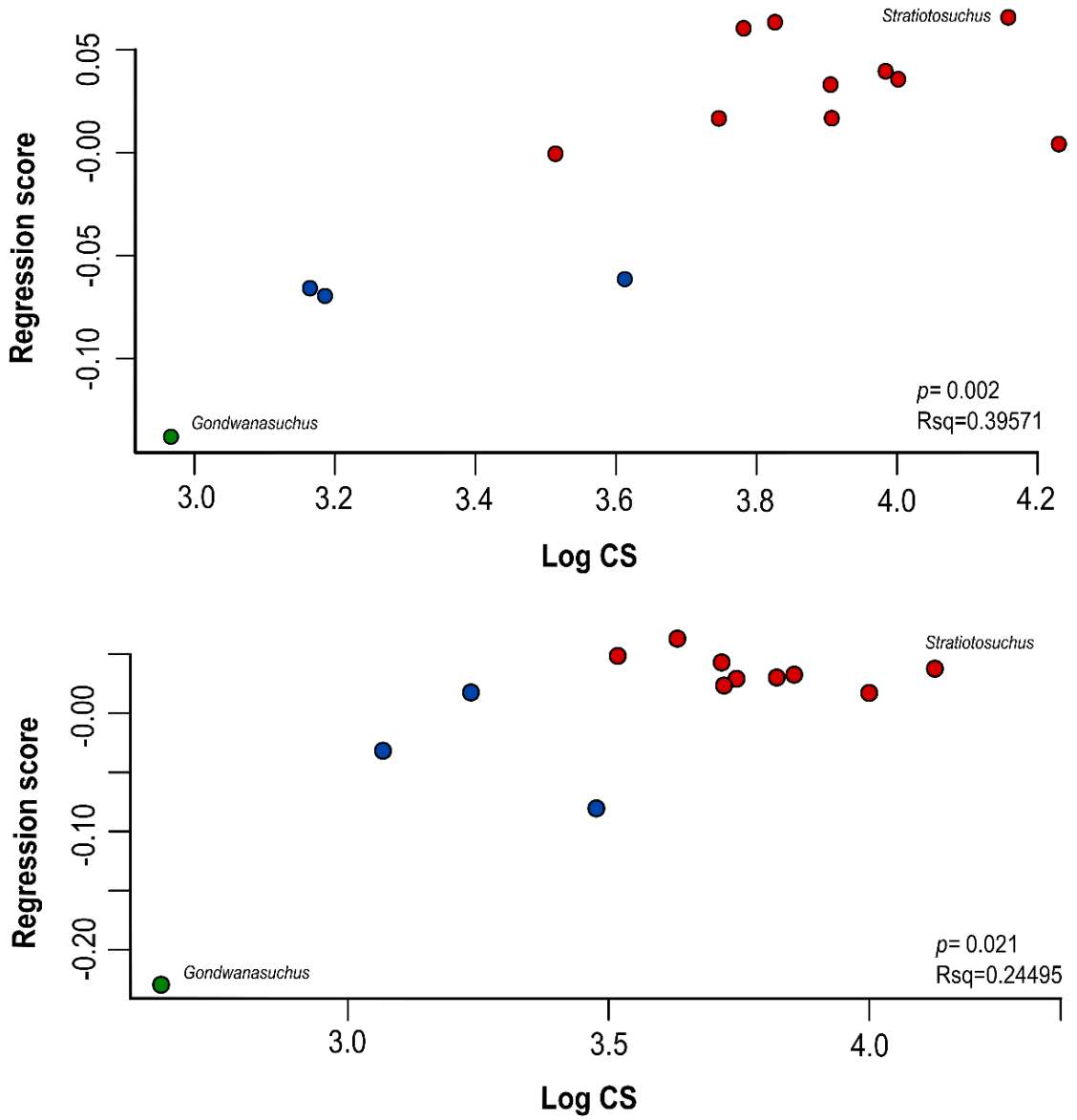


**Figure 4. Regression scatterplots of shape *vs.* log centroid size for both views. The nature of curves and their respective p-values support an ontogenetic signal. P-values and Rsq are provided in the bottom right corner. Red circles comprise larger skulls, while blue and green represent intermediate and small skulls, respectively.**

## 4. Discussion

The PCA analyses allowed for the characterization of the origins of shape variance amongst baurusuchids, consistently relating to ontogenetic growth. This sheds light into the nature of their in-group morphospace occupation, and thus provides substance for a more detailed discussion on their levels of diversity and disparity. Here, the geometric morphometric results are discussed in the context of baurusuchid taxonomy, paleoecology, and biogeography within the Bauru Basin, given the substantial allometric relationship found between size and shape.

### 4.1 Ontogenetic biases

Ontogenetic variations in skull shape and proportions described by the PCA and regression data (e.g. relatively large orbits, short and gracile rostra) are in line with previous morphometric (Foth et al. 2015; Foth et al. 2018; Blanco et al. 2018; Angulo-Bedoya et al. 2019) and comparative anatomy and development studies (Vieira et al. 2018; Drumheller and Wilberg 2020) involving crocodyliforms. More specifically to baurusuchids is the conspicuous heterochronic development of their rostrum, comprising most of the total skull length in adult individuals, clearly visible along the PC1 on both views, that creates a morphological gap between adults and young juveniles, in close accordance to the findings of Godoy et al. (2018).

The mapped contrasts between adults and juveniles work as a framework that allows the placement of known specimens along an ontogenetic series. This is of special importance given that new taxa have been erected in the past without the proper acknowledgement of ontogenetic biases, leading to an artificial overestimation

of past diversity (Horner and Goodwin 2006; Horner and Goodwin 2009; Scannella and Horner 2010; Woodward et al. 2020; Carr 2020).

Modern crocodylians and closely related fossil neosuchians undergo substantial shifts with growth (**Figure 5**), so it is only natural that divergent morphologies should be interpreted as being of phylogenetic origin in isolated fossil finds without particular special attention to the matter (Grigg 2015; Drumheller et al. 2021). Morphological divergences amongst semaphoronts have been identified in broader terms for sauropsids (Griffin et al. 2021), and were echoed by Santos et al.(chapter III) for the specific case of baurusuchids, identifying several cranial characters affected by growth, mostly in the sculpturing/ornamentation development of dermatocranium bones and enlargement of adductor musculature and associated origin and attachment sites.

As both anatomical and morphometric lines of evidence seem to suggest, *Gondwanasuchus scabrosus* has been described utilizing an early juvenile, perhaps the youngest ever identified excluding a baurusuchid yearling specimen (Santos et al. 2021), and so its autapomorphies cannot be properly disentangled from shifts associated with growth. Therefore, it is not known whether its defining characters, such as apicobasal ridges/sulci, also found in the posteriormost maxillary teeth of IFSP-VTP/PALEO 0003, might actually be common for baurusuchid individuals of similar stages or in fact unique to a new species, lacking a growth control that would bolster the case for a new taxon, especially as an entire new genus has also been erected. In the light of the shape analysis here presented, we reinforce the position that *Gondwanasuchus* should then be considered a *nomem dubium*, but also call attention to the possibility that *Stratiotosuchus* might represent a larger, and most likely older, individual attributable to species in the *Baurusuchus* genus (judging by its

morphospace position) because of its tendency to fall on the opposite end of the regression distributions.

It also needs to be recognized that, despite the proclivity of adult individuals to generally group together, it is hard to determine if this tendency is ascribable to an intraspecific signal or the morphospace overlap of several species, which is known to occur amongst modern crocodylians (Watanabe and Slice 2014; Foth et al. 2018). A case-by-case approach, in unison with paleoecological and paleogeographical arguments is thus advised in order to evaluate such pattern.

### 4.2 Paleoecological implications

The heterochronic growth in baurusuchid rostra bridges the significant gap between young juveniles and adults, starting from short and shallows snouts with gracile teeth and larger diastema, to long and deeper rostra with incrassate teeth. The relatively undeveloped adductor aponeuroses and relatively lack of tooth wear in juveniles, described in the previous chapter, in addition to rostrum development, most likely precluded young individuals from having pursued similar foraging strategies to adults due to differences in prey size and bite force (Erickson et al. 2003; Gignac and Erickson 2015; Gignac and Erickson 2016; Gignac and O'Brien 2016).

These observations fit the concept of and strengthen the case for ontogenetic dietary shifts and thus intraspecific niche partitioning with baurusuchidae, a common feature in modern crocodylians, where juveniles usually begin by consuming aquatic invertebrates then proceed to larger, less pliant prey, including vertebrates, avoiding competition with older semaphoronts (Dodson 1975; Tucker et al. 1996; Borteiro et al. 2009).

We hold that baurusuchids likely displayed similar dietary shifts throughout their life history, culminating in the osteophagous hypercarnivory of adults (Godoy et al. 2014; Oliveira et al. 2021). This is further supported by a ~ 30% difference in Hg concentrations in bone hydroxyapatite among adults and juveniles found by Cardia et al. (2018), an independent line of evidence likely indicating that different baurusuchid semaphoronts feed on different prey. Consequently, in spite of small egg clutch sizes (Oliveira et al. 2011; Marsola et al. 2016), we consider unlikely that baurusuchids displayed greater parental care levels than extant crocodylians (r/k spectrum of selection theory), which could require juvenile consumption of prey captured by adults, likely producing similar mercury concentrations than the ones presently observed (MacArthur and Wilson 1967; Godoy et al. 2018).

### 4.3 The effects of stratigraphy, distribution and ecology on taxonomy

Baurusuchid remains in Brazil are specific to the bioturbated, massive reddish sandstone facies of the Adamantina Formation, interpreted as a product of an extensive sandy braided river system (Batezelli 2010). These depositional systems are highly dynamic and are characterized by shallow, multiple anastomosed channels interspersed by sigmoidal sand bars (Boggs 2012; Schuurman and Kleinhans 2015). As previously mentioned, a few baurusuchid articulated skeletons have been found, and some were dipped in respect to the horizontal plane, suggesting high sediment volume due to their size and complicating stratigraphic interpretations (Vasconcellos and Carvalho 2010). It is reasonable then to suggest that frequent bar migration and channel dynamics were responsible for rapid burial and subsequent preservation of semi-complete skeletons (Araújo Júnior and Silva Marinho 2013; Rhoads 2020). This particular depositional context, lacking significant vertical distribution, decreases the

possibility that part of currently recognized baurusuchid diversity might be explained by anagenesis within a few closely related lineages, as it has been suggested, for instance, for the *Daspletosaurus* species from the Two Medicine Formation, Montana (Carr et al. 2017). However, it also creates an ecological and paleogeographical problem, with 10 similar-sized species of top-tier predators, collected in similar sedimentological contexts, with low morphological disparity and in sympatry within a relatively small geographical area lacking major geographical barriers.

The nine valid species of baurusuchids in the Bauru Basin have been divided into two distinct subfamilies, Baurusuchinae and Pissarrachampsine, by previous phylogenies that focus on the detailed relationships of sebecosuchians (Montefeltro et al. 2011; Godoy et al. 2014; Darlim, Montefeltro, et al. 2021).

Given their high predatory status, even being regarded as possible theropod mimics and/or likely competitors to South American abelisaurids (Riff and Kellner, 2011), though they might not have shared the same environments (Bandeira et al. 2018), an assessment of their diversity is paramount for the understanding of local food webs.

Excluding *Gondwanasuchus scabrosus*, which is distinctively small-bodied, the clade seems to present very low levels of disparity, with its holotypes, mostly composed of cranial material, being of similar dimensions, and lacking major anatomical differences that might indicate partitioning.

Curiously, this diversity of baurusuchid species seems not to have emerged from widely spaced and distinctively separate sites within the basin but is mainly restricted to a few outcrops where the abovementioned facies can be found within the western portions of the Adamantina Formation (**Figure 5**). These localities are bound

nowadays by the Tietê and Paranaíba rivers and represent a small area along the states of São Paulo and Minas Gerais, where baurusuchinae and pissarrachampinae species were collected, respectively. The holotypes of five species, *B. pachecoi*, *B. albertoi*, *B. salgadoensis*, *Gondwanasuchus*, and *Aplestosuchus* have all originated from the vicinities of General Salgado municipality, being the latter three from an outcrop of the very same farm (Price 1945; Carvalho et al. 2005; Nascimento and Zaher 2010; Marinho et al. 2013; Godoy et al. 2014).

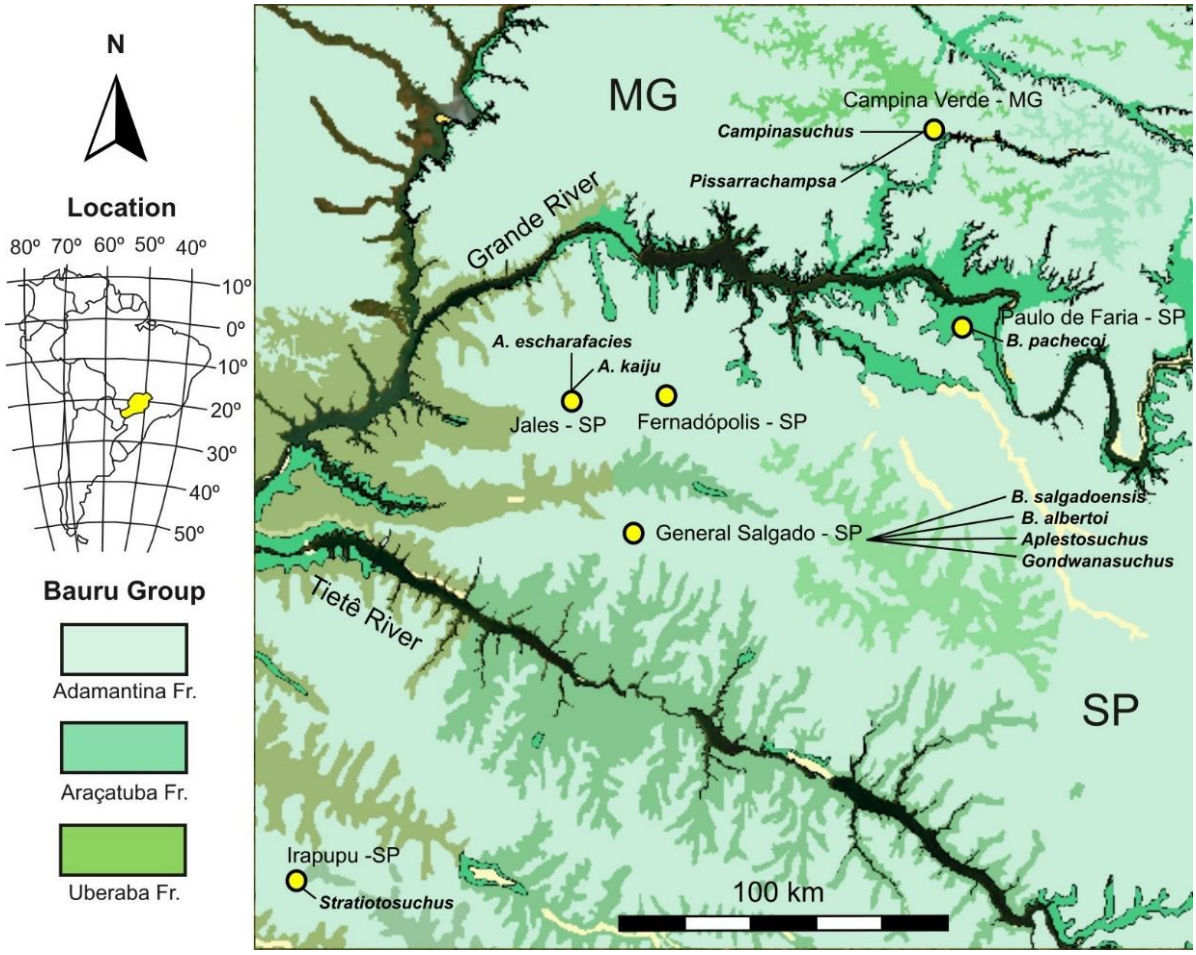


**Figure 5. Geological map of the northern Bauru Group, showing collecting sites and municipalities of all nine presently recognized baurusuchid species (in yellow). Curiously, the pissarrachampinae and baurusuchinae subfamilies are separated by the Grande River, between the states of Minas Gerais and São Paulo. The city of General Salgado-SP concentrates the highest number of species, four in total, coming from roughly the same site, within the same farm. *Stratiotosuchus maxhechti* is an outlier, being found south of the Tietê River.**

This condition greatly contrasts the present distributions and sympatric relationships of modern crocodylians (**Figure 6**), as the following cases exemplify. In spite of the recent recognition of *Crocodylus suchus* (Schmitz et al. 2003; Hekkala et al. 2011), the geographical range of *Crocodylus niloticus* Laurenti, 1768 vastly dwarfs that of brazilian baurusuchids. Similarly, the six caimanine species that occur in the Brazilian territory all have somewhat well-defined and vast biogeographical zones, and when in sympatry do not directly compete due to disparate sizes and rostral shapes (Roberto et al. 2021; Barreto-Lima et al. 2021).

In Colombia, the *Caiman crocodilus* complex is comprised of four subspecies, distributed along coastal, mountainous, and distinct river drainages separated by sharp geographical barriers (Angulo-Bedoya et al. 2019). These subspecies show surprising levels of cranial disparity considering their close relatedness, including a longirostrine form endemic to the Apaporis River (*C.crocodilus apaporiensis*) that oddly does not present significant molecular divergences from populations of *C.crocodilus crocodilus* (Balaguera-Reina et al. 2020).

In yet another example, the *Mescistops* genus, which used to be monospecific, now includes two morphologically similar species, *M. cataphractus* and *M. lepytorhyncus*, but these occur on distinct biogeographical zones on West Africa separated the Cameroon Volcanic Line (CVL) (Shirley et al. 2018). In fact, Africa, the second largest continent on Earth, currently supports only 5 crocodylian species, even after efforts to disentangle cryptic species. A comparison of such geographical distributions with the limited occurrences sites and single outcrops yielding high diversity in the Bauru Basin raises questions of about this unusual diversity of similar, sympatric, high-tier predators.

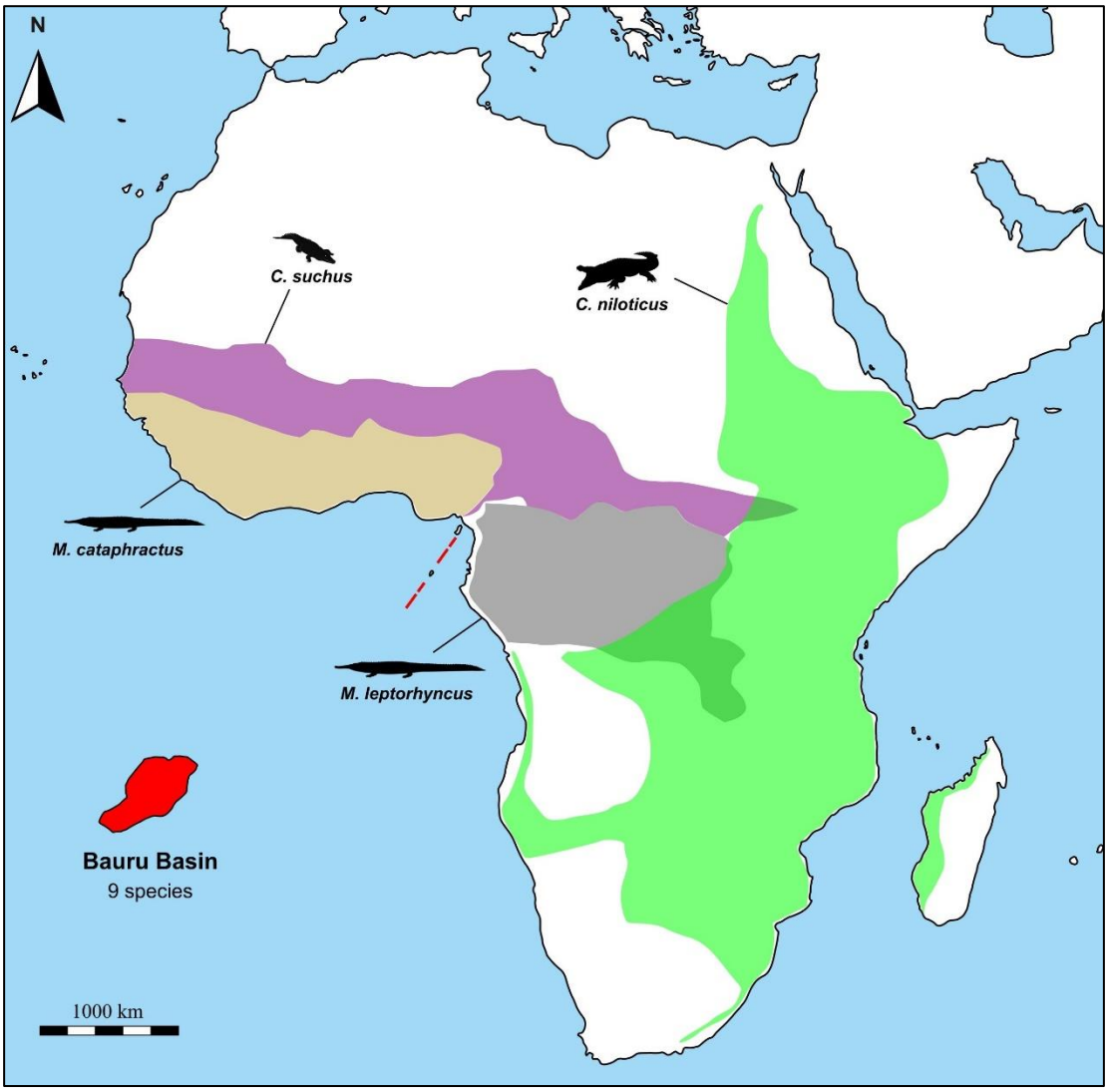


**Figure 6. Biogeographical zones of four species of crocodylids in Africa. The western light brown zone corresponds to the occurrence of *M. cataphractus*, while the light grey is where *M. leptorhyncus* can be found. These are separated by the Cameroon Volcanic Line (red dashed lines) and do not overlap. African members of the *Crocodylus* genus, *C. niloticus* and *C. suchus* are shown in purple and green, respectively. *Crocodylus* locally occurs in sympatry with both *Mecistops* and *Osteolaemus*. Adapted from the work of Matthew H. Shirley.**

Predators in modern terrestrial ecosystems, such as the African savannah, are of low diversity and anatomically disparate (lions, hyenas, cheetahs, leopards, and spotted dogs) and usually develop a series of avoidance mechanisms, such as niche/temporal partitioning, in order to decrease or prevent interspecific competition in the large predator guilds (Van Valkenburgh and Wayne 1994; Hayward and Slotow 2009; Sogbohossou et al. 2017).

Ecosystems where modern and fossil crocodylians play or played major ecological roles also display similar mechanisms, which allows for increased local diversity of distinct predators (Young et al. 2011; Salas-Gismondi et al. 2015; Souza et al. 2016; Staniewicz et al. 2018; Drumheller et al. 2021). Although behavioural/temporal partitioning would be almost unattainable from their fossil record, one should expect recognizable levels or anatomical disparity between baurusuchid species, which is lacking. This, in addition to the somewhat biased collection sites, brings into question the known levels of baurusuchid diversity, and demonstrates the necessity for taxonomy revision of the family.

We hold that a possible overestimation of diversity may have arisen from two main issues. The first is an inherent limitation of phylogenetic systematics itself, that is not able to discern between individuals of the same species, generating a terminal for every entry, no matter how closely related they are (even if they comprise individuals representing the same species). This likely results in a lack of incentives, under the newly published Phylocode, to distinguish new *specimens* from new *species* and *genera*, treating those as artificial entities instead of natural kinds and emptying the information retaining value of these taxonomy rankings (Dayrat et al. 2008; Cantino and De Queiroz 2020). Another issue is that the diagnoses of some species heavily rely on characters that may vary intraspecifically. For instance, the diagnosis of *B. albertoi* (Nascimento and Zaher, 2010) includes characters that make subjective assertions on the comparative robustness of structures, like "…*jugal with a triangular and rugose ventrolateral projection in the anterior portion, more ventrally developed than in other Baurusuchidae*", and also refers to structures as topological references such as in "*well-developed ventromedial crest of the quadrate, dividing the descendent body of the quadrate into a medial and an anterior face*". A fan-shaped depression on

the lateral facet of the jugal's anterior ramus is a feature present in all baurusuchid specimens (Montefeltro et al. 2011; Godoy et al. 2014), varying with age and taphonomic distortions, and compared to others there seems to be no objective reason to describe it as being an unique feature, while the latter crest most likely pertains to the quadrate aponeurosis (B' crest sensu Iordansky, 1964), thus universally distributed and prone to be developed in most skeletally mature skulls.

Ultimately, to increase stability of new taxa, diagnosis should concentrate on characters that are less affected by these processes in adult forms, such as the disposition of bone sutures and considerable architectural differences between major structures, like divergences in the pterygoid-choanal complex in baurusuchines and pissarrachampsines, which might be correlated with function (Darlim et al. 2021).

Considering the ontogenetic and morphometric findings presented here, as well as the arguments above, it seems probable that *B.salgadoensis*, *B.albertoi*, *Stratiotosuchus*, and *Aplestosuchus sordidus* might represent not distinct species (and genus), but specimens of *B. pachecoi*, as it takes precedent (Price 1945).

It is also possible that a future revision might result in the merger of *Pissarrachampsa* and *Campinasuchus*, due to their close dimensions, morphological similarity, and collecting site proximity (**Figure 5**). In summary, we recommend a conservative approach towards the erection of new taxa, and anticipate the possibility that a future taxonomic revision might support the invalidation some species that could be assigned either to *Baurusuchus pachecoi* or *Pissarrachampsa sera*, that possess more cohesively distinct characters, as defined by Montefeltro et al. (2011).

## 5. Conclusions

Using geometric morphometrics in two cranial views, including specimens of variable size and age, we have showed that the majority of baurusuchid skulls can be clearly separated into three groupings of adult, juvenile, and younger individuals in a PCA analysis. This does not necessarily mean that clustered holotypic material belong to a single species, given that they share a morphospace, but raises questions about overestimation of diversity and the levels of intraspecific variation within baurusuchidae. Anova analysis and regression of shape *vs.* log centroid size produced very strong to strong statistical support for size-controlled shape variation, robust evidence pointing to an ontogenetic signal. The baurusuchid skull sustained remarkable shape changes, with rostrum development being the most conspicuous and consequential, as it directly relates to predation capabilities and possible niche partitioning.

The size and shape contrast between the holotypes of *Gondwanasuchus* and *Stratiotosuchus*, and their behavior in the data, allows them to be considered as semaphoronts of previously erected species, like *B. pachecoi*, showing that their distinct characters may be reinterpreted as a consequence of growth instead of phylogeny (see chapter III).

The more restricted baurusuchid distribution allied with the high diversity and low disparity pose a geographical and ecological problem that could be explained, at least partially, by intraspecific variations. We advocate a more conservative approach towards their taxonomy, restricting diagnostic characters to fewer variable structures, which might result in a reduction of known baurusuchid diversity, more in line with the current understanding of top-predator ecology.

## 6. Acknowlegments

This study was financed in part by the Coordenação de Aperfeiçoamento de Pessoal de Nível Superior – Brasil (CAPES) – Finance Code 001.

The authors thank CAPES, a brazilian funding agency, for their financial support of DMS, and Dr. Julia Klaczko, of the University of Brasília (UnB), for her support and teachings.

## 7. Conflict of interest

No conflicts of interest were declared.

## References

Adams DC, Collyer M, Kaliontzopoulou A, Sherratt E. 2023. Geomorph: Software for geometric morphometric analyses.

Angulo-Bedoya M, Correa S, Benítez HA. 2019. Unveiling the cryptic morphology and ontogeny of the Colombian Caiman crocodilus: a geometric morphometric approach. Zoomorphology. 138(3):387–397.

Araújo Júnior HI de, Silva Marinho T da. 2013. Taphonomy of a Baurusuchus (Crocodyliformes, Baurusuchidae) from the Adamantina Formation (Upper Cretaceous, Bauru Basin), Brazil: Implications for preservational modes, time resolution and paleoecology. Journal of South American Earth Sciences. 47:90–99. https://doi.org/10.1016/j.jsames.2013.07.006

Arbour JH, Brown CM. 2014. Incomplete specimens in geometric morphometric analyses. Methods in Ecology and Evolution. 5(1):16–26. https://doi.org/10.1111/2041-210X.12128

Baken EK, Collyer ML, Kaliontzopoulou A, Adams DC. 2021. geomorph v4. 0 and gmShiny: Enhanced analytics and a new graphical interface for a comprehensive morphometric experience. Methods in Ecology and Evolution. 12(12):2355–2363.

Balaguera-Reina SA, Vargas-Ramírez M, Ordóñez-Garza N, Hernández-González F, Densmore LD. 2020. Unveiling the mystery: assessing the evolutionary trajectory of the Apaporis caiman population (Caiman crocodilus apaporiensis, Medem

1955) via mitochondrial molecular makers. Biological Journal of the Linnean Society. 131(1):163–171.

Bandeira KLN, Brum AS, Pêgas RV, Cidade GM, Holgado B, Cidade A, de Souza RG. 2018. The Baurusuchidae vs Theropoda record in the Bauru Group (Upper Cretaceous, Brazil): a taphonomic perspective. J Iber Geol. 44(1):25–54. https://doi.org/10.1007/s41513-018-0048-4

Barreto-Lima A, Santos M, Nóbrega Y. 2021. TRATADO DE CROCODILIANOS DO BRASIL. [place unknown].

Batezelli A. 2010. Arcabouço tectono-estratigráfico e evolução das Bacias Caiuá e Bauru no Sudeste brasileiro. Revista Brasileira de Geociências. 40(2):265–285.

Blanco FMV, Cassini GH, Bona P. 2018. Skull ontogeny of extant caimans: a three-dimensional geometric morphometric approach. Zoology. 129:69–81. https://doi.org/10.1016/j.zool.2018.06.003

Boggs S. 2012. Principles of Sedimentology and Stratigraphy. [place unknown]: Pearson Prentice Hall.

Borteiro C, Gutiérrez F, Tedros M, Kolenc F. 2009. Food habits of the Broad-snouted Caiman (Caiman latirostris: Crocodylia, Alligatoridae) in northwestern Uruguay. Studies on Neotropical Fauna and Environment. 44(1):31–36. https://doi.org/10.1080/01650520802507572

Campos DA. 2001. Short note on a new Baurusuchidae (Crocodyliformes, Metasuchia) from the Upper Cretaceous of Brazil. Museu Nacional.

Cantino PD, De Queiroz K. 2020. PhyloCode: a phylogenetic code of biological nomenclature. [place unknown]: CRC Press Boca Raton.

Cardia FMS, Santucci RM, Bernardi JVE, Andrade MB de, Oliveira CEM de. 2018. Mercury concentrations in terrestrial fossil vertebrates from the Bauru Group (Upper Cretaceous), Brazil and implications for vertebrate paleontology. Journal of South American Earth Sciences. 86:15–22. https://doi.org/10.1016/j.jsames.2018.06.006

Carr TD. 2020. A high-resolution growth series of Tyrannosaurus rex obtained from multiple lines of evidence. PeerJ. 8:e9192. https://doi.org/10.7717/peerj.9192

Carr TD, Varricchio DJ, Sedlmayr JC, Roberts EM, Moore JR. 2017. A new tyrannosaur with evidence for anagenesis and crocodile-like facial sensory system. Sci Rep. 7(1):44942. https://doi.org/10.1038/srep44942

Carvalho I de S, Arruda Campos A de C, Henrique Nobre P. 2005. Baurusuchus salgadoensis, a New Crocodylomorpha from the Bauru Basin (Cretaceous), Brazil. Gondwana Research. 8(1):11–30. https://doi.org/10.1016/S1342-937X(05)70259-8

Carvalho IDS, Teixeira VDPA, Ferraz MLDF, Ribeiro LCB, Martinelli AG, Neto FM, Sertich JJW, Cunha GC, Cunha IC, Ferraz PF. 2011. Campinasuchus dinizi gen.

et sp. nov., a new Late Cretaceous baurusuchid (Crocodyliformes) from the Bauru Basin, Brazil. Zootaxa. 2871(1):19–42. https://doi.org/10.11646/zootaxa.2871.1.2

Collyer ML, Adams DC. 2018. RRPP: An r package for fitting linear models to high-dimensional data using residual randomization. Methods in Ecology and Evolution. 9(7):1772–1779.

Darlim G, Carvalho I de S, Tavares SAS, Langer MC. 2021. A new Pissarrachampsinae specimen from the Bauru Basin, Brazil, adds data to the understanding of the Baurusuchidae (Mesoeucrocodylia, Notosuchia) distribution in the Late Cretaceous of South America. Cretaceous Research. 128:104969. https://doi.org/10.1016/j.cretres.2021.104969

Darlim G, Montefeltro FC, Langer MC. 2021. 3D skull modelling and description of a new baurusuchid (Crocodyliformes, Mesoeucrocodylia) from the Late Cretaceous (Bauru Basin) of Brazil. Journal of Anatomy [Internet]. [accessed 2021 Jun 3] n/a(n/a). https://doi.org/10.1111/joa.13442

Dayrat B, Cantino PD, Clarke JA, de Queiroz K. 2008. Species Names in the PhyloCode: The Approach Adopted by the International Society for Phylogenetic Nomenclature. Systematic Biology. 57(3):507–514. https://doi.org/10.1080/10635150802172176

Dodson P. 1975. Functional and ecological significance of relative growth in Alligator. Journal of Zoology. 175(3):315–355. https://doi.org/10.1111/j.1469-7998.1975.tb01405.x

Drumheller SK, Adams TL, Maddox H, Noto CR. 2021. Expanded Sampling Across Ontogeny in <I>Deltasuchus motherali</I> (Neosuchia, Crocodyliformes): Revealing Ecomorphological Niche Partitioning and Appalachian Endemism in Cenomanian Crocodyliforms. Elements of Paleontology [Internet]. [accessed 2023 Jan 19]. https://doi.org/10.1017/9781009042024

Drumheller SK, Wilberg EW. 2020. A synthetic approach for assessing the interplay of form and function in the crocodyliform snout. Zoological Journal of the Linnean Society. 188(2):507–521. https://doi.org/10.1093/zoolinnean/zlz081

Erickson GM, Lappin AK, Vliet KA. 2003. The ontogeny of bite-force performance in American alligator (Alligator mississippiensis). Journal of Zoology. 260(3):317–327. https://doi.org/10.1017/S0952836903003819

Fonseca PHM, Martinelli AG, Marinho T da S, Ribeiro LCB, Schultz CL, Soares MB. 2020. Morphology of the endocranial cavities of Campinasuchus dinizi (Crocodyliformes: Baurusuchidae) from the Upper Cretaceous of Brazil. Geobios. 58:1–16. https://doi.org/10.1016/j.geobios.2019.11.001

Foth C, Bona P, Desojo JB. 2015. Intraspecific variation in the skull morphology of the black caiman Melanosuchus niger (Alligatoridae, Caimaninae). Acta Zoologica. 96(1):1–13. https://doi.org/10.1111/azo.12045

Foth C, Fernandez Blanco MV, Bona P, Scheyer TM. 2018. Cranial shape variation in jacarean caimanines (Crocodylia, Alligatoroidea) and its implications in the taxonomic status of extinct species: The case of *Melanosuchus fisheri*. Journal of Morphology. 279(2):259–273. https://doi.org/10.1002/jmor.20769

Gignac P, O'Brien H. 2016. Suchian Feeding Success at the Interface of Ontogeny and Macroevolution. Integrative and Comparative Biology. 56(3):449–458. https://doi.org/10.1093/icb/icw041

Gignac PM, Erickson GM. 2015. Ontogenetic changes in dental form and tooth pressures facilitate developmental niche shifts in American alligators. Journal of Zoology. 295(2):132–142. https://doi.org/10.1111/jzo.12187

Gignac PM, Erickson GM. 2016. Ontogenetic bite-force modeling of Alligator mississippiensis: implications for dietary transitions in a large-bodied vertebrate and the evolution of crocodylian feeding. Journal of Zoology. 299(4):229–238. https://doi.org/10.1111/jzo.12349

Godoy PL, Ferreira GS, Montefeltro FC, Nova BCV, Butler RJ, Langer MC. 2018. Evidence for heterochrony in the cranial evolution of fossil crocodyliforms. Palaeontology. 61(4):543–558. https://doi.org/10.1111/pala.12354

Godoy PL, Montefeltro FC, Norell MA, Langer MC. 2014. An Additional Baurusuchid from the Cretaceous of Brazil with Evidence of Interspecific Predation among Crocodyliformes. PLOS ONE. 9(5):e97138. https://doi.org/10.1371/journal.pone.0097138

Gould SJ. 1966. Allometry and size in ontogeny and phylogeny. Biol Rev Camb Philos Soc. 41(4):587–640. https://doi.org/10.1111/j.1469-185x.1966.tb01624.x

Griffin CT, Stocker MR, Colleary C, Stefanic CM, Lessner EJ, Riegler M, Formoso K, Koeller K, Nesbitt SJ. 2021. Assessing ontogenetic maturity in extinct saurian reptiles. Biological Reviews. 96(2):470–525. https://doi.org/10.1111/brv.12666

Grigg G. 2015. Biology and Evolution of Crocodylians. [place unknown]: Csiro Publishing.

Gunz P, Mitteroecker P, Neubauer S, Weber GW, Bookstein FL. 2009. Principles for the virtual reconstruction of hominin crania. Journal of Human Evolution. 57(1):48–62. https://doi.org/10.1016/j.jhevol.2009.04.004

Hayward MW, Slotow R. 2009. Temporal partitioning of activity in large African carnivores : tests of multiple hypotheses : research article. South African Journal of Wildlife Research. 39(2):109–125. https://doi.org/10.10520/EJC117325

Hekkala E, Shirley MH, Amato G, Austin JD, Charter S, Thorbjarnarson J, Vliet KA, Houck ML, Desalle ROB, Blum MJ. 2011. An ancient icon reveals new mysteries: mummy DNA resurrects a cryptic species within the Nile crocodile. Molecular ecology. 20(20):4199–4215.

Holliday CM, Porter WR, Vliet KA, Witmer LM. 2020. The Frontoparietal Fossa and Dorsotemporal Fenestra of Archosaurs and Their Significance for Interpretations

of Vascular and Muscular Anatomy in Dinosaurs. The Anatomical Record. 303(4):1060–1074. https://doi.org/10.1002/ar.24218

Horner JR, Goodwin MB. 2006. Major cranial changes during Triceratops ontogeny. Proceedings of the Royal Society B: Biological Sciences. 273(1602):2757–2761. https://doi.org/10.1098/rspb.2006.3643

Horner JR, Goodwin MB. 2009. Extreme Cranial Ontogeny in the Upper Cretaceous Dinosaur Pachycephalosaurus. PLOS ONE. 4(10):e7626. https://doi.org/10.1371/journal.pone.0007626

Iordansky NN. 1964. The jaw muscles of the crocodiles and some relating structures of the crocodilian skull. Anatomischer Anzeiger [Internet]. [accessed 2023 Mar 2] 115. https://pubmed.ncbi.nlm.nih.gov/14327484/

Macarthur RH, Wilson EO. 1967. The Theory of Island Biogeography [Internet]. REV-Revised. [place unknown]: Princeton University Press; [accessed 2023 Jan 19]. https://www.jstor.org/stable/j.ctt19cc1t2

Mariani TF, Romano PSR. 2017. Intra-specific variation and allometry of the skull of Late Cretaceous side-necked turtle Bauruemys elegans (Pleurodira, Podocnemididae) and how to deal with morphometric data in fossil vertebrates. PeerJ. 5:e2890. https://doi.org/10.7717/peerj.2890

Marinho T da S, Iori FV, Carvalho I de S, de Vasconcellos FM. 2013. Gondwanasuchus scabrosus gen. et sp. nov., a new terrestrial predatory crocodyliform (Mesoeucrocodylia: Baurusuchidae) from the Late Cretaceous Bauru Basin of Brazil. Cretaceous Research. 44:104–111. https://doi.org/10.1016/j.cretres.2013.03.010

Marsola JC de A, Batezelli A, Montefeltro FC, Grellet-Tinner G, Langer MC. 2016. Palaeoenvironmental characterization of a crocodilian nesting site from the Late Cretaceous of Brazil and the evolution of crocodyliform nesting strategies. Palaeogeography, Palaeoclimatology, Palaeoecology. 457:221–232. https://doi.org/10.1016/j.palaeo.2016.06.020

Martinelli AG, Pais DF. 2008. A new baurusuchid crocodyliform (Archosauria) from the Late Cretaceous of Patagonia (Argentina). Comptes Rendus Palevol. 7(6):371–381. https://doi.org/10.1016/j.crpv.2008.05.002

Martins KC, Queiroz MV, Ruiz JV, Langer MC, Montefeltro FC. 2023. A new Baurusuchidae (Notosuchia, Crocodyliformes) from the Adamantina Formation (Bauru Group, Upper Cretaceous), with a revised phylogenetic analysis of Baurusuchia. Cretaceous Research.:105680. https://doi.org/10.1016/j.cretres.2023.105680

Montefeltro FC, Larsson HCE, Langer MC. 2011. A New Baurusuchid (Crocodyliformes, Mesoeucrocodylia) from the Late Cretaceous of Brazil and the Phylogeny of Baurusuchidae. PLOS ONE. 6(7):e21916. https://doi.org/10.1371/journal.pone.0021916

Murray CM, Russo P, Zorrilla A, McMahan CD. 2019. Divergent morphology among populations of the New Guinea crocodile, Crocodylus novaeguineae (Schmidt, 1928): diagnosis of an independent lineage and description of a new species. Copeia. 107(3):517–523.

Nascimento PM, Zaher H. 2010. A new species of Baurusuchus (Crocodyliformes, Mesoeucrocodylia) from the Upper Cretaceous of Brazil, with the first complete postcranial skeleton described for the family Baurusuchidae. Papéis Avulsos de Zoologia. 50(21):323–361. https://doi.org/10.1590/S0031-10492010002100001

Oliveira CEM, Santucci RM, Andrade MB, Fulfaro VJ, Basílio J a. F, Benton MJ. 2011. Crocodylomorph eggs and eggshells from the Adamantina Formation (Bauru Group), Upper Cretaceous of Brazil. Palaeontology. 54(2):309–321. https://doi.org/10.1111/j.1475-4983.2010.01028.x

Oliveira FA de, Santucci RM, Oliveira CEM de, Andrade MB de. 2021. Morphological and compositional analyses of coprolites from the Upper Cretaceous Bauru Group reveal dietary habits of notosuchian fauna. Lethaia [Internet]. [accessed 2021 Jun 28]. https://doi.org/10.1111/let.12431

Price. 1945. A new reptile from the Cretaceous of Brazil. Rio de Janeiro, Departamento Nacional da Produção Mineral, Notas preliminares e estudos. Boletim 25.

Rhoads BL. 2020. River dynamics: geomorphology to support management. [place unknown]: Cambridge University Press.

Riff D, Kellner AWA. 2011. Baurusuchid crocodyliforms as theropod mimics: clues from the skull and appendicular morphology of Stratiotosuchus maxhechti (Upper Cretaceous of Brazil). Zoological Journal of the Linnean Society. 163(suppl_1):S37–S56. https://doi.org/10.1111/j.1096-3642.2011.00713.x

Roberto IJ, Bittencourt PS, Hernández-Rangel SM. 2021. Taxonomia e biologia geral dos crocodilianos do Brasil. Tratado de Crocodilianos do Brasil.:60–93.

Rohlf FJ, Corti M. 2000. Use of two-block partial least-squares to study covariation in shape. Systematic biology. 49(4):740–753.

Rohlf FJ, Slice D. 1990. Extensions of the Procrustes method for the optimal superimposition of landmarks. Systematic zoology. 39(1):40–59.

Salas-Gismondi R, Flynn JJ, Baby P, Tejada-Lara JV, Wesselingh FP, Antoine P-O. 2015. A Miocene hyperdiverse crocodylian community reveals peculiar trophic dynamics in proto-Amazonian mega-wetlands. Proceedings of the Royal Society B: Biological Sciences. 282(1804):20142490. https://doi.org/10.1098/rspb.2014.2490

dos Santos D, Santucci R, Andrade M, Oliveira CEM. 2021. A baurusuchid yearling (Mesoeucrocodylia, Crocodyliformes), from the Adamantina Formation, Bauru Group, Upper Cretaceous of Brazil. Historical Biology. https://doi.org/10.1080/08912963.2021.2001807

Scannella JB, Horner JR. 2010. Torosaurus Marsh, 1891, is Triceratops Marsh, 1889 (Ceratopsidae: Chasmosaurinae): synonymy through ontogeny. Journal of Vertebrate Paleontology. 30(4):1157–1168. https://doi.org/10.1080/02724634.2010.483632

Schmitz A, Mansfeld P, Hekkala E, Shine T, Nickel H, Amato G, Böhme W. 2003. Molecular evidence for species level divergence in African Nile Crocodiles Crocodylus niloticus (Laurenti, 1786). Comptes Rendus Palevol. 2(8):703–712. https://doi.org/10.1016/j.crpv.2003.07.002

Schuurman F, Kleinhans MG. 2015. Bar dynamics and bifurcation evolution in a modelled braided sand-bed river. Earth Surface Processes and Landforms. 40(10):1318–1333. https://doi.org/10.1002/esp.3722

Shirley MH, Carr AN, Nestler JH, Vliet KA, Brochu CA. 2018. Systematic revision of the living African slender-snouted crocodiles (Mecistops Gray, 1844). Zootaxa. 4504(2):151–193.

Sogbohossou EA, Kassa BD, Waltert M, Khorozyan I. 2017. Spatio-temporal niche partitioning between the African lion (Panthera leo leo) and spotted hyena (Crocuta crocuta) in western African savannas. Eur J Wildl Res. 64(1):1. https://doi.org/10.1007/s10344-017-1159-5

Souza RG, Cidade GM, Campos DDA, Riff D. 2016. New crocodylian remains from the Solimões Formation (lower Eocene–Pliocene), State of Acre, Southwestern Brazilian Amazonia. Rev bras paleontol. 19(2):217–232. https://doi.org/10.4072/rbp.2016.2.06

Staniewicz A, Behler N, Darmansyah S, Jones G. 2018. Niche partitioning between juvenile sympatric crocodilians in Mesangat Lake, East Kalimantan, Indonesia. The Raffles Bulletin of Zoology. 66:528–537.

Tucker AD, Limpus CJ, McCallum HI, McDonald KR. 1996. Ontogenetic Dietary Partitioning by Crocodylus johnstoni during the Dry Season. Copeia. 1996(4):978–988. https://doi.org/10.2307/1447661

Van Valkenburgh B, Wayne RK. 1994. Shape Divergence Associated with Size Convergence in Sympatric East African Jackals. Ecology. 75(6):1567–1581. https://doi.org/10.2307/1939618

Vasconcellos F, Carvalho IS. 2010. Paleoichnological assemblage associated with Baurusuchus salgadoensis remains, a Baurusuchidae Mesoeucrocodylia from the Bauru Basin, Brazil (Late Cretaceous). New Mexico Museum of Natural History and Science Bulletin [Internet]. [accessed 2021 Jul 6] 51. https://www.semanticscholar.org/paper/PALEOICHNOLOGICAL-ASSEMBLAGE-ASSOCIATED-WITH-%2C-A-%2C-Vasconcellos-Carvalho/17496caef24e65fe4344fe06523224aec37a07bd

Vieira LG, Santos ALQ, Hirano LQL, Menezes-Reis LT, Mendonça JS, Sebben A. 2018. Ontogeny of the skull of the Black Caiman (Melanosuchus niger) (Crocodylia: Alligatoridae). Canadian Journal of Zoology [Internet]. [accessed 2021 Feb 14]. https://doi.org/10.1139/cjz-2018-0076

Watanabe A, Slice DE. 2014. The utility of cranial ontogeny for phylogenetic inference: a case study in crocodylians using geometric morphometrics. Journal of Evolutionary Biology. 27(6):1078–1092. https://doi.org/10.1111/jeb.12382

Wilson JA, Malkani MS, Gingerich PD. 2001. NEW CROCODYLIFORM (REPTILIA, MESOEUCROCODYLIA) FROM THE UPPER CRETACEOUS PAB FORMATION OF VITAKRI, BALOCHISTAN (PAKISTAN). Contributions from the Museum of Paleontology.

Woodward AS. 1896. On two mesozoic crocodilians Notosuchus (genus novum) and Cynodontosuchus (genus novum) from the red sandstones of the territ ory of Neuquen (Argentine republic)= Sobre dos cocodrilos mesozoicos Notosuchus (genus novum) y Cynodontosuchus (genus novum) de las areniscas rojas del territorio del Neuquen (República Argentina). (No Title).

Woodward HN, Tremaine K, Williams SA, Zanno LE, Horner JR, Myhrvold N. 2020. Growing up Tyrannosaurus rex: Osteohistology refutes the pygmy “Nanotyrannus” and supports ontogenetic niche partitioning in juvenile Tyrannosaurus. Science Advances. 6(1):eaax6250. https://doi.org/10.1126/sciadv.aax6250

Young MT, Bell MA, De Andrade MB, Brusatte SL. 2011. Body size estimation and evolution in metriorhynchid crocodylomorphs: implications for species diversification and niche partitioning. Zoological Journal of the Linnean Society. 163(4):1199–1216.

## Supplemental information (chapter IV)

Here we provide, for both vistas: (1) Procrustes analyses; (2) PLS analyses graphs and (3) raw statistical data for regression scores.

Lateral

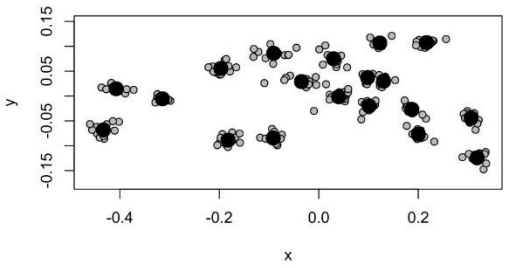


**Analysis of Variance, using Residual Randomization**
**Permutation procedure: Randomization of null model residuals**
**Number of permutations: 1000**
**Estimation method: Ordinary Least Squares**
**Sums of Squares and Cross-products: Type I**
**Effect sizes (Z) based on F distributions**

| | Df | SS | MS | Rsq | F | Z | Pr(>F) | |
|---|---|---|---|---|---|---|---|---|
| log(Csize) | 1 | 0.034301 | 0.034301 | 0.39571 | 7.8579 | 2.6789 | 0.002 | ** |
| Residuals | 12 | 0.052382 | 0.004365 | 0.60429 | | | | |
| Total | 13 | 0.086683 | | | | | | |

**---**
**Signif. codes: 0 '***' 0.001 '**' 0.01 '*' 0.05 '.' 0.1 ' ' 1**

**PLS1 Plot: Block 1 (X) vs. Block 2 (Y)**

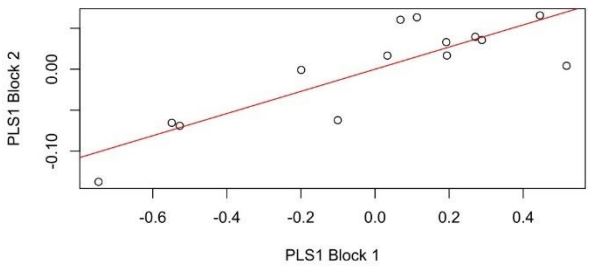


**r-PLS: 0.842**

**Effect Size (Z): 2.0614**

**P-value: 0.011**

**Based on 1000 random permutations**

Dorsal

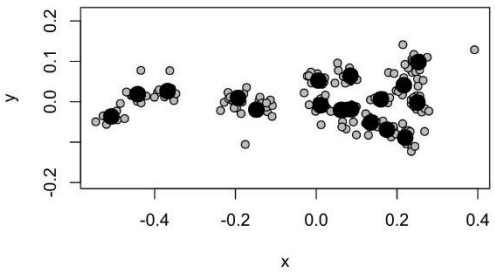


**Analysis of Variance, using Residual Randomization**
**Permutation procedure: Randomization of null model residuals**
**Number of permutations: 1000**
**Estimation method: Ordinary Least Squares**
**Sums of Squares and Cross-products: Type I**
**Effect sizes (Z) based on F distributions**

| | Df | SS | MS | Rsq | F | Z | Pr(>F) | |
|---|---|---|---|---|---|---|---|---|
| log(Csize) | 1 | 0.043714 | 0.043714 | 0.24495 | 3.5686 | 2.0416 | 0.021 | * |
| Residuals | 11 | 0.134748 | 0.012250 | 0.75505 | | | | |
| Total | 12 | 0.178462 | | | | | | |

**---**
**Signif. codes: 0 '***' 0.001 '**' 0.01 '*' 0.05 '.' 0.1 ' ' 1**

**PLS1 Plot: Block 1 (X) vs. Block 2 (Y)**

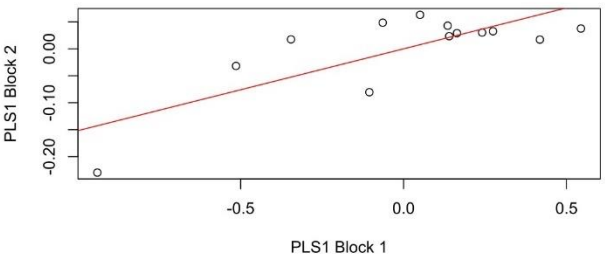


**r-PLS: 0.77**

**Effect Size (Z): 1.6912**

**P-value: 0.043**

**Based on 1000 random permutations**

# APÊNDICE

**Santos et al., 2022. A baurusuchid yearling (Mesoeucrocodylia, Crocodyliformes), from the Adamantina Formation, Bauru Group, Upper Cretaceous of Brazil. *Historical Biology*, *34*(11), pp.2137-2151.**

Historical Biology

An International Journal of Paleobiology

ISSN: (Print) (Online) Journal homepage: https://www.tandfonline.com/loi/ghbi20

# A baurusuchid yearling (Mesoeucrocodylia, Crocodyliformes), from the Adamantina Formation, Bauru Group, Upper Cretaceous of Brazil

**Daniel Martins dos Santos, Rodrigo Miloni Santucci, Carlos Eduardo Maia de Oliveira & Marco Brandalise de Andrade**

**To cite this article:** Daniel Martins dos Santos, Rodrigo Miloni Santucci, Carlos Eduardo Maia de Oliveira & Marco Brandalise de Andrade (2021): A baurusuchid yearling (Mesoeucrocodylia, Crocodyliformes), from the Adamantina Formation, Bauru Group, Upper Cretaceous of Brazil, Historical Biology, DOI: 10.1080/08912963.2021.2001807

**To link to this article:** https://doi.org/10.1080/08912963.2021.2001807

Published online: 19 Dec 2021.

HISTORICAL BIOLOGY
https://doi.org/10.1080/08912963.2021.2001807

Taylor & Francis
Taylor & Francis Group



# A baurusuchid yearling (Mesoeucrocodylia, Crocodyliformes), from the Adamantina Formation, Bauru Group, Upper Cretaceous of Brazil

Daniel Martins dos Santos[a], Rodrigo Miloni Santucci[b], Carlos Eduardo Maia de Oliveira[c] and Marco Brandalise de Andrade[d]

[a]Zoology Graduate Program, Institute of Biological Sciences, University of Brasília, Brasília, Brazil; [b]University of Brasília, Planaltina Campus (FUP), Brasília, Brazil; [c]Federal Institute of Education, Science and Technology of São Paulo, Votuporanga Campus (IFSP), Votuporanga, Brazil; [d]Pontifical Catholic University of Rio Grande do Sul, Porto Alegre, Brazil

**ABSTRACT**

Occurrences of young and immature individuals, relatively rare in the fossil record, are important due to the great amount of morphological and evolutionary information they reveal about a lineage's development. Although crocodylomorphs are the most abundant terrestrial vertebrates found in the Bauru Basin, south-eastern Brazil, even outnumbering dinosaurian materials, much remains to be understood about their anatomy, ecology, and ontogeny. Egg fragments, nests and nesting sites attributed to *Baurusuchus* have been previously described, but unfortunately none of these yielded embryonic or hatchling remains. Here, we describe, for the first time, skeletal material of a small notosuchian yearling, recovered from the Adamantina Formation, with osteological features consistent with a baurusuchid affinity. We provide and discuss osteological and histological evidence of its ontogenetic stage, revealing morphological characters distinct from most adult forms, including conspicuous centro-parapophyseal laminae and developed ventral keels. Computerised tomography data also allowed for the identification of incipient ossification and a novel ontogenetic feature in the diminishing volume of the frontal´s internal recesses. Similar materials will increase our understanding of notosuchian ontogeny and diversity, thus requiring growth characters to be integrated into future phylogenies.

**ARTICLE HISTORY**
Received 9 September 2021
Accepted 31 October 2021

**KEYWORDS**
Crocodylomorpha; notosuchia; baurusuchidae; ontogeny; Bauru Group

## Introduction

The notosuchian clade of mesoeucrocodylian crocodyliforms, originally erected by Gasparini (1971) to encompass terrestrial forms from Gondwana (*Notosuchus, Sphagesaurus, Uruguaysuchus* and *Araripesuchus*), now includes a myriad of taxa (Pol and Leardi 2015), with distinct diet specialisations including herbivory (Buckley et al. 2000; Pol 2003; Oliveira et al. 2021), carnivory (Riff and Kellner 2011; Montefeltro et al. 2020), as well as taxa bearing an extensive cover of ornate dermal shields (e.g., Marinho and Carvalho 2009; Hill 2010). The Upper Cretaceous Bauru Basin in southeastern Brazil is particularly rich in notosuchians of different clades, with an ever-growing list of described species (e.g., Price 1945, 1950, 1955; Carvalho and Bertini 1999; Nobre and de Carvalho 2006; Marinho and Carvalho 2009; Riff et al. 2012; Pol et al. 2014; Martinelli et al. 2018; Darlim et al. 2021). Its fossil record is unusual due to the occurrence of several sympatric, high-tier predators, including nine species of baurusuchids (Price 1945; Campos et al. 2001; Carvalho et al. 2005; Nascimento and Zaher 2010; Montefeltro et al. 2011; Carvalho et al. 2011; Marinho et al. 2013; Godoy et al. 2014; Darlim et al. 2021) which are one of the most abundant fossil materials found in the basin. Regardless of the abundance of specimens, few notosuchians have had their postcranial skeletons described in detail (Riff 2003; Riff and Kellner 2011; Nobre and de Carvalho 2013; Godoy et al. 2016; Cotts et al. 2017; Martinelli et al. 2018; Cunha et al. 2020), fewer still have been the works dedicated to material of different ontogenetic stages, despite some authors identifying juvenile characteristics on published specimens (Geroto and Bertini 2012; Marinho et al. 2013; Godoy et al. 2018; Martinelli et al. 2018).

The discovery and description of extensive fossil eggs and nesting sites attributed to *Baurusuchus* (see Oliveira et al. 2011) brought new information regarding site fidelity in Crocodylomorpha and egg ultrastructure, but unfortunately no embryos were recovered and no notosuchian early-stage younglings have been found. Here, we present the osteology of a baurusuchid yearling, collected around the Fernandópolis region (Adamantina Formation), State of São Paulo, Brazil. This specimen is the youngest notosuchian individual described so far and its ontogenetic stage was inferred from both osteological cues and histological data, helping to bridge the vast morphological and developmental gaps between hatchling individuals and the adult forms described in past years. Early stage crocodyliform semaphoronts are known from Palaeocene (Tongue River Formation) and Eocene (Green River Formation) deposits of North America (Erickson 1976; Langston and Rose 1978), however, these were neosuchian mesoeucrocodylians, and similar notosuchian cases of such young individuals are absent in the literature.

Although present, juvenile crocodylomorph individuals are rare in the Brazilian fossil record, and none of the known specimens are considered yearlings (Salisbury et al. 2003; Figueiredo and Kellner 2009; Geroto and Bertini 2012; Godoy et al. 2018). Nevertheless, semaphoronts comprise an important

**CONTACT** Daniel Martins dos Santos danielmartinsantos@hotmail.com Zoology Graduate Program, Institute of Biological Sciences, University of Brasília, Brasília-DF, Brazil



Published online 19 Dec 2021

supply of information that contribute not only to a more comprehensive understanding of the growth series of a species but also improve our grasp on the true diversity of fossil taxa, even clarifying longstanding controversies (e.g., Horner and Goodwin 2009; Carr 2020).

## Anatomical abbreviations

**ar**, anterior ramus; **cb**, cortical bone; **cc**, *crista cranii*; **cct**, criss-cross texture. **cf**, cranial fragment; **cpl**, centro-parapophyseal lamina; **cv**, cervical vertebra; **dr**, dorsal ribs; **dv**, dorsal vertebrae; **el**, endosteal lamellae; **fae**, *facies articularis externa*; **fr**, frontal bone; **frre**, *repli frontals*; **gl**, glenoid; **hy**, hypapophysis; **ioc**, infraorbital crest; **j**, jugal bone; **ldc**, lateral depression of centra; **lk**, longitudinal keel; **mc**, medullary cavity; **mr**, medial recess; **na**, neural arch; **ncs**, neurocentral suture; **nvf**, neurovascular foramen; **ot**, olfactory tract; **p**, parietal bone; **pa**, parapophysis; **pb**, postorbital bar; **pc**, posterior concavity of scapula; **pfb**, parallel-fibred bone; **pl**, *pars laterale*; **pm**, *pars mediale*; **po**, primary osteons; **pob**, postorbital bone; **pp**, palpebral; **pr**, posterior ramus of jugal; **prz**, prezygapophysis; **s**, scapular bone; **sb**, scapular blade; **sbt**, scapular butress; **sc**, sagittal crest; **scf**, sagittal crest of frontal; **so**, supraoccipital bone; **sq**, squamosal bone; **ss**, scapular shaft; **stf**, supratemporal fenestra; **vk**, ventral keel; **wfb**, woven-fibred bone.

## Institution abbreviations

**IFSP-VTP** – Federal Institute of Education, Science and Technology of São Paulo, Votuporanga Campus. **UFRJ-DG** – Federal University of Rio de Janeiro, Department of Geosciences.

## Geological setting

The Bauru Basin (Figure 1) is an Upper Cretaceous sedimentary sequence deposited mostly over the central and southeastern part of Brazil, covering the states of Goiás, Mato Grosso, Mato Grosso do Sul, Minas Gerais, São Paulo, and Paraná, with an estimated area of 370.000 km$^2$ (Fernandes 2004). Its genesis is commonly associated with the massive basaltic lava flows that produced the Serra Geral Formation during the early opening stages of the Atlantic Ocean (Schobbenhaus and Brito Neves 2003), generating a crust depression onto which the sequence was deposited (Fernandes and Coimbra 2000; Fernandes 2004).

The main stratigraphic subdivision for the Bauru Basin is the one between the Caiuá and Bauru Groups, with the former most likely representing red beds deposited under desert-like conditions, composed of the Rio Paraná, Goio Erê, and Santo Anastácio formations, while the most widely adopted division for the latter includes the Araçatuba, Adamantina, Uberaba, and Marília Formations (Fernandes and Coimbra 1996; Batezelli 2010). The Bauru Group depositional system started with the accommodation of thinly laminated pelitic rocks of the Araçatuba lacustrine environments (Batezelli et al. 1999), progressively obliterated upwards through the rock succession by the braided fluvial sand deposits of the Adamantina Formation (Batezelli 2010). The younger Marília and the local Uberaba Formations, with their basal conglomerates followed by sandstones, would then represent higher-energy alluvial fan deposits (Soares et al. 1980).

Several age estimates based on distinct techniques have yielded different, but somewhat overlapping, age intervals for the Bauru Group. Goldberg and Garcia (2000) estimated a Coniacian-Campanian deposition age for the sequence, while Bertini (1993) and Dias-Brito et al. (2001), making use of the vertebrate, microfossil and charophyte assemblages, inferred a Maastrichtian age for

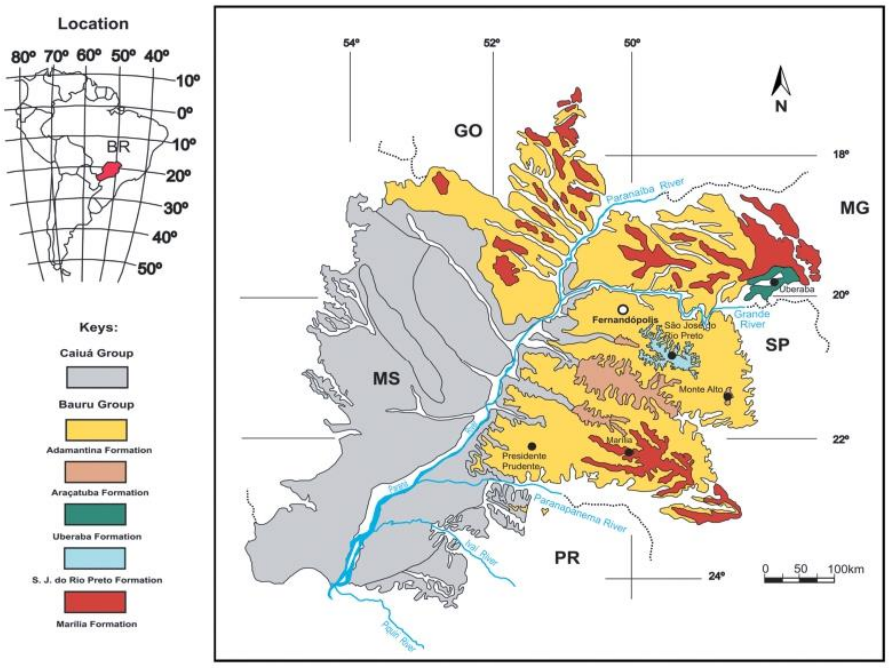


Figure 1. Geographical locality of the Bauru Basin within South America and its geological map. Stratigraphic units are colour coded. Fossil recovery locality is highlighted in white.

**Table 1.** List of taxa selected for osteological comparisons, their respective sources and original descriptions.

| Taxon | Source |
|---|---|
| *Baurusuchus salgadoensis* | Carvalho et al. (2005) |
| *Baurusuchus albertoi* | Nascimento and Zaher (2010) |
| *Caipirasuchus paulistanus* | Iori et al. (2016) |
| *Caipirasuchus mineirus* | Martinelli et al. (2018) |
| *Campinasuchus dinizi* | Cotts et al. (2016) |
| *Mariliasuchus amarali* | Nobre and de Carvalho (2013) |
| *Melanosuchus niger* | Vieira et al. 2018a,b) |
| *Notosuchus terrestris* | Pol (2005); Fiorelli and Calvo (2008) |
| *Pissarrachampsa sera* | Godoy et al. (2016) |
| *Sebecus icaeorhinus* | Pol et al. (2012) |
| *Simosuchus clarki* | Georgi and Krause (2010); Sertich and Groenke (2010) |
| *Stratiotosuchus maxcheti* | Riff (2007); Riff and Kellner (2011) |
| *Yacarerani boliviensis* | Pol et al. (2015) |

the Marília Formation. Recent efforts to obtain radioisotopic ages for the Bauru Group have been successful, with ages placing them between the Campanian and Maastrichtian (Castro et al. 2018; Dias et al. 2021). The young individual described here was found in sandstone outcrops attributed to the Adamantina Formation, near the municipality of Fernandópolis, in the State of São Paulo (Figure 1). This unit is the sole horizon known to yield baurusuchid remains (Campos et al. ; Carvalho et al. 2005; Nascimento and Zaher 2010; Riff and Kellner 2011; Godoy et al. 2014).

## Materials and methods

The osteological nomenclature for the axial skeleton followed the work of Wilson (1999) and Georgi and Krause (2010). Montefeltro (2019) was used as reference for nomenclature on osteoderm morphology. A list of taxa selected for osteological comparisons is presented in the table below (Table 1). These include adult baurusuchids in addition to small-bodied ziphosuchians and a modern juvenile caimanine (*Melanosuchus niger*) with skeletal elements of similar size to the specimen herein described. Specimens of *Baurusuchus salgadoensis, Baurusuchus albertoi, Caipirasuchus paulistanus*, and *Mariliasuchus amarali* were first-hand examined by the authors. Information on other taxa was extracted from the literature.

The fossil specimen herein described – IFSP-VTP/PALEO 0004 – was recovered in the field still mostly embedded in sediment, along with other fossil occurrences and sedimentary samples. In order to fully assess the preservation state and morphology, the material was scanned at IMEB (Imagens Médicas Brasília-DF) with a Revolution EVO model, yielding 511 slices (0.5 mm each, 512 × 512 pixels, 140 kv and 240 mA). The CT data was processed using the open-source medical software *InVesalius* (Amorim et al. 2015), developed by the Renato Archer Information Technology Center. Tomographic images of previously studied specimens (baurusuchids) were used for comparison (FUP-Pv 000020 and IFSP-VTP/PALEO-0003, see Dumont Jr et al. 2020, Figure 1, p. 4). A histological slide of a fragmentary long bone was prepared to evaluate the age of the animal before death, following the protocols described in Padian and Lamn (2013).

## Results

### Systematic palaeontology

CROCODYLOMORPHA Walker and Westoll (1970)
CROCODYLIFORMES Hay (1930)
MESOEUCROCODYLIA Whetstone and Whybrow (1983)
NOTOSUCHIA de Gasparini (1971) sensu Ruiz et al. (2021)
BAURUSUCHIDAE Price (1945) sensu Darlim et al. (2021)
**IFSP-VTP/PALEO 0004**

### Referred specimen and repository

The vertebrate palaeontology collection of the Federal Institute of Education, Science and Technology of São Paulo in Votuporanga (IFSP-VTP), was the chosen locality to house the specimen. It was thus assigned a corresponding identifier: IFSP-VTP/PALEO 0004. It consists of both cranial fragments and postcranial material.

### Locality and horizon

The material was discovered near the city of Fernandópolis, State of São Paulo, in a mostly horizontal outcrop exposure comprised of reddish, massive, fine to medium-grained sandstones, characterised by root marks, invertebrate burrows and, more rarely, egg clutches (see Cunha et al. 2020 for a more detailed description). Most importantly, it was found in close association with the second specimen of *Armadillosuchus* Marinho and Carvalho (2009), recently described by Cunha et al. (2020), in the same horizon of the fluvial sandstones of the Adamantina Formation, Upper Cretaceous (Campanian – Maastrichtian) of the Bauru Basin.

### Osteological description

IFSP-VTP/PALEO 0004 specimen consists of the following elements: a fragmented skull, represented by skull-roof elements, including a partial parietal-frontal complex, a jugal and putative palate fragment, an almost complete cervical series, composed of six postaxial vertebrae, along with eight partially preserved dorsal vertebrae, articulated rib fragments and an osteoderm (Figure 2 (a–c)). Additional material is scattered around the main elements, and most are too fragmentary to be properly identified. Despite being broken or fractured, most likely by erosional dynamics, the bones still retain their original textures.

Surprisingly, the cervical and the anterior sequence of thoracic vertebrae were found still articulated and close to cranial remains, indicating that the carcase was not submitted to extensive transport. The CT images of the block allowed the observation of a putative 'death mask', marked by a distinct density change between the sandstone immediately surrounding the small carcase and the remaining block (Figure 2b$_1$). These images also reveal reworking of the sediment by invertebrates, as indicated by intense bioturbation, with conspicuous tubular perforations preserved (Figure 2b$_1$).

### Fragmented cranial elements

Unfortunately, the articulated pattern into which the vertebral centra were fossilised did not extend to the cranial region of the skeleton, being preserved as several fragmented skull bones, and dispersed into a small area around the cervical series. The fragmentary and indistinguishable aspect of some pieces hindered a correct identification of their original position and nature, while others less damaged and more complete, were either confidently recognised as major elements composing the skull roof or interpreted as elements composing the cheek region of this specimen (Figure 3). Nevertheless, we provide three-dimensional reconstructions of unidentified elements (Figure 3c$_1$-c$_2$). The following description focuses on the identifiable cranial fragments and their most distinct morphological features.

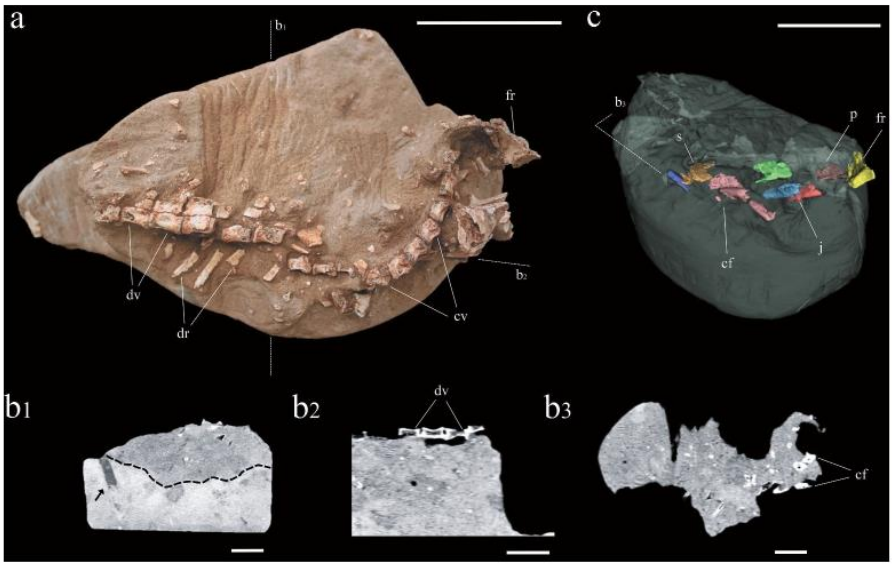


**Figure 2.** Photograph of IFSP-VTP/PALEO-0004 specimen and additional CT images showing both the structure of surrounding sediment and the three-dimensional reconstruction of cranial fragments. a) – Whole-block view of the prepared skeleton highlighting disposition of cranial and postcranial material. $b_1$ - $b_3$) – CT frames, from left to right, in axial, sagittal and axial cross-sections, respectively. Image $b_1$ reveals the presence of vertical bioturbations, indicated by the dark arrow, as well as a distinct density difference between the sediment adjacent to the skeleton and the overall block. The poorly ossified dorsal vertebral centra are visible in image $b_2$ and the fragmented nature of the cranial bones is shown in $b_3$. c) – Close-up view of segmented cranial and appendicular fragments, some of which are identified. Scale bars: a = 5 cm; b = 1 cm; c = 5 cm.

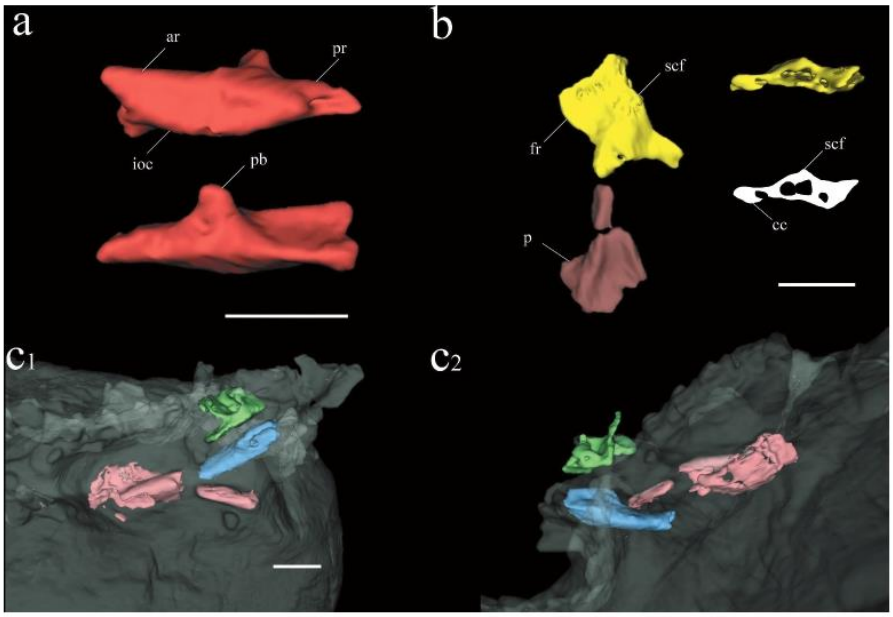


**Figure 3.** Three-dimensional reconstruction of cranial fragments. a) – Left jugal bone in lateral (above) and medial (below) views, highlighting a dorsoventral expansion of the anterior ramus. b) – Frontal-parietal in dorsal view and oblique cross-section of the frontal exposing internal recesses. $c_1$-$c_{2)}$ – Unidentified cranial bones shown in two distinct perspectives. All scale bars = 1 cm.

***Jugal.*** One of the largest cranial bones preserved possesses a triradial profile and due to its shape and proximity to other cranial elements, was thus identified as the left jugal (Figure 3(a)). It is somewhat triangular in lateral view, with a convex dorsal margin and a concave ventral one. The medial surface is smooth, with a shallow depression anteriorly. Its anterior ramus is incomplete but is clearly marked by a dorsoventral expansion and a crest that runs anteroposteriorly, reaching the posterior ramus. Ventral to this crest, an incipient depression develops. The posterior ramus tapers to a tubular aspect as it progresses posteriorly though it is also not complete. Roughly at mid-length, there is an ascending dorsomedial process interpreted here to represent the jugal contribution to

the postorbital bar. As in adult crocodyliform specimens, it marks the transition between the anterior and posterior jugal ramus. Interestingly, the tomography images revealed a high level of pneumatization, with a neurovascular foramen running its length and connecting the anterior and posterior rami. Similar features are also observed in crocodyliforms of larger size, with a major jugal foramen dominating the posterior ramus, reaching anteriorly, and emerging at the lateral surface as a small vascular foramina.

***Frontal.*** This is a single bone that makes up the anterior portion of the skull roof and is herein characterised by a trapezoidal shape in dorsal view, being narrow anteriorly and transversely expanded posteriorly, in addition to being dorsoventrally flattened (Figure 3(b)). The right anterolateral portion has been broken off at an oblique angle, close to a transverse cross-section through the bone, exposing a series of small cavities that mark the internal structure of the bone. It is also marked by a sagittal crest running medially along its dorsal surface. This crest does not reach the parietal, tapering posteriorly before it reaches their contact, and, due to the fracturing mentioned above, it is not possible to determine how far it extended anteriorly.

In anterior view, one can observe the frontal to be roughly symmetrical, both sides adjacent to the sagittal crest equally matched, their dorsal surface slightly concave, and the apical region of the latter moderately sharp. The anterolateral margins of the frontal are flat and ventromedially inclined, most likely forming the dorsal border of the orbits and serving as a platform for the attachment of the palpebrals. A small and ovate element, with incipient sculpturing, found next to the parietals (Figure 7$b_1$-$b_2$), is morphologically consistent with it being one of the posterior palpebrals, most likely being dislocated posteriorly by taphonomic processes. The posterior region of the frontal decreases in width as it approaches the frontal-parietal contact, which is transversely placed. The contact region has an incipient sculpturing pattern on its surface, marked by small, anteroposteriorly directed striations that continue on to the anterior portion of the parietal dorsal surface. The posterolateral margins, which delineate the supratemporal fenestrae, are not well preserved, having an irregular pattern. Ventrally, the frontal is smooth and slightly bulged upwards, lacking any major features.

As mentioned above, an oblique fracture exposed a series of recesses, which prompted further investigation using the CT reconstruction. It revealed an element marked by a pair of medial, rounded recesses separated by a central strut, ventral to the sagittal crest. Lateral to these, close to the still undeveloped *cristae cranii*, there are two additional similar-sized elliptical recesses that are slightly laterally inclined (*repli frontal sensu* Martinelli and Pais 2008). Unlike what is observed with larger individuals, this specimen lacks well-developed, deep carving ornamentation, most likely due to its young age. A similar process is observed in modern members of the crown-group Crocodylia, such as *Crocodylus porosus*, that undergoes extensive development of dermal bone ornamentation in the skull during its ontogenetic progression (Grigg 2015).

***Parietal.*** The parietal is represented by a medial process, made up of fused left and right elements, possessing raised lateral margins and an anteriorly thinning portion that contacts the frontal anteriorly. Posteriorly, the thin parietal medial region thickens as it becomes transversely expanded closer to the occipital region. It forms the anteromedial margins of the supratemporal fenestra, the margins of which are well marked by ridges, being medially vertical and having little observable fossa (Figure 3(b)). Dorsally, it displays lateral raised margins and a slightly concave inner surface. As in the frontal, it lacks the deep-carving ornamentation seen in adults, displaying in its posterior region only shallow longitudinal grooves (Figure 7(b)).

## Axial skeleton

***Cervical vertebrae.*** The preserved cervical series consists of the axis and six post-axial vertebral centra (Figure 4a,b), all of which display rounded articular facets in anterior and posterior views. These centra have slightly concave articular surfaces and therefore are amphicoelous. The axis has ventrally faced parapophyses on the anterior and ventrolateral surfaces of its centrum, which is roughly rectangular in lateral view, being only slightly longer than tall. The former is also lateromedially constricted at mid length and ventrally concave, with a poorly developed ventral keel in comparison with posterior elements (Figure 4$b_1$-$b_2$). Given that its anterior margin is damaged, with no odontoid process preserved, the surfaces for the attachments of the atlas neural arch and intercentrum could not be identified. Despite not being preserved, it could be assessed that the neural arch ran the entire length of the centrum due to the breakage pattern of the pedicles. Zygapophyses are not preserved nor are the neural spines.

The third cervical vertebra is marked by a more prominent development of the ventral keel, and the enlargement and onset of dorsal migration of the parapophyses, located anterolaterally on the centrum, close to the border of the anterior articular facet. The centrum continues to be roughly as wide as it is tall, only slightly anteroposteriorly elongated. The preserved parapophysis is sustained by a robust process and centroparapophyseal lamina that emerges from the midlateral surface of the centrum and is dorsoventrally flattened. The parapophysis and its lamina are both dorsally and ventrally surrounded by shallow depressions. These increase in depth along the posterior vertebrae, as the centroparapophyseal laminae and the ventral keels increase in size. In lateral view, the articular surfaces of the parapophyses progressively change from elliptical to kidney-shaped, along the cervical series (Figure 4$a_1$-$a_2$). The fourth cervical is set apart by a shortening of the centrum, a trend that continues posteriorly, and a more developed ventral keel. The latter is sharply more pronounced than in the third cervical vertebra, with a dorsoventrally expanded anterior portion, tapering posteriorly but running the entire length of the centrum. It is structurally consistent with a hypapophysis (sensu Pol et al. 2012) and is herein treated as such. Unfortunately, they are not all well preserved, being mostly broken at some point along their length, roughly revealing a triangular cross section. The fifth, sixth, and seventh cervicals have the same pattern, with their centra becoming more quadrangular in lateral view and anteroposteriorly shorter in comparison to anterior vertebrae. Their hypapophyses expand dorsoventrally. The articular facet of the parapophysis expands with a wider attachment area, shifting to a more dorsal position, and the centroparapophyseal laminae become thicker, while the lateral depressions of the centra become more conspicuous.

***Dorsal vertebrae.*** There are eight partially preserved dorsal vertebrae, of which only the last three are reasonably complete. They were identified based on the presence or absence of a hypapophysis, length of centrum, and alignment of transverse process and zygapophyses, to be anterior to mid dorsal elements. These have a centrum, a neural arch, right prezygapophyses and broken transverse processes preserved, but lack postzygapophyses and neural spines (Figure 4$c_1$-$c_2$).

The anterior dorsals follow the morphology of the posterior cervicals, being shorter anteroposteriorly and still displaying ventral keels of decreasing sizes, posteriorly. Middle dorsals are distinguished by their elongated, longer than tall, laterally constricted centra, the typical spool-like aspect also found in other notosuchians. The neural arches also follow the anteroposterior stretching of the centrum and run the entire length of the centrum. The neurocentral suture remains open and unfused, indicating an

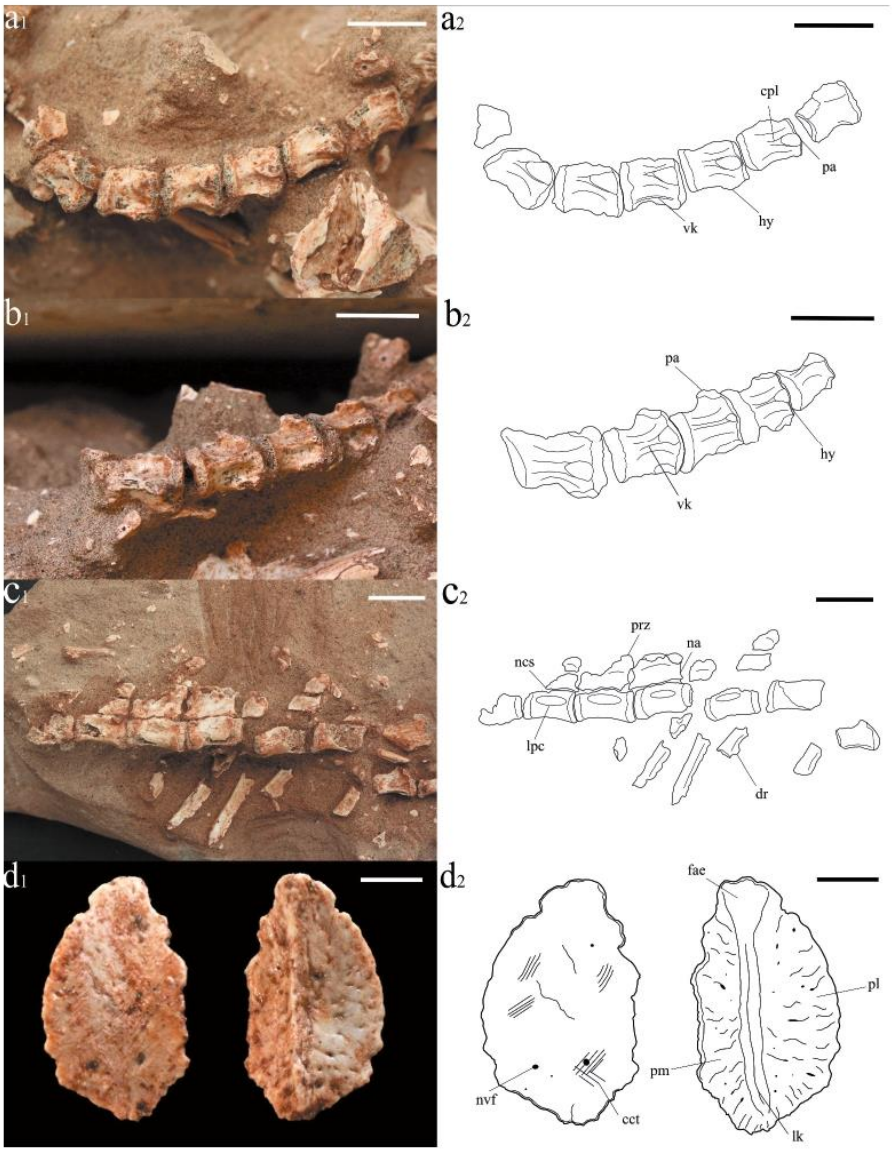


**Figure 4.** Postcranial skeleton of IFSP-VTP/PALEO-0004, including a posterior dorsal osteoderm, and their respective anatomical schematics. $a_1$-$a_2$) – Cervical series, including axis, in lateral view. $b_1$-$b_2$) – Cervical series in ventral view. $c_1$-$c_2$) – Anterior dorsal vertebra in addition to posterior dorsal series with articulated ribs in lateral view. $d_1$-$d_2$) – Posterior dorsal osteoderm in superficial and deep views. Scale bars: a, b and c = 1 cm; d = 5 mm.

early ontogenetic stage for this specimen, following the proposal by Brochu (1996). The characteristic lateral constriction of these vertebrae increases posteriorly, creating enlarging anteroposteriorly long elliptical depressions onto the lateral surfaces of the centra.

Prezygapophyses are roughly vertically oriented and seem to be located slightly dorsal to the transverse process on the last three vertebrae preserved, and dorsally develop a spinoprezygapophyseal lamina that connects it to the anterolateral margin of the neural spine, bounding a subtle prespinal fossa, dorsal to the anterior end of the neural canal. Due to a lack of well-preserved articular facets, the exact shape of these structures is not fully resolved, but based on larger specimens, these most likely were elliptical, with major axis transversely aligned. Laterally, the anterior and posterior edges of the neural arch are concave, creating an oval space between two consecutive vertebrae as they articulate. The anterior concavity is less pronounced, giving the neural arch a slight anterior inclination.

***Dorsal ribs.*** A total of five partially preserved and fragmentary dorsal ribs are preserved, all of them to the left side, semi-articulated with their respective vertebra. Owing to the way the carcase was preserved, lying on the left side of the body, only the medial surfaces of these ribs have been exposed. They comprise dorsoventrally elongated, lateromedially flattened elements, which are medially bent at their proximal and distal ends, forming and arch-shaped structure bulged outwards (Figure 4$c_1$-$c_2$).

A transverse cross-section reveals an elliptical shape with the major axis anteroposteriorly aligned. In medial view, all the preserved rib fragments have crest-like features that run dorsoventrally along their length, from the base of their bifurcating proximal expansion to their distal ends. These are mostly dislocated posteriorly and seem to become increasingly so as the series progresses, the anteriormost rib fragment displaying a more anteriorly placed crest and the posterior ones with crests bordering their posterior margins. This crest-like feature creates a thinner, anterior lamina. A more prominent development of the lamina is seen on the second, third, and fourth rib fragments, giving them a slight anteroposterior expansion.

The fourth rib still preserves its proximal articulating end, characterised by an anterior tuberculum, anterodorsally inclined, and a lower, posterior capitulum. Their divergence generates a y-shaped proximal end, marked medially by a depression between the two articulating processes. Distally, the capitular process gets lateromedially compressed, while the tubercular one thickens, developing the features described above.

### Appendicular elements

***Scapula.*** Using the CT images, a relatively large and flattened element, still embedded in the sandstone matrix, was located near the last cervical vertebra. Given its location and overall morphology, it was interpreted as the left scapular bone (Figure 5(b)). It is characterised by a large, blade-like dorsal portion, of which the anterior margin is highly fragmented, as well as a ventral portion marked by a posteroventral process. These two are separated by an anteroposterior constriction at mid length. The posterior margin is rectilinear dorsally and more concave ventrally, close to the scapular buttress, as is common with other crocodyliforms (Pol 2005; Nascimento and Zaher 2010). The posteroventral glenoid process is transversely expanded with a medial depression separating its lateral and medial edges. The scapular contribution to the glenoid articular surface is damaged but is clearly posteroventrally oriented. The outline of the dorsal scapular blade could not be determined due to its state of preservation, but the material allows the inference that it was dorsoventrally taller than anteroposteriorly deeper.

### Dermal skeleton

***Osteoderm.*** The material yielded a single osteoderm, found near the dorsal vertebrae, but not spatially associated with any single vertebra, being uncovered by itself within the sandstone matrix. In superficial view, it is marked by an oval shape and irregular lateral and medial margins (Figure 4$d_1$-$d_2$). It is ventrally convex and dorsally concave, with anterior and posterior ends arching dorsally. The medial edge of the element displays a more rectilinear border in comparison to the right one, giving it a D-like shape. It also has more conspicuous irregularities, being interpreted here as likely being the sutured medial edge of the osteoderm, where it transversely attached to its left-side counterpart across the midline of a dorsal sagittal row.

A major feature is the presence of longitudinal keel that is medially offset, creating a smaller medial area (*pars mediale*), and a larger lateral area (*pars laterale*). Consequently, this asymmetrical setting creates a superficial area with a somewhat steep medial side and a lateral one with a smoother incline. Thus, a cross-section through the mid portion of the osteoderm would reveal a typical triangular shape, with a convex deep surface. Anteriorly it possesses an external articulating surface (*facies articularis externa*), while posteriorly the border is blunt. This anterior surface gives this osteoderm a somewhat sharp anterior tip, responsible for the articulation with the preceding osteoderm. The longitudinal keel does not progress onto the anteriormost articulating surface. At mid-length (central area), both medial and lateral superficial areas adjacent to the crest are slightly concave. The longitudinal keel is less developed than on larger individuals with similar osteoderms.

The sculpturing is incipient, as expected, the superficial surface being only dotted with small shallow rounded pits and grooves, as well as vascular foramina. These features are preferentially transversely aligned, emerging from either the keel or centre area, with some

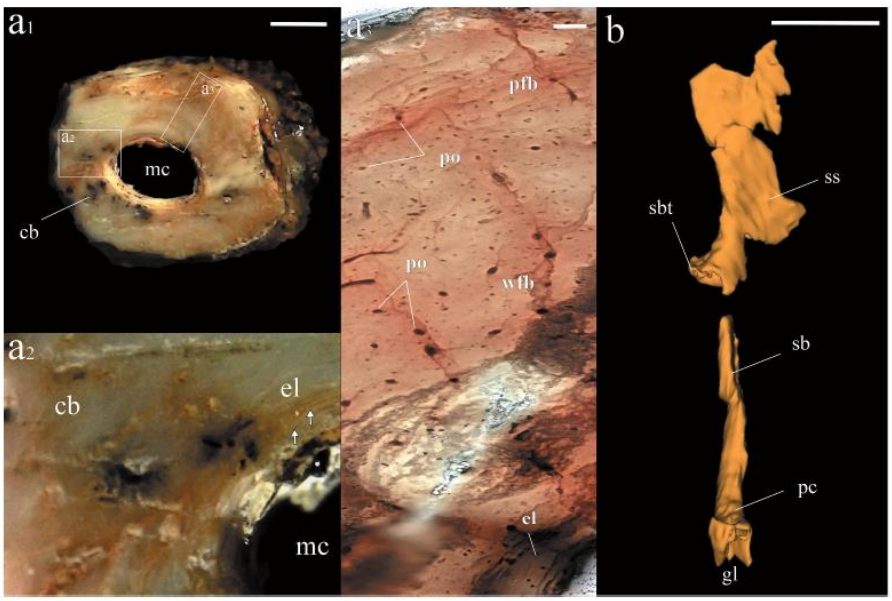


**Figure 5.** Appendicular skeleton, comprised of a long, unidentified bone and the right scapula. $a_1$-$a_2$) – detail of long bone cross-section, displaying the medullary cavity surrounded by cortical bone. Arrows point to endosteal lamellae in the perimedullary region. $a_3$) – Micrograph of thin section slide encompassing the medullary cavity, surrounded by endosteal lamellae and cortex composed mostly by longitudinal primary osteons in a woven-fibred-like bone and less vascularised parallel-fibred-like texture towards the periosteum. b) – Fragmented scapula in lateral and posterior views. Scale bars: a1 = 1 mm; a3 = 100 µm; b = 1 cm.

radial arrangement. The deep surface of the osteoderm is marked by the classic criss-cross type texture described for fossil and modern forms (Seidel 1979), in addition to pits and nutritious foramina.

### Long bone histology

Adjacent to the last cervical vertebra, there is a fractured elongated element, with a circular cross-section and open medullary cavity surrounded by compact bone (Figure 5a$_1$). This unidentified long bone most likely was part of an anterior limb, given its position in relation to the axial skeleton. One of the epiphyses is still present, and its dorsoventral expansion is similar to an ulnar proximal epiphysis, with the development of the olecranon process. Thus, despite the lack of characteristic features, its position and morphology indicate it may have composed an anterior zeugopod.

Its thin section encompasses a fragment of cortical bone containing portions of both the endosteal surface, surrounding the medullary cavity, and the periosteum (Figure 5a$_1$-a$_2$). The cortex is characterised by compact bone, lacking major cancellous or trabecular regions, while the perimedullary region is encircled by endosteal lamellae (EL, sensu Enlow 1962), marked by low vascularity. Succeeding the deposition of this tissue, deep in the cortex, there is the prevalence of somewhat randomly dispersed primary osteons, with disorganised collagen fibrils, typifying a woven-fibred -like bone (WFB) architecture and an incipient fibrolamellar system. Primary osteons and haversian canals are preferentially longitudinal, with localised anastomoses. Vascularity seems to decrease periostealy, where fewer primary osteons are visible, in addition to a higher degree of fibre orientation, likely transitioning to a parallel-fibred-like tissue (PFB). Nevertheless, primary osteons are still found close to the periosteal surface, and no annuli or LAGs had yet formed at the time of death. Consequently, the thin section shows no evidence of external fundamental tissue formation (EFS). In spite of the known distinct trajectories CGM (cyclical growth marks) formation may take inside different appendicular elements, these seem to only become conspicuous in more mature individuals (Woodward et al. 2014), thus not compromising histological interpretations on young juveniles.

## Discussion

### Phylogenetic relationships

Using the data matrix of Cunha et al. (2020) (440 characters, 114 taxa, modified from Martinelli et al. 2018), this semaphoront, specimen IFSP-VTP/PALEO-0004, possesses 28 potentially codifiable characters (6.3% of the total number of characters), including cranial and postcranial elements, a similar percentage to some well-resolved taxa, and would be suitable for a subsequent phylogenetic analysis. Even so, in accordance with Sharma et al. (2017), which asserts that treating ontogenetic stages as terminals may violate principles of systematics, considering this specimen as a terminal would most likely produce topological artefacts, given that such an early juvenile may not have yet developed all the synapomorphies that would aid its placement. Thus, its relationships are inferred by comparing the preserved osteological features with other crocodyliforms, and also considering the known diversity of adjacent fossil sites.

The specimen possesses characteristic features that allowed a family-level positioning, including its osteoderm morphology and a typical baurusuchid cranial synapomorphy (triangular depression on the lateral surface of the jugal sensu Montefeltro et al. 2011). Below, in-depth comparisons are provided, and subsequent conclusions are presented.

### Osteological comparisons and taxonomic placement

#### Cranial material

Overall, the evidence in the form of the cranial and postcranial features described above, likely including a synapomorphic one (a triangular depression on the lateral surface of the jugal (sensu Montefeltro et al. 2011), points to a baurusuchid affinity for this specimen. The parietal/frontal skull roof elements differ most substantially, both in terms of morphology and sculpturing type, from modern crocodylians and other eusuchians. The frontals in *Melanosuchus niger*, for instance, are extremely elongated anteroposteriorly and constricted at mid length, right above the eye sockets, having a concave dorsal surface with no sagittal crest. The parietals display an inverted 'T' shape and are much wider than on IFSP-VTP/PALEO-0004. Both bones are strongly ornamented with deep-excavating rounded pits even on smaller, skeletally immature *Melanosuchus* specimens (Vieira et al. 2018b).

Peirosaurids share with neosuchians a similar sculpturing of dermal bones (Gasparini et al. 1991; Carvalho et al. 2004; Larsson and Sues 2007; Carvalho et al. 2007; Campos et al. 2011), which allows for their exclusion as candidates for a taxonomic placement for this specimen, given the contrasting pattern of incipient ornamentation of shallow grooves seen in IFSP-VTP/PALEO-0004. Also, peirosaurids are not known from the site where the specimen was collected. Comparison with derived notosuchians, such as members of the clade Ziphosuchia, yielded more widely shared traits for comparison. Derived, small-bodied sphagesaurids such as members of the genus *Caipirasuchus* (Pol et al. 2014; Martinelli et al. 2018), display anteroposteriorly elongated frontals, which are usually as long as the nasals, with low sagittal crests. These crests are not as transversely wide as in IFSP-VTP/PALEO-0004 and are also anteriorly dislocated, failing to reach posteriorly to the frontal-parietal suture. Their parietals, in dorsal view, have thickened lateral bulges running along the margins of the border with the supratemporal fenestrae, are laterally constricted at mid length and anteriorly, as well as posteriorly concave at their contact with the supraoccipitals, the latter not being part of the skull roof on sebecosuchians. The main difference between the parietals in Baurusuchidae and Sphagesauridae is that, in the former, the medial process is highly laterally constricted, developing only a thin bone wall, and transversely expanding at the frontal-parietal suture, while in the latter this process is much wider transversely, being symmetrical along its length.

A similar pattern of anteroposteriorly elongate frontals is observed in advanced notosuchians outside of sphagesauridae, with similarly sized forms like *Mariliasuchus amarali* or *Notosuchus terrestris* differing from IFSP-VTP/PALEO-0004 by either lacking a sagittal crest or displaying a low relief one (Zaher et al. 2006; Fiorelli and Calvo 2008). An important additional observation is the apparent vertical lateral surface of the parietal, which forms the medial wall of the supratemporal fenestra, highlighting the lack of a substantial fossae in IFSP-VTP/PALEO-0004, which also differs from the abovementioned clades in relation to baurusuchids. This condition indicates a fully open supratemporal fenestrae early in their development, which raises questions about their role on such a small individual.

Finally, despite the limited number of identifiable cranial elements, the similarities with baurusuchid crania are most noticeable. Although not complete and broken at its right lateral side, the frontal in IFSP-VTP/PALEO-0004 is losangular and transversely wide, bearing a midline crest, as is common for baurusuchids with such element preserved, like *Baurusuchus salgadoensis, Stratiotosuchus maxcheti, Campinasuchus dinizi, Pissarrachampsa sera*, and *Aplestosuchus sordidus* (Riff 2003; Carvalho et al. 2005;

Carvalho et al. 2011; Montefeltro et al. 2011; Godoy et al. 2014). Moreover, the preserved anterior jugal ramus displays a baurusuchid synapomorphy in the form of a putative triangular depression on its lateral surface (Montefeltro et al. 2011).

Following the work of Godoy et al. (2018), the observation of fully open supratemporal fenestrae at this stage may indicate an even earlier onset of peramorphic development during the ontogeny of baurusuchids, raising important questions on the functional significance of such feature and the likely repercussions for niche partitioning between juveniles and adults. It is possible that, given its large size relative to the skull roof in adult forms, early post-hatchling development started with fully open supratemporal fenestrae in order to reach its mature, enlarged state lacking broad fossae. It has been demonstrated that modern crocodylians, as well as fossil neosuchian crocodyliforms, show dietary shifts across ontogeny, with the coupling of functional changes of the rostrum, dentition and, consequently, bite force, with the acquisition of different prey items (Tucker et al. 1996; Gignac and Erickson 2016; Gignac and O'Brien 2016; Gignac and Santana 2016; Drumheller and Wilberg 2020; Drumheller et al. 2021). A similar process could also have applied to notosuchians, with juveniles and adults occupying distinct ecomorphotypes.

Curiously, the internal recess pattern of the frontal provided an additional character that linked this material to Baurusuchidae. Martinelli and Pais (2008) briefly described frontal cavities being present in their description of the argentine baurusuchid *Wargosuchus australis*, and a remarkably similar pattern is also observed in our specimen. Assuming the early juvenile nature of IFSP-VTP/PALEO-0004 and to further clarify the ontogenetic nature of this character, we compared the pattern found here with two other still undescribed baurusuchid specimens (to be described elsewhere), belonging to two distinct growth stages (subadult and adult individuals), with known histological age estimates (Ricart 2017; Dumont Jr et al. 2020). This comparison suggests a strong correlation between age and recess volume within the bone (Figure 6). At their earliest stage of development, medial and lateral recesses comprise a substantial volume of the bone. Dorsally, the sagittal crest tapers to a sharp end and possesses a conspicuous relief, while ventrally the lateral processes bound the olfactory tract (*cristae cranii*). The intermediate growth stage shows a lateral expansion of the frontals, enlarged repli frontals and substantially developed cristae cranii, which are now clearly visible and associated with a medial process that divides the olfactory tract. The central strut thickens, and the medial recesses decrease in size, at the same time as the sagittal crest reduces its relief relative to the dorsal surface. Expectedly, the adult individual presents a more ossified element, with abundant compact bone matrix, where the medial network of recesses does not extend anteroposteriorly throughout the bone and are only observed along a few CT slices. The repli frontals are much smaller and the *cristae cranii* much closer medially, marking a lateral constriction of the olfactory tract along the anteroventral portion of the frontal, as seen in recent endocast reconstructions (Dumont Jr et al. 2020; Fonseca et al. 2020). The sagittal crest is much diminished, but still distinguishable, and surface sculpturing is extensive, marked by shallow grooves.

### *Cervical vertebrae*

Advancing the comparisons to the postcranial remains, the cervical vertebrae of IFSP-VTP/PALEO-0004 differ most from the neosuchian condition, here represented by *Melanosuchus niger* (Vieira et al. 2018b), with its anteroposteriorly stretched (longer than tall), procelous centra contrasting the shorter (roughly as tall as it is long), amphicoelous centra of the present material. The hypapophyses, despite also becoming more conspicuous posteriorly, taper into a ventral keel, being much less developed dorsoventrally than on *Melanosuchus*, and do not display anteriorly inclined distal tips. Parapophyses on anterior cervicals have similarly shaped elliptical articular facets, but unlike IFSP-VTP /PALEO-0004, on *Melanosuchus* these have the same overall shape throughout the series.

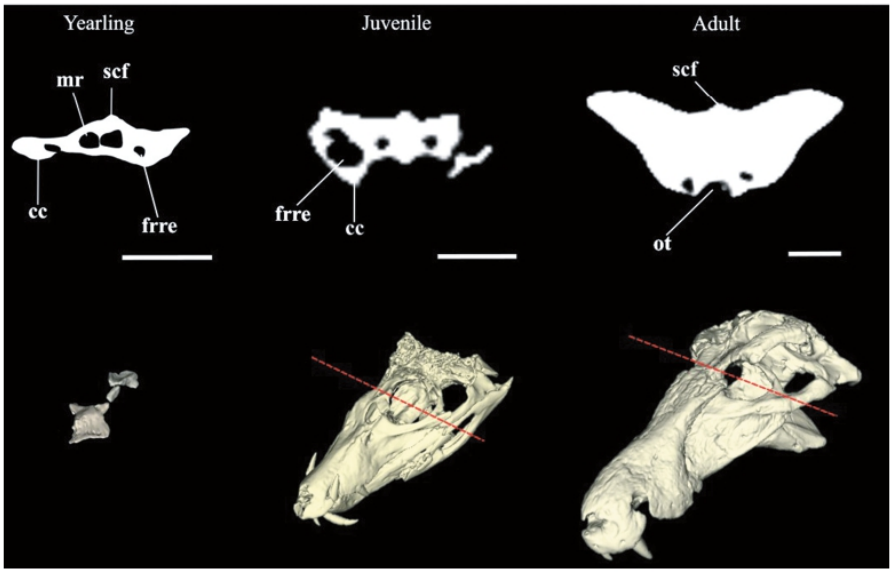


**Figure 6.** The ontogeny of frontal internal structure in Baurusuchidae. As the *crista cranii* develop and the olfactory tract becomes more defined, both medial and lateral recesses are substituted by compact bone. Red dashed lines indicate cross-section slide. Scale bars = 1 cm. Skull reconstructions not to scale.

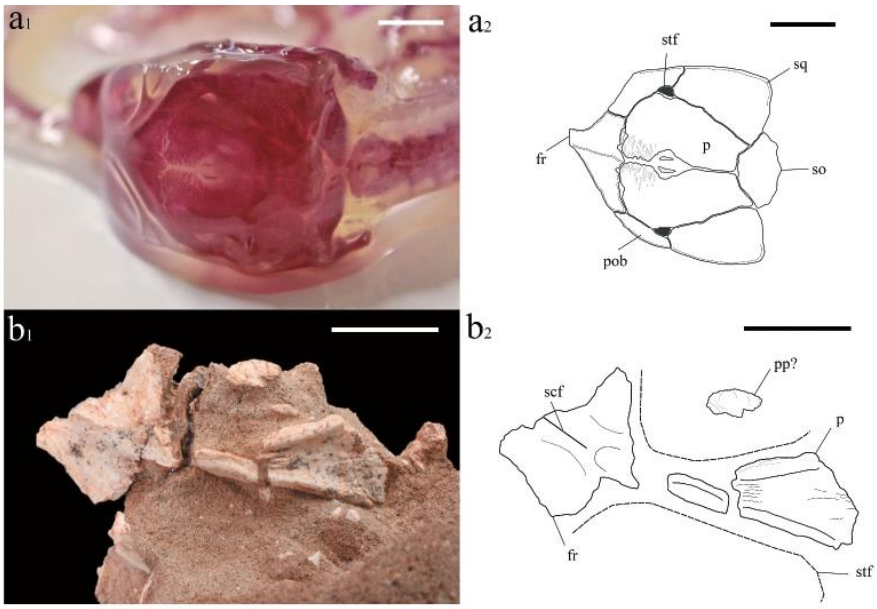


**Figure 7.** Skull roof osteology of IFSP-VTP/PALEO-0004. $a_1$-$a_2$) – Comparison with late-stage, pre-hatchling *Melanosuchus niger* embryo. Note unfused parietals and two distinct centres of ossification. $b_1$-$b_2$) – Frontal-parietal of IFSP-VTP/PALEO-0004 with the crest-like parietals between the supratemporal fenestrae, similar to baurusuchids. In contrast, most other notosuchians display a flattened, evidently broader dorsal parietal surface. Scale bars = 1 cm.

The features observed are much closer to the notosuchian pattern, such as in basal ziphosuchians like *Simosuchus clarki*, the sphagesaurid *Yacarerani boliviensis*, and sebecosuchians for which we have well-preserved and/or published cervical material, like *Sebecus icaeorhinus, Baurusuchus salgadoensis*, and *Baurusuchus albertoi* (Carvalho et al. 2005; Nascimento and Zaher 2010; Georgi and Krause 2010; Pol et al. 2012; Leardi et al. 2015). These taxa, like the specimen herein described, display anteroposteriorly shorter amphicoelous centra in comparison with neosuchians, becoming increasingly taller in posterior elements. They also share slight lateral depressions located dorsally and ventrally in relation to the parapophyses and concave ventral surfaces.

Although not formally described for baurusuchids, cervical hypapophysis-like structures are clearly visible on the UFRJ-DG -255 *Baurusuchus* specimen, becoming both dorsoventrally and longitudinally expanded as the series progresses, and tapering on anterior dorsals. Despite not being considered as such by the authors (Nascimento and Zaher 2010), a similar pattern was seen in *Baurusuchus albertoi* and, like IFSP-VTP/PALEO-0004 and *Y. boliviensis*, they transition posteriorly into a ventral keel, contrasting the anteriorly limited hypapophyses of *Sebecus icaeorhinus* and *Simosuchus clarki*. *S. icaeorhinus* had the most dorsoventrally deep hypapophyses of the taxa considered.

Differences between parapophyses provided more scope for comparisons. As mentioned before, these in IFSP-VTP/PALEO-0004 enlarge posteriorly and gradually vary from round to a more kidney-like shape starting on C5, just like in *Baurusuchus*, but differently from *S. icaeorhinus*, where parapophyses remains elliptical and elongate until C7, expanding dorsoventrally abruptly only on C8 or D1, and also distinct from the sphagesaurid *Y. boliviensis*, that retains the same shape along the series. *Simosuchus clarki*, a basal ziphosuchian, presents a similar modification of the parapophyseal articular facet in posterior cervicals as some baurusuchids, but it does not proceed posteriorly in the same fashion, and so far, has only been found in Madagascar.

### *Dorsal vertebrae*

As expected, IFSP-VTP/PALEO-0004 dorsal vertebrae have spool-shaped centra, with lateral depressions, and become anteroposteriorly stretched in comparison to their cervical counterparts, a widely observed morphology in notosuchians (Pol 2005) and, to some extent, also seen in *Melanosuchus niger* (Vieira et al. 2018b). Anterior dorsals in IFSP-VTP/PALEO-0004 still retain ventral keels, though not as developed as the anterior ones, sharply differing from the eusuchian condition, but much like what is seen in the already mentioned notosuchians. Clearly visible hypapophyses are persistent up to D5 in *S. icaeorhinus*, D3 in UFRJ-DG-255, at least up to D2 in *Y. boliviensis* and D3 in *S. clarki*. Assuming the preserved anterior dorsals in IFSP-VTP/PALEO-0004 represent a continuous sequence with the cervical series, which lacks C8, hypapophyses would still be distinguishable on D2 or D3, approaching the latter three taxa. In lateral view, IFSP-VTP/PALEO-0004 displays anteriorly and posteriorly concave margins of the neural arch, the posterior one has a noticeably deeper concavity, a standard condition in notosuchians, but different from *Simosuchus*, where the posterior edge advances anteriorly, giving its neural arches an anteriorly inclined form.

Despite the paucity of postcranial materials and detailed published descriptions, some workers have been successful at identifying postcranial synapomorphies for Notosuchia and clades within it (Clark 1994; Pol et al. 2012; Leardi et al. 2015). Most of these, though, when relating to the axial skeleton, are concentrated on features of the neural arch, and not on the centra themselves and associated hypapophyseal and paraphophyseal processes. Since the referred material, IFSP-VTP/PALEO-0004, preserves mostly the centra and, in the case of the mid-dorsals, a portion of the neural arches and prezygapophyses, proper distinctions between taxa could not be brought to light. Notwithstanding the similarities observed between the cervicals of IFSP-VTP/PALEO-0004 and baurusuchids, the vertebral material alone is not sufficient to safely support this assignment.

### Scapula

As noted by Sertich and Groenke (2010), a dorsally wide scapular blade is common to basal mesoeucrocodylians, contrasting to the narrow condition found eusuchians, including extant crocodylians. As a result, am eusuchian affinity can be easily dismissed, given that the specimen displays a clear dorsal anteroposterior expansion in relation to the scapular shaft, thus pointing to a notosuchian affinity, consistent with the morphological features of the cranial and axial materials. Although roughly similar, within Ziphosuchia scapular anatomy also varies: basal advanced notosuchians like *Simosuchus clarki* and *Mariliasuchus amalari* (Sertich and Groenke 2010; Nobre and de Carvalho 2013) and sphagesaurids, like *Caipirasuchus* (Pol et al. 2014; Martinelli et al. 2018) display taller scapular shafts and rectilinear posterior margins of the dorsal blade, while sebecosuchians (e.g. baurusuchidae) lack a conspicuous scapular prominence and have a more rounded lateral outline of the dorsal blade (Nascimento and Zaher 2010; Cotts et al. 2017). The scapula of IFSP-VTP/PALEO-0004 seems to have a dorsoventrally short scapular shaft, but, due to it still being embedded in sediment and poor preservational state, more detailed descriptions were not possible, hindering further comparisons with characters shared by less inclusive clades.

### Osteoderm

The preserved osteoderm is the most distinct and taxonomically relevant element of IFSP-VTP/PALEO-0004, and, along with the jugal, the one that allowed a family-level phylogenetic placement within Baurusuchidae. Although osteoderms share similarities throughout crocodylomorpha (Montefeltro 2019), some clades of highly-specialised forms have adapted their parasagital rows to different ends, with the marine metryorhynchids lacking them altogether (Young et al. 2010), and large sphagesaurids like *Armadillosuchus* developing extensive defensive armours (Marinho and Carvalho 2009).

As thoroughly reviewed recently by Montefeltro (2019), the baurusuchid dermal shields are somewhat unusual for Crocodylomorpha due to a mix of plesiomorphic and apomorphic characters. While possessing the ancestral paravertebral rows of longitudinally keeled osteoderms, features such as the ovate profile, along with a poorly ornamented superficial surface (mostly by shallow grooves and pits that excavate little into the surface) and, in some cases, non-imbricating elements, contrast sharply with the rectangular osteoderms with deeply intruding and highly ornate pits such as the ones found not only outside of Notosuchia but also in clades within this group, such as the peirosaurids (Tavares et al. 2017).

In fact, there are very few taxa that have morphologically comparable osteoderms, and that assisted the efforts to narrow down possible candidates. Sebecids are one of them, but, thus far, all have come from Cenozoic beds (including in Brazil, see Kellner et al. 2014), with one exception (Sellés et al. 2020), and work by Ortega (2004) and Martin (2014) on European sebecosuchians (*Iberosuchus* sp.), showed that, despite being closely related to baurusuchids and sharing a similar sculpturing pattern, their dorsal elements are more elongate and display a taller and sharper sagittal keel that makes up a larger fraction of osteoderm height.

Within Ziphosuchia, but outside of Baurusuchidae, only some forms of advanced notosuchians share similar osteoderms (Montefeltro 2019). The small-bodied sphagesaurid *Caipirasuchus mineirus* (Martinelli et al. 2018) shares the oval shape of presacral osteoderms, described by the authors as 'D-shaped', a term also utilised here and by Nascimento and Zaher (2010) when referring to dorsal osteoderms belonging to *Baurusuchus albertoi*. However, as recognised by the authors, the dorsal shield of *C. mineirus* are non-imbricating, lacking an exterior articular surface, present in our material and differs from other specimens of its genera by being smaller. Additionally, there are features, besides body size, identified in *C. mineirus* which indicate that it might be a juvenile, thus raising the possibility that it was not fossilised in its final form.

Other species with osteoderms that share features with Baurusuchidae include *Notosuchus terrestris*, which is only found in Argentina (Pol 2005; Fiorelli and Calvo 2008), and *Mariliasuchus amarali*, which possesses only superficially similar dorsal osteoderms. In the latter, they do not imbricate, are much rounder in superficial view (higher length to width ratio), have concave deep surfaces rather than convex, and display a more developed ornamentation with secondary transverse crests (Nobre and de Carvalho 2013), a character not seen in baurusuchids or IFSP-VTP/PALEO-0004.

## Bone histology and considerations on the possible age at the time of death

The histology thin section revealed tissues consistent with a lamellar-zonal bone system, typically observed in modern crocodylians and fossil eusuchians, where periods of more rapid growth of woven-fibred bone deposition alternate with parallel-fibred annuli (Hutton 1986; Lee 2004; Klein et al. 2009; Woodward et al. 2014). The woven-fibred tissue, marked here by longitudinally oriented primary osteons, follows a general crocodylomorph pattern, with less vascularisation than its counterparts seen in avemetatarsalians (Horner et al. 2001; Padian et al. 2004). Unlike specimens analysed by the previously cited authors, IFSP-VTP/PALEO-0004 did not complete a full cycle of growth before dying, but shows evidence of slower deposition towards the periosteum, where more organised tissue was being formed, pointing to it being an early juvenile, perhaps less than a year old. A less than a year-old *A. mississippiensis* tibia showing similar histologic features was described by Horner et al. (2001) (Figure 2(d)), it also did not form any CGMs, and similarly seems to have been forming parallel-fibred bone towards to periosteum. Additionally, the near-term embryo shown by Horner et al. (Figure 2b,c) possesses a known pattern of a large medullary cavity surrounded by a relatively thin cortex (roughly 78% of the radius is composed by the inner medulla) that differs markedly from the older, abovementioned semaphoront. IFSP-VTP/PALEO-0004 shows a pattern similar to the former, we estimate the medulla of major axis comprising only 36% of the radius, pointing to a more mature individual.

Previous work on long bone histology of embryonic, neonate or older juvenile archosaurs point to common features that may indicate the likely ontogenetic stage of a given specimen. Data indicates that the presence of EFS (external fundamental system) is evidence of ceasing growth and skeletal maturity (Ricqlès et al. 2003; Klein et al. 2009; Woodward et al. 2011, 2014). Likewise, neonate and early juveniles usually lack intensive remodelling, with fewer secondary osteons, and do not display secondary cancellous bone, despite a reported 18-month-old *Alligator mississippiensis* already showing incipient cortical remodelling (Horner et al. 2001; Woodward et al. 2014). Consistent with the absence of CGMs, IFSP-VTP/PALEO-0004 shows no signs of remodelling and lacks an EFS.

Research on notosuchian growth has seen important recent developments with the analysis of the long-bone histology of *Iberosuchus* and *Pepesuchus* (Cubo et al. 2017; Sena et al. 2018), these, unfortunately, represent older individuals, hindering a proper peer-to-peer comparison with IFSP-VTP/PALEO-0004. *Iberosuchus* displays intense remodelling of the perimedullary cavity, with large resorption cavities (Figure 1, p. 3), while *Pepesuchus*, despite still possessing an endosteal lamellae, developed a classic harversian-type bone, with multiple generations of secondary osteons (Figure 4, p. 339).

We evaluate that some osteological features of IFSP-VTP/PALEO-0004 also indicate a yearling individual, in contrast to younger or more mature ones. Firstly, the parietals seem to be fully fused medially (Figure 7), contrasting the unsutured condition seen in pre-hatchling embryos of modern crocodylian taxa, such as the *Alligator mississippiensis*, and caimans like *Caiman latirostris* and *Melanosuchus niger* (Rieppel 1993b; Iungman et al. 2008; Vieira et al. 2018b). The parietals have two separate ossification centres that consolidate slowly, resulting in open skull roofs late in their development (Figure 7$a_1$-$a_2$), but given the paucity of embryological work on extant crocodylids, this may either be a widely distributed characteristic in Crocodylia or a derived developmental feature of Alligatoridae. If notosuchians followed a similar ossification pattern, then medial contact of parietals could then be used as a measure for rough ontogenetic development estimates for small individuals. Although paired frontals have been cited as valuable characters to identify juvenile crocodylomorphs (Rieppel 1993; Schwarz and Salisbury 2005), know and putative notosuchian juveniles already had fully fused frontals (Marinho et al. 2013; Godoy et al. 2018), therefore not being a suitable character for ontogenetic evaluation in this case.

Research on the osteological indicators of maturity in crocodylians and, more broadly, archosaurs, mainly focuses on the nature of the neurocentral suture, with workers pointing to the necessity of it being coupled with specimen size to properly assess maturity (Brochu 1996; Irmis 2007). The former author also points to the aspect of the sutural surface of the pedicle, becoming increasingly wider and more rugose during the growth series. Developmental and histological work showed that while ossification proceeds anteroposteriorly, neurocentral sutures closure advances caudocranially, with *Alligator mississippiensis* adults still retaining partially open sutures on their cervical vertebrae (Rieppel 1993; Vieira et al. 2018b). Given what has been described in the literature, the state of these characters on the present specimen do not meet the criteria even for partially closed neurocentral sutures, with neural arches barely contacting the centra on the preserved dorsal vertebrae, and smooth, undeveloped pedicles of cervical vertebrae providing additional evidence of its skeletal maturity.

The presence of a fully ossified osteoderm is also particularly revealing. Work done by Vickaryous and Hall (2008) on dermal skeleton development in *Alligator mississippiensis* showed that osteoderms are one of the very last elements to ossify, starting from the keeled region and radiating outwards, but not developing completely until after the first year of life of the youngling with a snout-vent length (SVL) of at least 175 mm. It is conceivable that the rate of development of these dermal ossifications is predicated on the metabolic rate and life strategy of a lineage and given the significant morphological and ecological differences between modern crocodylians (semiaquatic forms) and notosuchians (mostly terrestrial), such processes most likely differed between the two groups. In the light of the two scenarios and the work abovementioned, a more conservative stance was assumed in terms of growth dynamics, and thus IFSP-VTP/PALEO-0004 is considered to be a post-hatchling, yearling individual, following an ossification pattern similar to modern crocodylians.

Notwithstanding the known diversity of small-bodied notosuchians with dimensions similar to the specimen herein described (Nobre and de Carvalho 2006; O'Connor et al. 2010; Pol et al. 2014; Leardi et al. 2015; Martinelli et al. 2018), the evidence at hand in the form of absence of CGMs and EFS, fully fused parietals, unfused and open neurocentral sutures, undeveloped and smooth pedicles, poorly ossified vertebral centra and poorly developed ornamentation on dermal plate, clearly points to it being an early post-hatchling baurusuchid semaphoront (Brochu 1996; Irmis 2007; Vieira et al. 2018b).

## Conclusions

The osteological description and known fossil diversity of the collection site, converge on supporting a baurusuchid affinity for this specimen. Moreover, the thin section analysis of a long bone supports it as an early juvenile, likely less than a year-old. Assuming this taxonomic placement, several features, with likely ontogenetic implications, are of relevance and deserve further discussion and investigation:

Neonates and yearlings of fossil crocodyliforms and modern crocodylians do not possess fully developed supratemporal fenestrae, which are intimately linked to bite force and show different diet and foraging strategies as they grow (Tucker et al. 1996; Gignac and Erickson 2016; Vieira et al. 2018b; Drumheller et al. 2021). Thus, given its oversized state in baurusuchids and its fully open nature in early semaphoronts, the onset of supratemporal fenestra enlargement could have taken place early in ontogeny.

In the case of IFSP-VTP/PALEO-0004 being a baurusuchid, the presence of ventral keels on cervical vertebrae, visible centroparapophyseal lamina and the absence of prezygapophyseal bulges, seem to have a strong ontogenetic influence, given that both are not seen in adult specimens and the former has been recovered as a possible postcranial synapomorphy for sebecosuchians (Pol et al. 2012);

Cranial dermal bones, like the frontal, seem to display ontogenetic features such as decreasing recess volumes, which may contribute to a more precise age assessment of suspected juvenile specimens without long-bone histology, such as *Gondwanasuchus scabrosus* (Marinho et al. 2013), given that proposing new species based on immature individuals is risky.

The observed osteological and histological evidence points to an early baurusuchid juvenile affinity for this specimen. The material presented here is the very first example of an early notosuchian ontogenetic stage recovered from the fossil record, and is spatially associated with nesting sites of *Bauroolithos fragilis* Oliveira et al. (2011), eggs attributed to *Baurusuchus*. Interestingly, the sediment surrounding this specimen is of a similar granulometric and structural nature to the reddish sandstones associated with these nesting sites found in the Adamantina Formation (Oliveira et al. 2011; Marsola et al. 2016). This semaphoront also provided insights into possible osteological divergences between it and its adult counterparts, including presence or absence of vertebral laminae and processes and expected absence of sculpturing of dermal skeleton. Despite the lack of more than two fully fledged synapomorphic characters, the presence of identifiable features on such an early ontogenetic stage brings hope that future specimens will be properly placed into clades, possibly allowing the study of more complete growth series for other notosuchian groups, which lack ontogenetic data. Finally, a renewed interest in postcranial descriptions is welcomed (Pol et al. 2012; Leardi et al. 2015; Godoy et al. 2016) but more is needed, and these data would increase the likelihood of proper assessment of future discoveries.

## Acknowledgments

The authors thank CAPES, for the financial support of DMS, and CNPq for the funding of this project. We would also like to express our gratitude to the students and participants involved in the fieldwork campaign to collect this specimen, as well as all the hosts from the vertebrate paleontology collections of UFRJ, ANM Museum, and MZUSP for their great hospitality. A special thanks also goes to Prof. Julia Klaczko and fellow lab members, from the University of Brasília, for their support with the *Melanosuchus* embryos.

## Disclosure statement

No potential conflict of interest was reported by the author(s).

## Funding

This work was supported by the CAPES [88887.508038/2020-00]; CNPQ [401784/2010-0].

## ORCID

Marco Brandalise de Andrade http://orcid.org/0000-0002-3452-801X

## References

Amorim P, Moraes T, Silva J, Pedrini H. 2015. InVesalius: an interactive rendering framework for health care support. In: Bebis G, Boyle R, Parvin B, Koracin D, Pavlidis I, Feris R, McGraw T, Elendt M, Kopper R, Ragan E, et al., editors. Adv Vis Comput. Cham: Springer International Publishing; pp. 45–54. doi:10.1007/978-3-319-27857-5_5.

Batezelli A. 2010. Arcabouço tectono-estratigráfico e evolução das Bacias Caiuá e Bauru no Sudeste brasileiro. Rev Bras Geociências. 40(2):265–285. doi:10.25249/0375-7536.2010402265285.

Batezelli A, Perinotto JDJ, Etchebehere MDC, Fulfaro VJ, Saad AR. 1999. Redefinição litoestratigráfica da unidade Araçatuba e da sua extensão regional na Bacia Bauru, Estado de São Paulo, Brasil. Simpósio Sobre O Cretáceo Bras. 5:195–200.

Bertini RJ. 1993. Paleobiologia do Grupo Bauru, Cretáceo Superior continental da Bacia do Paraná, com ênfase em sua fauna de amniotas. Rio de Janeiro: Universidade Federal do Rio de Janeiro.

Brochu CA. 1996. Closure of neurocentral sutures during crocodilian ontogeny: implications for maturity assessment in fossil archosaurs. J Vertebr Paleontol. 16(1):49–62. doi:10.1080/02724634.1996.10011283.

Buckley GA, Brochu CA, Krause DW, Pol D. 2000. A pug-nosed crocodyliform from the Late Cretaceous of Madagascar. Nature. 405(6789):941–944. doi:10.1038/35016061.

Campos DA, Oliveira GR, Figueiredo RG, Riff D, Azevedo SAK, Carvalho LB, Kellner AWA. 2011. On a new peirosaurid crocodyliform from the Upper Cretaceous, Bauru Group, southeastern Brazil. An Acad Bras Ciênc. 83 (1):317–327. doi:10.1590/S0001-37652011000100020.

Campos DA, Suarez, JM, Riff, D, and Kellner, AWA. 2001. Short note on a new baurusuchidae (Crocodyliformes, Metasuchia) from the Upper Cretaceous of Brazil. Mus Nac. 57: 1–7. 0080–3200.

Carr TD. 2020. A high-resolution growth series of *Tyrannosaurus rex* obtained from multiple lines of evidence. PeerJ. 8:e9192. doi:10.7717/peerj.9192.

Carvalho IDS, Teixeira VDPA, Ferraz MLDF, Ribeiro LCB, Martinelli AG, Neto FM, Sertich JJW, Cunha GC, Cunha IC, Ferraz PF. 2011. *Campinasuchus dinizi* gen. et sp. nov., a new Late Cretaceous baurusuchid (Crocodyliformes) from the Bauru Basin, Brazil. Zootaxa. 2871(1):19–42. doi:10.11646/zootaxa.2871.1.2.

Carvalho IDS, Vasconcellos FMD, Tavares SAS. 2007. *Montealtosuchus arrudacamposi*, a new peirosaurid crocodile (Mesoeucrocodylia) from the Late Cretaceous Adamantina Formation of Brazil. Zootaxa. 1607(1):35–46. doi:10.11646/zootaxa.1607.1.3.

Carvalho IS, Bertini RJ. 1999. *Mariliasuchus*: um novo Crocodylomorpha (Notosuchia) do Cretáceo da Bacia Bauru, Brasil. Geol Colomb. 24:83–105.

Carvalho IS, Borges Ribeiro LC, Dos Avilla LS. 2004. *Uberabasuchus terrificus* sp. nov., a New Crocodylomorpha from the Bauru Basin (Upper Cretaceous), Brazil. Gondwana Res. 7(4):975–1002. doi:10.1016/S1342-937X(05)71079-0.

Carvalho IS, de Arruda Campos AC, Henrique Nobre P. 2005. *Baurusuchus salgadoensis*, a New Crocodylomorpha from the Bauru Basin (Cretaceous), Brazil. Gondwana Res. 8(1):11–30. doi:10.1016/S1342-937X(05)70259-8.

Castro MC, Goin FJ, Ortiz-Jaureguizar E, Vieytes EC, Tsukui K, Ramezani J, Batezelli A, Marsola JCA, Langer MC. 2018. A Late Cretaceous mammal from Brazil and the first radioisotopic age for the Bauru Group. R Soc Open Sci. 5 (5):180482. doi:10.1098/rsos.180482.

Clark JM. 1994. Patterns of evolution in Mesozoic Crocodyliformes. Cambridge: Camb Univ Press Camb UK. (In the Shadow of the Dinosaurs: Early Mesozoic Tetrapods.).

Cotts L, Pinheiro AEP, Da Silva Marinho T, de Souza Carvalho I, Di Dario F. 2017. Postcranial skeleton of *Campinasuchus dinizi* (Crocodyliformes, Baurusuchidae) from the Upper Cretaceous of Brazil, with comments on the ontogeny and ecomorphology of the species. Cretac Res. 70:163–188. doi:10.1016/j.cretres.2016.11.003.

Cubo J, Köhler M, de Buffrénil V. 2017. Bone histology of *Iberosuchus macrodon* (Sebecosuchia, Crocodylomorpha). Lethaia. 50(4):495–503. doi:10.1111/let.12203.

Cunha GO, Santucci RM, de Andrade MB, de Oliveira CEM. 2020. Description and phylogenetic relationships of a large-bodied sphagesaurid notosuchian from the Upper Cretaceous Adamantina Formation, Bauru Group, São Paulo, southeastern Brazil. Cretac Res. 106:104259. doi:10.1016/j.cretres.2019.104259.

Darlim G, Montefeltro FC, Langer MC. 2021. 3D skull modelling and description of a new baurusuchid (Crocodyliformes, Mesoeucrocodylia) from the Late Cretaceous (Bauru Basin) of Brazil. J Anat. 239:622–662. doi:10.1111/joa.13442.

Dias ANC, Chemale F, Candeiro CRA, Lana CC, Guadagnin F, Sales ASW. 2021. Unraveling multiple tectonic events and source areas in the intracratonic Bauru Basin through combined zircon geo and thermochronological studies. J South Am Earth Sci. 106:103061. doi:10.1016/j.jsames.2020.103061.

Dias-Brito D, Musachio EA, Castro JC, Maranhão MSAS, Suarez JM, Rodrigues R. 2001. Bauru Group: a continental Cretaceous unit in Brazil - concepts based on micropaleontological, oxygen isotope and stratigraphic data. Rev Paléobiol. 20(1):245–304.

Drumheller SK, Adams TL, Maddox H, Noto CR. 2021. Expanded sampling across ontogeny in *Deltasuchus motherali* (Neosuchia, Crocodyliformes): revealing ecomorphological niche partitioning and appalachian endemism in Cenomanian Crocodyliforms. Elem Paleontol. doi:10.1017/9781009042024.

Drumheller SK, Wilberg EW. 2020. A synthetic approach for assessing the interplay of form and function in the crocodyliform snout. Zool J Linn Soc. 188(2):507–521. doi:10.1093/zoolinnean/zlz081.

Dumont Jr MV, Santucci RM, de Andrade MB, de Oliveira CEM. 2020. Paleoneurology of *Baurusuchus* (Crocodyliformes: Baurusuchidae), ontogenetic variation, brain size, and sensorial implications. Anat Rec. doi:10.1002/ar.24567.

Enlow DH. 1962. A study of the post-natal growth and remodeling of bone. Am J Anat. 110(2):79–101. doi:10.1002/aja.1001100202.

Erickson BR. 1976. Osteology of the Early Eusuchian Crocodile *Leidyosuchus formidabilis*, Sp. Nov. Sci Mus Minn. Paleontology. 2:63.

Fernandes LA. 2004. Mapa litoestratigráfico da parte oriental da Bacia Bauru (PR, SP, MG), escala 1: 1.000. 000. Bol Parana Geociências. 55: 53–66.

Fernandes LA, Coimbra AM. 1996. A Bacia Bauru (Cretáceo Superior, Brasil). An Acad Bras Ciênc. 68(2):195–206.

Fernandes LA, Coimbra AM. 2000. Revisão estratigráfica da parte oriental da Bacia Bauru (Neocretáceo). Rev Bras Geociências. 30(4):717–728. doi:10.25249/0375-7536.2000304717728.

Figueiredo RG, Kellner AWA. 2009. A new crocodylomorph specimen from the Araripe Basin (Crato Member, Santana Formation), northeastern Brazil. Paläontol Z. 83(2):323. doi:10.1007/s12542-009-0016-6.

Fiorelli LE, Calvo J 2008. New remains of *Notosuchus terrestris* Woodward, 1896 (Crocodyliformes: Mesoeucrocodylia) from Late Cretaceous of Neuquén, Patagonia, Argentina. Arq Mus Nac [Internet]. [accessed 2021 Feb 25]. https://ri.conicet.gov.ar/handle/11336/81084

Fonseca PHM, Martinelli AG, Da Marinho TS, Ribeiro LCB, Schultz CL, Soares MB. 2020. Morphology of the endocranial cavities of *Campinasuchus dinizi* (Crocodyliformes: Baurusuchidae) from the Upper Cretaceous of Brazil. Geobios. 58:1–16. doi:10.1016/j.geobios.2019.11.001.

Gasparini ZB. 1971. Los Notosuchia de Cretacico de America del Sur como un nuevo infraodern de los mesosuchia (crocodilia). Ameghiniana. 8(2):83–103.

Gasparini Z, Chiappe LM, Fernandez M. 1991. A new Senonian peirosaurid (Crocodylomorpha) from Argentina and a synopsis of the South American Cretaceous crocodilians. J Vertebr Paleontol. 11(3):316–333. doi:10.1080/02724634.1991.10011401.

Georgi JA, Krause DW. 2010. Postcranial axial skeleton of *Simosuchus clarki* (Crocodyliformes: Notosuchia) from the Late Cretaceous of Madagascar. J Vertebr Paleontol. 30(sup1):99–121. doi:10.1080/02724634.2010.519172.

Geroto CFC, Bertini RJ. 2012. Descrição de um espécime juvenil de baurusuchidae (Crocodyliformes: Mesoeucrocodylia) do Grupo Bauru (Neocretáceo): considerações preliminares sobre ontogenia. Rev Inst Geológico. 33 (2):13–29. doi:10.5935/0100-929X.20120007.

Gignac PM, Erickson GM. 2016. Ontogenetic bite-force modeling of *Alligator mississippiensis*: implications for dietary transitions in a large-bodied vertebrate and the evolution of crocodylian feeding. J Zool. 299(4):229–238. doi:10.1111/jzo.12349.

Gignac PM, Santana SE. 2016. A bigger picture: organismal function at the nexus of development, ecology, and evolution: an introduction to the symposium. Integr Comp Biol. 56(3):369–372. doi:10.1093/icb/icw080.

Gignac P, O'Brien H. 2016. Suchian feeding success at the interface of ontogeny and macroevolution. Integr Comp Biol. 56(3):449–458. doi:10.1093/icb/icw041.

Godoy PL, Bronzati M, Eltink E, de Marsola JCA, Cidade GM, Langer MC, Montefeltro FC. 2016. Postcranial anatomy of *Pissarrachampsa sera* (Crocodyliformes, Baurusuchidae) from the Late Cretaceous of Brazil: insights on lifestyle and phylogenetic significance. PeerJ. 4:e2075. doi:10.7717/peerj.2075.

Godoy PL, Ferreira GS, Montefeltro FC, Nova BCV, Butler RJ, Langer MC. 2018. Evidence for heterochrony in the cranial evolution of fossil crocodyliforms. Palaeontology. 61(4):543–558. doi:10.1111/pala.12354.
Godoy PL, Montefeltro FC, Norell MA, Langer MC. 2014. An additional baurusuchid from the Cretaceous of Brazil with evidence of interspecific predation among crocodyliformes. PLOS ONE. 9(5):e97138. doi:10.1371/journal.pone.0097138.
Goldberg K, Garcia AJV. 2000. Palaeobiogeography of the Bauru Group, a dinosaur-bearing Cretaceous unit, northeastern Parana Basin, Brazil. Cretac Res. 21(2):241–254. doi:10.1006/cres.2000.0207.
Grigg G. 2015. Biology and evolution of crocodylians. Clayton South: Csiro Publishing.
Hay OP 1930. Second bibliography and catalogue of the fossil vertebrata of North America.
Hill RV. 2010. Osteoderms of *Simosuchus clarki* (Crocodyliformes: Notosuchia) from the Late Cretaceous of Madagascar. J Vertebr Paleontol. 30(sup1):154–-176. doi:10.1080/02724634.2010.518110.
Horner JR, Goodwin MB. 2009. Extreme cranial ontogeny in the Upper Cretaceous Dinosaur *Pachycephalosaurus*. PLOS ONE. 4(10):e7626. doi:10.1371/journal.pone.0007626.
Horner JR, Padian K, de Ricqlès A. 2001. Comparative osteohistology of some embryonic and perinatal archosaurs: developmental and behavioral implications for dinosaurs. Paleobiology. 27(1):39–58. doi:10.1666/0094-8373(2001)027<0039:COOSEA>2.0.CO;2.
Hutton JM. 1986. Age determination of living nile crocodiles from the cortical stratification of bone. Copeia. 1986(2):332–341. doi:10.2307/1444994.
Irmis RB. 2007. Axial skeleton ontogeny in the Parasuchia (Archosauria: Pseudosuchia) and its implications for ontogenetic determination in archosaurs. J Vertebr Paleontol. 27(2):350–361. doi:10.1671/0272-4634-(2007)27[350:ASOITP]2.0.CO;2.
Iungman J, Piña CI, Siroski P. 2008. Embryological development of *Caiman latirostris* (Crocodylia: Alligatoridae). Genesis. 46(8):401–417. doi:10.1002/dvg.20413.
Kellner AWA, Pinheiro AEP, Campos DA. 2014. A new sebecid from the paleogene of Brazil and the crocodyliform radiation after the K–Pg Boundary. PLOS ONE. 9(1):e81386. doi:10.1371/journal.pone.0081386.
Klein N, Scheyer T, Tütken T. 2009. Skeletochronology and isotopic analysis of a captive individual of *Alligator mississippiensis* Daudin, 1802. Foss Rec. 12(2):121–131. doi:10.1002/mmng.200900002.
Langston JW, Rose H. 1978. A yearling crocodilian from the Middle Eocene Green River formation of Colorado on JSTOR. J Paleontol. 52(1):122–125.
Larsson HCE, Sues H-D. 2007. Cranial osteology and phylogenetic relationships of *Hamadasuchus rebouli* (Crocodyliformes: Mesoeucrocodylia) from the Cretaceous of Morocco. Zool J Linn Soc. 149(4):533–567. doi:10.1111/j.1096-3642.2007.00271.x.
Leardi JM, Pol D, Novas FE, Riglos MS. 2015. The postcranial anatomy of *Yacarerani boliviensis* and the phylogenetic significance of the notosuchian postcranial skeleton. J Vertebr Paleontol. 35(6):e995187. doi:10.1080/02724634.2014.995187.
Lee AH. 2004. Histological organization and its relationship to function in the femur of *Alligator mississippiensis*. J Anat. 204(3):197–207. doi:10.1111/j.0021-8782.2004.00275.x.
Marinho TS, Carvalho IS. 2009. An armadillo-like sphagesaurid crocodyliform from the Late Cretaceous of Brazil. J South Am Earth Sci. 27(1):36–41. doi:10.1016/j.jsames.2008.11.005.
Marinho TS, Iori FV, de Carvalho IS, de Vasconcellos FM. 2013. *Gondwanasuchus scabrosus* gen. et sp. nov., a new terrestrial predatory crocodyliform (Mesoeucrocodylia: Baurusuchidae) from the Late Cretaceous Bauru Basin of Brazil. Cretac Res. 44:104–111. doi:10.1016/j.cretres.2013.03.010.
Marsola JCA, Batezelli A, Montefeltro FC, Grellet-Tinner G, Langer MC. 2016. Palaeoenvironmental characterization of a crocodilian nesting site from the Late Cretaceous of Brazil and the evolution of crocodyliform nesting strategies. Palaeogeogr Palaeoclimatol Palaeoecol. 457:221–232. doi:10.1016/j.palaeo.2016.06.020.
Martin JE. 2014. A sebecosuchian in a Middle Eocene Karst with comments on the Dorsal Shield in crocodylomorpha. Acta Palaeontol Pol. 60(3):673–680. doi:10.4202/app.00072.2014.
Martinelli AG, Marinho TS, Iori FV, Ribeiro LCB. 2018. The first *Caipirasuchus* (Mesoeucrocodylia, Notosuchia) from the Late Cretaceous of Minas Gerais, Brazil: new insights on sphagesaurid anatomy and taxonomy. PeerJ. 6:e5594. doi:10.7717/peerj.5594.
Martinelli AG, Pais DF. 2008. A new baurusuchid crocodyliform (Archosauria) from the Late Cretaceous of Patagonia (Argentina). Comptes Rendus Palevol. 7(6):371–381. doi:10.1016/j.crpv.2008.05.002.
Montefeltro FC. 2019. The osteoderms of baurusuchid crocodyliforms (Mesoeucrocodylia, Notosuchia). J Vertebr Paleontol. 39(2):e1594242. doi:10.1080/02724634.2019.1594242.
Montefeltro FC, Larsson HCE, Langer MC. 2011. A new baurusuchid (Crocodyliformes, Mesoeucrocodylia) from the Late Cretaceous of Brazil and the phylogeny of baurusuchidae. PLOS ONE. 6(7):e21916. doi:10.1371/journal.pone.0021916.
Montefeltro FC, Lautenschlager S, Godoy PL, Ferreira GS, Butler RJ. 2020. A unique predator in a unique ecosystem: modelling the apex predator within a Late Cretaceous crocodyliform-dominated fauna from Brazil. J Anat. 237(2):323–333. doi:10.1111/joa.13192.
Nascimento PM, Zaher H. 2010. A new species of *Baurusuchus* (Crocodyliformes, Mesoeucrocodylia) from the Upper Cretaceous of Brazil, with the first complete postcranial skeleton described for the family baurusuchidae. Papéis Avulsos Zool. 50(21):323–361. doi:10.1590/S0031-10492010002100001.
Nobre PH, de Carvalho IS. 2006. *Adamantinasuchus navae*: a new Gondwanan Crocodylomorpha (Mesoeucrocodylia) from the Late Cretaceous of Brazil. Gondwana Res. 10(3):370–378. doi:10.1016/j.gr.2006.05.008.
Nobre PH, de Carvalho IS. 2013. Postcranial skeleton of *Mariliasuchus amarali* Carvalho and Bertini, 1999 (Mesoeucrocodylia) from the Bauru Basin, Upper Cretaceous of Brazil. Ameghiniana. 50(1):98–113. doi:10.5710/AMGH.15.8.2012.500.
O'Connor PM, Sertich JJW, Stevens NJ, Roberts EM, Gottfried MD, Hieronymus TL, Jinnah ZA, Ridgely R, Ngasala SE, Temba J. 2010. The evolution of mammal-like crocodyliforms in the cretaceous period of Gondwana. Nature. 466(7307):748–751. doi:10.1038/nature09061.
Oliveira CEM, Santucci RM, Andrade MB, Fulfaro VJ, Basílio JAF, Benton MJ. 2011. Crocodylomorph eggs and eggshells from the Adamantina Formation (Bauru Group), Upper Cretaceous of Brazil. Palaeontology. 54(2):309–321. doi:10.1111/j.1475-4983.2010.01028.x.
Oliveira FA, Santucci RM, de Oliveira CEM, de Andrade MB. 2021. Morphological and compositional analyses of coprolites from the Upper Cretaceous Bauru Group reveal dietary habits of notosuchian fauna. Lethaia. doi:10.1111/let.12431.
Ortega F. 2004. Historia evolutiva de los cocodrilos Mesoeucrocodylia. Madrid (Spain): Universidad Autónoma de Madrid.
Padian K, Horner JR, De Ricqlès A. 2004. Growth in small dinosaurs and pterosaurs: the evolution of archosaurian growth strategies. J Vertebr Paleontol. 24(3):555–571. doi:10.1671/0272-4634(2004)024[0555:GISDAP]2.0.CO;2.
Padian K, Lamn E-T 2013. Bone histology of fossil tetrapods. University of California Press. https://www.degruyter.com/document/doi/10.1525/9780520955110/html
Pol D. 2003. New remains of *Sphagesaurus huenei* (Crocodylomorpha: Mesoeucrocodylia) from the Late Cretaceous of Brazil. J Vertebr Paleontol. 23(4):817–831. doi:10.1671/A1015-7.
Pol D. 2005. Postcranial remains of *Notosuchus terrestris* Woodward (Archosauria: Crocodyliformes) from the upper Cretaceous of Patagonia, Argentina. Ameghiniana. 42(1):21–38.
Pol D, Leardi JM 2015. Diversity patterns of Notosuchia (Crocodyliformes, Mesoeucrocodylia) during the cretaceous of Gondwana. https://ri.conicet.gov.ar/handle/11336/60525
Pol D, Leardi JM, Lecuona A, Krause M. 2012. Postcranial anatomy of *Sebecus icaeorhinus* (Crocodyliformes, Sebecidae) from the Eocene of Patagonia. J Vertebr Paleontol. 32(2):328–354. doi:10.1080/02724634.2012.646833.
Pol D, Nascimento PM, Carvalho AB, Riccomini C, Pires-Domingues RA, Zaher H. 2014. A new notosuchian from the Late Cretaceous of Brazil and the phylogeny of advanced notosuchians. PLOS ONE. 9(4):e93105. doi:10.1371/journal.pone.0093105.
Price. 1945. A new reptile from the Cretaceous of Brazil. Rio Jan Dep Nac Produção Miner Notas Prelim E Estud. Boletim 25.
Price. 1950. Os crocodilídeos da fauna da formação Bauru, do Cretáceo terrestre do Brasil meridional. An Acad Bras Ciênc. 22(4):473–490.
Price. 1955. Novos crocodilídeos dos arenitos da Série Bauru, Cretáceo do Estado de Minas Gerais. An Acad Bras Ciênc. 27(4):487–498.
Ricart RSD 2017. Paleohistologia dos fósseis de crocodilomorfos das regiões de Jales e Fernandópolis-SP, Formação Adamantinaa, Grupo Bauru, Cretáceo Superior [Masters dissertation]. https://repositorio.unb.br/handle/10482/24366
Ricqlès AJ, Padian K, Horner JR. 2003. On the bone histology of some Triassic pseudosuchian archosaurs and related taxa. Ann Paléontol. 89(2):67–101. doi:10.1016/S0753-3969(03)00005-3.
Rieppel O. 1993. Studies on skeleton formation in reptiles. v. Patterns of ossification in the skeleton of *Alligator mississippiensis* Daudin (Reptilia, Crocodylia). Zool J Linn Soc. 109(3):301–325. doi:10.1111/j.1096-3642.1993.tb02537.x.
Riff D 2003. Descrição morfológica do crânio e mandíbula de *Stratiotosuchus maxhechti* (Crocodylomorpha, Cretáceo Superior do Brasil) e seu posicionamento filogenético [Masters dissertation]. http://pantheon.ufrj.br/handle/11422/3437

Riff D, Kellner AWA. 2011. Baurusuchid crocodyliforms as theropod mimics: clues from the skull and appendicular morphology of *Stratiotosuchus maxhechti* (Upper Cretaceous of Brazil). Zool J Linn Soc. 163(suppl_1):S37–S56. doi:10.1111/j.1096-3642.2011.00713.x.

Riff D, Souza RGD, Cidade GM, Martinelli AG, Souza-Filho JP. 2012. Crocodilomorfos: a maior diversidade de répteis fósseis do Brasil. Terræ. 9 (1/2):12–40.

Ruiz JV, Bronzati M, Ferreira GS, Martins KC, Queiroz MV, Langer MC, Montefeltro FC. 2021. A new species of *Caipirasuchus* (Notosuchia, Sphagesauridae) from the Late Cretaceous of Brazil and the evolutionary history of Sphagesauria. J Syst Palaeontol. 19(4):265–287. doi:10.1080/14772019.2021.1888815.

Salisbury SW, Frey E, Martill DM, Buchy M-C. 2003. A new crocodilian from the Lower Cretaceous crato formation of north-eastern Brazil. Palaeontogr Abt A. 19. 3–47.

Schobbenhaus C, Brito Neves BBD. 2003. A geologia do Brasil no contexto da plataforma Sul-Americana. Rio de Janeiro: Geol Tectônica E Recur Minerais Bras. (CPRM); p. 5–25.

Schwarz D, Salisbury SW. 2005. A new species of *Theriosuchus* (Atoposauridae, Crocodylomorpha) from the Late Jurassic (Kimmeridgian) of Guimarota, Portugal. Geobios. 38(6):779–802. doi:10.1016/j.geobios.2004.04.005.

Seidel MR. 1979. The osteoderms of the American alligator and their functional significance. Herpetologica. 35(4):375–380.

Sellés AG, Blanco A, Vila B, Marmi J, López-Soriano FJ, Llácer S, Frigola J, Canals M, Galobart À. 2020. A small cretaceous crocodyliform in a dinosaur nesting ground and the origin of sebecids. Sci Rep. 10(1):15293. doi:10.1038/s41598-020-71975-y.

Sena MVA, Andrade RCLP, Sayão JM, Oliveira GR. 2018. Bone microanatomy of *Pepesuchus deiseae* (Mesoeucrocodylia, Peirosauridae) reveals a mature individual from the Upper Cretaceous of Brazil. Cretac Res. 90:335–348. doi:10.1016/j.cretres.2018.06.008.

Sertich JJW, Groenke JR. 2010. Appendicular skeleton of simosuchus clarki (Crocodyliformes: Notosuchia) from the Late Cretaceous of Madagascar. J Vertebr Paleontol. 30(sup1):122–153. doi:10.1080/02724634.2010.516902.

Sharma PP, Clouse RM, Wheeler WC. 2017. Hennig's semaphoront concept and the use of ontogenetic stages in phylogenetic reconstruction. Cladistics. 33 (1):93–108. doi:10.1111/cla.12156.

Soares PC, Landim PMB, Fúlfaro VJ, Neto AFS. 1980. Ensaio de caracterização estratigráfica do cretáceo no Estado de São Paulo: Grupo Bauru. Rev Bras Geociências. 10(3):177–185. doi:10.25249/0375-7536.1980177185.

Tavares SAS, Branco FR, de Carvalho IS, Maldanis L. 2017. The morphofunctional design of *Montealtosuchus arrudacamposi* (Crocodyliformes, Upper Cretaceous) of the Bauru Basin, Brazil. Cretac Res. 79:64–76. doi:10.1016/j.cretres.2017.07.003.

Tucker AD, Limpus CJ, McCallum HI, McDonald KR. 1996. Ontogenetic dietary partitioning by *Crocodylus johnstoni* during the dry season. Copeia. 1996 (4):978–988. doi:10.2307/1447661.

Vickaryous MK, Hall BK. 2008. Development of the dermal skeleton in *Alligator mississippiensis* (Archosauria, Crocodylia) with comments on the homology of osteoderms. J Morphol. 269(4):398–422. doi:10.1002/jmor.10575.

Vieira LG, Lima FC, Mendonôa SHST, Menezes LT, Hirano LQL, Santos ALQ. 2018b. Ontogeny of the postcranial axial skeleton of *Melanosuchus niger* (Crocodylia, Alligatoridae). Anat Rec. 301(4):607–623. doi:10.1002/ar.23722.

Vieira LG, Santos ALQ, Hirano LQL, Menezes-Reis LT, Mendonça JS, Sebben A. 2018a. Ontogeny of the skull of the Black Caiman (*Melanosuchus niger*) (Crocodylia: Alligatoridae). Can J Zool. doi:10.1139/cjz-2018-0076.

Walker AD, Westoll TS. 1970. A revision of the Jurassic reptile *Hallopus victor* (Marsh), with remarks on the classification of crocodiles. Philos Trans R Soc Lond B Biol Sci. 257(816):323–372. doi:10.1098/rstb.1970.0028.

Whetstone KN, Whybrow PJ. 1983. A cursorial crocodilian from the Triassic of Lesotho (Basutoland) Southern Africa. Occas Pap Mus Nat Hist Univ Kans. 106:1–37.

Wilson JA. 1999. A nomenclature for vertebral laminae in sauropods and other saurischian dinosaurs. J Vertebr Paleontol. 19(4):639–653. doi:10.1080/02724634.1999.10011178.

Woodward HN, Horner JR, Farlow JO. 2011. Osteohistological Evidence For Determinate Growth in the American alligator. J Herpetol. 45(3):339–342. doi:10.1670/10-274.1.

Woodward HN, Horner JR, Farlow JO. 2014. Quantification of intraskeletal histovariability in *Alligator mississippiensis* and implications for vertebrate osteohistology. PeerJ. 2:e422. doi:10.7717/peerj.422.

Young MT, Brusatte SL, Ruta M, de Andrade MB. 2010. The evolution of Metriorhynchoidea (Mesoeucrocodylia, Thalattosuchia): an integrated approach using geometric morphometrics, analysis of disparity, and biomechanics. Zool J Linn Soc. 158(4):801–859. doi:10.1111/j.1096-3642.2009.00571.x.

Zaher H, Pol D, Carvalho AB, Riccomini C, Campos D, Nava W. 2006. Redescription of the cranial morphology of *Mariliasuchus amarali*, and its phylogenetic affinities (Crocodyliformes, Notosuchia). Am Mus Novit. 2006 (3512):1–40. doi:10.1206/0003-0082(2006)3512[1:ROTCMO]2.0.CO;2.